Trinity College Dublin
Coláiste na Tríonóide, Baile Átha Cliath
The University of Dublin

Thiol-Ene Mediated Strategies for Peptide Cyclisation and Bioconjugation

Nikita Ostrovitsa

April 2025

Supervisor: Prof. Eoin M. Scanlan

Submitted to the School of Chemistry for

the degree of Doctor of Philosophy

I declare that this thesis has not been submitted as an exercise for a degree at this or any other university and it is entirely my own work.

I agree to deposit this thesis in the University's open access institutional repository or allow the Library to do so on my behalf, subject to Irish Copyright Legislation and Trinity College Library conditions of use and acknowledgement.

I consent to the examiner retaining a copy of the thesis beyond the examining period, should they so wish (EU GDPR May 2018).

Signed: Nikita Ostrovitsa Date: 04/05/2025

Abstract

This thesis presents innovative methodologies for peptide cyclisation, functionalisation, and bioconjugation, providing advanced tools for biomedical research and drug discovery. Central to this work is the application of the radical thiol-ene chemistry, enabling precise on-resin peptide hydrothiolation and versatile chemical modifications.

Chapter 2 details the synthesis of vasopressin and somatostatin analogues with tailored ring sizes to study neuropeptide activity. Using a novel on-resin regioselective thiol installation strategy and subsequent disulfide bond formation, high-purity cyclic analogues of vasopressin and somatostatin were produced, offering insights into the effect of the ring size on biological function.

Chapter 3 expands the methodology of the on-resin peptide hydrothiolation to native chemical ligation (NCL), streamlining the synthesis of thiolated amino acid analogues at the *N*-terminus of peptide sequences. This chapter also demonstrates on-resin conjugation of fluorophores, eliminating intermediate purification steps and paving the way for efficient bioconjugation strategies.

Chapter 4 introduces a novel approach for late-stage modifications of cyclic peptide by combining chloroacetyl peptide cyclisation with post-cyclisation thiol-ene reactions. An unsaturated vasopressin analogue was utilised as a model peptide to demonstrate compatibility with diverse thiol substrates.

Chapter 5 focuses on the development of thiol-containing chemical probes for selective targeting of crotonylation post-translational modifications. Optimised TEC reactions enabled the covalent modification of crotonylated peptides and opened a new avenue for applications in chemoproteomics and protein targeting in complex biological systems.

Abbreviations

AA	Amino acid
Abz	Aminobenzamide
Ac_2O	Acetic anhydride
AcN	Acetonitrile
ADH	Antidiuretic hormone
Agl	Allylglycine
AIBN	2,2-Azobis(isobutryonitrile)
AIP	Autoinducing Peptide
alloc	*N*-Allyloxycarbonyl
AML	Auxiliary mediated ligation
AMP	Antimicrobial peptide
APCI	Atmospheric Pressure Chemical Ionization
Aq.	Aqueous
Ar	Aromatic
Arg; R	Arginine
Asn; N	Asparagine
Asp; D	Aspartic Acid
ATE	Acyl Thiol-Ene
AuNPs	Gold nanoparticles
AVP	Arginine vasopressin
BDT	1,4-Butanedithiol
Boc	*tert*-butyloxycarbonyl
BPB	Bromophenol Blue
BSA	Bovine Serum Albumin
B2RP	Brevin-2-related peptide
Bzl	benzyl
Cbz	Carboxybenzyl
$CDCl_3$	Chloroform
CLipPA	Cysteine Lipidation on a Peptide or Amino Acid
$COCl_2$	Oxalyl chloride

CuAAC	Copper-Catalysed Azide Alkyne Cycloaddition
Cys; C	Cysteine
d	Doublet
Dbz	3,4-diaminobenzoic acid
DBU	1,8-diazabicyclo-[5.4.0]-undec-7-ene
DCC	*N,N'*-dicyclohexylcarbodiimide
DCU	*N,N'*-dicyclohexylurea
dd	Doublet of Doublets
DIAD	Diisopropyl azodicarboxylate
DIC	Diisopropylcarbodiimide
DIPEA	Diisopropylethylamine
DMAP	4-(Dimethylamino)pyridine
DMF	Dimethylformamide
DMP	2,2-dimethoxypropane
DMSO	Dimethylsulfoxide
DPAP	2,2-Dimethoxy-2-Phenylacetophenone
DTT	Dithiothreitol
EDC·HCl	*N*-Ethylcarbodiimide hydrochloride
EDT	Ethanedithiol
EPO	Erythropoietin
Equiv.	Equivalents
ESI-MS	Electrospray Ionisation Mass Spectrometry
Et_2O	Diethyl Ether
EtOAc	Ethyl Acetate
FDA	Food and Drug Administration
Fmoc	Fluorenylmethoxycarbonyl
Fmoc-OSu	Fluorenylmethoxycarbonyl-succinimide
Gdn·HCl	Guanidinium hydrochloride
Gln	Glutamine
GLP-1	Glucagon-like peptide-1
Glu	Glutamic Acid
Gly	Glycine

GnRH	Gonadotropin-releasing hormone
GPCRs	G-protein-coupled receptors
GSH	Glutathione
h	hour
H_2O	Water
HATU	Hexafluorophosphate azabenzotriazole tetramethyl uronium
Hag	1-homoallylglycine
HBTU	(2-(1H-Benzotriazol-1-yl)-1,1,3,3-Tetramethyluronium
HCl	Hydrochloric acid
HCl·Cys	L-cysteine hydrochloride
HCl·Cys-OMe	L-cysteine hydrochloride methyl ester
HCTs	Histone crotonyl transferases
HDCs	Histone decrotonylases
HF	Hydrofluoric acid
His; H	Histidine
HIV-1 PR	Human immunodeficiency virus-1 protease
HOBt	Hydroxybenzotriazole
HPLC	High-Performance Liquid Chromatography
hPTHrP	Human parathyroid hormone
HRMS	High Resolution Mass Spectrometry
I_2	Iodine
IIDQ	2-Isobutoxy-1-Isobutoxycarbonyl-1,2-Dihydroquinoline
Ile; I	Isoleucine
IL-8	Interleukin 8
J	Coupling Constant
KCr	Crotonylation
LAP	(2,4,6-trimethylbenzoyl) phosphinate
LC	Liquid Chromatography
LC-MS	Liquid Chromatography - Mass Spectrometry
LED	Light-Emitting Diode
Leu; L	Leucine
LiOH	Lithium hydroxide

Lys	Lysine
m	Multiplet
m/z	Mass to Charge Ratio
MAP	4-Methoxyacetophenone
MeNbz	*N*-acyl-*N*'-methylurea
MeOH	Methanol
Met; M	Methionine
min	Minutes
Mmt	Monomethoxytrityl
MPAA	4-mercaptophenylacetic acid
MsCl	Methenesulfonyl chloride
Mtt	Methyltrityl
NaCr	Sodium crotonylate
Nbz	*N*-acyl-benzimidazolinone
NCL	Native chemical ligation
NHS-Cr	*N*-hydroxy succinimide
NMM	*N*-methylmorpholine
NMP	*N*-methylpyrolidinone
NMR	Nuclear Magnetic Resonance
NaOAc	Sodium acetate
OBt	O-benzotriazole
PG	Protecting groups
Phe; F	Phenylalanine
PPh_3	Triphenyl phosphine
PPI	Protein-protein interaction
Pro; P	Proline
PSCaa	Photoswitchable click amino acid
PTM	Post Translational Modification
PTSA	p-toluenesulfonic acid
PyBOP	Benzatriazol-1-yl-oxytripyrrolidinophosphonium hexafluorophosphate
RaPID	Random nonstandard peptides integrated discovery
RCM	Ring closing metathesis

RGD	Arginine-glycine-aspartic acid
RP	Reverse Phase
RP-HPLC	Reverse-phase high-performance liquid chromatography
rt	Room Temperature
s	Singlet
SEA	bis(2-sulfanylethyl)amido
Ser; S	Serine
$SOCl_2$	Thionyl chloride
SPAAC	Strain promoted azide alkyne cycloaddition
SPPS	Solid phase peptide synthesis
t	Triplet
***t*Bu**	*tert*-butyl
***t*BuSH**	*tert*-butyl thiol
TCEP·HCl	Tris(2-carboxyethyl)phosphine hydrochloride
TEA	Triethylamine
TEC	Thiol-Ene Click
TES	Triethylsilane
TFA	Trifluoroacetic acid
THF	Tetrahydrofuran
TLC	Thin Layer Chromatography
Thr; T	Threonine
Trp	Tryptophan
Tris	tris(hydroxymethyl)aminomethane
Trityl; Trt	Triphenylmethyl
Tyr; Y	Tyrosine
UAA	Unnatural amino acids
VA-044	2,2'-azobis[2-(2-imidazolin-2-yl) propane] dihydrochloride
Val; V	Valine
Vgl	Vinylglycine

Acknowledgments

Firstly, I would like to thank my supervisor, Professor Eoin Scanlan, for providing me the opportunity to join his research group as a PhD student. I really appreciate his guidance and never-ending support throughout the course of this work. Thank you for supporting me to attend conferences and for providing me the opportunity to complete a 3-month placement at the University of Utrecht. I would also like to thank Science Foundation Ireland (SFI) for funding my PhD.

I would like to thank Professor Marc Devocelle for allowing me to use the Liberty Blue peptide synthesiser in his research group at Royal College of Surgeons in Ireland (RCSI). I am so grateful to Dr. John O' Brien for his non-stop work that he has done for my projects, especially for the full characterisation of all the amino acid derivatives that I made. Your skills and enthusiasm in NMR characterisation are remarkable. I would like to thank Dr. Manuel Ruether for fixing any technical issues with the instruments and ensuring that everything is running smoothly. I wish to thank Dr. Gary Hessman for his support with mass spectrometry.

I have no words to describe how thankful I am to Dr. Rita Petracca who is an assistant Professor at the University of Utrecht. Thank you very much for having me in your research group for 3 months and involving me in amazing research projects. I always develop new skills when I work with you- you made my PhD experience much better. I would like to thank Sebastian for being an amazing friend for years and for spending some good time with me during my staying in Utrecht. Finally, I would like to thank Ilhan, Helena and Marinda for being amazing friends and for always making me feel welcome in a new country.

I would like to thank all the members of the Scanlan group that I worked and collaborated with. Finishing my PhD, I will have very nice memories with Laura, Alby, Ines, Conor (also known as Mr Williams), Lucy, Matthew, Dillon, and Glenna. Laura, fuiste la persona más importante que conocí en Dublín. No tengo palabras para decir lo mucho que me has ayudado durante todos estos años y lo cariñosa que has sido conmigo. I would like to thank Alby for making me feel welcome in the group since the first day of my PhD and Mr Williams for sharing the same fume cupboard for 2 years of

non-stop philosophy sessions. Ines thank you for bringing all your positivity in our group and for being a good friend and person to work with. Finally, I would like to thank all the previous members of the Scanlan group and especially, Ale-ale-jandro, Katie, Dylan, Harlei and Josh.

I would like to thank Valerio, Connor, and André from the Mcgouran group for providing me good times of laughing all these years. I would also like to thank the members of the Connon group that I shared the lab for the 4 years of my PhD. It was amazing to work in the lab with Lee, Pierre, Ian, and Lorenzo. I will miss our never-ending conversations, stories, and bad jokes along with the very particular music playlists!!! I would also like to thank Adam and Connie from the Gunnlaugsson group.

I want to give a special mention to my best-friends from Greece, Sotiris Panagiotis, Nikos, and Stavros for being so important for me all these years. We were not as close the last years because of the distance but I always had the best moments of my life whenever I would meet you. Special thank you to my very good friends from London, Shristi, Shub, Michael, Vasilis, Natalia, Ragadh, and Yasir for the beautiful reunions we had very frequently in London during the years of my PhD. I am hoping to spend more time with you from now on!!

Finally, I want to express my gratitude to my parents, Άννα and Ανδρέας, and grandparents, Γιάννης and Κωνσταντίνα, for the unconditional love, support and help during all the years of my studies, including the 4 years of my PhD. My parents have taught me not to give up no matter the circumstances, so this PhD work is dedicated to them.

Publications

1) I. Rabadan Gonzalez, J.T. McLean, **N. Ostrovitsa**, S. Fitzgerald, A. Mezzetta, L. Guazzelli, D.F. O'Shea, E.M. Scanlan, A thiol-ene mediated approach for peptide bioconjugation using 'green' solvents under continuous flow, *Org. Biomol. Chem.*, 2024, **22**, 2203-2210.
2) T.W. Craven, M.D. Nolan, J. Bailey, S. Olatunji, S.J. Bann, K. Bowen, **N. Ostrovitsa**, T.M. Da Costa, R.D. Ballantine, D. Weichert, P.M. Levine, L.J. Stewart, G. Ghardwaj, J.A. Geoghegan, S.A. Cochrane, E.M. Scanlan, M. Caffrey and D. Baker, Computational Design of Cyclic Peptide Inhibitors of a Bacterial Membrane Lipoprotein Peptidase, *ACS Chem. Biol*., 2024, **19**, 1125-1130.
3) M. Westerveld, K. Besermenji, D. Aidukas, **N. Ostrovitsa** and Dr. R. Petracca, Cracking Lysine Crotonylation (Kcr): Enlightening a Promising Post-Translational Modification, *ChemBioChem*, 2024, e202400639.
4) P. Krawinski, L. Smithers, L. Dalsen, C. Boland, **N. Ostrovitsa**, J. Pérez and M. Caffrey, 7.10 MAG. A Novel Host Monoacylglyceride for *In Meso* (Lipid Cubic Phase) Crystallization of Membrane Proteins, *Cryst. Growth Des*. 2024, **24**, 2985-3001.

Table of Contents

Chapter 1 - Introduction

Chapter 2 - On-resin Hydrothiolation Towards Peptide Cyclisation

Chapter 3 - On-resin Hydrothiolation Towards Peptide Ligation and Modification

Chapter 4 - Thiol-ene Mediated Late-stage Modifications of Cyclic Peptides

Chapter 5 - Development of a Photochemical Method to Specifically Label and Detect Lysine- crotonylated (KCr) Proteins.

Chapter 6 - Conclusions

Chapter 7 - Experimental

Chapter 1

Introduction

1.1 Peptide Therapeutics

Peptide therapeutics play a crucial role in drug discovery and have numerous pharmaceutical applications. Peptides can function as neurotransmitters, hormones, cell surface ligands, and antimicrobial agents[1] and are used for the treatment of a wide range of diseases including cancer,[2,3] cardiovascular diseases,[4] pain,[3] and infections.[5] The history of peptide-based drugs dates back to 1921, when Frederick Banting successfully isolated insulin from bovine pancreas.[6] In 1923, insulin became the first commercially available peptide therapeutic for treatment of diabetes, an achievement that earned Banting and John MacLeod the Nobel Prize in Physiology or Medicine.[6] A significant milestone in peptide therapeutics was the synthesis of oxytocin (**1**) in solution by du Vigneaud and coworkers in 1954.[7] Oxytocin is a human peptide hormone produced in the hypothalamus of brain which plays an important role in human social behaviour, anxiety and depression.[8] Its cyclic structure consists of nine amino acid residues, with a disulfide bridge between the cysteine (Cys, C) residues (**Figure 1.1.A, left**).[8] Oxytocin was the first polypeptide to be sequenced and synthesised, leading to Vincent du Vigneaud receiving the Nobel Prize in Chemistry in 1955.[7,9] The successful total synthesis of oxytocin opened new possibilities towards the development of synthetic human signalling hormones including vasopressin, somatostatin, and gonadotropin-releasing hormone (GnRH). Notably, goserelin acetate and leuprolide acetate are two highly efficient GnRH agonists that are widely used for treatment of prostate and breast cancer.[10] Another major class of therapeutic peptides is those derived from natural products isolated from bacteria, plants, and animals. Cyclosporine A (**2**) is a cyclic peptide comprised of eleven amino acids that was initially isolated from *fungi imperfecti* and approved as an immunosuppressive drug in 1983.[10–12] Cyclosporine A exhibits excellent pharmacokinetic properties due to Its high degree of *N*-methylation, the presence of unnatural amino acids (UUAs), and its conformational rigidity (**Figure 1.1.A, right**). In addition, peptide drug discovery has demonstrated considerable interest in animal venom-derived peptides as potential therapeutic agents. Animal venoms contain a mixture of potent bioactive peptides that target a wide range of proteins, including G-protein-coupled receptors (GPCRs) and ion channels.[13] In 2005, exenatide, derived from the venomous lizard Gila monster (*Heloderma suspectum*), was

approved as a highly effective agonist of the Glucagon-like peptide-1 (GPL1) receptor for the treatment of type 2 diabetes.[10,14]

Over the past six decades, the approval of peptide therapeutics has steadily increased, with the global peptide therapeutics market experiencing an average growth rate of 7.7%.[10] Peptide therapeutics account for 5% of the global pharmaceutical market and in 2019 global sales of peptide drugs exceeded $70 billion.[10] As of 2022, more than 80 peptides reached the global pharmaceutical market, with over 170 additional peptides in active clinical development and 400-600 peptides in the pre-clinical stage.[10]

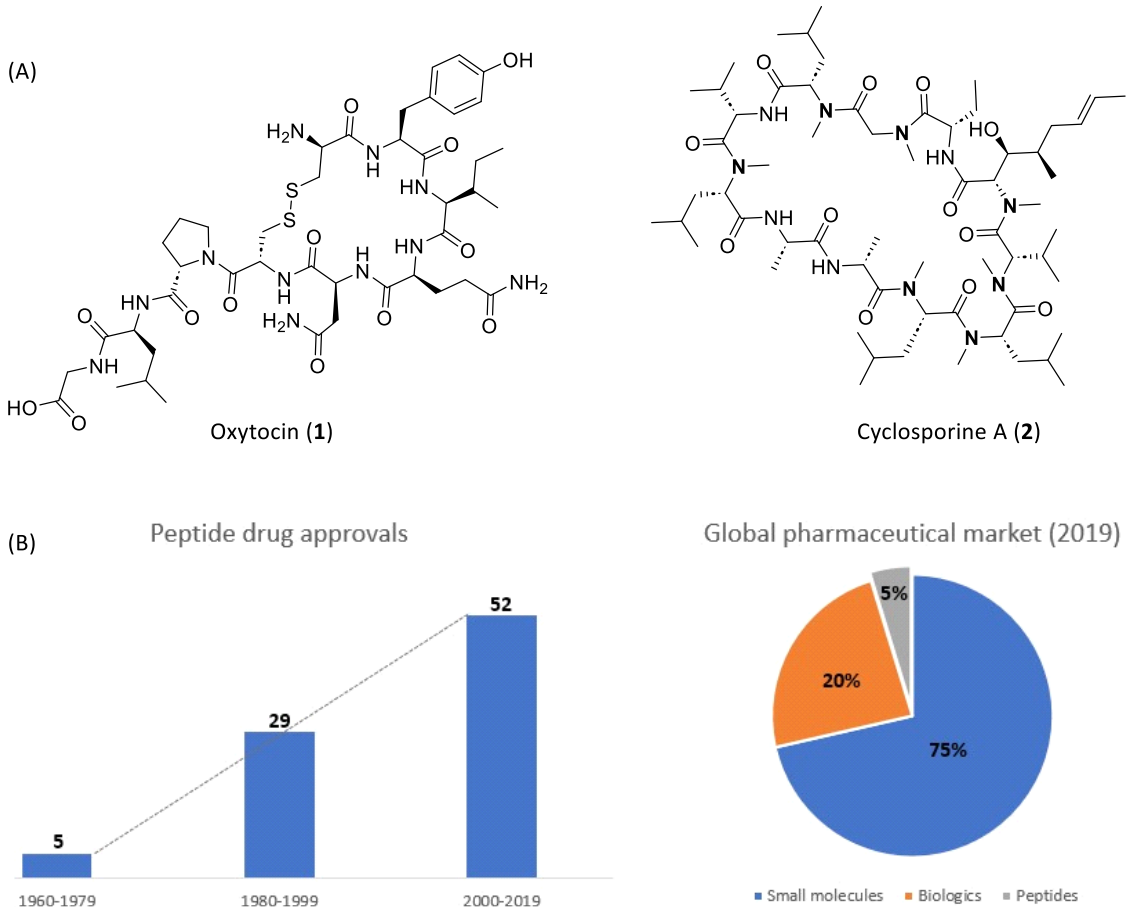

Figure 1.1. (A) The chemical structures of oxytocin (**1**) and cyclosporine (**2**). (B) Approval of peptide drugs over the last six decades (left) and types of drugs in the pharmaceutical market as of 2019 (right).[10]

1.1.2 Peptides in Drug Discovery

The pharmaceutical market is traditionally divided into two main categories of drugs: small-molecule drugs, which have a molecular weight of less than 500 Da, and biologics, which are typically larger than 5000 Da.[15] Small-molecule drugs are

characterised by high bioavailability and cell permeability, while biologics exhibit extremely high specificity and affinity for their targets. Peptide-based drugs fill the gap between these two traditional classes of molecules, combining the advantageous properties of both in the development of modern therapies for a plethora of diseases. Even though small molecule drugs comprise the majority of therapeutics, their small size results in many extracellular and intracellular off-target binding interactions which raises safety issues.[15] Peptides are biological molecules comprised of amino acids, therefore their metabolites are significantly less harmful than small molecules to the human body which lowers the risk of toxicity.[16] Additionally, peptides are more appropriate candidates than small molecules for the disruption of protein-protein interactions (PPIs) which are usually classified as "undruggable" targets.[17] PPIs play a critical role in regulating many biological pathways and are directly associated with a number of diseases, including cancer and autoimmune diseases, rendering their inhibition a very active topic in drug discovery.[18,19] PPIs generally involve large, flat surface areas ranging from 1500-3000 Å², whereas small molecules can only cover 300-1000 Å² of the protein surface.[15] By contrast, peptides have much larger sizes, flexible backbones, and the ability to precisely mimic the binding interface between the two interacting proteins, which make them very promising inhibitors of PPIs.

Despite their therapeutic potential, peptide drugs face significant challenges, particularly related to their pharmacokinetic profile.[20] Peptides are prone to rapid degradation by proteolytic enzymes in the plasma and digestive system, resulting in low bloodstream stability and short *in vivo* half-life (1-2 minutes).[21] The short *in vivo* half-life is also attributed to their rapid removal from the bloodstream by the liver and the kidney.[21,22] The extensive hydrogen bonding and the highly polar surfaces of peptides lower their cell membrane permeability, restricting their effectiveness primarily to extracellular targets.[23] In addition, peptide-based drugs generally demonstrate very poor oral bioavailability. Hence, they are typically injected intramuscularly or intravenously, which leads to low patient compliance.[24] Over the past 30 years, peptide chemists have developed many chemical strategies to improve the unfavourable pharmacokinetic properties of peptides, including the use of unnatural or D- amino acids

within the peptide sequence, *N*-methylated peptides, pseudo-peptides and peptidomimetic molecules.[10,25]

Of particular interest and research focus is the use of cyclic peptides that have several advantages for drug development compared to linear peptides. Peptide macrocycles have constrained ring structures which improves their binding properties.[26] The conformational rigidity of cyclic peptides reduces their entropic penalty, thereby improving the affinity towards the biological target of interest.[27] Furthermore, cyclic peptides show increased resistance to hydrolysis by degrading enzymes due to the lack of a *C*- or *N*- terminus, resulting in higher *in vivo* stability and longer half-life.[26,28] Potent macrocyclic peptide binders can be developed through high-throughput screening technologies such as phage display or mRNA display.[29] In addition, modern computational methods allow for the *de novo* generation of cyclic peptides with increased potency and enhanced drug-like properties such as improved cell permeability.[30] From 2017 to 2023, one in ten drugs approved by the Food and Drug Administration (FDA) were peptides and nearly half of these were cyclic peptides.[27] Thus, the development of novel synthetic methodologies for peptide cyclisation is a very active research area which is gathering increased attention in peptide drug discovery.

1.1.3 Cyclic Peptides in Nature

Peptide macrocycles can be categorised into head-to-tail, side chain-to-side chain, head-to-side chain, and side chain-to-tail cyclisations (**Figure 1.2.A**). In head-to-tail cyclisation there is a direct covalent link *via* an amide bond between the *C*- and *N*-terminus of the peptide chain. Head-to-tail cyclic peptides have been observed in microorganisms and plants. Prominent examples are gramicidin *S* (**3**, **Figure 1.2.B**) which is produced by the gram-positive *Brevibacillus brevis* and was used as a topical antibiotic, and bacteriocin AS-48 which is a 70-residue cyclic peptide produced by the bacterium *Enterococcus faecalis.*[27,31,32] Side chain-to-side chain is another common loop, and it involves covalent linkage between two side chain residues. This motif is found in many naturally occurring hormones including oxytocin, vasopressin, and in a series of synthetic "stapled" peptides for disruption of PPIs.[7,15] On the other hand, termini-to-side chain cyclisation links *via* the *C*- or *N*-terminus to a side chain residue are

observed, for example, in the antibiotic polymyxin B (**4**, **Figure 1.2.B**) which is isolated from *Bacillus polymyxa* and binds and disrupts the out cell of Gram-negative bacteria.[33,34] Finally, several naturally occurring peptide macrocycles contain multiple staples, which are referred to as bicycles and tricycles. This class of cyclic peptides, are garnering increasing interest as potential therapeutics due to their improved binding characteristics compared to monocyclic peptides.[27,35]

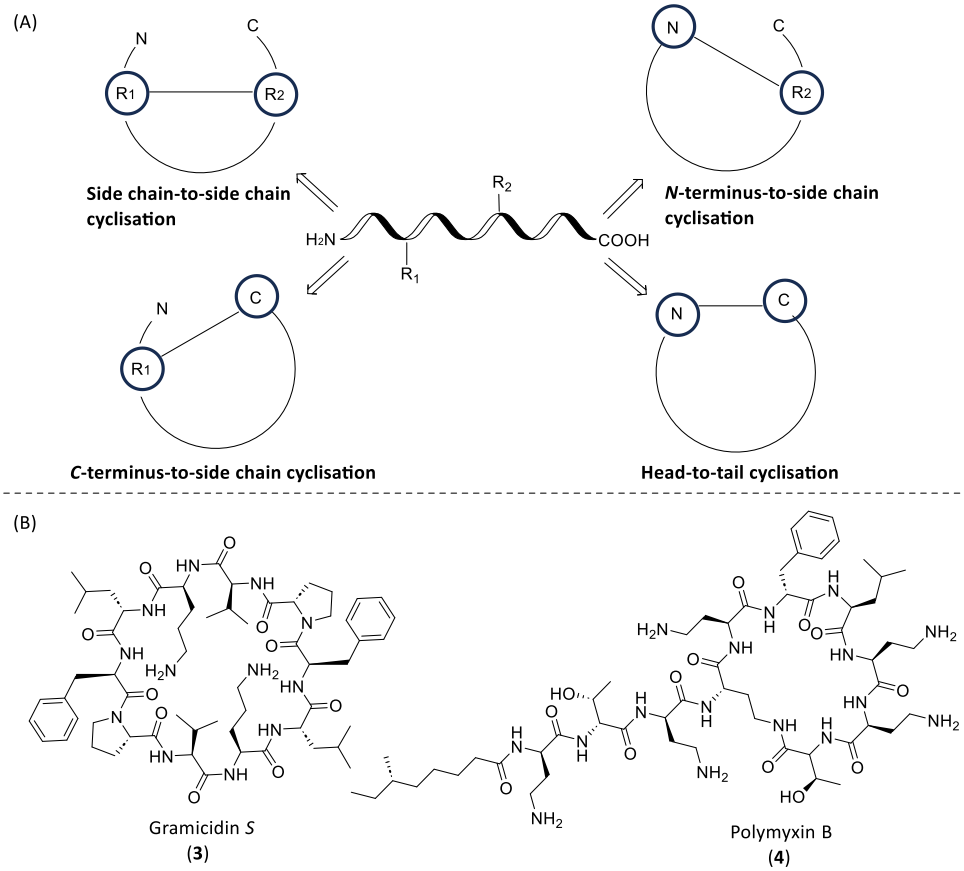

Figure 1.2. (A) Types of peptide macrocycles. (B) Chemical structures of Gramicidin *S* (**3**) and Polymyxin B (**4**).

1.1.4 Synthetic Strategies for Peptide Macrocyclisation

Over the last century, a plethora of synthetic methodologies have been developed aimed at accessing cyclic peptides. The traditional macrolactone cyclisation involves the direct ester bond formation, usually between the hydroxyl group of threonine (Thr, T) or serine (Ser, S) and the activated carboxylate group of aspartic acid (Asp, D), glutamic acid (Glu, E) or the *C*-terminal of the sequence (**Figure 1.3.A**). Depsipeptides are natural products bearing an ester linkage and examples have been shown to demonstrate

excellent anti-tumour and antiviral properties.[36,37] However, the ester moiety is very prone to hydrolysis, rendering macrolactone cyclic peptides unstable *in vivo*, and thus limiting their therapeutic potential.[38] This problem can be addressed through replacement of the labile ester linkage with a more stable amide bond resulting in a macrolactam macrocycle (**Figure 1.3.B**). The intramolecular amide forming process usually occurs between free the amine group of the *N*-terminus or lysine (Lys, K) side chain and a reactive carboxylate group such as an activated ester, anhydride, acyl azide or acyl halide.[39] Nevertheless, macrolactam formation is not a biocompatible synthetic method for peptide cyclisation since it requires the use of fully protected reactive side chains to prevent side reactions.

An alternative synthetic method to cyclise peptides involves the formation of a reversible covalent bond between the thiol moieties of two Cys residues (**Figure 1.3.C**). Disulfide bridges are commonly observed in nature, often resulting in conformational constraint of proteins and peptides. For example, cyclotides are disulfide-rich mini proteins derived from plants that share a common structural feature of a Cys knot motif comprised of three or more disulfide bridges.[40] Kalata B1 is a cyclotide isolated from African herb *Oldenlandia affinis* with a head-to-tail cyclic structure and three internal disulfide bridges, which shows increased chemical and thermal stability.[41] Intramolecular disulfides can form synthetically under air oxidation or in the presence of stronger oxidative agents at near-neutral pH and room temperature, and this reaction is deemed highly biocompatible because it is not affected by the presence of reactive side chains of other residues.[42] Margaret Brimble and coworkers achieved the oxidative folding of the 63-mer snakin 1 protein in tris(hydroxymethyl)aminomethane (Tris) buffer at pH 8 in presence of cysteine over 21 hours.[43] Dimethylsulfoxide (DMSO) and iodine (I_2) are widely used as effective oxidising agents for rapid cyclisation of Cys-rich peptides *via* disulfide bond formation.[42] The main disadvantage of disulfide-based cyclic peptides is the relatively low stability *in vivo* due to their susceptibility to reducing enzymes such as reductases.[44] Aiming to improve this, peptide chemists have developed a number of synthetic methods for bioisosteric replacement of the disulfide linkage with more stable moieties.

The copper-catalysed [3 + 2]-azide–alkyne cycloaddition (CuAAC) developed concurrently by Sharpless and Meldal, is a very powerful 'click' reaction that links an alkyne and an azide group *via* a [1,2,3]-triazole heterocycle (**Figure 1.3.D**). The use of alkyne- and azide-containing amino acids has enabled the development of triazole-based peptide macrocycles that display improved helicity, stability, and binding affinity.[27] However, a significant limitation of the CuAAC reaction is the requirement for a copper catalyst that can non-specifically bind to the peptide, complicating purification.[27] To address this issue, Bertozzi and coworkers developed a copper-free, strain-promoted [3 + 2]-azide-alkyne cycloaddition which has since become a widely used method for metal-free bioconjugation in living systems. For their pioneering work in these fields, Meldal, Sharpless, and Bertozzi were awarded the Nobel Prize in Chemistry in 2022. In addition, ruthenium-catalysed ring closing metathesis (RCM) between two alkenyl amino acids has also emerged as a useful surrogate of the disulfide group for peptide stapling applications (**Figure 1.3.E**).[27]

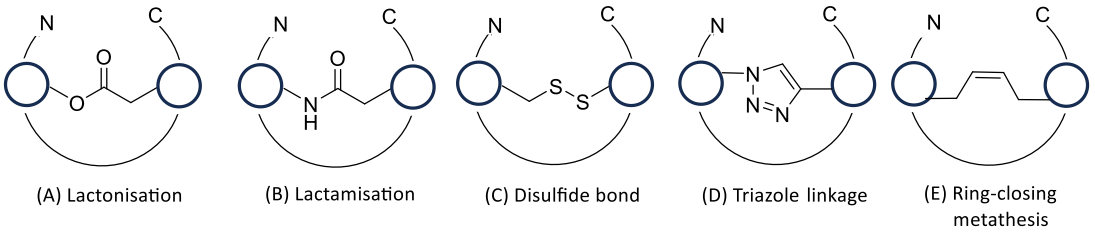

Figure 1.3. Synthetic strategies towards peptide cyclisation.

1.2 Chemical Peptide Synthesis

1.2.1 Solution Phase Peptide Synthesis

The formation of amide bonds between carboxylic acids and amines is a fundamental reaction in traditional solution phase peptide synthesis. Direct condensation of carboxylic acids with amines to form amides can be achieved using high temperatures (>200 °C) or microwave irradiation.[45] However, such harsh conditions are generally incompatible with the synthesis of peptides. Consequently, the carboxylic acid is typically preactivated and transformed into a reactive intermediate to facilitate the acylation of the amine group, furnishing the final amide bond. Traditionally, thionyl

chloride ($SOCl_2$) and oxalyl chloride ($COCl_2$) have been employed to form highly reactive acyl chloride intermediates.[46,47] However, the generation of hydrochloric acid (HCl) upon amine acylation renders their use unsuitable for peptides containing acid-labile protecting groups. To address this limitation, acyl chlorides can be replaced by acyl azides which are highly potent synthetic intermediates used for the direct preparation of amines, amides, isocyanates, and carbodiimides.[48,49] The primary advantage of acyl azides over many coupling reagents is their ability to facilitate rapid amide formation in the presence of an amine group, while preserving the chiral integrity of the α-carbon atom. Racemisation, a common side reaction during peptide coupling, involves the inversion of the stereochemistry of the α-carbon due to the increased acidity of the α-hydrogen atom upon activation (**Figure 1.4**).[50] Despite their advantages, acyl azides are highly unstable, reactive, and explosive, which limits their widespread application as coupling reagents in peptide synthesis.[49]

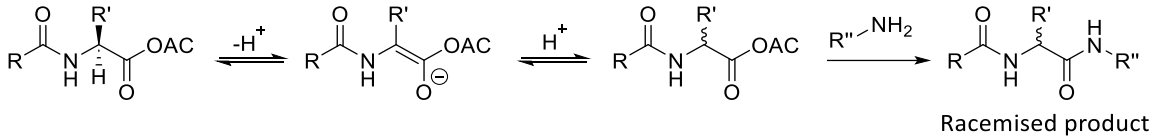

Figure 1.4. Base-catalysed racemisation of the α-carbon during activation of the free carboxylic acid.

Carbodiimides were amongst the first modern reagents employed for amide coupling, specifically tailored for peptide synthesis. Nucleophilic attack of the carboxylic acid to the carbodiimide moiety generates the reactive *O*-acylisourea intermediate which rapidly undergoes aminolysis in presence of the amine component, yielding the final amide bond. In 1955, Sheenan and Hess reported the use of *N,N'*-dicyclohexylcarbodiimide (**5**, DCC, **Figure 1.5.A**) for the efficient synthesis of tripeptides.[51] However, DCC produces *N,N'*-dicyclohexylurea (DCU) as a byproduct, which is highly insoluble and complicates the amide purification step. To mitigate this issue, a new generation of carbodiimides was developed, including *N,N'*-diisopropylcarbodiimide (**6**, DIC, **Figure 1.5.A**) and 1-ethyl-3-(3-dimethylaminopropyl) carbodiimide hydrochloride (**7**, EDC·HCl, **Figure 1.5.A**), that produce less problematic urea by-products.[52] For example, the urea byproduct produced by EDC·HCl can be removed through slightly acidic aqueous washings, significantly simplifying the purification step.[53] Despite their advantages, carbodiimides as coupling reagents have a

major drawback: the formation of racemised amide products. This racemisation occurs because the *O*-acylisourea activated ester increases the acidity of the α-hydrogen atom upon activation. To address this issue, uronium/iminium and phosphonium derived coupling reagents were developed as milder activating agents that suppress racemisation.[54] Both types share a common benzotriazole structural motif that forms an *O*-benzotriazole (OBt) activated ester. The aromatic structure of OBt is believed to shield the α-hydrogen atom more effectively, thereby reducing racemisation. Hexafluorophosphate azabenzotriazole tetramethyl uronium (**8**, HATU, **Figure 1.5.B**), hexafluorophosphate benzotriazole tetramethyl uronium (**9**, HBTU, **Figure 1.5.B**), and benzotriazol-1-yl-oxytripyrrolidinophosphonium hexafluorophosphate (**10**, PyBOP, **Figure 1.5.C**) have been widely used as very safe, cost-effective, and potent activators in peptide synthesis.[54]

Despite recent advancements in the development of potent coupling reagents for amide bond formation, peptide synthesis in solution faces significant limitations. This process necessitates multiple coupling and protection/deprotection steps to maintain selectivity, and chromatographic purification is typically required after each step. Solution phase peptide synthesis is generally feasible for short peptides, typically up to 5-6 amino acids in length, due to the limited solubility of the growing protected peptide in organic solvents. This insolubility often results in inefficient couplings and deprotections when attempting to further elongate the peptide sequence. These significant limitations were addressed with the advent of the revolutionary Solid Phase Peptide Synthesis (SPPS) approach for peptide synthesis.

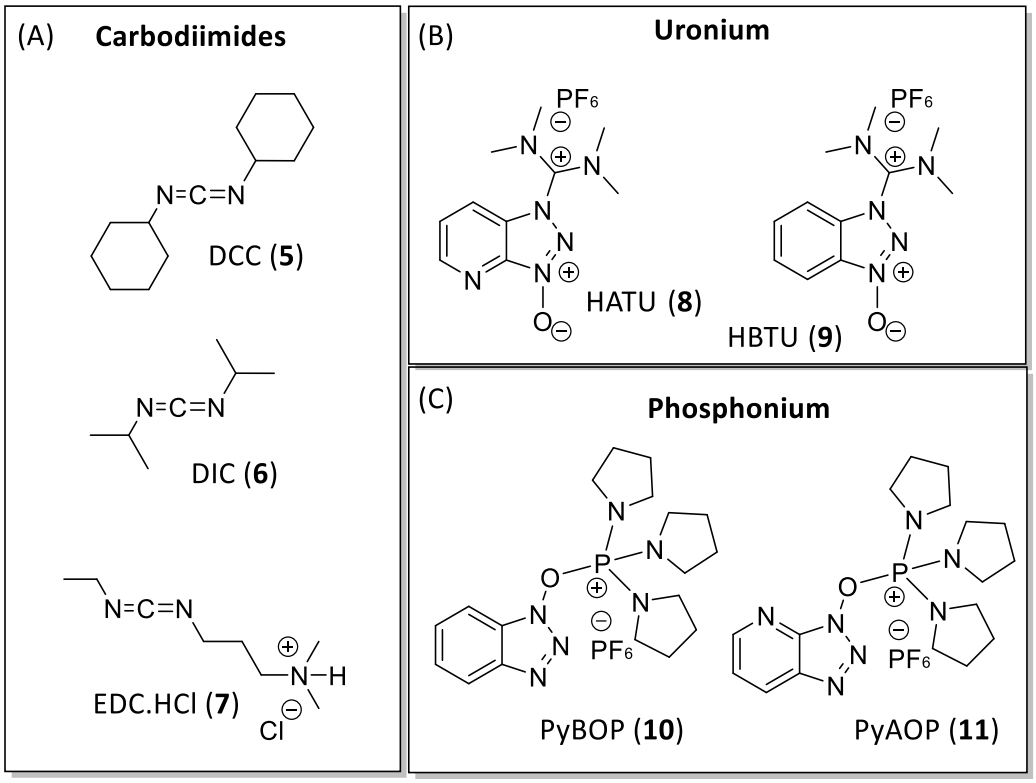

Figure 1.5. Chemical structures of the (A) carbodiimide-based coupling reagents DCC (**5**), DIC (**6**), and EDC.HCl (**7**), (B) uronium-based coupling reagents HATU (**8**) and HBTU (**9**), (C) phosphonium-based coupling reagents PyBOP (**10**) and PyAOP (**11**).

1.2.2 Solid Phase Peptide Synthesis (SPPS)

SPPS was first developed by Merrifield *et al*. in 1963, with the initial synthesis of the tetrapeptide NH_2-Leu-Ala-Gly-Val-OH.[55] The defining feature of SPPS is the covalent attachment of the *N*-protected amino acid to an insoluble polymeric resin. The carboxyl group of the initial amino acid is activated using a variety of amide specific coupling reagents in the presence of a base aiming for coupling on the resin. Following coupling of the first amino acid, the resin is thoroughly washed to remove excess reagents and byproducts.[56] The synthesis then proceeds through a series of cycles involving *N*-terminal deprotections and couplings of subsequent activated *N*-protected amino acids until the peptide sequence is fully assembled (**Scheme 1.1**). After each coupling and deprotection step, the resin is washed extensively to eliminate byproducts, thereby simplifying the final peptide purification process by obviating the need for intermediate purification steps typical of solution phase synthesis. Additionally, nucleophilic side chains of the amino acids are protected during SPPS to reduce potential side reactions throughout the synthesis. Upon completion of the peptide chain, global deprotection of

the side chains and cleavage of the peptide from the resin under acidic conditions yield the final unprotected peptide.[56] The innovative nature of this methodology earned Bruce Merrifield the Nobel Prize in Chemistry in 1984.[57] Since then, SPPS has become the predominant method for synthesising peptides, including chemically modified variants such as phosphopeptides,[58] glycopeptides,[59] lipopeptides,[60] peptidomimetics,[61] and larger polypeptides *via* fragment-based approaches.[62]

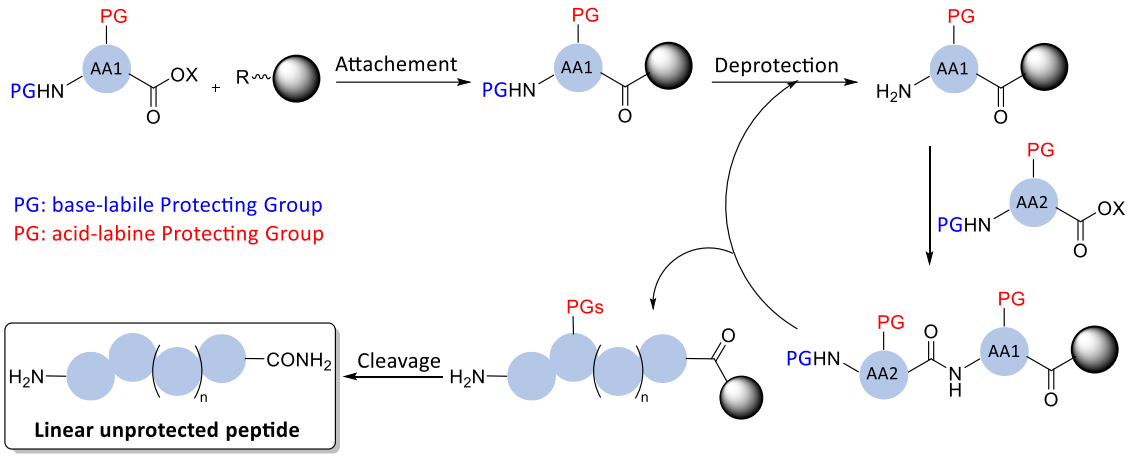

Scheme 1.1. Workflow of SPPS (PG= Protective Groups X= activating group).

1.2.2 Protecting Group Strategies in SPPS

Two principal strategies for SPPS have been established, leveraging the orthogonality between *N*-terminal and side chain protecting groups (PGs). These include the base-labile 9-fluorenylmethoxycarbonyl (Fmoc)/*tert*-butyl (*t*Bu) strategy and the acid-labile *tert*-butyloxycarbonyl (Boc)/benzyl (Bzl) strategy. Both methods allow the selective removal of *N*-terminal PGs (Fmoc or Boc) while preserving side-chain PGs, thus facilitating repeated cycles of amino acid coupling and *N*-terminal deprotection without the generation of side products.

The Boc/Bzl strategy was introduced by Merrifield and coworkers in 1967 and it was predominantly used from the 1960s through the 1980s.[63] This approach requires the use of strong acids, such as hydrogen fluoride (HF), for peptide cleavage from the resin.[64] The Boc *N*-terminal PG is sensitive to milder acids like trifluoroacetic acid (TFA), while Bzl-based side chain PGs remain stable under TFA but are cleaved in presence of HF.[63,64] This differential stability allows selective Boc deprotection in the presence of Bzl

side-chain PGs. Despite its initial prominence and successful application for the chemical synthesis of biologically relevant proteins and enzymes-including interleukin-3,[65] ribonuclease A,[66] and HIV-1 aspartyl protease,[67] Boc/Bzl SPPS poses several challenges. The use of highly toxic HF requires careful handling and specialist training, and the repeated Boc deprotection cycles can inadvertently remove some Bzl PGs, resulting in byproducts.[68,69] The strongly acidic conditions required are also incompatible with acid-sensitive peptides such as glycopeptides and phosphopeptides.[69]

The Fmoc/*t*Bu strategy, developed by Carpino and coworkers in 1972, operates under mild basic conditions for *N*-terminal deprotection, applicable to both primary and secondary amines (**Scheme 1.2.B**).[70] Fmoc deprotection is usually achieved using 20% piperidine in DMF and the characteristic λ_{max} of the dibenzofulvene-piperidine side product liberated from the reaction can be used to monitor the success of deprotection steps. This strategy offers superior orthogonality compared to Boc/Bzl, as Fmoc deprotection occurs under basic conditions while side chain deprotection and peptide cleavage are performed under acidic conditions.[71] The Fmoc/*t*Bu approach is generally preferred due to its milder cleavage conditions and by 1998, only 2% of peptide synthesis laboratories employed Boc/Bzl methods regularly.[72] The popularity of Fmoc SPPS has led to the widespread use of cheap commercially available Fmoc-protected amino acids bearing acid labile side chain protecting groups such as trityl (Trt), *t*Bu, and Boc groups, which can be typically removed with 90% TFA in water.

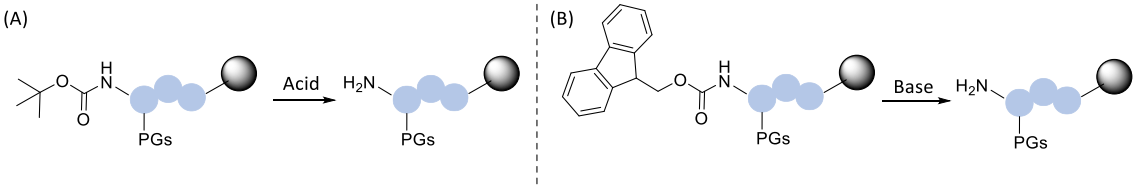

Scheme 1.2. (A) Acid-catalysed *tert*-butyloxycarbonyl (Boc) deprotection. (B) Base-catalysed 9-fluorenylmethoxycarbonyl (Fmoc) deprotection.

1.2.3 Limitations of SPPS

Although SPPS is a well-established technique for routine peptide synthesis, it encounters limitations when dealing with peptides >50 amino acids. The elongation of peptide chains during SPPS can induce aggregation due to non-covalent interactions

among adjacent hydrophobic residues.[73] This aggregation substantially reduces amide coupling efficiency, resulting in poor chromatographic separation and low yields. Additionally, the high solvent volumes, excess reagents, and multi-step linear nature of SPPS contribute to its high cost, making it less attractive for use outside of specialised chemical laboratories. In contrast, recombinant protein expression technologies offer a solution to these challenges by enabling the rapid and cost-effective production of large protein substrates.[74] However, these technologies come with significant drawbacks, including the absence of post-translational modifications (PTMs) such as phosphorylation, glycosylation, and lipidation, which are critical for the functional properties of many proteins.[75] Furthermore, the separation and purification of expressed proteins is often complex and difficult. The incorporation of chemical entities, such as fluorescent tags, and UAAs into recombinant proteins is also frequently limited, requiring advanced genome engineering techniques. Given the constraints of both SPPS and recombinant protein expression methodologies, there is a clear need for innovative approaches in chemical protein synthesis.[75] One promising strategy involves the assembly of large biomolecules through the conjugation of smaller, unprotected peptide fragments.

1.3 Chemical Protein Synthesis

1.3.1 Native Chemical Ligation

Native chemical ligation (NCL) is a chemoselective process that involves the condensation of two unprotected peptide fragments under mild reaction conditions, efficiently generating a native amide bond in high yield.[76] Initially reported by Kent and coworkers in 1994,[77] NCL involves the reaction between a peptide bearing a *C*-terminal thioester and another peptide bearing an *N*-terminal Cys residue. The mechanism proceeds through an initial, reversible *trans*-thioesterification step between the Cys side chain and the *C*-terminal acyl donor, forming a transient thioester linkage between the two peptide segments. This unstable intermediate then undergoes a rapid, irreversible intramolecular *S*-to-*N* acyl transfer, resulting in the formation of a native peptide bond at the ligation site.[76,78] A critical feature of NCL is its operation at neutral pH with excellent chemoselectivity, allowing the use of unprotected linear peptide fragments.

The inclusion of a chaotropic agent, such as guanidinium chloride (Gdn·HCl), is essential to enhance solubility and prevent the formation of secondary structures.[79] The first total synthesis of a protein *via* NCL was achieved by Kent and coworkers in 1994, culminating in the synthesis of the cytokine protein IL-8 (**Scheme 1.3**).[77] This pioneering work combined SPPS with NCL and revolutionised the field of chemical protein synthesis. Since these initial efforts, NCL has been employed for the synthesis of a wide variety of biologically significant protein targets, including the *D*-Dpo4 enzyme,[80] erythropoietin (EPO),[81] human immunodeficiency virus-1 protease (HIV-1 PR),[82] and P2 deoxyribonucleic acid (DNA) polymerase IV.[83]

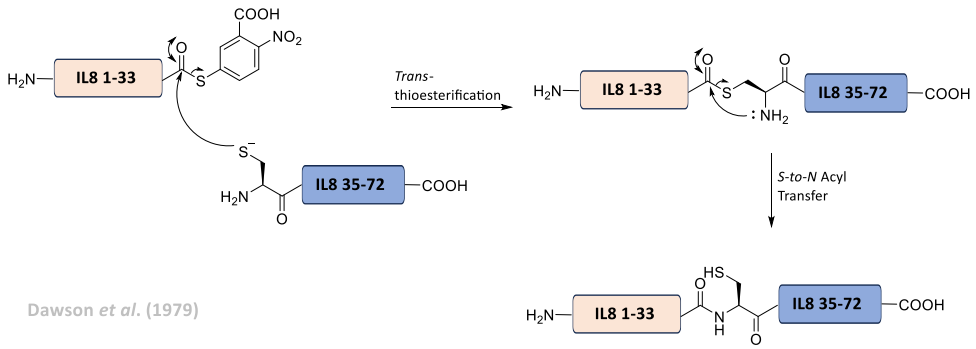

Scheme 1.3. First example of native chemical ligation for the synthesis of interleukin 8 (IL-8).[73]

1.3.2 Synthesis of Peptide Thioesters

The rate of NCL is significantly influenced by the steric and electronic properties of the *C*-terminal thioester. Acyl donors with sterically unhindered residues, such as glycine (Gly, G), alanine (Ala, A), and phenylalanine (Phe, F), facilitate rapid ligation rates. Conversely, sterically hindered residues on the thioester component, including isoleucine (Ile,I), valine (Val, V), threonine (Thr, T), and proline (Pro, P), can decrease the ligation rate by up to 20-fold, necessitating extended reaction times of up to 48 hours.[79] The trans-thioesterification step of NCL is accelerated with the use of exogenous thiol catalysts (aryl- or alkyl-thiols), which generate reactive thioester intermediates *in situ*.[84] Aryl thiols, such as 4-mercaptophenylacetic acid (MPAA) and thiophenol, are preferred due to their lower pK_a values, making them excellent leaving groups and thus more effective in forming reactive thioesters.[85] The development of novel synthetic methods for accessing *C*-terminal acyl donors is a dynamic research area within NCL methodologies. Various strategies have been devised to generate peptide thioesters using both Fmoc/*t*Bu and Boc/Bzl SPPS chemistries.[86] Peptide thioesters are typically

generated *in situ* from more stable precursors due to their inherent instability under the basic conditions of SPPS and the challenges associated with their purification.

Dawson and coworkers pioneered a thioester forming strategy using *N*-acyl-benzimidazolinone (Nbz) peptides.[87] This approach involves covalent attachment of a 3,4-diaminobenzoic acid (**12**, Dbz) linker to the SPPS resin, followed by peptide elongation *via* standard Fmoc/*t*Bu chemistry (**Scheme 1.4.A**). Treatment of the resin-bound peptide with p-nitrophenylchloroformate (**13**) and base induces rapid cyclisation of the Dbz moiety to form *N*-acylurea.[87,88] Acidic cleavage from the resin furnishes the stable unprotected Nbz peptide, which can be purified *via* reverse-phase high-performance liquid chromatography (RP-HPLC). The addition of a suitable thiol additive, such as MPAA, generates the corresponding thioester *in situ* prior to ligation. In 2011, Liu and coworkers developed a novel method for *in situ* thioester generation using peptide acyl hydrazides.[89] Resin functionalisation with hydrazine hydrate permits conventional Fmoc/*t*Bu SPPS chemistry and upon cleavage yields the peptide hydrazide stable to RP-HPLC purification (**Scheme 1.4.B**). Oxidation of the peptide hydrazide with $NaNO_2$ furnishes the intermediate peptide azide, susceptible to substitution by MPAA to form the active peptide thioester suitable for ligation *in situ* (**Scheme 1.4.B**). More recently, Melnyk and coworkers described an innovative approach utilising bis(2-sulfanylethyl)amido (SEA) groups.[90] Reduction the peptide with tris(2-carboxyethyl)phosphine (TCEP) generates the reactive thioester moiety *via* intramolecular *N*-to-*S* acyl transfer (**Scheme 1.4.C**).

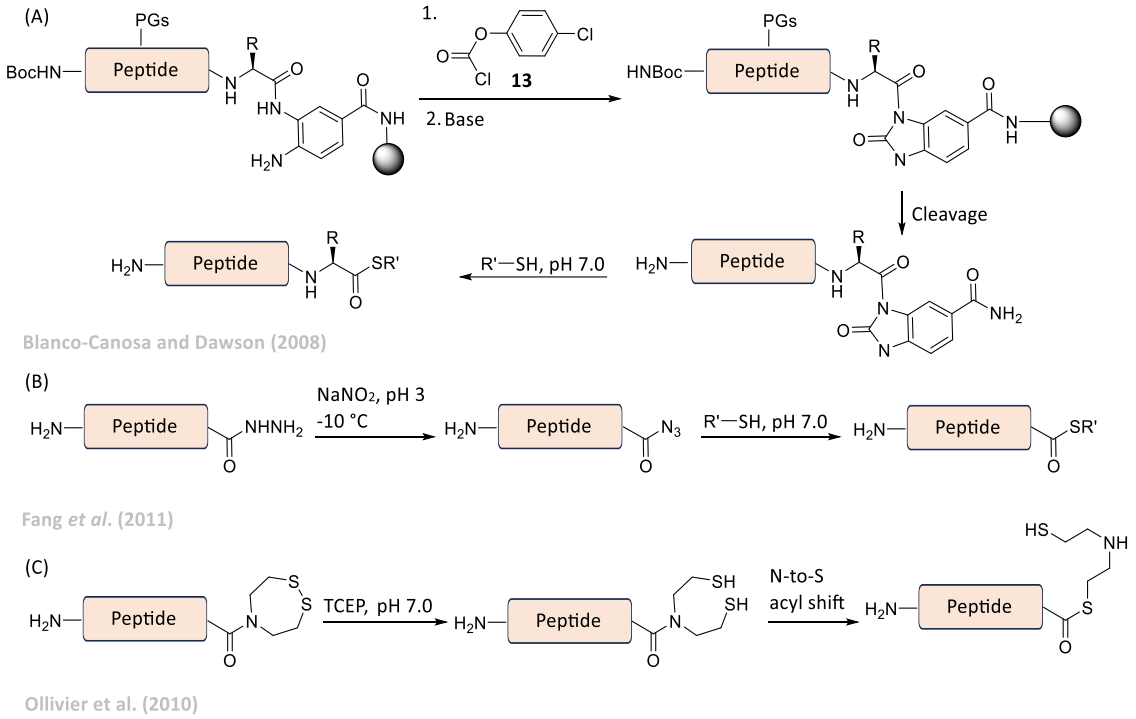

Scheme 1.4. (A) Synthesis of peptide thioesters using the Dbz linker. (B) Synthesis of peptide thioesters *via* activation of peptide acyl hydrazides. (C) SEA$^{on/off}$ ligation thioester generation.

1.3.3 Non-Cysteine Native Chemical Ligation

Despite the significant advantages of NCL, its requirement for a Cys residue at the ligation site poses a limitation due to the low natural abundance of Cys (~ 1.7%) in proteins, thus restricting the applicability of classical NCL in chemical protein synthesis.[88] Auxiliary mediated ligation (AML) was developed in the early 2000s, enabling ligation at non-Cys residues. This methodology employs *N*-terminal thiolated auxiliaries capable of generating reactive peptide thioesters and facilitating reliable *S*-to-*N* acyl transfer.[88] Following ligation, the auxiliary is cleaved to yield the native peptide target. In 2001, Kent and coworkers achieved the chemical synthesis of cytochrome b562 using 1-phenyl-2-mercaptoethyl (**14**) as a removable thiol-containing auxiliary group.[91] Following *trans*-thioesterification and *S*-to-*N* acyl shift, the auxiliary group was removed quantitatively under acidic conditions (**Scheme 1.5**). Although AML methodologies have expanded the scope of NCL, they present distinct disadvantages compared to conventional NCL. The increased steric bulk at the ligation site can impede *S*-to-*N* acyl transfer, resulting in significantly slower reaction rates.[91] Extended reaction

times can lead to the formation of hydrolysis and epimerization byproducts, which, along with the often-challenging auxiliary removal step, reduce the overall yield of the desired peptide.

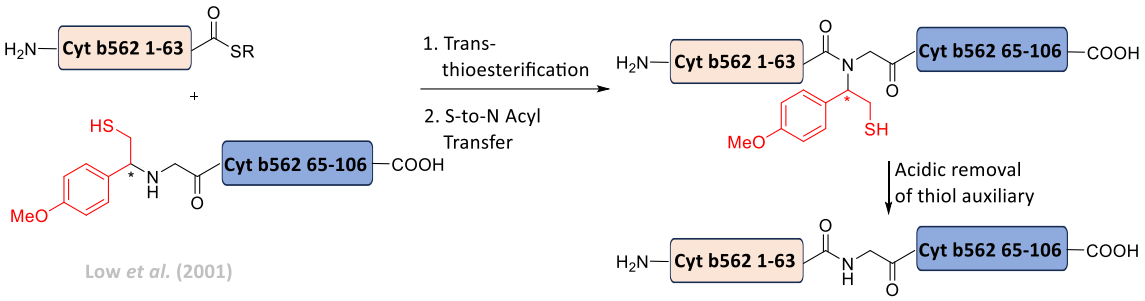

Scheme 1.5. Chemical synthesis of cytochrome b562 using the acid labile 1-phenyl-2-mercaptoethyl (**14**) auxiliary.

A key advancement in expanding the scope of traditional NCL is the combination of sequential NCL with desulfurisation chemistries. In 2001, Dawson and coworkers introduced the post-ligation desulfurisation concept, where a native Ala residue at the ligation site is replaced with a Cys residue.[92] Following NCL, the sulfhydryl group of Cys is removed by treating the peptide with either Raney Ni or Pd/Al_2O_3, yielding the native Ala junction. This method leverages the higher natural abundance of Ala (~8.9%), thereby increasing the number of possible ligation sites.[93] The metal-based desulfurisation strategy has been employed for the chemical synthesis of several Cys-free protein targets. However, the high excess of metal catalysts required can result in undesired side reactions, including tryptophan (Trp, W) hydrogenation and methionine (Met, M) demethylthiolation.[93] Additionally, the separation of metal catalysts from the ligated peptide product using conventional RP-HPLC purification is challenging.[93]

In 2007, Danishefsky and coworkers developed a novel metal-free desulfurization strategy under mild aqueous conditions, employing the water-soluble radical initiator 2,2'-azobis[2-(2-imidazolin-2-yl) propane] dihydrochloride (VA-044, **15**) in the presence of TCEP and a thiol additive such as *tert*-butyl thiol (*t*BuSH).[94] This radical-mediated process initiates with the thermal decomposition of VA-044 to generate a carbon-centered radical, which abstracts a hydrogen from the sulfhydryl group to form a thiyl radical (**Scheme 1.6**). The thiyl radical reacts with TCEP to create a

phosphine radical intermediate, which undergoes C-S bond scission to form an alanyl radical. The alanyl radical abstracts a hydrogen atom from the exogenous thiol, restarting the cycle and yielding the native ligation product (**Scheme 1.6**).[95] These conditions are compatible with a wide range of reactive functional groups.

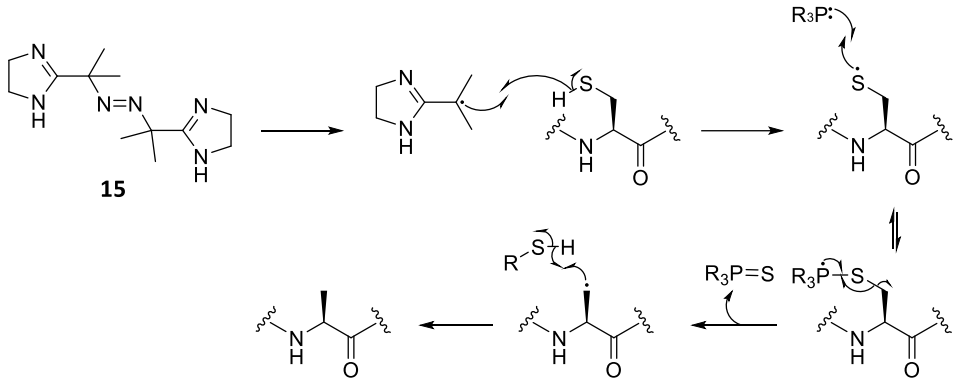

Scheme 1.6. Proposed mechanism for the radical-mediated desulfurisation of Cys to Ala using VA-044.

The advancement of metal-free desulfurisation significantly enhanced the ability of chemical protein synthesis to produce valuable polypeptide products. Desulfurisation sparked considerable interest in creating synthetic thiolated amino acids that can be incorporated at the *N*-terminus of peptide fragments. These fragments, after undergoing *trans*-thioesterification, *S*-to-*N* acyl transfer, and desulfurisation, furnish native peptides at various ligation sites.[93] Several methods have been developed for the total synthesis of β-thiol, γ-thiol, and δ-thiol derivatives of amino acids. In 2007, β-thiol Phe was the first thiol-derived amino acid used in NCL, and subsequent desulfurisation produced a native Phe at the ligation site.[96] To date, 15 synthetic thiolated AAs have been developed and utilised in ligation chemistry, significantly increasing the potential ligation junctions within protein targets.[93] Ligation-desulfurisation chemistry has been applied to synthesise a variety of biological targets, including human parathyroid hormone (hPTHrP),[97] ATAD bromodomain,[98] human erythropoietin (EPO),[99] and human α-synuclein.[100] However, the lack of commercial availability and the complex synthesis processes of these thiolated derivatives have limited their widespread use.

1.4 The Thiol-ene Reaction

The Thiol-ene Click (TEC) was first reported in 1905 by Posner and since then has become a versatile and powerful synthetic tool.[101] This reaction involves the anti-Markovnikov hydrothiolation of an olefin group, resulting in the formation of a saturated sulfide product. The radical mediated TEC is often initiated *via* a thermal or photomediated process.[102] In the case of photoinitiation, radical initiation occurs *via* the formation of radicals upon absorption of light by the photoinitiator, which in turn abstracts a hydrogen from a thiol residue to generate the reactive thiyl radical. Two widely used initiators for the radical TEC reaction are 2,2-azobis(isobutryonitrile) (AIBN, **16**) and 2,2-dimethoxy-2-phenylacetophenone (DPAP, **17**).[103] Upon absorption of UV light (365 nm), DPAP undergoes homolytic fragmentation producing a carbon-centred radical which abstracts the thiol proton and forms the thiyl radical (**Figure 1.6.A**).[103] On the other hand, AIBN is a thermal initiator which, under high temperature (~ 90 °C), generates radicals similarly to VA-044 (**Figure 1.6.A**).

The TEC reaction may be described as a radical chain reaction which starts with the formation of the reactive thiyl radical *via* homolytic cleavage of the S-H group.[104] Next, the thiyl radical undergoes anti-Markovnikov addition to the alkene, forming a carbon-centred radical. This radical can then abstract a hydrogen atom from another thiol molecule, thereby propagating the reaction cycle and furnishing the thioether product (**Figure 1.6.B**) The relatively low bond dissociation energy of the S-H bond (~ 87 kcal/mol) compared to that of C-H bonds (~ 101 kcal/mol) facilitates the homolytic cleavage of the sulfhydryl S-H bond by a carbon-centred radical initiator.[105] The radical-mediated thiol-ene reaction is often classified as a 'click' reaction due to the high yield and atom economy, compatibility with a wide range of functional groups and aqueous conditions, and mild reaction conditions.[103] As a result, the TEC reaction has found extensive application across diverse fields, including polymer chemistry,[106] surface chemistry,[107] carbohydrate chemistry,[108] peptide chemistry and chemical biology.[109,110]

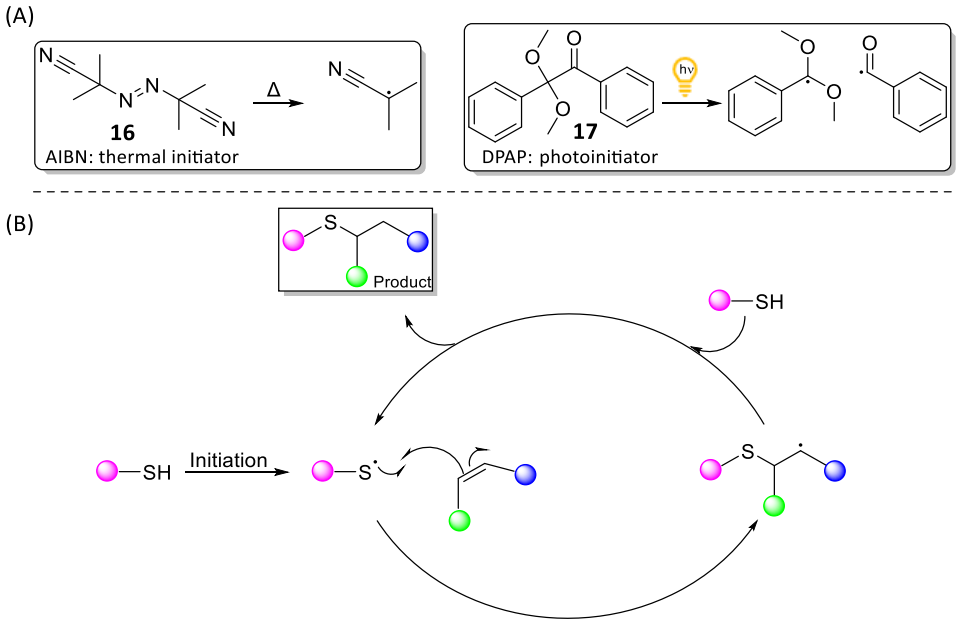

Figure 1.6. (A) Initiation reaction of AIBN (**16**) and DPAP (**17**). (B) Mechanism of the radical TEC reaction.

1.4.1 The TEC Reaction in Biomolecular Synthesis

The thiol-ene reaction is a powerful metal-free click reaction which is extensively used in biomolecular synthesis and modification. TEC has proven particularly valuable in the synthesis of glycosylated peptides and proteins, often employing thiolated or unsaturated carbohydrates under radical-mediated conditions. Protein glycosylation is a post-translational modification found in more than 50% of proteins in human cells and plays a crucial role in protein folding, stability, and activity.[111,112] Dodoni *et al.* used the radical TEC reaction to access *S*-linked glycoproteins by using alkene-containing monosaccharides.[113] Initial optimisation was conducted using DPAP as a photoinitiator in DMF, with an excess of the Fmoc-protected Cys **18** derivative and the monosaccharide **19** bearing a terminal alkene at the anomeric position (**Scheme 1.7.A**). Following chromatographic purification, the ligated product **20** was isolated in a 92% yield. Subsequently, the reaction was performed using a nonapeptide bearing a Cys residue and the monosaccharide **19** with DPAP as a photoinitiator in DMSO/Phosphate buffer (pH 7.4). The *S*-ligated product was quantitatively formed as confirmed by liquid chromatography-mass spectrometry (LC-MS). These optimised conditions were later applied for the *S*-glycosylation of the globular bovine serum albumin (BSA) which has a Cys residue at position 35 and a disulfide bridge between positions 75 and 91. Upon

irradiation for 5 minutes, site-specific glycosylation of all three Cys residues with the monosaccharide **19** was achieved.[113] In 2009, Floyd *et al.* introduced a "tag-modify" approach for site-specific glycosylation using the TEC reaction.[114] This work describes the radical-mediated conjugation of glycosyl thiols to proteins bearing L-homoallylglycine (Hag) as a "tag" in place of Met in the primary structure. Initial optimisation of the reaction was performed using VA-044 as a photoinitiator and the glycosyl thiol **21** with the Boc-protected L-homoallylglycine **22**. The progress of the reaction was evaluated across a pH range of 4 to 7, furnishing the glycoconjugate product **23** in high conversions. Next, they recombinantly expressed in *Escherichia coli* bacteria the model protein *Ss*βG where the Hag tag was introduced at a single Met site. The TEC reaction of SsβG-Hag with the unprotected thiosugar **24** in acetate buffer resulted in the formation of glycosylated SsβG-Hag with greater than 95% conversion at pH < 7 (**Scheme 1.7.B**).[114]

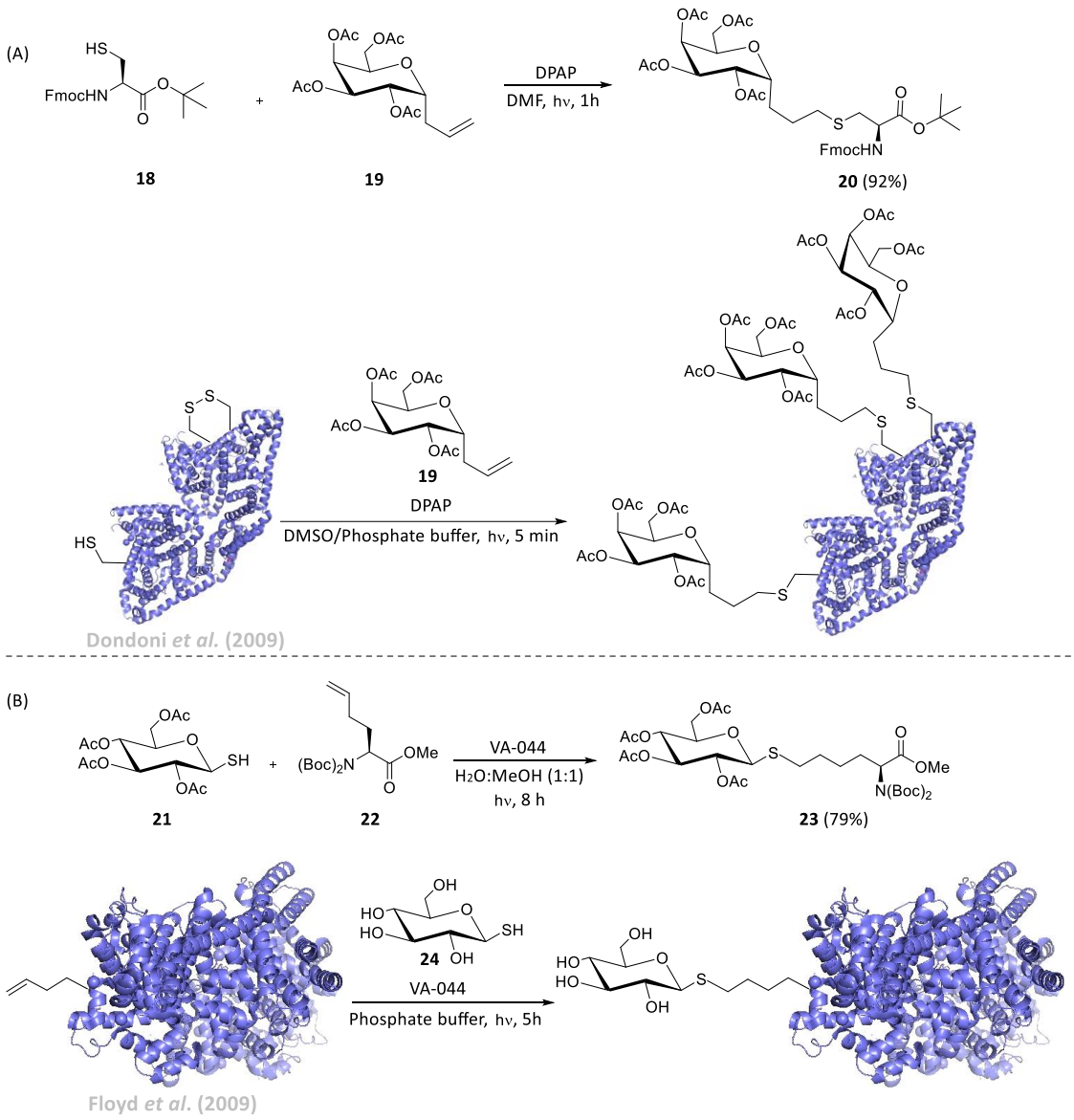

Scheme 1.7. (A) Work of Dondoni *et al*. including the optimisation of the TEC reaction between the protected Cys **18** the unsaturated sugar **19** and, and glycosylation of the Cys residues at positions 34, 75 and 91 of BSA.[113] (B) Work of Floyd *et al*. including the optimisation of the TEC reaction between the thiolated sugar **21** and the alkenyl amino acid **22**, and the site-specific glycosylation of the model protein *Ss*βG with **24**.[114]

Protein and peptide lipidation, akin to glycosylation, has garnered significant attention in drug discovery, particularly for its potential to enhance therapeutic efficacy. Naturally occurring lipopeptides have shown promise as potent antimicrobial agents as well as other therapeutic applications.[115] The incorporation of lipid moieties onto the peptide backbone has been demonstrated to improve pharmacokinetic properties, including enhanced enzymatic stability, bioavailability, and cellular permeability.[116,117] The TEC reaction has been widely utilised in both the synthesis of lipidated amino acids

for use in SPPS and the direct lipidation of peptide sequences.[103] In 2008, Triola *et al.* reported the use of TEC to generate lipidated Cys derivatives with minimal racemisation, suitable for SPPS.[118] Building on this, Brimble and coworkers introduced the Cysteine Lipidation on Peptide or Amino Acid (CLipPA) methodology in 2013, enabling the direct lipidation of unprotected peptides bearing a Cys residue.[119] This novel approach allowed the synthesis of the *N*-lipidated antigenic peptide **27** which can stimulate $CD8^+$ cytotoxic T-cells. The peptide **25** bearing a Cys residue at the *N*-terminus of the sequence was accessed *via* conventional Fmoc/*t*Bu SPPS strategy. Global cleavage and lipidation of the linear unprotected peptide **25** followed using the vinyl palmitate **26**, DPAP as a photoinitiator and dithiothreitol (DTT) to prevent the possible formation of disulfides (**Scheme 1.8.A**). RP-HPLC and Electrospray Ionisation Mass Spectrometry (ESI-MS) analysis indicated successful conversion to the final palmitoylated product **27**.[119] Since then, CLipPA has emerged as a powerful synthetic approach for the development of biologically interesting lipopeptides, including Battacin analogues with varying lipid chains,[120] analogues of Connexin 43 channel inhibitory Peptide5,[121] and *S*-lipidated teixobactin analogues.[122] Notably, the Brimble group demonstrated the effective combination of NCL and the TEC reaction to access a library of synthetic cyclic lipopeptide analogues of iturin A (**Scheme 1.8.B**).[123] The linear unprotected peptide **28**, containing a *C*-terminal thioester and an *N*-terminal Cys, was built *via* a traditional Boc-SPPS strategy. The peptide **28** was cyclised under NCL conditions in phosphate buffer pH 7.5 and using TCEP as a reducing agent. Following cyclisation, the sulfhydryl group of the cyclic peptide **29** was employed as a chemical handle for lipidation *via* CLipPA by using a wide range of vinyl esters including lipid chains of different sizes, branched chains, and phenyl groups. The conversions to the final cyclic lipopeptides were notably high, ranging from 80% to 86%.[123]

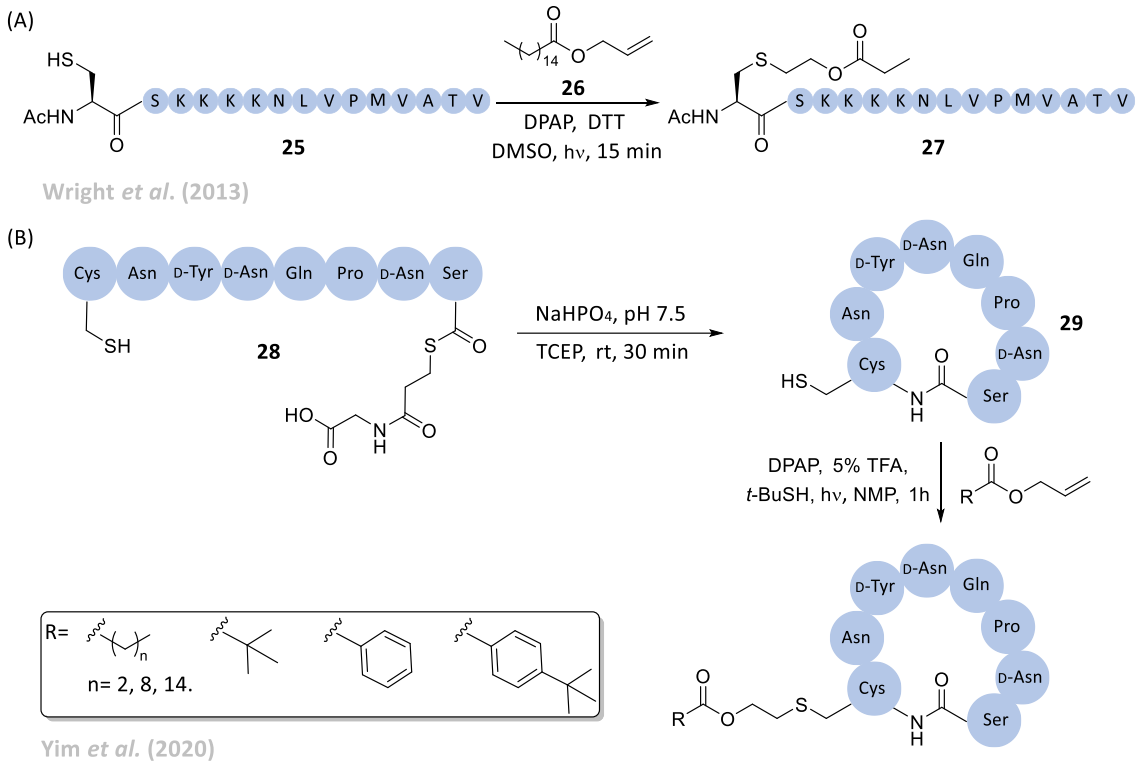

Scheme 1.8. (A) Palmitoylation of the peptide **25** *via* TEC reaction.[119] (B) Application of sequential NCL and ClipA to generate a library of iturin A analogues.[123]

1.4.2 The TEC Reaction in Peptide Macrocyclisation and Stapling

The radical TEC reaction offers an efficient synthetic tool for the development of "stapled" peptides which are conformationally constrained peptides, usually obtaining α-helix or β-sheet secondary structures, and are widely employed for the disruption of PPIs. The stable thioether linkage contributes to the stabilisation of active peptide conformations, thereby reducing the entropic cost of binding and enhancing the overall stability of peptide therapeutics. The TEC reaction has been widely employed as an effective method for peptide stapling in both one- and two-component systems, with successful applications reported in both solution-phase and solid-phase synthesis.[103] A key advantage of on-resin peptide stapling is the facile removal of excess reagents and byproducts through extensive washing of the resin.[124] However, it has been observed that on-resin peptide stapling *via* radical TEC may result in reduced yields of the final stapled product, potentially due to the restricted diffusion of radical species within the polymeric matrix.

In one-component systems, peptide cyclisation occurs between a Cys residue and an alkene-containing unnatural amino acid, located within the peptide sequence, without the introduction of additional external linkers.[103] A primary challenge associated with one-component stapling systems is the potential formation of dimers, which is typically mitigated by employing highly dilute conditions. Hoppmann *et al*. developed a photoswitchable click amino acid (PSCaa) that features an azobenzene moiety and a terminal alkene handle.[125] This amino acid can be incorporated into peptide sequences using conventional SPPS techniques. In this work, PSCaa was incorporated to the helical peptide motif **31** bearing a Cys residue at position 9. The unprotected linear peptide **30** underwent TEC-mediated cyclisation using VA-044 as a photoinitiator, with a *trans*-to-*cis* isomerisation of the azo group (**Scheme 1.9.A**), and RP-HPLC and ESI-MS analysis indicated full consumption of the starting material **30**.[125] Similarly, Levalley *et al.* successfully demonstrated the combination of the TEC-mediated peptide cyclisation with the azide-alkyne cycloaddition for further peptide functionalisation.[126] Their study focused on the cyclisation of a linear peptide containing the arginine-glycine-aspartic acid (RGD) motif and a reactive azide group at the *C*-terminus. The cyclisation occurred between a Cys residue at the *N*-terminus and an allyloxycarbonyl (alloc)- protected lys residue using lithium phenyl (2,4,6-trimethylbenzoyl) phosphinate (LAP) as a free radical initiator. Upon irradiation for 10 minutes, the cyclic thioether peptide product was obtained in 70% yield and the free azide group was used as a synthetic handle for hydrogel conjugation *via* CuAAC.[126] Recently, Scanlan and coworkers investigated the application of the TEC reaction to develop stable thioether-bridged neuropeptides as disulfide mimetics (**Scheme 1.9.B**).[127] This work primarily focused on the neuropeptide oxytocin which is a nonapeptide containing a disulfide bridge between positions 1 and 6, rendering the peptide susceptible to reduction *in vivo*. To address this issue, the authors substituted the Cys residue at position 6 with allyl-glycine (Agl), which is stable under standard SPPS conditions. Intramolecular TEC of the pure linear unprotected peptide **32** was achieved upon irradiation for 1 h using the DPAP photoinitiator, yielding the thioether cyclic analogue **33** with >90% conversion based on ^{1}H-NMR and RP-HPLC analysis. Remarkably, the cyclic peptide **33** was obtained in high purity following extraction, eliminating the need for additional purification steps.[127]

In 2010, Aimetti *et al.* reported the first on-resin peptide cyclisation *via* the TEC coupling reaction.[128] The researchers synthesised a linear RGD peptide displaying an alloc-protected lysine at the *C*-terminus and a monomethoxytrityl (Mmt)-protected Cys at the *N*-terminus of the sequence. Selective removal of the Mmt protecting group was achieved upon treating the resin-bound peptide with 2% TFA in dichloromethane (CH_2Cl_2), thereby exposing the free sulfhydryl group. On-resin cyclisation was performed by irradiating the resin-bound peptide with UV light for 15 minutes in the presence of the VA-044 photoinitiator (**Scheme 1.9.C**)[128] This approach significantly streamlined the synthetic process by eliminating multiple purification steps typically required in solution-phase cyclisation reactions. Building upon this methodology, Zhao *et al*. conducted on-resin intramolecular TEC using alkyl chains with terminal alkenes ranging from four to six carbons in length within the peptide sequence.[129] Notably, they demonstrated the compatibility of this cyclisation strategy with longer peptide sequences, successfully synthesising a bioactive peptide consisting of 11 residues.[129]

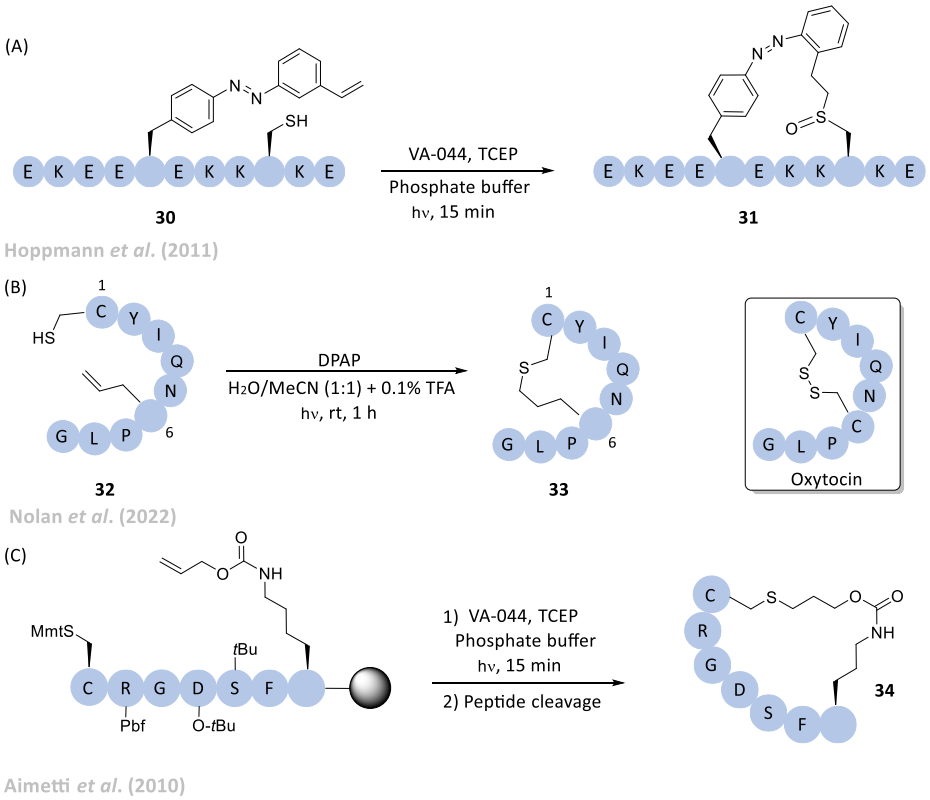

Scheme 1.9. (A) One-component stapling of peptide **30** using a photoswichable linker.[125] (B) Intramolecular TEC for the synthesis of the thioether-linked oxytocin analogue **33**.[127] (C) On-resin peptide cyclisation *via* TEC reaction yielding the cyclic RGD peptide **34**.[128]

In two-component systems, peptide stapling involves the use of a bifunctional external linker, resulting in a two-step cyclisation. This method typically involves the reaction between two native Cys residues within the peptide sequence and an external diene linker under radical-mediated conditions.[103] The first step is the intermolecular TEC reaction of the linker and the peptide to yield a linear thioether coupled precursor, followed by a second intramolecular TEC to furnish the final cyclic peptide.[103] The TEC-mediated two-component stapling technique allows for the incorporation of various dienes, enabling the development of a diverse library of dithioether-based stapled peptides for subsequent biological screening. However, a significant challenge associated with this approach is the potential formation of byproducts due to the double addition of dienes onto the same peptide. This issue can be mitigated by employing high dilution conditions and by strategically positioning the unreacted alkene moiety of the synthetic brace in proximity to the second Cys residue.

The first instance of two-component peptide stapling using the TEC reaction was reported by Wang and Chou.[130] This reaction was optimised using the unprotected linear octapeptide **35** containing two Cys residues within its sequence, along with a series of dienes, including both aliphatic and aromatic variants. Initial studies identified DPAP as the most effective photoinitiator, while the use of *N*-methyl-2-pyrrolidone (NMP) as the reaction solvent significantly enhanced yields. Under these optimised conditions, the stapled peptides were obtained in isolated yields ranging from 85% to 92%. Subsequent application of these conditions enabled the synthesis of an *i, i+7*-stapled p53 mimetic using 1,8-nonadiene **36** (**Scheme 1.10.A**). The resulting dithioether-stapled peptide exhibited robust α-helical structure and effectively disrupted the p53-MDM2 interaction.[130] The same research group extended the applicability of this methodology to aqueous environments, achieving successful macrocyclisation of peptides and recombinantly expressed proteins by employing water-soluble diallylurea staples and the VA-044 photoinitiator.[131] For example, TEC-mediated peptide stapling of **38** was achieved in aqueous conditions using the divinyl urea linker **39**, affording the product **40** in a 95% yield (**Scheme 1.10.B**).More recently, the Brimble group adapted the conditions from the CLipPA methodology to develop stapled peptides *via* TEC reaction.[132] This approach utilises exogenous divinyl esters as stapling agents of linear

peptides containing two Cys residues. The stapled peptides generated through this method were isolated in high yields and purity and demonstrated strong helical properties and effective disruption of PPIs.[132]

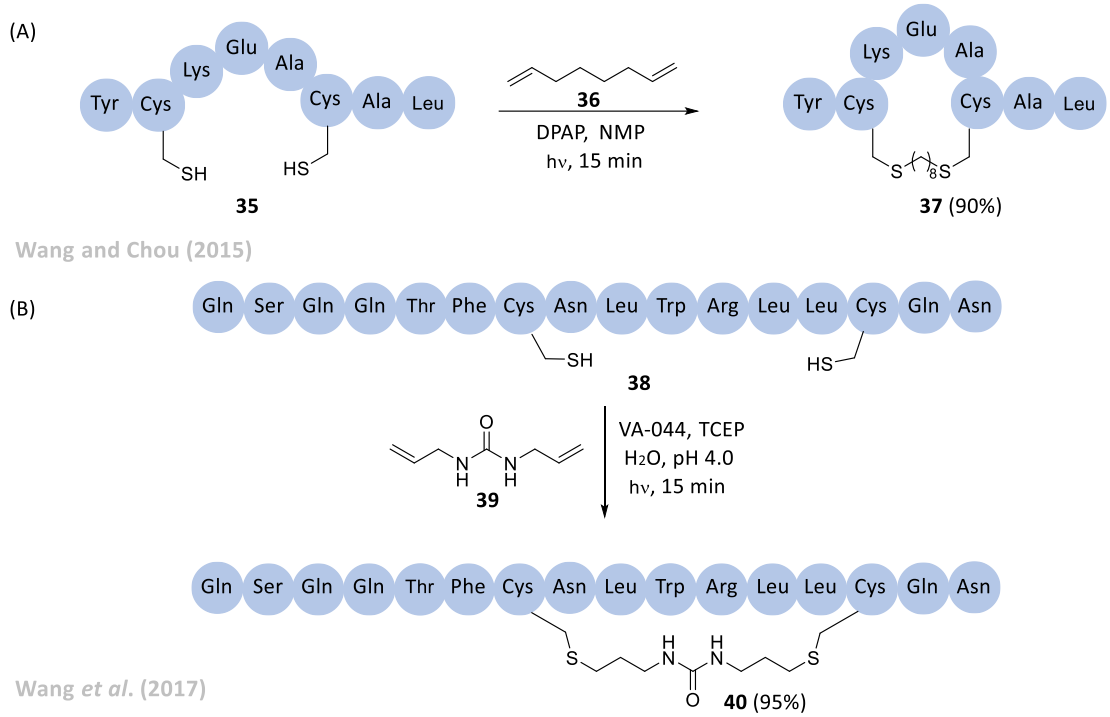

Scheme 1.10. (A) Two-component stapling of the peptide **35** using the diene linker **36** to furnish the stapled peptide **37**.[130] (B) TEC-mediated stapling of the peptide **38** in aqueous media with the use of the water-soluble divinyl urea linker **39** yielding the stapled peptide **40** quantitatively.[131]

1.4.3 The Acyl Thiol-ene Reaction

The acyl thiol-ene (ATE) reaction represents the acyl counterpart of the thiol-ene reaction, characterised by the radical-mediated addition of a thioacid group onto an alkene, furnishing a thioester product. ATE is understood to have a similar mechanistic pathway to the previously discussed thiol-ene reaction (**Figure 1.7**). The thioacid functional group exhibits greater acidity and nucleophilicity compared to the corresponding carboxylic group and possess a similar bond dissociation energy to alkyl thiols (~ 87 kcal/mol).[133] This enables the formation of radicals in the presence of a photo- or thermal initiator.

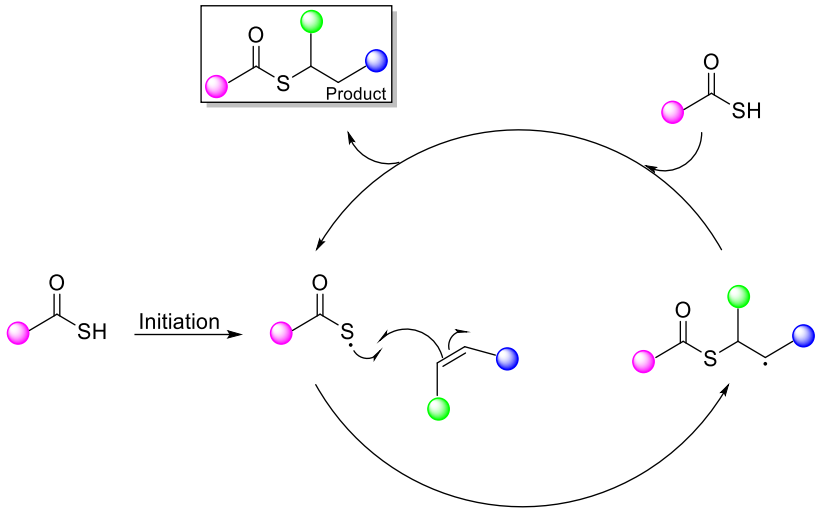

Figure 1.7. Mechanism of the radical ATE reaction.

The ATE reaction has been extensively reported in the literature as a robust method for direct thiolation *via* thioester hydrolysis under basic, acidic, or reductive conditions, furnishing the free thiol in quantitative yields (**Scheme 1.11.A**).[134,135] Following *S*-deacetylation, the free thiol has been extensively used as a versatile synthetic handle for surface functionalisation of gold nanoparticles (AuNPs) with different ligands including peptides and carbohydrates.[136,137] Inspired by this approach, the Scanlan group leveraged the free thiol to access δ-thiolactones, which are of significant interest in chemical biology, drug discovery, and materials science.[138] This approach involves a sequential process involving ATE coupling of a terminal alkene with thioacetic acid to generate an intermediate thioester, followed by *S*-deacetylation to produce a free thiol. This thiol residue subsequently forms a δ-thiolactone in the presence of a carboxylic acid group under Steglich conditions (**Scheme 1.11.B**). ATE coupling between the alkene **41** and thioacetic acid in presence of DPAP and 2-methoxyacetophenone (MAP) as a photosensitiser, yielded the thioester **42** in 94% yield following chromatographic purification. Subsequent *S*-deacetylation and ethyl ester hydrolysis were accomplished in a single step under basic conditions using sodium hydroxide, furnishing the free thiol **43** in a quantitative yield. Finally, thiolactonisation under standard Steglich conditions furnished the δ-thiolactone **44** in an isolated yield of 71%.[138]

Moreover, the same group demonstrated the efficient synthesis of thiolactones *via* a C-S bond disconnection strategy, employing a direct intramolecular

ATE reaction (**Scheme 1.11.C**).[139] Photolysis of the thioacid **45** in the presence of DPAP and MAP selectively produced the 5-exo-trig γ-thiolactone product **46** in 88% isolated yield, without any formation of the competing 6-endo-trig product. This methodology was further validated using various unsaturated carboxylic derivatives, with the ATE cyclisation proceeding in high yields and with complete regioselectivity.

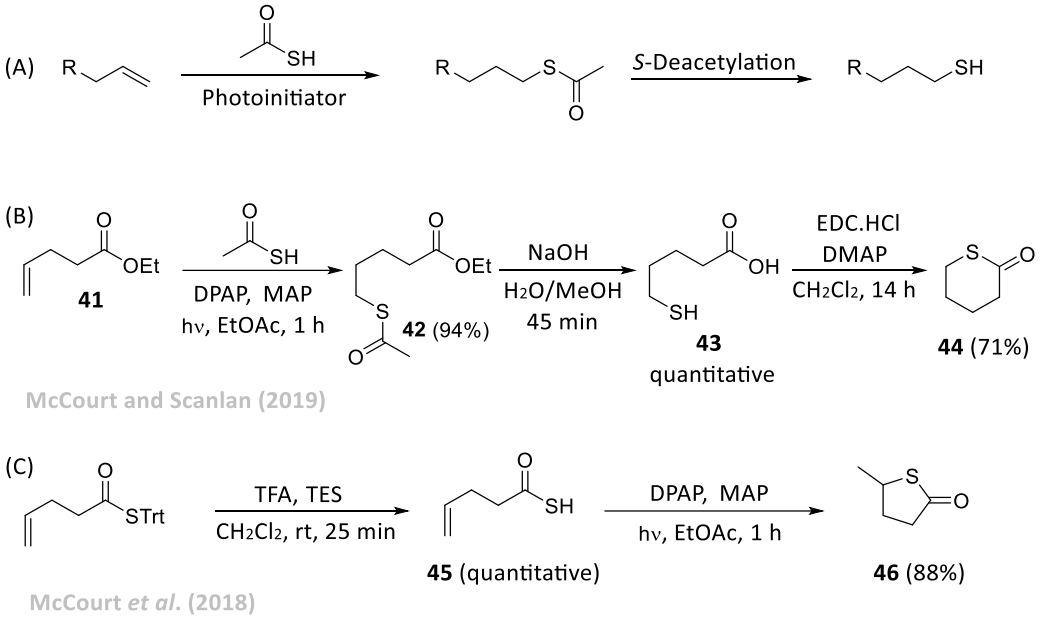

Scheme 1.11. (A) Sequential ATE and *S*-deacetylation for direct substrate thiolations. (B) A sequential ATE and thiolactonisation method for synthesis of δ-thiolactone **44**.[138] (C) ATE-mediated synthesis of thiolactone **46**.[139]

Recent work by Benny and Scanlan employed the intramolecular ATE reaction for the efficient synthesis of macrocyclic thiolactone peptides.[140] This study explored the radical-mediated cyclisation of unprotected linear peptides displaying both an alkene and a thioacid residue, forming biologically relevant peptide thiolactones. The linear peptide **47** bearing thioaspartic acid at the *N*-terminus and AgI was obtained in high purity using conventional Fmoc/*t*Bu SPPS. Irradiation of peptide **47** with UV light for 15 minutes in presence of DPAP led to the formation of the peptide thiolactone **48** in 90% conversion as confirmed by analytical RP-HPLC (**Figure 1.8**). The scope of this novel macrocyclization method was further evaluated using structurally diverse peptides containing amines, carboxylic acids, alcohols, and phenols. Notably, the reaction demonstrated full compatibility with these reactive functional groups, resulting

in the formation of cyclic thiolactones with high conversion rates as determined by RP-HPLC analysis.

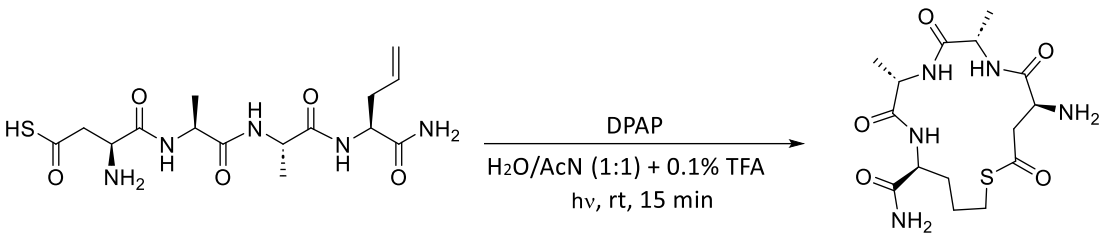

47 **48** (90%)

Benny and Scanlan (2024)

Figure 1.8. ATE reaction towards direct peptide macrocyclisation.

In conclusion, it is clear that synthetic advances in peptide synthesis, purification and characterisation over recent decades have advanced the state-of-the-art in peptide synthesis and enabled discovery and development of many important therapeutics. The ability to conduct peptide synthesis, macrocyclisation and covalent modification reactions on solid supports has revolutionised the field and enabled peptide synthesis to become an automated process. Advances in chemo- and regioselective chemical ligation reactions, primarily those based on either redox or radical-mediated reactions involving sulfur containing functional groups, including thiols and thioesters, have enabled the chemical synthesis of complex and diverse peptides, including proteins and macrocycles. The field continues to advance at a rapid rate and novel methods for peptide synthesis, macrocyclisation and ligation are of ever increasing importance.

1.5 Work Described Within This Thesis

As highlighted in **Section 1.4**, TEC demonstrates considerable promise for chemoselective modification of complex substrates, including applications in biomolecular systems. Nonetheless, there are several unexplored areas where TEC could be further investigated and applied.

Chapter 2 describes the synthesis of vasopressin and somatostatin analogues with expanded ring sizes and preserved disulfide moieties to explore neuropeptide activity. A novel on-resin regioselective thiol incorporation methodology, followed by

disulfide bond formation in solution, was developed to produce high-purity cyclic analogues of diverse ring sizes, providing valuable insights into the influence of the ring size on the biological function of each neuropeptide.

Chapter 3 extends the on-resin peptide hydrothiolation strategy developed in Chapter 2 to native chemical ligation (NCL), enabling streamlined synthesis of thiolated amino acid analogues at the *N*-terminus of peptide sequences *via* two simple sequential on-resin steps. This allows for subsequent NCL-desulfurisation processes employed in chemical protein synthesis. This chapter also showcases on-resin fluorophore conjugation by employing the same on-resin peptide hydrothiolation strategy. This avoids the requirement for any intermediate purification steps facilitating efficient peptide bioconjugation workflows.

Chapter 4 presents a new strategy for late-stage modifications of cyclic peptides by combining chloroacetyl-mediated peptide cyclisation with post-cyclisation TEC reactions. A vasopressin analogue bearing an unsaturated moiety was used as a model system to demonstrate compatibility with various thiol-containing substrates.

Chapter 5 highlights the creation of thiol-containing chemical probes designed for selective targeting of crotonylation post-translational modifications. Optimised TEC reactions enabled covalent labelling of crotonylated peptides, laying the groundwork for applications in chemoproteomics and protein targeting within complex biological systems.

Chapter 6 contains experimental details and characterisation data for the compounds synthesised over the course of this work.

Chapter 2

On-resin Hydrothiolation Towards Peptide Cyclisation

2.1 Introduction and Aims

As outlined in the introduction, the radical-mediated TEC reaction is widely utilised in peptide chemistry for diverse applications including macrocyclisation and chemical modifications including lipidation and glycosylation (**Sections 1.4.1, 1.4.2, and 1.4.3**). However, applications of TEC for the direct hydrothiolation of peptide substrates to introduce reactive thiol residues suitable for further modification remain underexplored. This chapter describes the application of sequential acyl thiol-ene (ATE) and *S*-deacetylation chemistries on-resin to obtain structurally diverse thiolated peptidic targets. Incorporation of commercially available unsaturated amino acids of diverse lengths during peptide assembly permits the facile installation of a thiol group under mild conditions, prior to global deprotection and peptide cleavage. Compared to the labour-intensive, multistep synthesis of thiolated building blocks for SPPS, this approach provides a significant advantage by enabling quantitative and regioselective thiol installation directly on the resin, with efficient removal of byproducts *via* washings. The resulting free thiol group serves as a versatile chemical handle for subsequent chemical modifications both on-resin and in solution. The aim of this work is to apply the new on-resin thiolation methodology for the development of disulfide-based analogues of vasopressin and somatostatin with enlarged ring sizes, aiming to investigate the effect of ring size on the activity of both neuropeptides. Replacement of one or two Cys residues of the native sequences with the commercially available AgI, and application of sequential ATE reaction with thioacetic acid and *S*-deacetylation, furnishes the free thiol on the resin (**Scheme 2.1**). Following acidic cleavage and deprotection, the linear unprotected peptide cyclises under oxidative conditions to yield the final disulfide-based neuropeptide analogue bearing an increased ring size (**Scheme 2.1**).

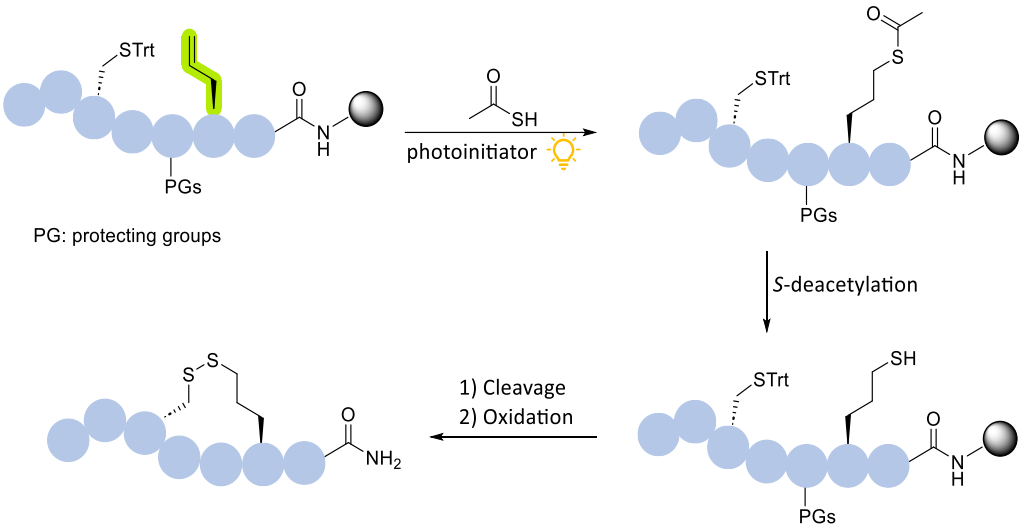

Scheme 2.1 Work described in this Chapter.

2.2 Results and Discussion

2.2.1 On-resin Optimisations

Initial studies were conducted by Dr. Joshua McLean to evaluate the suitability of ATE chemistry for on-resin applications, utilising a 4-pentenoic acid-capped tripeptide **49** tethered to the Rink amide resin (**Figure 2.1.C**). The resin-bound peptide **49** was synthesised manually on Rink Amide resin using repetitive steps of amino acid couplings, with PyBOP and *N*-methylmorpholine (NMM) as coupling reagents, and Fmoc deprotection prior to each coupling step. Subsequently, an ATE reaction was performed directly on the resin-bound unsaturated peptide using thioacetic acid under UV-irradiated conditions. The reaction was facilitated by the initiator/photosensitiser pair DPAP and MAP and irradiation with UV light at 365 nm in DMF yielding the corresponding resin-bound peptide thioacetate **50**. Following this, multiple washings of the resin were carried out to remove excess reagents from the resin surface. Peptide cleavage was achieved by treating the resin-bound peptide with TFA/H_2O (98:2) and removal of the cleavage cocktail under reduced pressure yielded mixtures of desired thioacetate **50** and alkene starting material **49** (**Table 2.1**). Conversion to thioacetate **50** was calculated utilising the relative integration of alkene and thioacetate signals recorded in ^{1}H NMR spectra of the mixtures obtained. The reaction proceeded cleanly in all cases, with no side products detected by ^{1}H NMR spectra. DMF was initially chosen for its superior resin swelling properties. Interestingly, at short reaction times of 5 and

10 minutes (**Table 2.1, entries 1–4 and 5–8**, respectively), conversion to thioacetate **50** decreased when higher equivalents of thioacetic acid and DPAP/MAP were used. However, using 20 equivalents of thioacetic acid and 10 equivalents of DPAP and MAP, respectively, resulted in a >95% conversion to the desired thioacetate peptide **50** within 15 minutes (**Table 2.1, entry 9**). The use of alternative solvents, such as NMP and CH_2Cl_2, which are commonly employed in SPPS, did not significantly affect the conversion to **50** (**Table 2.1, entries 10 and 11**). Furthermore, unsaturated peptides synthesised on Wang resin and 2-chlorotrityl resin (2-ClTrt), both allowing the isolation of *C*-terminal peptide carboxylic acid **51**, were found to be compatible with the ATE conditions (**Table 2.1, entries 12 and 13**). This finding is particularly relevant for the 2-ClTrt resin, which facilitates the isolation of fully protected peptides following SPPS, highlighting the potential for ATE/S-deacetylation chemistries in the synthesis of protected thiolated peptides, enabling facile in-solution thiol modifications. Finally, the ATE reaction was successfully initiated using a low-power (36 W) nail lamp, as opposed to the laboratory-scale Luzchem photoreactor used for all other reactions (**Table 2.1, entries 1–13**). Under optimised conditions (**Table 2.1, entry 14**), the nail lamp achieved full conversion within 25 minutes, demonstrating that on-resin ATE methodologies, and thiol-ene reactions in general, are accessible to laboratories without specialized UV-mediated chemistry equipment.

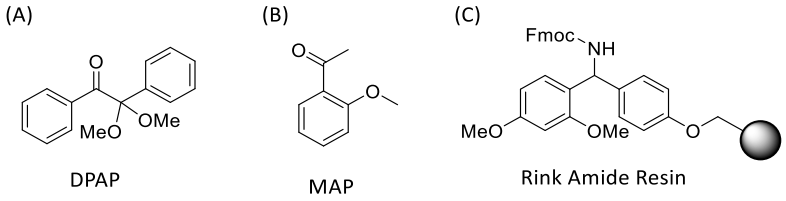

Figure 2.1. Chemical structures of (A) DPAP phoroinitiator, (B) MAP photosensitizer, and (C) rink amide resin.

Table 2.1. Optimisation table for the on-resin ATE reaction between the unsaturated peptide **49** and thioacetic acid to yield peptide thioacetates **50** (-$CONH_2$ at the *C*-terminus using Rink Amide resin) and **51** (-COOH at the *C*-terminus using Wang or 2-ClTrt resins).

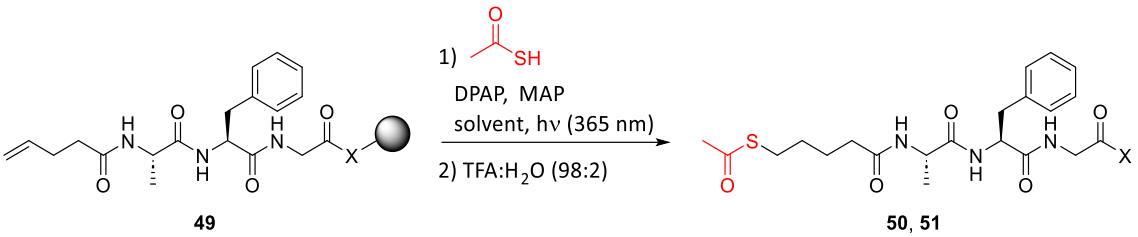

49 **50**, **51**

Entry	Eq. Thioacetic acid	Eq. DPAP/MAP	Time (min)	Solvent	Resin	Power (W)	Conv. (%)
1	10	5	5	DMF	Rink amide	110	24
2	50	25	5	DMF	Rink amide	110	22
3	100	50	5	DMF	Rink amide	110	17
4	200	100	5	DMF	Rink amide	110	12
5	10	5	10	DMF	Rink amide	110	90
6	50	25	10	DMF	Rink amide	110	76
7	100	50	10	DMF	Rink amide	110	67
8	200	100	10	DMF	Rink amide	110	59
9	20	10	15	DMF	Rink amide	110	>95
10	20	10	15	NMP	Rink amide	110	88
11	20	10	15	CH_2Cl_2	Rink amide	110	>95
12	20	10	15	DMF	Wang	110	>95
13	20	10	15	DMF	2-ClTrt	110	>95
14	20	10	25	DMF	Rink Amide	36	>95

Building on the optimised conditions identified for the on-resin ATE reaction, optimisation process for the on-resin *S*-deacetylation reaction followed (**Table 2.2**). The resin-bound thioacetate **50**, synthesised *via* conventional SPPS and the aforementioned on-resin ATE reaction, was subjected to various thiol-containing mixtures to induce *S*-deacetylation. DMF was chosen as the solvent due to its favourable resin-swelling properties. Previous reports by Wan and coworkers provided a foundation for exploring *S*-deacetylation conditions of anomeric thioacetates during thioglycoside synthesis.[141] Inspired by NCL, initial attempts utilised L-cysteine hydrochloride (HCl·Cys) and L-cysteine hydrochloride methyl ester (HCl·Cys-OMe) to irreversibly *S*-deacetylate *via*

sequential intermolecular *S*-to-*S* and intramolecular *S*-to-*N* acyl transfers (**Table 2.2, entries 1 and 2**). Triethylamine (TEA) was employed as a base to neutralize the internal HCl cysteine salts, facilitating proton transfer within the reaction medium. However, the solubility of these additives in DMF was poor, resulting in only 20% conversion to the resin-bound thiolated peptide **52** (**Table 2.2, entries 1 and 2**). Mild *S*-deacetylation has been reported using potassium carbonate (K_2CO_3) in methanol (MeOH) by Lee and coworkers.[142] However, the inability of MeOH to adequately swell the resin prevented effective *S*-deacetylation (**Table 2.2, entry 3**). DTT was next evaluated as a nucleophilic agent due to its good solubility in DMF. Treatment of the resin-bound thioacetate **50** with DTT and TEA resulted in a 56% conversion to thiol **52** (**Table 2.2, entry 4**). Subsequent screening of alternative bases, including NMM and DIPEA did not enhance reaction conversion (**Table 2.2, entries 5 and 6**). Extending the reaction time significantly increased conversion to 78%, but a 3-hour reaction was considered impractical for SPPS, prompting further optimization efforts. Replacement of the *S*-deacetylation cocktail every 15 min over the course of 1 h (**Table 2.2, entry 8**) resulted in a similar conversion to that observed with extended reaction times. DTT and HCl·Cys-OMe were used in a DMF:Phosphate buffer (8:2) system to enable efficient resin swelling but also enhance solubility of the two reagents (**Table 2.2, entries 9 and 10**). Ultimately, treating of the resin-bound peptide with a solution of 100 equiv. of DTT and HCl·Cys-OMe, respectively, in DMF:Phosphate buffer at pH 8.5 led to a conversion of >95% after 1 h.

Table 2.2. Optimisation table for the on-resin *S*-deacetylation of peptide thioacetate **50** to yield thiolated peptide **52**.

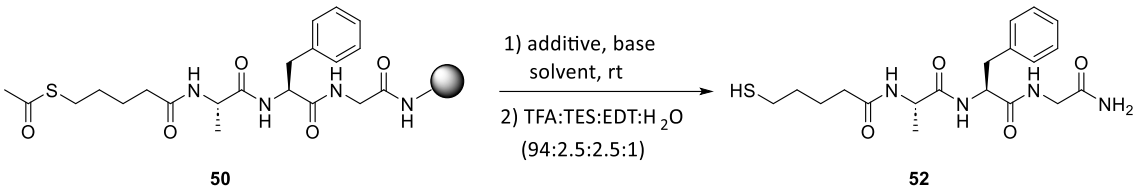

50 **52**

Entry	Additive	Eq. Additive	Base	Eq. Base	Time (min)	Solvent	Conv. (%)
1	HCl·Cys	10	TEA	10	60	DMF	20
2	HCl·Cys-OMe	10	TEA	10	60	DMF	20
3	-	-	K_2CO_3	10	60	MeOH	-
4	DTT	100	TEA	100	60	DMF	56
5	DTT	100	DIPEA	100	60	DMF	40
6	DTT	100	NMM	100	60	DMF	53
7	DTT	100	TEA	100	180	DMF	78
8	DTT	100	TEA	100	4 x 15	DMF	75
9	DTT+ HCl·Cys-OMe	100	TEA	100	60	DMF+PB	64
10	DTT+ HCl·Cys-OMe	100	-	-	60	DMF+PB (pH 8.5)	>95

2.2.2 Synthesis of Disulfide-linked Vasopressin Analogues

Vasopressin (**53**), also known as arginine vasopressin (AVP) or antidiuretic hormone (ADH), is a cyclic peptide hormone comprised of nine amino acids which is produced in the hypothalamus.[143] Structurally analogous to oxytocin, the cyclic structure of vasopressin consists of a disulfide bond between Cys residues at positions 1 and 6 (**Figure 2.2.A**).[143] Vasopressin's primary physiological roles include the induction of vasoconstriction in arterioles, leading to increased peripheral vascular resistance and a subsequent rise in arterial blood pressure.[144] Additionally, it promotes water reabsorption without solutes in the renal tubules, enhancing the return of water to the systemic circulation.[144] Emerging evidence suggests that vasopressin also influences social behaviours and sexual motivation.[145] Clinically, vasopressin is utilised in the treatment of central diabetes insipidus, a condition resulting from a deficiency in

antidiuretic hormone.[146] Off-label medical applications include its use in managing gastrointestinal haemorrhage and vasodilatory shock.[144] We sought to investigate the developed methodology for direct on-resin peptide thiolation to access two disulfide-based vasopressin analogues **54** and **55**, with extended ring sizes by two and four carbons, respectively (**Figure 2.2.B**). Biological evaluation of the two analogues, in collaboration with Prof. Markus Muttenthaler at the University of Vienna, is currently in process to investigate the effect of the ring size on the activity of vasopressin.

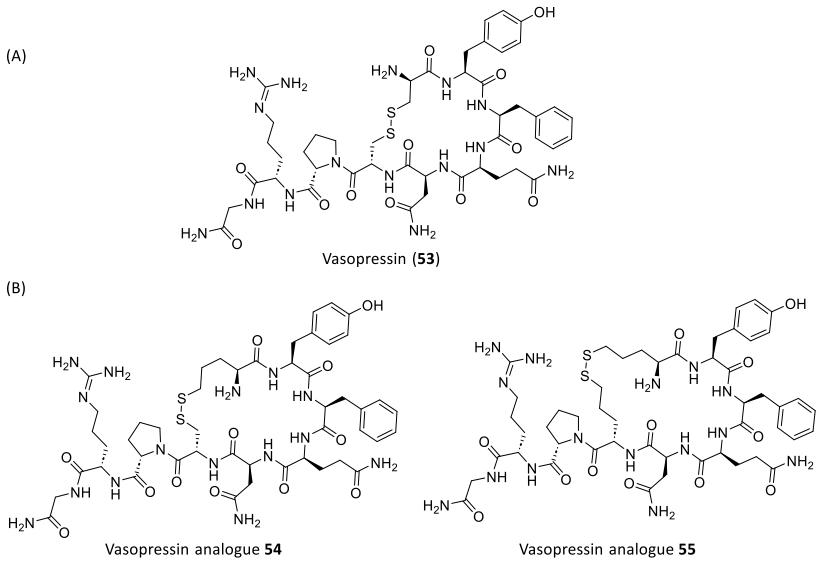

Figure 2.2. (A) The chemical structure of vasopressin. (B) The chemical structure of the disulfide-linked vasopressin analogues **54** and **55** synthesised in this work.

The first analogue, vasopressin analogue **54**, was designed to incorporate two additional carbon atoms relative to the native structure. This modification was achieved by substituting the Cys residue at position 1 (*N*-terminus) with AgI and subsequently installing a thiol moiety onto the terminal alkene *via* the two sequential on-resin reactions. The protected peptide **56** was synthesised on a Rink Amide resin (initial loading: 0.65 mmol/g), which yields an amide group at the *C*-terminus of the peptide upon cleavage from the resin. Peptide elongation proceeded up to the Tyr residue on a CEM Liberty Blue peptide synthesiser at Royal College of Surgeons in Ireland (RCSI), employing repetitive cycles of amino acid couplings and Fmoc deprotections under microwave-assisted conditions and elevated temperature. Amide couplings were carried out using DIC (3 equiv.) as a coupling reagent and Oxyma Pure (6 equiv.) as an activating additive, and Fmoc deprotections were achieved upon treatment of the resin-

bound peptide with 20% (v/v) piperidine in DMF. The combination of DIC and Oxyma Pure in both manual and automated synthesis is known as an effective racemisation-free method for amide formation.[147] The final coupling of the commercially available Boc-AgI-OH was carried out manually by treating the resin bound peptide with a solution of Boc-AgI-OH (3 equiv.), PyBOP (3 equiv.) and NMM (6 equiv.) in DMF for 45 minutes. Progress of the coupling reaction was monitored qualitatively using the bromophenol blue (BDB) test, as described by Krchnak *et al*.[148] In this test, a small portion of the resin-bound peptide was treated with a bromophenol solution in CH_2Cl_2, allowing the detection of free amines. Incomplete coupling was indicated by the appearance of blue colour in the resin, prompting a second coupling under identical conditions.

Subsequently, the on-resin ATE reaction was carried out using the optimised conditions outlined in **Section 2.2.1**, resulting in the formation of the thioacetate group at the *N*-terminus of the protected **57** on-resin (**Scheme 2.2**). This reaction was performed using a maximum quantity of 100 milligrams of resin-bound peptide, ensuring efficient agitation and reagent mixing during irradiation at 365 nm. Following the reaction, the resin-bound peptide was thoroughly washed to remove any residual reagents and byproducts. Next, on-resin *S*-deacetylation was carried out under the optimised conditions described in **Section 2.2.1**, furnishing the free thiol at the *N*-terminus of the protected peptide **58** on-resin (**Scheme 2.2**). Finally, the peptide was cleaved from the resin and globally deprotected upon treatment with a TFA cleavage cocktail (**Scheme 2.2**). Triethylsilane (TES) was incorporated into the cocktail to scavenge reactive carbocations generated upon the removal of side chain protecting groups. Ethanedithiol (EDT) was also included in the cleavage cocktail to maintain the two sulfhydryl groups in the reduced form. The peptide cleavage and global deprotection were achieved upon treatment of the resin-bound peptide with a TFA/TES/EDT/H_2O mixture in a ratio of 94:2.5:2.5:1 for two hours. The crude product was then concentrated and precipitated using diethyl ether (Et_2O). The linear unprotected peptide **59** was obtained in high purity based on analytical RP-HPLC (**Figure 2.2.C**) and was used for the final cyclisation step without the need for further purification.

The peptide **59** was cyclised *via* disulfide formation between the Cys residue of position 6 and the free thiol group at the *N*-terminus of the sequence (**Scheme 2.2**). Peptide cyclisation *via* disulfide formation between two Cys residues has been extensively studied in the literature.[42] The oxidative folding process can be facilitated by electron-accepting reagents such as molecular oxygen (O_2) or hydrogen peroxide, or by disulfide-based small molecules like cystine, cystamine, and oxidized glutathione (GSH).[149] Factors such as peptide concentration, temperature, ionic strength, and pH significantly influence intramolecular disulfide formation. The efficiency of disulfide bond formation is dependent on thiolate concentration, proceeding rapidly at pH 9.0, but gradually slowing down at pH values below the pK_a (~ 8.7).[149] Additionally, the reaction requires highly diluted conditions (1–100 mM) in order to avoid oligomeric byproduct formation. Inspired by the work of Muttenthaler and coworkers, the linear peptide **59** was cyclised using 10% of DMSO as an oxidising agent in 1:1 mixture of H_2O/Phosphate buffer (pH 8.5) at a final concentration of 1 mM.[150] The reaction mixture was stirred at room temperature for 24 hours and purification of the crude product was performed *via* semi-preparative RP-HPLC on a C_{18} stationary phase, utilising a gradient of 0–100% acetonitrile (AcN) in water (H_2O) with 0.1% TFA. The final vasopressin analogue **54** was isolated in a 24% overall yield and with >95% purity, as confirmed by analytical RP-HPLC (Experimental Chapter, page 101).

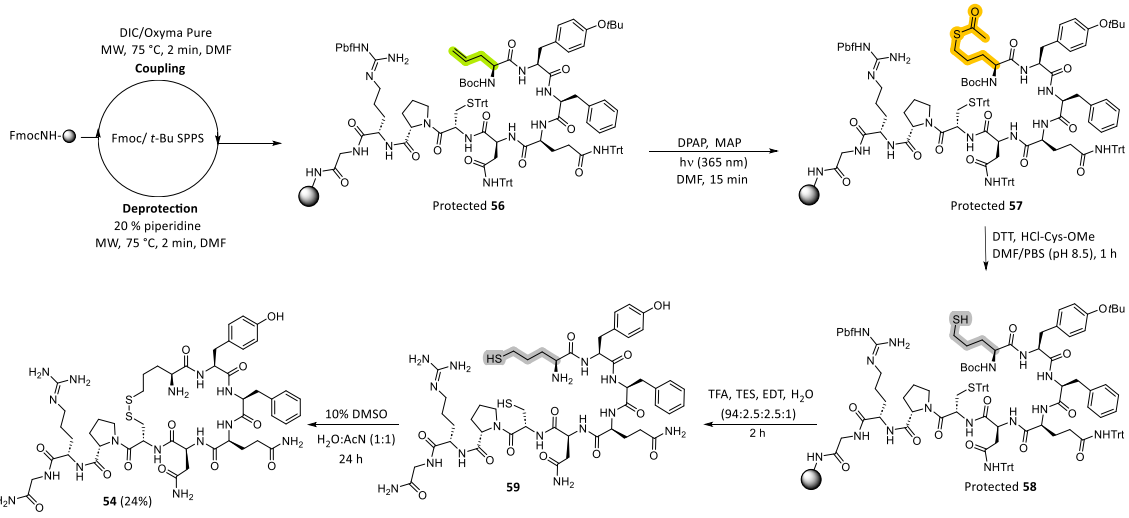

Scheme 2.2. Synthetic route undertaken to access vasopressin analogue **54**.

To monitor the progress of the two on-resin reactions, small-scale peptide cleavage and global deprotection of each intermediate was performed. Following

removal of TFA under reduced pressure, the linear unprotected intermediate products were analysed by RP-HPLC and ESI-MS. As illustrated from the RP-HPLC in **Figure 2.3.A**, the linear unprotected starting material **56**, displaying a terminal alkene at the *N*-terminus, was obtained in high purity. The mass of the linear unprotected peptide **56** was identified under the main RP-HPLC peak, with a retention time of 9.808 minutes. Following the first on-resin ATE reaction, the protected thioacetate **57** was subjected to small-scale cleavage and RP-HPLC analysis. Gratifyingly, the RP-HPLC trace demonstrated complete consumption of the starting unprotected peptide **56** and the emergence of a new main peak with a retention time of 10.240 minutes, corresponding to the mass of the linear unprotected peptide **57** with the thioacetate group at the *N*-terminus (**Figure 2.3.B**). Subsequently, *S*-deacetylation was conducted on-resin, and the resulting product was analysed using the same procedure. The analytical RP-HPLC trace confirmed the full consumption of the starting unprotected thioacetate **57**, with a new main peak observed at a retention time of 10.080 minutes, corresponding to the mass of the dithiol linear peptide **59** (**Figure 2.3.C**). Gratifyingly, the analysis of the intermediate products confirmed the efficiency of the two sequential on-resin reactions developed for direct peptide thiolation. Both on-resin reactions proceeded quantitatively, yielding products of high purity.

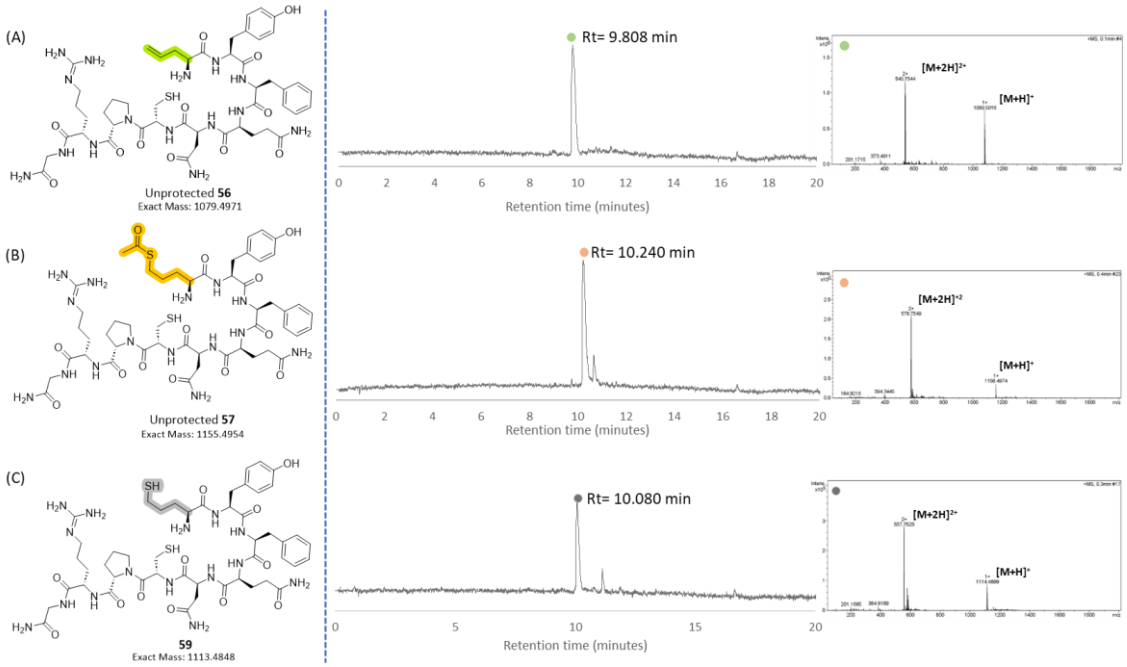

Figure 2.3. (A) Analytical RP-HPLC (220 nm) trace of the unprotected starting material **56.** ESI-MS analysis of the main peak with a retention time of 9.880 minutes confirmed the mass of the unprotected peptide **56** (1080.5016, $[M+H]^{+1}$ requires 1080.4871, 540.7544, $[M+2H]^{+2}$ requires 540.7485). (B) Analytical RP-HPLC (220 nm) trace of the unprotected peptide **57**. ESI-MS analysis of the main peak with a retention time of 10.240 minutes confirmed the mass of the unprotected peptide **57** (1156.4974, $[M+H]^{+1}$ requires 1156.4954, 578.7549, $[M+2H]^{+2}$ requires 578.7477). (C) Analytical RP-HPLC (220 nm) trace of the peptide **59**. ESI-MS analysis of the main peak with a retention time of 10.080 minutes confirmed the mass of the peptide **59** (1114.4899, $[M+H]^{+1}$ requires 1113.4848, 557.7525, $[M+2H]^{+2}$ requires 557.7424).

The second vasopressin analogue, **55**, was designed by incorporating an additional four carbon atoms relative to the native peptide. This structural modification was achieved by substituting both Cys residues at positions 1 (*N*-terminus) and 6 with AgI. The installation of thiol moieties at these positions was carried out through the two sequential on-resin reactions, enabling finally peptide cyclisation *via* disulfide bond formation (**Scheme 2.3**).

The protected peptide **60** was synthesised on the Liberty Blue peptide synthesiser as described above. Due to the presence of two alkene sites, the on-resin ATE reaction was performed under the previously optimised conditions resulting in the protected peptide **61** on-resin bearing two thioacetate groups (**Scheme 2.3**). On-resin *S*-deacetylation under the optimised conditions yielded the protected dithiol peptide **62** on-resin (**Scheme 2.3**). Cleavage of the peptide from the resin, along with global

deprotection, was achieved by treatment with a solution of TFA/TES/EDT/H_2O (94:2.5:2.5:1) for 2 h. Following concentration and precipitation, the linear unprotected dithiol **63** was obtained in high purity and used directly in the final cyclisation step without further purification. The oxidative folding of **63** was achieved under the same conditions by using DMSO as an oxidative agent. Given the increased distance between the two thiol groups, the reaction was left under stirring for 48 hours to ensure the formation of intramolecular disulfide bond. The final product was purified *via* semi-preparative RP-HPLC and the vasopressin analogue **55** was isolated in a 22% overall yield and with >95% purity, as confirmed by analytical RP-HPLC (Experimental Chapter, page 102).

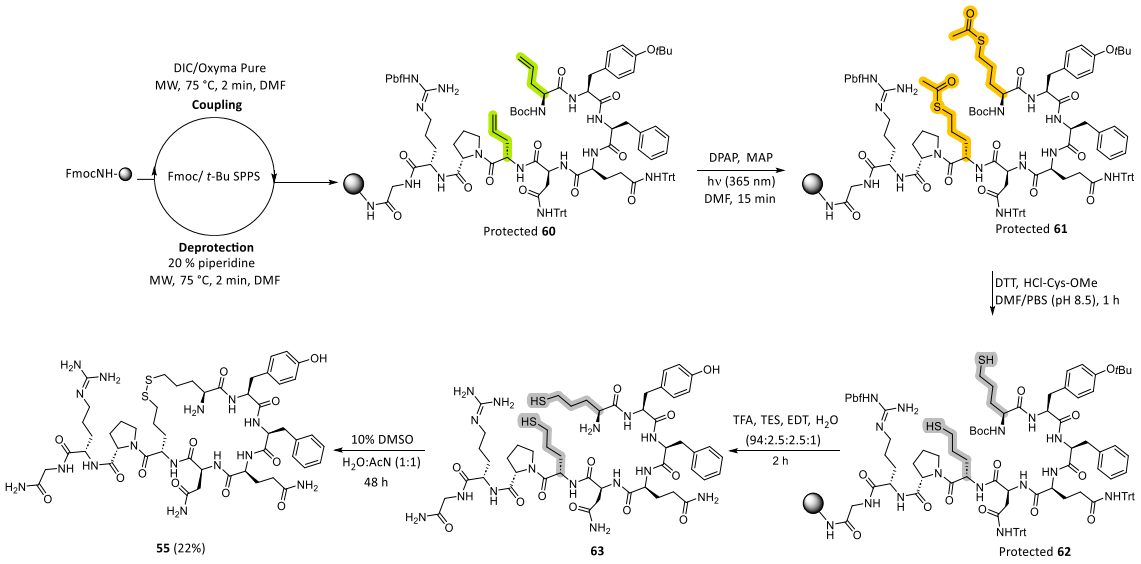

Scheme 2.3. Synthetic route undertaken to access vasopressin analogue **55**.

Similar to the synthesis of the vasopressin analogue **54**, the progress of both on-resin reactions was monitored *via* small-scale peptide cleavage and deprotection, and subsequent analysis of the intermediate unprotected products by RP-HPLC and ESI-MS. As illustrated in **Figure 2.4.A**, the unprotected starting material **60**, containing two terminal alkene groups, was obtained with excellent purity. The mass of the unprotected peptide **60** was identified under the main RP-HPLC peak, with a retention time of 9.975 minutes. Gratifyingly, the installation of thioacetate groups at both alkene sites was successfully achieved through the on-resin ATE reaction. The RP-HPLC trace indicated complete consumption of the unprotected starting material **60** and the appearance of a new peak at a retention time of 10.817 minutes, corresponding to the

mass of the unprotected peptide **61** bearing two thioacetate groups, as confirmed by ESI-MS (**Figure 2.4.B**). Additionally, the on-resin *S*-deacetylation also proceeded with complete consumption of the unprotected starting material **61** and a quantitative formation of peptide **63** as confirmed by analytical RP-HPLC and ESI-MS analysis (**Figure 2.4.C**). Importantly, this work underscores the potential and broad applicability of the developed methodology, which can facilitate the direct on-resin thiolation of multiple sites within a peptide sequence.

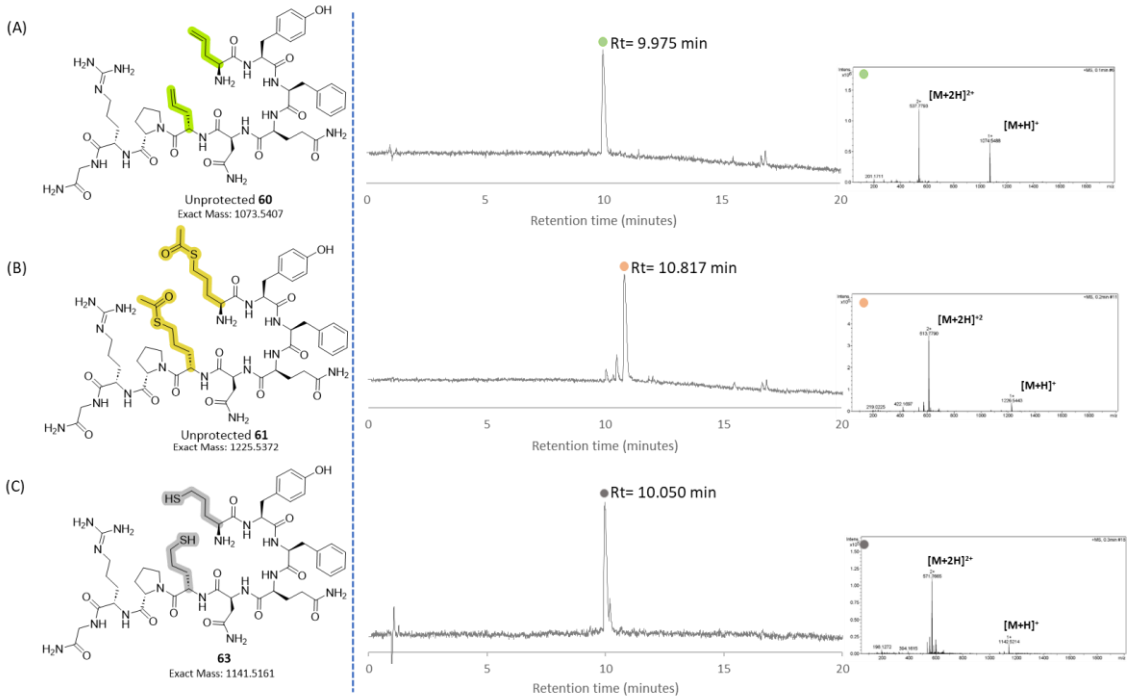

Figure 2.4. (A) Analytical RP-HPLC (220 nm) trace of the unprotected starting material **60**. ESI-MS analysis of the main peak with a retention time of 9.975 minutes confirmed the mass of the unprotected peptide **60** (1074.5488, $[M+H]^{+1}$ requires 1074.5407, 537.7793, $[M+2H]^{+2}$ requires 537.7703). (B) Analytical RP-HPLC (220 nm) trace of the unprotected peptide **61**. ESI-MS analysis of the main peak with a retention time of 10.817 minutes confirmed the mass of the unprotected peptide **61** (1226.5443, $[M+H]^{+1}$ requires 1226.5372, 613.7790, $[M+2H]^{+2}$ requires 613.7686). (C) Analytical RP-HPLC (220 nm) trace of the peptide **63**. ESI-MS analysis of the main peak with a retention time of 10.050 minutes confirmed the mass of the peptide **63** (1142.5214, $[M+H]^{+1}$ requires 1142.5161, 571.7665, $[M+2H]^{+2}$ requires 571.7580).

After successfully synthesizing the two vasopressin analogues **54** and **55**, the impact of the ring size expansion on the activity of vasopressin was investigated by Professor Markus Muttenthaler's research group at the University of Vienna. To assess

the derivatives' ability to interact with this receptor, functional cellular assays (HTRF IP-One G_q Detection Kit, Revvity) were carried out on HEK-293 cells, stably overexpressing the human V_{1a} receptor ($hV_{1a}R$). To check for agonism, analogues **54** and **55** were tested at 10 µM, but even at these high concentrations, no receptor activity above the baseline level was detected (**Figure 2.5A-C**). To further see whether the compounds could possibly act as antagonists, 10 µM of vasopressin analogues **54** and **55** were added to the vasopressin dilution series, but no competitive ligand displacement (shift of the sigmoidal curve to the right) was observed, indicating that the derivatives did not interact with the orthosteric binding pocket of the receptor (**Figure 2.5B-C**). These results highlight the importance and sensitivity of the macrocyclic ring system to increased ring size.

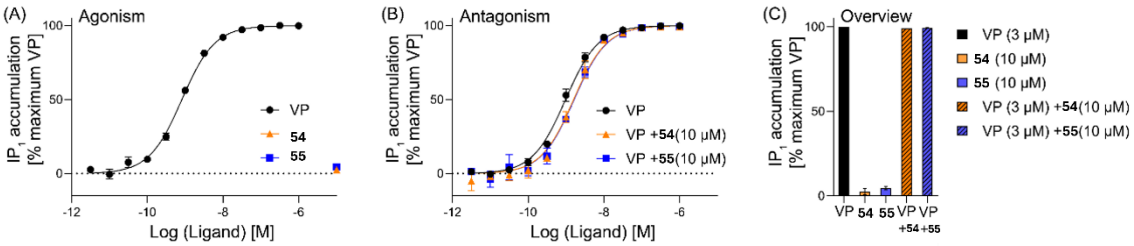

Figure 2.5. Biological evaluation of vasopressin analogues **54** and **55**. Functional IP_1 assays were performed on stable HEK-293 cells overexpressing the human $V_{1a}R$. (A) Single point measurement of **54**/**55** at 10 µM to determine potential agonism. (B) Addition of 10 µM **54**/**55** to a dilution series of vasopressin (3 µM -30 pM) to determine potential antagonism. (C) Overview of IP_1 assay results for agonism and antagonism. Each point represents three (agonism) or two (antagonism) independent measurements with technical triplicates. Results normalized to the highest vasopressin activity (100%) and vehicle control (0%). Error bars indicate the standard error of the mean (SEM).

2.2.3 Synthesis of Disulfide-linked Somatostatin Analogues

Somatostatin (**64**), also known as growth hormone-inhibiting hormone, is a cyclic polypeptide produced in several locations within the human body, including the hypothalamus, pancreas, gastrointestinal (GI) tract, and central nervous system.[151] Its structure comprises fourteen amino acids with a disulfide bridge formed between Cys residues at positions three and fourteen (**Figure 2.6**).[151] Somatostatin exerts its biological effects by binding to specific receptors, classified as G protein-coupled receptors (SSTR1–SSTR5).[152] These interactions are known to inhibit pancreatic, exocrine, and pituitary secretions, in addition to suppressing angiogenesis and cancer

cell proliferation.[151,152] Similar to the work described in **Section 2.2.2**, two novel and previously not mentioned from the literature disulfide-bridged analogues of somatostatin featuring expanded ring sizes by two and four carbons, respectively, were developed (**Figure 2.6**). This was accomplished through the systematic substitution of Cys residues with AgI, followed by direct peptide thiolation using the two on-resin reactions, and final cyclisation *via* disulfide bond formation.

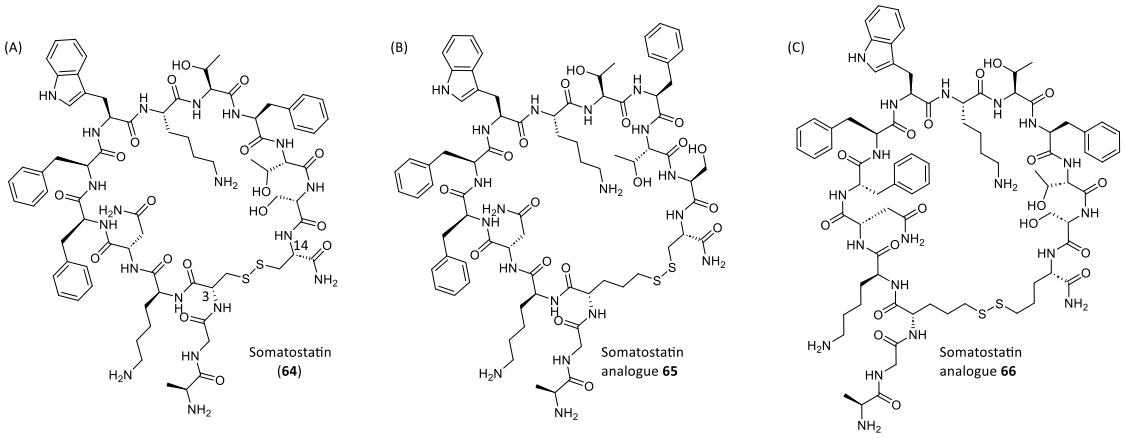

Figure 2.6. (A) The chemical structure of somatostatin (**64**). (B) The chemical structure somatostatin analogue **65** synthesised in this work**.** (C) The chemical structure of somatostatin analogue **66** synthesised in this work.

The synthesis of somatostatin analogue **65** was achieved by applying traditional SPPS protocols, in which the Cys at position 3 was replaced with AgI, followed by on-resin hydrothiolation. Gratifyingly, the two sequential on-resin reactions proceeded in full conversion as confirmed by the RP-HPLC and ESI-MS analysis of the linear unprotected intermediate products. Following peptide cleavage and deprotection, the disulfide formation was achieved under identical conditions as discussed in **Section 2.2.2**. The final somatostatin analogue **65** bearing two more carbons compared to the native structure, was isolated in a 14% yield and with >95% purity as confirmed by analytical RP-HPLC (Experimental Chapter, page 104). The very low yield is attributed to the extensive loss of peptide material during semi-preparative RP-HPLC purification which is a common issue of peptide synthesis.

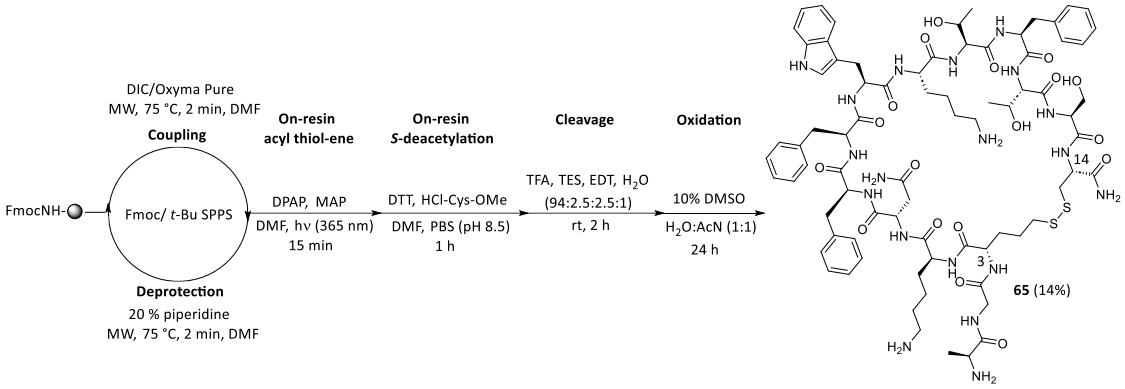

Scheme 2.4. Synthetic route undertaken to access somatostatin analogue **65**.

For the synthesis of somatostatin analogue **66**, which contains an extension of four carbon atoms, both Cys residues at positions 3 and 14, respectively, were replaced with AgI. Utilising the two sequential on-resin reactions, the thiol groups were quantitatively introduced at both sites, as confirmed by RP-HPLC and ESI-MS analysis. The final cyclisation *via* disulfide formation was successfully performed under analogous conditions and following purification, somatostatin analogue **66** was isolated in a 12% yield and with >95% purity as confirmed by analytical RP-HPLC (Experimental Chapter, page 105).

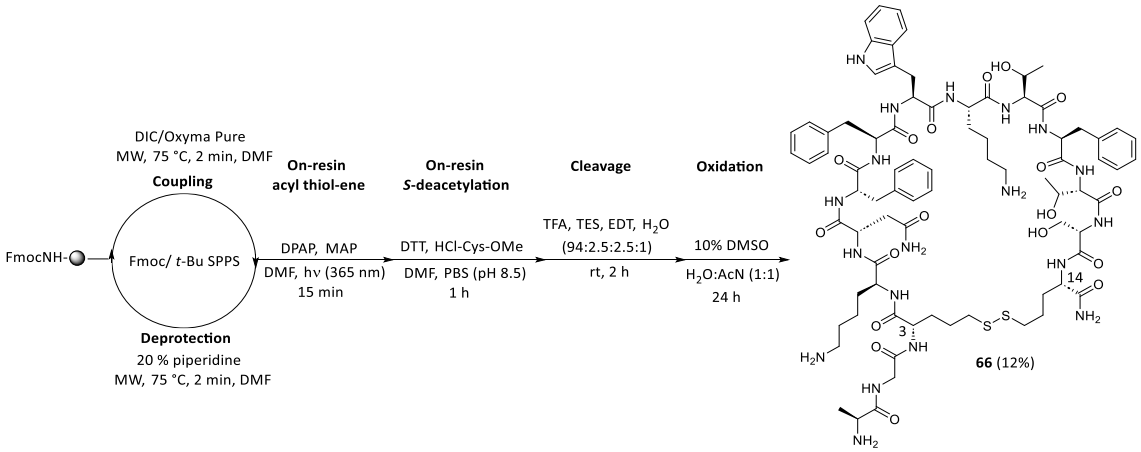

Scheme 2.5. Synthetic route undertaken to access somatostatin analogue **66**.

2.3 Conclusions and Future Work

In conclusion, this study reports the development of novel vasopressin and somatostatin analogues with extended ring sizes and preserved disulfide bonds, aiming to investigate the effect of ring size on the activity of each neuropeptide. To achieve

this, the radical TEC reaction was employed for the first time for direct peptide hydrothiolation on-resin, generating thiolated amino acids of different lengths, which were subsequently used for peptide cyclisation *via* disulfide bond formation. The use of commercially available alkenyl amino acids, in combination with sequential ATE reaction using thioacetic acid followed by *S*-deacetylation on-resin, enabled the regioselective installation of a thiol residue onto the peptide.

Initially, optimisation of the two on-resin reactions was performed using the 4-pentenoic acid-capped tripeptide **49**. The use of thioacetic acid (20 equiv.), DPAP (10 equiv.), MAP (10 equiv.), and irradiation of the resin-bound peptide for 15 minutes led to the formation of the thioacetate group with >95% conversion (**Table 2.1, entry 9**). Subsequent on-resin removal of the acetyl group was achieved using DTT (100 equiv.) and HCl·Cys-OMe (100 equiv.) in DMF/phosphate buffer (pH 8.5), resulting in >95% conversion (**Table 2.2, entry 10**). These optimised conditions were then utilised for the synthesis of disulfide-based analogues of vasopressin and somatostatin. This involved the systematic substitution of Cys residues in the sequences of vasopressin and somatostatin with the commercially available AgI, followed by regioselective hydrothiolation *via* the two on-resin reactions. Importantly, both on-resin reactions, under the optimised conditions, proceeded with complete conversion. Following peptide cleavage and deprotection, cyclisation occurred *via* disulfide bond formation under oxidative conditions, yielding vasopressin and somatostatin analogues with enlarged ring sizes in very high purity, suitable for biological testing.

Future work will include the biological evaluation the synthesised somatostatin analogues **65** and **66**, with binding affinity studies currently being conducted by Professor Markus Muttenthaler's research group at the University of Vienna. These results will elucidate the significance of ring size for the biological activity of somatostatin. Furthermore, future directions will explore the formation of the disulfide bond on-resin, applied to other cyclic peptides of biological interest, towards in drug-discovery efforts. In cases where both Cys residues are replaced with AgI, following on-resin thiolation, the protected peptide will be subjected to on-resin cyclisation *via* disulfide formation under similar conditions by using DMSO or I_2 as oxidising agents. Alternatively, if only one of the two Cys is replaced with AgI, a Cys with an Mmt

protecting group will be incorporated into the peptide sequence. Following on-resin hydrothiolation, selective removal of the Mmt group using 1% TFA will expose the second free sulfhydryl group, facilitating peptide cyclisation on-resin. Finally, inspired by these results, future work will explore the use of other commercially available unsaturated amino acids, with the aim of further diversifying the ring size and structure of these neuropeptides.

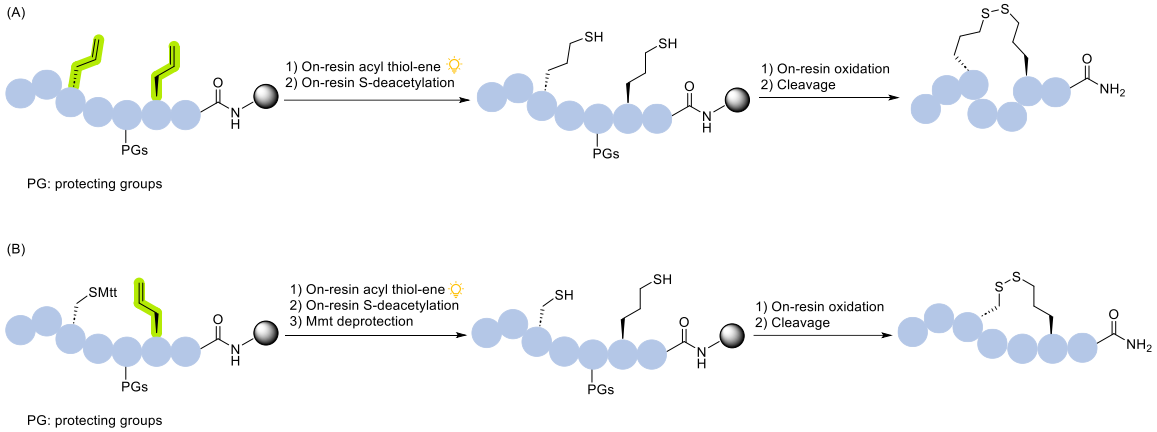

Scheme 2.6. (A) Future directions for on-resin disulfide formation by substituting both Cys sites with AgI. (B) Future directions for on-resin disulfide formation by substituting only the one Cys with AgI.

Chapter 3

On-resin Hydrothiolation Towards Peptide Ligation and Modification

3.1 Introduction and Aims

As discussed in **Section 1.3**, NCL has revolutionised the field of chemical protein synthesis since its discovery in 1994, particularly with the advancement of sequential NCL and desulfurisation chemistries for non-Cys ligation sites. However, the limited commercial availability and the complex synthetic routes required for thiolated amino acids specifically designed for NCL and desulfurisation have restricted their broader application.[95] The aim of this project is the application of the developed methodology for direct on-resin peptide thiolation within the context of NCL. As illustrated in **Scheme 3.1**, the incorporation of commercially available unsaturated analogues of natural amino acids at the *N*-terminus enables the direct introduction of a thiol residue. Upon cleavage and deprotection, this thiol group can then be employed in sequential NCL and desulfurisation reactions, resulting in the formation of the native amino acid at the ligation site. This approach offers a streamlined, two-step procedure for accessing thiolated peptide substrates for NCL, circumventing the labor-intensive and lengthy synthesis processes traditionally required for thiolated natural amino acids. Finally, to further broaden the utility of this methodology, this chapter also explores the on-resin covalent attachment of fluorophores to biologically relevant peptides.

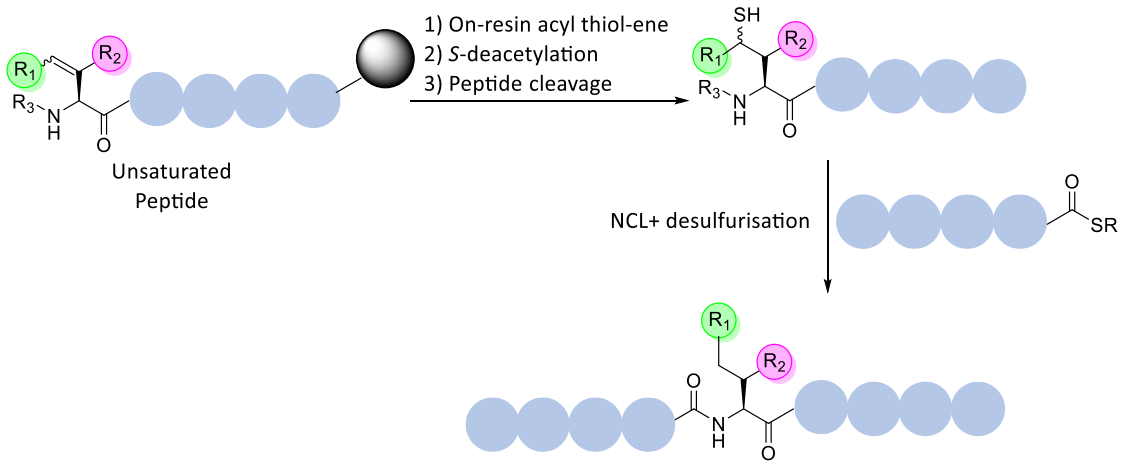

Scheme 3.1. Application of the sequential on-resin ATE and *S*-deacetylation chemistries in chemical protein synthesis.

3.2 Results and Discussion

3.2.1 Use of Dehydrovaline

The first unsaturated amino acid to be investigated for direct thiolation and subsequent application in NCL was Boc-L-3,4-didehydrovaline (Boc-Dhv-OH, **67**) which is commercially available. Valine is highly abundant in human proteins, accounting for approximately 6.8% of their amino acid content, which enhances the applicability of synthetic strategies incorporating valine at ligation sites.[153] In 2008, Danishefsky and coworkers reported the use of γ-thiolated valine in NCL.[153] However, their synthetic approach required over seven steps and numerous intermediate purification stages to obtain the final thiolated valine.[153] The current study aims to achieve γ-thiolated valine by employing Boc-Dhv at the *N*-terminus and introducing the thiol group *via* two on-resin, quantitative reactions without any requirement for intermediate purification.

Ixosin is a 23 amino acid antimicrobial peptide (AMP) isolated from the salivary glands of the hardtick *Ixodes sinensis,* possessing the following primary sequence: GLHKVMREVLGYERNSYKKFFLR.[154] Ixosin has shown high antimicrobial activity against *Escherichia coli*, *Staphylococcus aureus*, and *Candida albicans in vitro.*[154] Ixosin [H_3A, E_8K, E_{13}L, S_{16}V] (**68**) is a mutated sequence reported by Angeles-Boza and coworkers with an amino acid sequence of GLAKVMR(KV)LGYLRNVYK.[155] This Ixosin mutant has shown activity against gram positive and negative bacteria, pathogenic fungi and cancers.[155] Ixosin [H_3A, E_8K, E_{13}L, S_{16}V] was deemed an ideal target for synthesis *via* the NCL/desulfurisation strategy (**Scheme 3.2**). The ligation site in the middle of sequence, located between Lys and Val, would permit the synthesis of peptide fragment **69** bearing γ-thiol valine at the *N*-terminus. This was accomplished by synthesising the protected peptide **70** and incorporating Boc-Dhv-OH at the *N*-terminus. On-resin hydrothiolation/deacetylation and subsequent peptide cleavage produced the 'ligatable' peptide fragment **69** in two efficient and quantitative steps (**Scheme 3.2**). Following NCL of peptide fragment **69** and peptide thioester **71**, desulfurisation would yield the final ligated product, Ixosin [H3A, E8K, E13L, S16V], incorporating valine at the ligation site (**Scheme 3.2**).

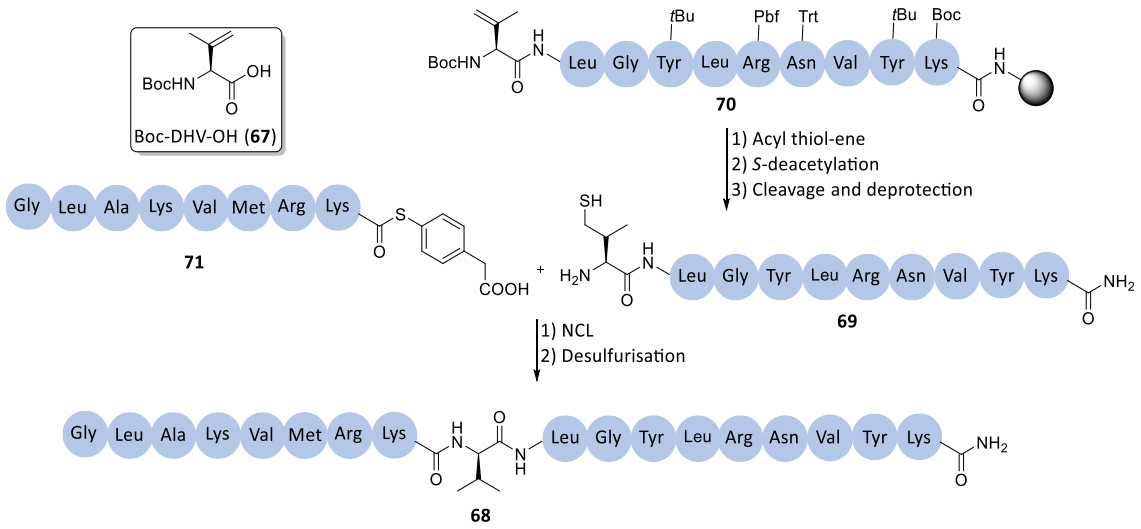

Scheme 3.2. Synthesis of Ixosin [H3A, E8K, E13L, S16V] *via* on-resin ATE and *S*-deacetylation reactions, followed by NCL/desulfurisation strategy.

Although Boc-Dhv-OH is commercially available, it was synthesized in-house (**Scheme 3.3**), as the procedure has been well-described by the Scanlan group.[156] The six-step synthesis of Boc-Dhv-OH (**67**) begins with D-Ser, which, through a number of functional group interconversions results in the target compound and an inversion of alpha carbon stereochemistry.[156] Initially, Boc protection of D-Ser methyl ester **72** furnished alcohol **73** in a 83% yield following purification *via* normal phase column chromatography. In the next step, protection of the serine derivative **73** was achieved upon treatment with 2,2-dimethoxypropane (DMP, **74**) and p-toluenesulfonic acid (PTSA), resulting in oxazolidine **75**. Due to poor chromatographic separation of the starting material **74** and oxazolidine **75** by thin layer chromatography (TLC), vacuum distillation was employed as a purification method rather than column chromatography, affording the desired product **75** in 76% yield. Grignard reaction of **75** with methyl magnesium bromide gave the tertiary alcohol **76** in quantitative yield following column chromatography. Subsequent one-pot mesylation and elimination of the tertiary alcohol **76** was undertaken with dropwise addition of methanesulfonyl chloride (MsCl) at -10 °C in the presence of the tertiary base TEA. Unfortunately, the terminal alkene **77** was isolated in only 26% yield after column chromatography. The mesylation/elimination step was extensively studied by two postdoctoral researchers within the Scanlan Group, Dr. Joshua McLean and Dr. Pierre Milbeo. The low yield obtained was attributed to Boc-deprotection of the starting alcohol **76** by HCl generated

upon addition of MsCl to the reaction mixture. Furthermore, formation of a mixture of the internal alkene (thermodynamic product) and the terminal alkene **77** (kinetic product) was observed, even at low temperatures. Various solvents, bases, and reaction conditions were screened aiming to decrease the side product formation and increase the overall yield. However, no improvement in yield was observed, with a slight improvement in alkene selectivity noted under Finkelstein conditions. Subsequently, alkene **77** underwent pseudoproline deprotection using a mixture of TFA:Tetrahydrofuran (THF):H_2O in a 4:2:1 ratio at 0 °C for 10 min prior to a basic quench at 0 °C. These pseudoproline deprotection conditions were reported by Fukuyama and coworkers and are highly selective in presence of the Boc group.[157] Finally, oxidation of alcohol **78** using 2.5 M Jones reagent in acetone furnished the final Boc-Dhv-OH (**67**) in quantitative yield (Experimental Chapter, page 112).

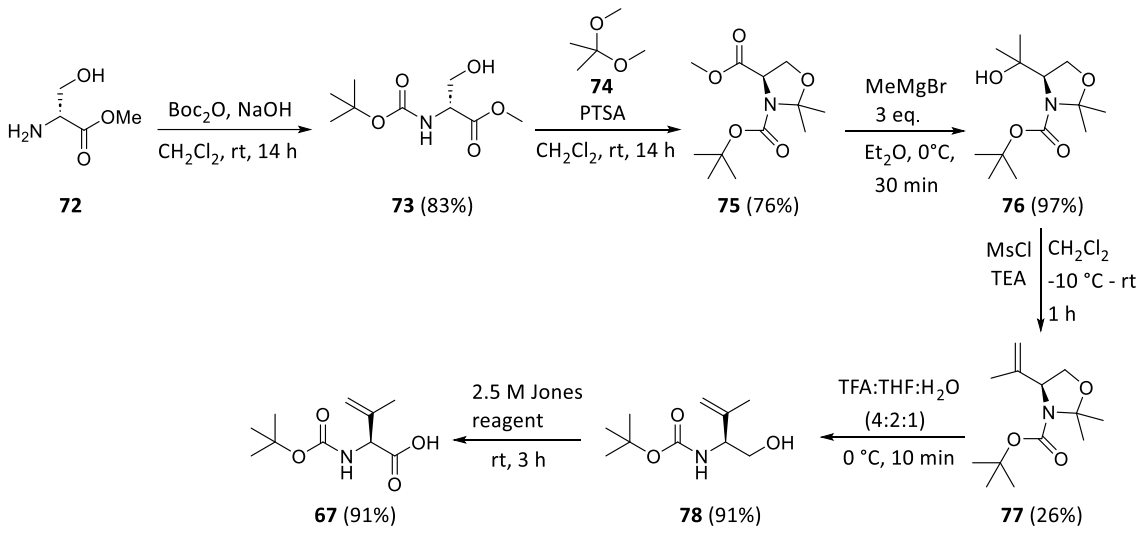

Scheme 3.3. Synthetic route undertaken to access Boc-Dhv-OH (**67**).[156]

The synthesis of Dhv containing fragment **70** was undertaken using manual standard Fmoc/*t*Bu SPPS protocols (**Scheme 3.4**). Fritted syringes were utilised as reaction vessels enabling sequential coupling, resin washing and deprotection cycles. The peptide sequence was built on a Rink amide resin (loading: 0.78 mmol/g). The amino acid couplings were accomplished by treating the resin bound peptide with a solution of Fmoc-AA-OH (3 equiv.), PyBOP (3 equiv.) and NMM (6 equiv.) in DMF for 45 minutes, and the progress of coupling steps was monitored using the bromophenol blue test. The final amino acid, Boc-Dhv-OH **67** was coupled using DIC and Oxyma Pure as coupling

reagents, to suppress epimerisation at this residue. Sequential on-resin ATE and *S*-deacetylation were subsequently carried out on the resin bound peptide under the optimised conditions discussed in **Section 2.2.1**, furnishing the γ-thiol valine residue at the *N*-terminus of the peptide sequence. Both on-resin reactions proceeded quantitatively as confirmed by small-scale peptide cleavage and analysis of the linear unprotected intermediates by RP-HPLC and ESI-MS. Finally, the peptide was cleaved from the resin and purified *via* semi-preparative RP-HPLC yielding the peptide fragment **69** in a 35% overall yield and with >95% purity, as confirmed by analytical RP-HPLC (Experimental Chapter, page 114).

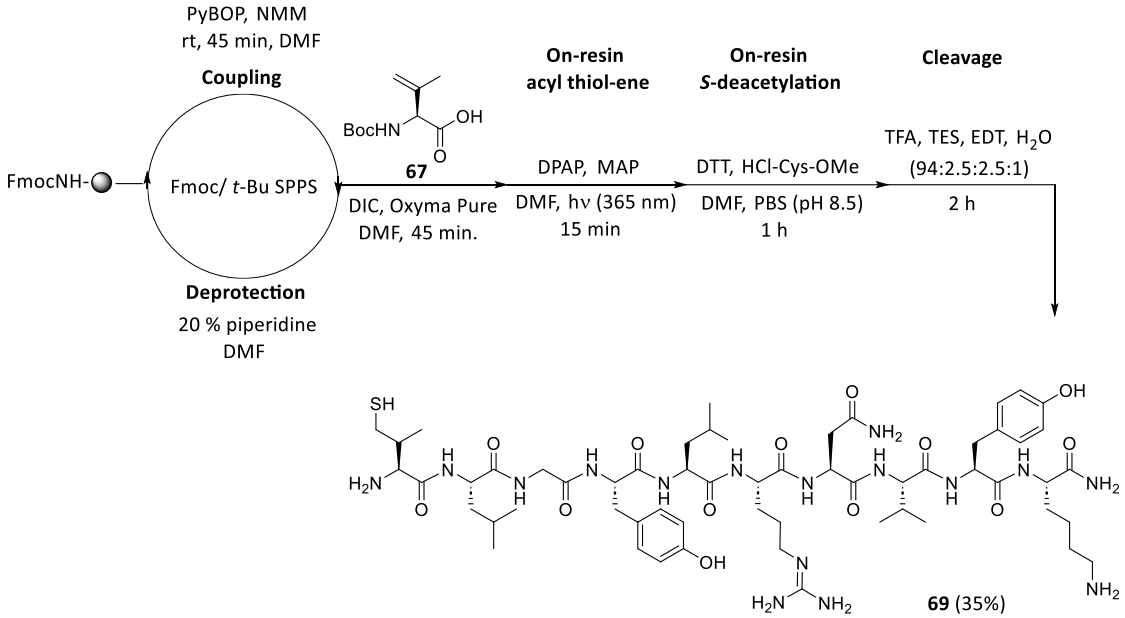

Scheme 3.4. Synthetic route undertaken to access peptide fragment **69**.

Peptide thioester fragment **71** was synthesised using the Dbz-methodology developed by Dawson and coworkers (**Scheme 1.4.A**).[87,158] The second generation of o-aminoaniline linker, the o-amino(methyl)aniline (**Scheme 3.5**, Fmoc-MeDbz (**79**)) was used, in which a methyl group is introduced onto the para-amino group to prevent acylation during SPPS, a side reaction observed with the first generation of the Dbz linker.[158] The *N*-acyl-*N*'-methylurea (MeNbz) group which derives from the on-resin cyclisation of the MeDbz linker at the *C*-terminus of the peptide (**Scheme 3.6,** peptide fragment **80**), permits *in situ* thiolysis during the ligation without any pre-activation.[158] Fmoc protected MeDbz linker **79** was synthesised to incorporate the linker through standard Fmoc/*t*Bu SPPS (**Scheme 3.5**). Starting from 4-fluoro-3-nitrobenzoic acid **81**,

nucleophilic aromatic substitution of the fluoro group with methylamine gave the aniline derivative **82** in a 90% yield. Reduction of the nitro group of **82** through catalytic hydrogenation with Pd/C furnished the diamino derivative **83** in a yield of 88%. Fmoc protection using Fmoc-succinimide (Fmoc-OSu) yielded the final Fmoc-MeDbz-OH linker **79** in a good yield of 80% (Experimental Chapter, page 113).

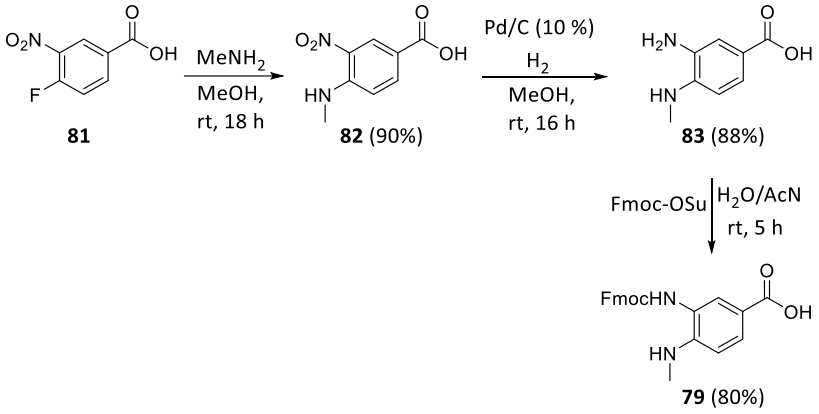

81 **82** (90%) **83** (88%) **79** (80%)

Scheme 3.5. Synthesis of Fmoc-MeDbz-OH (**79**).[158]

The synthesis of **80** was undertaken manually. Due to the high steric hindrance of Fmoc-MeDbz-OH, a glycine spacer was first coupled to Rink amide resin to facilitate efficient coupling of **79** to the resin (**Scheme 3.6**). Fmoc-MeDbz-OH was subsequently coupled using HBTU as an activating agent and DIPEA as the base in DMF. Subsequent amino acid couplings were achieved using PyBOP and NMM. Following assembly of the desired sequence, the resin-bound peptide was treated with a solution of *p*-nitrophenyl chloroformate in CH_2Cl_2, followed by cyclisation under basic conditions using DIPEA in DMF to form the MeNbz at the *C*-terminus of the sequence (**Scheme 3.6**). Peptide cleavage and purification *via* semi-preparative RP-HPLC yielded the linear unprotected peptide fragment **80** bearing the MeNbz group at the *C*-terminus in a 65% with >95% purity as confirmed by analytical RP-HPLC (Experimental Chapter, page 115).

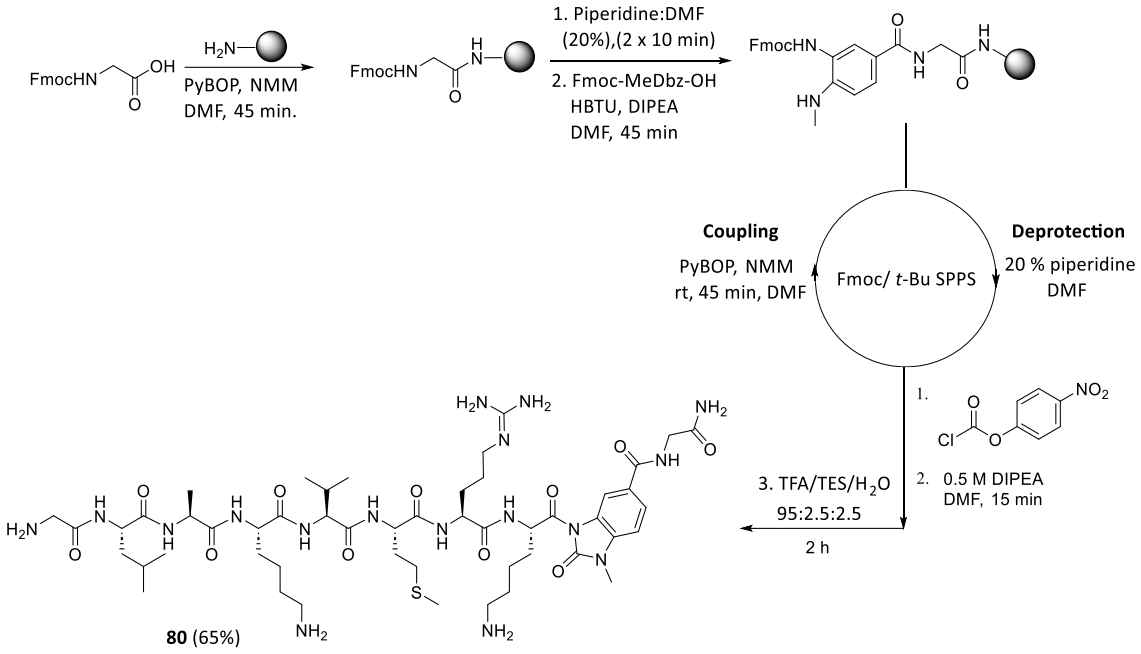

Scheme 3.6. Synthetic route undertaken to access peptide fragment **80**.

Native chemical ligation of peptide fragments **69** and **80** was carried out using the protocol reported by Dawson and coworkers (**Figure 3.1**).[159] A fresh ligation buffer was prepared containing 6 M Gnd.HCl, 200 mM sodium phosphate dibasic (Na_2HPO_4), 20 mM TCEP.HCl, and 200 mM MPAA. TCEP.HCl was used to prevent the formation of disulfide bonds, and MPAA was used as an external aryl thiol for the *in situ* formation of the more reactive thioester at the *C*-terminus of **71** during the ligation reaction (**Scheme 3.2**). Equimolar amounts of the two peptide fragments were dissolved in the ligation buffer at a concentration of 2 mM and the pH was adjusted to 7.0. The ligation reaction was agitated under argon and the ligated product **84** was observed *via* analytical RP-HPLC ESI-MS after 1 h of reaction. After 18 h, the ligated product **84** was the main product with full consumption of the starting materials **69** and **71** observed (**Figure 3.1**). Work is currently ongoing to optimise the purification and desulfurisation of the ligated product **84** to afford the final native peptide product **68**.

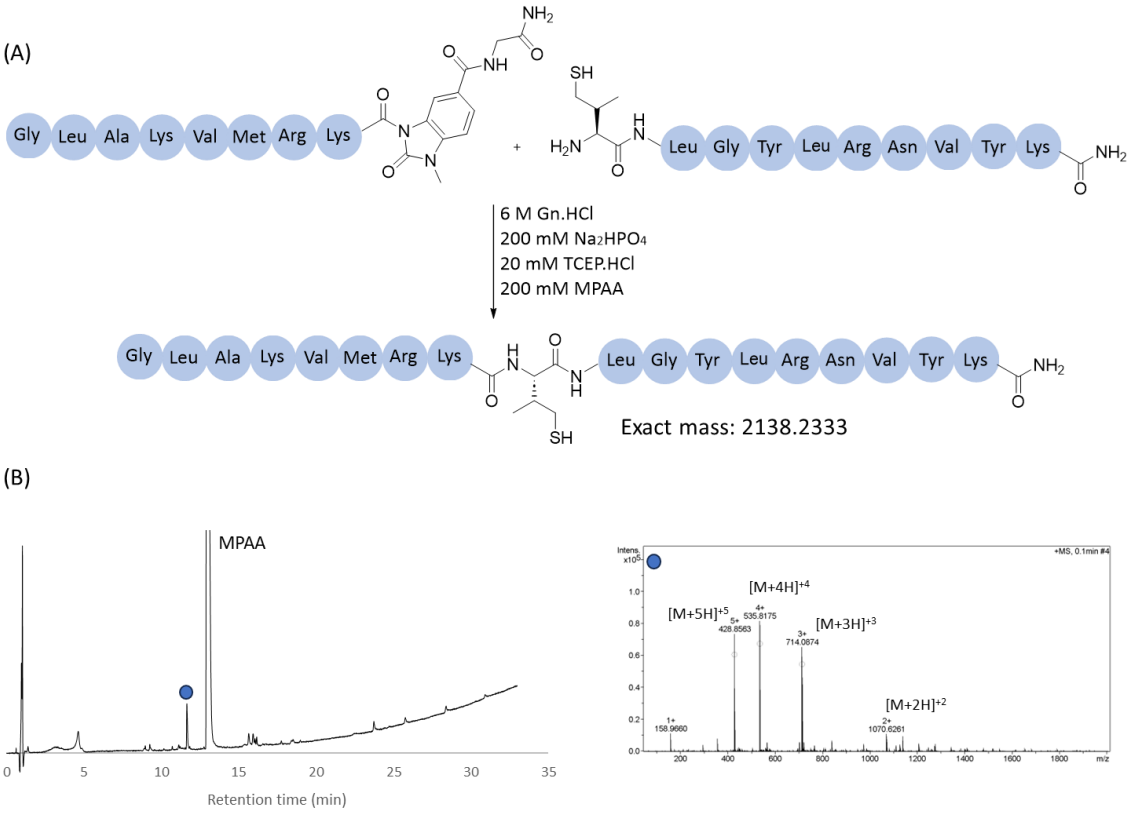

Figure 3.1. (A) NCL between peptide fragments **69** and **80** towards the formation of the ligated product **84** containing γ-thiol valine at the ligation site. (B) RP-HPLC (220 nm) of the crude material. ESI-MS analysis of the peak highlighted with the blue sphere confirmed the mass of the ligated product **84**.

3.2.2 Use of Vinylglycine (Vgl)

The next unsaturated amino acid employed in NCL to yield methionine at the ligation junction was commercially available vinylglycine (Vgl). In this study, Boc-Vgl-OH (**85**) was incorporated at the *N*-terminus of a peptide sequence, and following on-resin thiolation, cleavage and NCL, methylation of the free thiol group of the ligated product furnishes the methionine residue at the ligation site. Brevinin-2-related peptide (B2RP), a potent antimicrobial peptide with the sequence GIWDTIK(SM)GKVFAGKILQNL, was selected as an ideal target for synthesis through sequential NCL and methylation.[160] The ligation site, positioned between serine and methionine, allowed the synthesis of peptide fragment **86**, bearing a free thiol group at the *N*-terminus. This was achieved by synthesising the protected peptide **87** bearing Boc-Vgl at its *N*-terminus. Then, efforts were undertaken for on-resin hydrothiolation/deacetylation and subsequent peptide cleavage aiming to produce the peptide fragment **86**, suitable for NCL, in two efficient

and quantitative steps (**Scheme 3.7**). The final step of this work will be the ligation between peptide fragment **86** and the thioester **88**, followed by *S*-methylation to furnish the native methionine residue of **89** (**Scheme 3.7**).

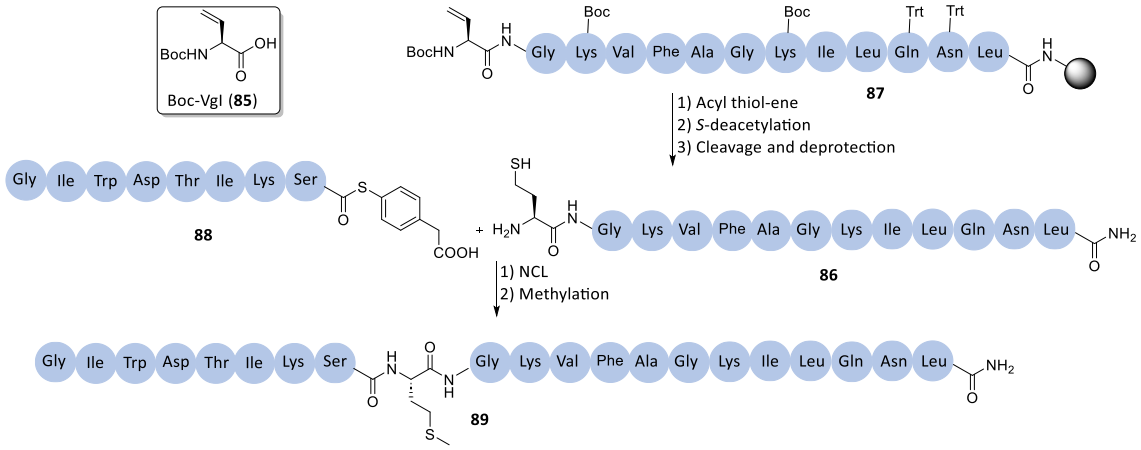

Scheme 3.7. Synthesis of B2RP *via* on-resin ATE and *S*-deacetylation reactions, followed by NCL/methylation strategy.

Even though Boc-VgI-OH is commercially available, it was decided to synthesise it in-house as shown in **Scheme 3.8**, since the procedure has been well-stablished by Rapoport and Afzali-Ardakani, and was then further optimised within the Scanlan group.[156,161] Initially, oxidation of Cbz-Met-OMe (**90**) towards the methyl sulfoxide **91** was achieved using sodium metaperiodate. The reaction proceeded quantitatively, and the product **91** was isolated *via* a simple work up with no need for chromatographic purification. Thermolysis of **91** towards the terminal alkene **92** was achieved by refluxing a solution of **91** in xylene for 72 h. TLC analysis of the crude reaction mixture indicated complete consumption of the starting material, but this step also produces the *cis*- and *trans*- isomers of the corresponding conjugated internal alkene, which lowers the overall yield significantly. The two internal alkene side-products were removed through multiple chromatographic purifications, and the protected terminal alkene **92** was isolated in a 22% yield. Simultaneous removal of Cbz and methyl ester protecting groups of **92** was achieved in 6 M aq. HCl under reflux for 3 h, followed by recrystallisation from acetone, yielding the VgI HCl salt **93** in a 75% yield. Finally, Boc protection of **93** was achieved with Boc_2O and $NaHCO_3$ under reflux in dioxane:H_2O (1:1), yielding the final Boc-VgI-OH (**85**) in 85% yield ready for incorporation in SPPS (Experimental Chapter, page 118).

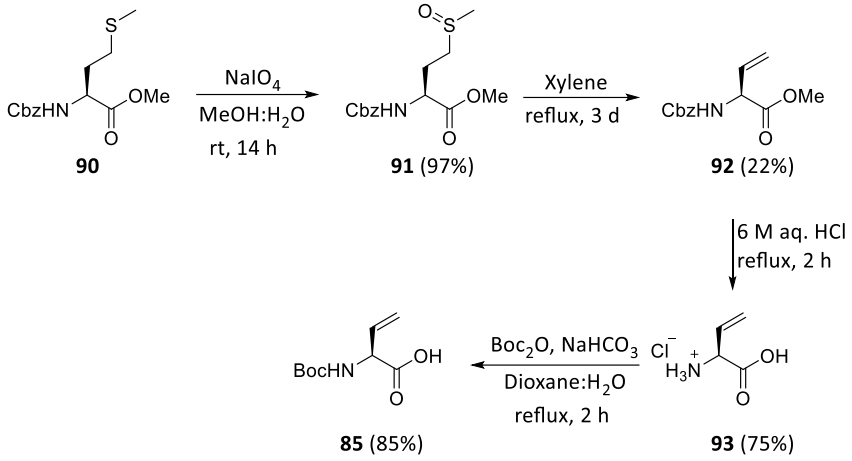

Scheme 3.8. Synthetic route undertaken to access Boc-VgI-OH (**85**).[156]

The synthetic strategy to access peptide fragment **86**, incorporating homocysteine at the *N*-terminus, is shown in **Scheme 3.9**. The peptide sequence was manually assembled using PyBOP and NMM as coupling agents. However, VgI is highly prone to isomerisation, leading to the formation of the internal alkene under basic conditions. To mitigate this issue, a base-free coupling protocol was employed for the acylation step of Boc-VgI-OH. The coupling was facilitated by using 2-isobutoxy-1-isobutoxycarbonyl-1,2-dihydroquinoline (IIDQ) in the absence of base. The *N*-deprotected resin-bound peptide was treated with a solution of Boc-VgI-OH (2 equiv.) and IIDQ (2 equiv.) in THF, with agitation over 120 hours. Successful coupling was confirmed *via* the bromophenol blue test. Following this, the resin-bound protected peptide was subjected to on-resin thiolation *via* the two on-resin reactions. On-resin ATE was performed under the optimised conditions, and the progress of the reaction towards the formation of the thioacetate group was checked by small-scale cleavage and deprotection and analysis of the linear intermediate by RP-HPLC and ESI-MS. Surprisingly, the RP-HPLC analysis revealed that the major product was the starting material, with VgI at the *N*-terminus, and only trace amounts of the desired thioacetate product were detected. Repeating the on-resin reaction under identical conditions yielded a thioacetate product with less than 5% conversion, as confirmed by RP-HPLC. Subsequent attempts to improve conversion involved varying irradiation times (1 h, 2 h, and 3 h) and repeating the reaction using significantly larger excess of thioacetic acid, DPAP, and MAP. However, no significant improvement in conversion was observed. Due

to the persistently low yields, the synthesis of the final linear unprotected peptide bearing *N*-terminal homocysteine could not be completed.

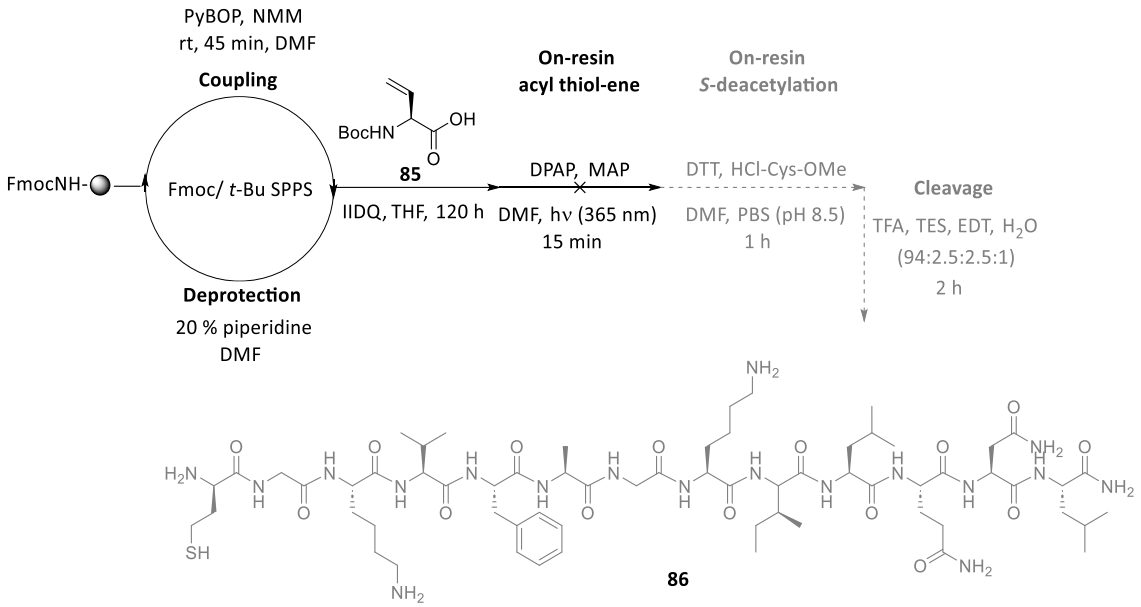

Scheme 3.9. Attempted synthetic route to access peptide fragment **86**.

The poor conversion of the on-resin thiol-ene reaction is attributed to the structural characteristics of VgI. As a terminal alkene, VgI contains one fewer methylene (-CH_2-) group than AgI, potentially making the alkene less exposed and thus, less reactive in a TEC reaction. However, the predominant explanation for the reduced reactivity of VgI compared to AgI is likely the amine-mediated inhibition of the radical TEC reaction. This phenomenon has been previously reported by Gautrot and coworkers, who conducted extensive studies on the reactivity of thiol-ene reactions.[162] Notably, their work demonstrated that allyl amines, such as VgI, exhibit significantly lower efficiency in radical TEC reactions, whether the amines are free or protected.[162] This is attributed to a reduced stability of the carbon-centred radical formed during the TEC reaction which is highly influenced by electronic effects of neighbouring atoms. In the case of allyl amines like VgI, the proximity of the amine group destabilises the carbon-centred radical intermediate, increasing the likelihood of a spontaneous fragmentation of this radical intermediate back to the initial alkene and thiyl radical. Conversely, AgI, which possesses an additional methylene group compared to VgI, is more reactive because the amine group does not exert a significant destabilising effect on the radical intermediate.

3.2.3 Use of Dehydroproline

The final unsaturated amino acid employed in the NCL project was Boc-3,4-Dehydro-L-proline (**94**). The aim of this work was to introduce the thiol group on the proline residue over two steps on-resin, followed by NCL and subsequent desulfurisation. SMAP-29 [9-29] is an antimicrobial peptide isolated from sheep with a sequence of KIAHGVKKY(GP)TVLRIIRIAG. SMAP-29 [9-29] was deemed as an ideal target for NCL and desulfurisation, utilising proline at the ligation site (**Scheme 3.10**).[163] As with previous targets, the goal was to install a thiol group on the proline residue of the protected **95** *via* sequential on-resin reactions. After cleavage, NCL between peptide fragment **96** and thioester **97**, followed by final desulfurization, would yield the native sequence of **98** (**Scheme 3.10**).

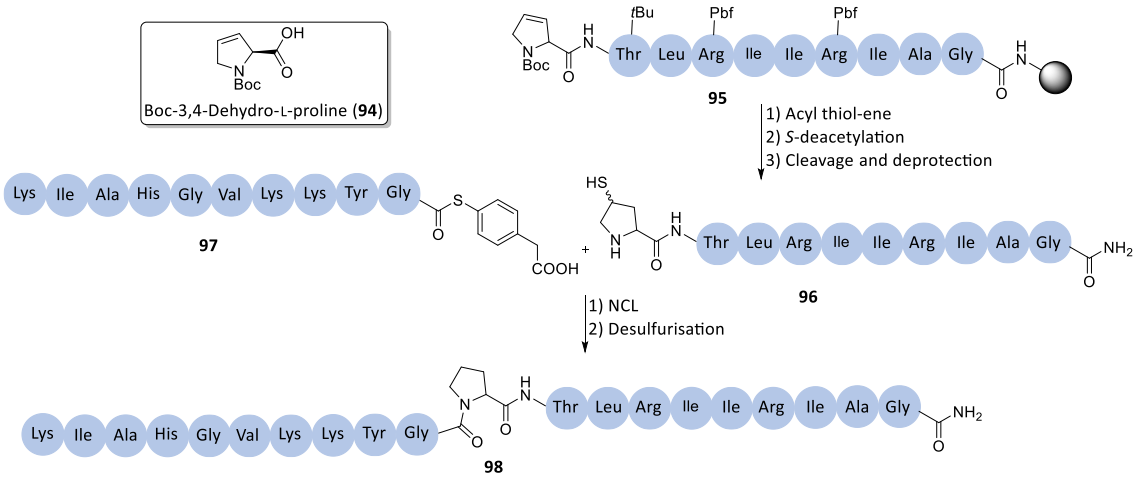

Scheme 3.10. Synthesis of SMAP-29 [9-29] *via* on-resin ATE and *S*-deacetylation reactions, followed by NCL/methylation strategy.

The unsaturated proline derivative **94** was also deemed a suitable substrate for direct on-resin thiolation due to well described literature syntheses of the compound.[164,165] The synthetic route described was undertaken as reported in the literature (**Scheme 3.11**).[164,165] Methyl ester protection of L-hydroxyproline **99** was carried out using $SOCl_2$ in methanol yielding **100** in a 98% yield. Boc protection of **100** was carried out directly to furnish alcohol **101** in a 79% yield following chromatographic purification. Next, conversion of alcohol **101** to *cis*-γ-iodoproline **102** was performed under Mitsunobu conditions with inversion of stereochemistry at the γ-position, using diisopropyl azodicarboxylate (DIAD), triphenyl phosphine (PPh_3) and iodomethane

(MeI). Formation of **102** was observed by TLC analysis (R_f 0.54), but the starting alcohol **101** was still present after 18 h. The crude product was purified *via* column chromatography and *cis*-γ-iodoproline **102** was isolated in a 39% yield. Elimination of iodide **102** was carried out by using 1,8-diazabicyclo-[5.4.0]-undec-7-ene (DBU) as a base in toluene, and the alkene **103** was isolated in 90% yield following column chromatography purification. The final ester hydrolysis of **103** was achieved under basic conditions using sodium hydroxide (NaOH) in THF/H_2O yielding the final unsaturated proline **94** in a 74% yield, ready for incorporation in SPPS (Experimental Chapter, page 121).

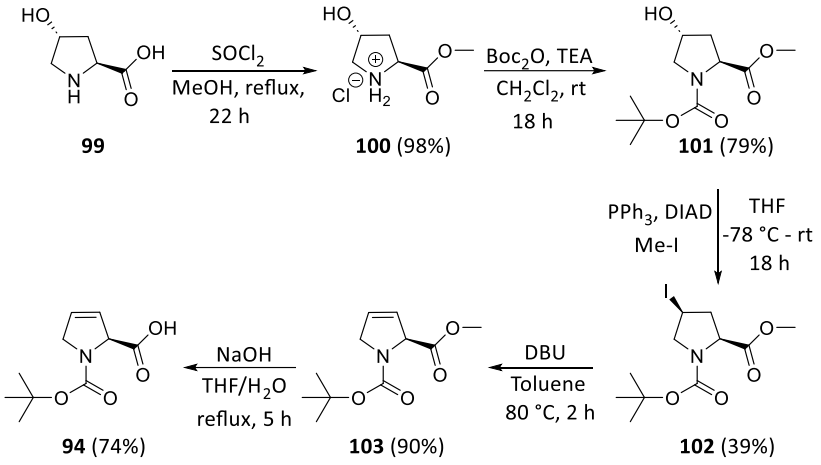

Scheme 3.11. Synthetic route undertaken to access Boc-L-3,4-Dehydroproline (**94**).[164,165]

The synthetic strategy to access peptide fragment **96**, containing thiol-proline at the *N*-terminus, is shown in **Scheme 3.12**. The peptide sequence was manually assembled using PyBOP and NMM as coupling reagents. For the final coupling of Boc-dehydroproline (**94**), DIC and Oxyma Pure were employed. Radical-mediated hydrothiolation of the proline derivative on resin was conducted under optimised conditions. However, RP-HPLC and ESI-MS analyses revealed very poor conversion in the on-resin ATE reaction step, with limited formation of the desired thioacetate product. Attempts to improve the reaction yield by extending reaction times and using a larger excess of thioacetic acid, DPAP, and MAP did not result in significant improvement. The observed inefficiency in the ATE reaction can be attributed to the same issue encountered with VgI. Boc-dehydroproline, like VgI, is an allyl amine. The carbon-centred radical generated during the reaction is possibly destabilised by the

proximity of the Boc-protected secondary amine group, likely leading back to the initial alkene. Consequently, the total synthesis of the final linear unprotected peptide fragment **96** could not be completed. These results suggest that the on-resin peptide thiolation methodology is effective for unsaturated amino acids only when the alkene group is located at least two carbon atoms away from the amine group.

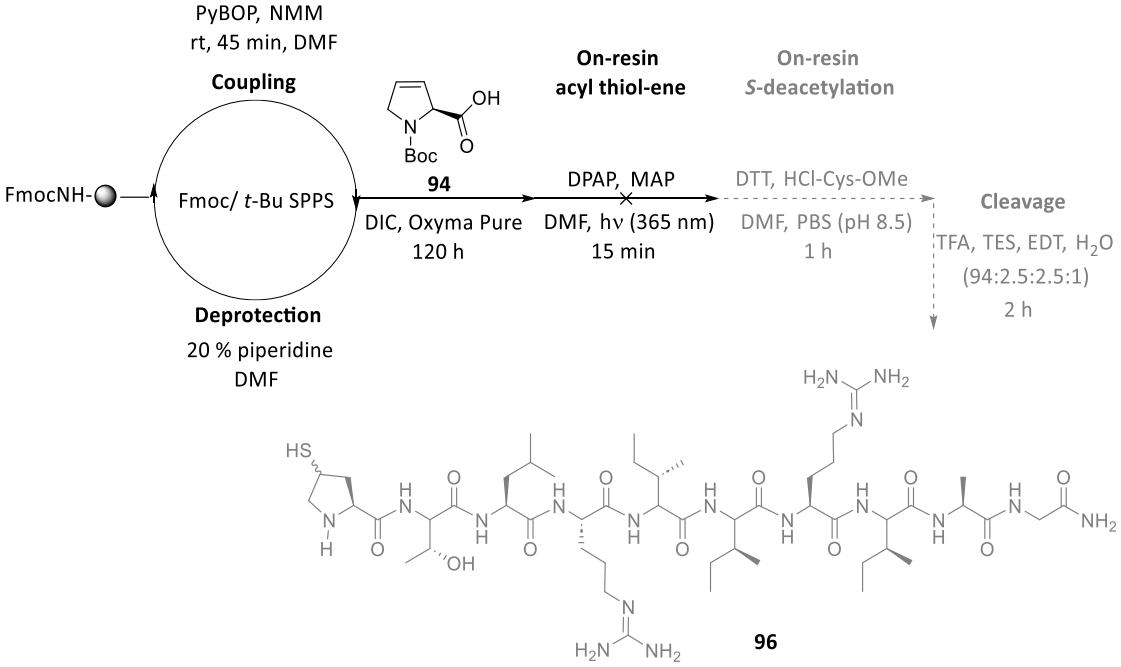

Scheme 3.12. Attempted synthetic route undertaken to access peptide fragment **96**.

3.2.4 Use Sequential ATE and *S*-deacetylation For On-resin Peptide Conjugation

To further extend the applicability of on-resin hydrothiolation, this approach was employed for the fluorescent labelling of a linear peptide containing the arginylglycylaspartic acid (RGD) motif. Peptides incorporating the RGD sequence are known to exhibit high affinity for the αvβ3 integrin receptor, which is overexpressed in various cancer cells.[166] Thereby, RGD-based agents have been widely used in cancer treatments, for both therapeutic and diagnostic purposes.[166,167] In 2002, Bansal and coworkers developed the ^{18}F-labelled linear RGD peptide **104** (KPQVTRGDVFTEG) to investigate its biodistribution in tumour-bearing mice.[168] As illustrated in **Figure 3.2**, the RGD motif was centrally positioned within the peptide, while 4-[^{18}F]fluorobenzoic acid

was conjugated to the side-chain amine of the *N*-terminal lysine residue. This peptide sequence was deemed an ideal target for on-resin thiolation and subsequent on-resin covalent attachment of a fluorescence tag by utilising the free thiol group. In this work, the *N*-terminal lysine residue of **104** was replaced with Boc-AgI. Following on-resin hydrothiolation, the exposed thiol group at the *N*-terminus of **105** served as a reactive site for covalent attachment of a fluorophore prior to peptide cleavage and deprotection.

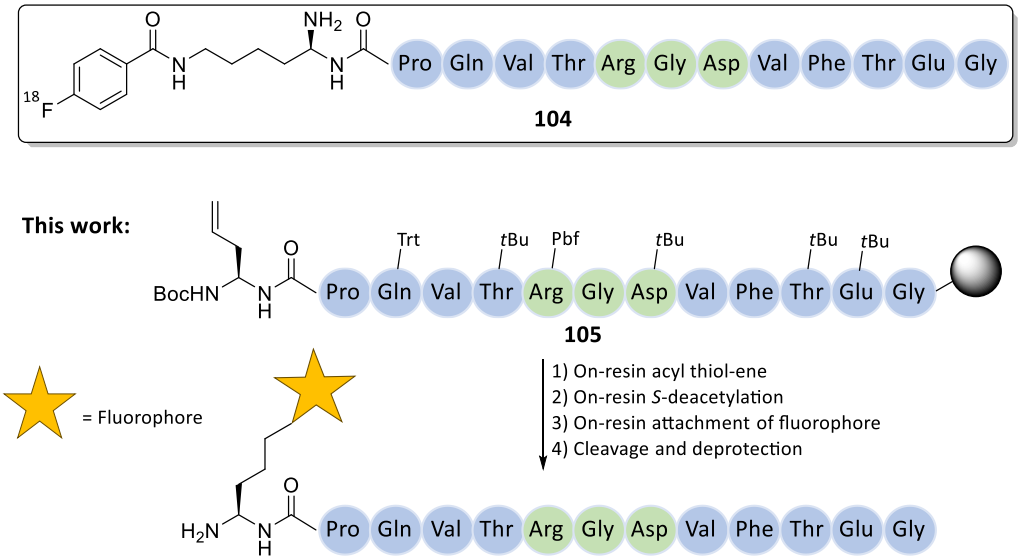

Figure 3.2. Application of the on-resin thiolation for the covalent attachment of a fluorophore tag onto the linear RGD peptide **105**.

Ortho-aminobenzoic acid (Abz) is a simple fluorescent molecule that was employed in this work.[169] The Abz fluorophore was linked through a small diamino spacer to a maleimide moiety which is highly reactive in presence of free thiols. The synthesis of the Boc-protected fluorophore **106** that was used for the on-resin covalent attachment has not been reported in the literature. **Scheme 3.13** shows the synthetic route that was designed to access the final compound **106**. The synthesis started with the Boc-protection of one of the two amines of 1,3-diaminopropane (**107**) as described by Gilon and coworkers, *via* dropwise addition of a solution of Boc_2O in a stirring solution of **107** in chloroform ($CHCl_3$).[170] The protected amine **108** was isolated in 88% yield following chromatographic purification. Next, condensation of **108** with maleic anhydride was carried out as described by Parthasarathy and coworkers.[171] Reaction of the free amine **108** with maleic acid and subsequent cyclisation using sodium acetate (NaOAc) in acetic anhydride (Ac_2O) furnished **109** in 35% yield over two steps. Near

quantitative Boc deprotection of **109** was achieved in a TFA/CH_2Cl_2 mixture leading to the TFA salt **110**. Finally, amide coupling of **110** with the commercially available Boc-Abz-OH was achieved by using EDC·HCl and HOBt as coupling reagents and DIPEA as an activating base and the final protected fluorophore **106** was isolated in a 69% yield after chromatographic purification (Experimental Chapter, page 123).

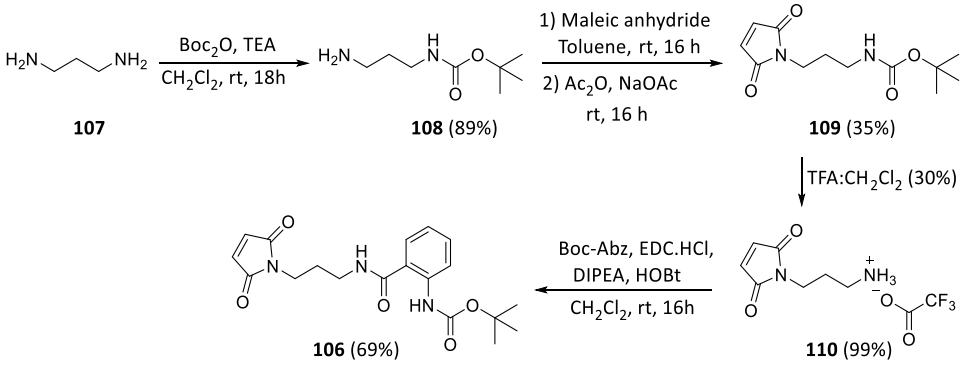

Scheme 3.13. Synthetic route undertaken to access **106**.

Scheme 3.14 shows the synthetic route undertaken to access the final RGD analogue **111** bearing the Abz fluorophore at the *N*-terminus of the sequence. The peptide was manually synthesised using PyBOP and NMM as coupling agents, with the final Boc-AgI coupled under similar conditions. The two sequential on-resin reactions for hydrothiolation followed using the previously described optimised conditions. As anticipated and shown in **Chapter 2**, both reactions proceeded with quantitative yields, yielding clean products, and successfully installing the thiol group at the *N*-terminus. These results align with the observation that the on-resin thiol-ene reaction is highly efficient for alkene groups positioned at least two carbon atoms away from the amine group. The final step was the on-resin covalent attachment of the protected fluorophore **106** *via* the nucleophilic attack of the free thiol moiety to the maleimide group. This achieved by treating the resin-bound peptide with a solution of **106** (10 equiv.) and TEA (10 equiv.) in DMF and agitation of the system for 1 h. TEA was employed as a base to ensure the deprotonation of the free thiol group and increase of its nucleophilicity. The progress of the covalent attachment of fluorophore **106** was checked by small-scale peptide cleavage and deprotection and analysis of crude product by RP-HPLC and ESI-MS. Upon cleavage, the Boc group of the fluorophore was removed, revealing the free Abz moiety at the *N*-terminus of the peptide. Gratifyingly, RP-HPLC analysis confirmed

complete consumption of the starting material, with the appearance of a new major peak corresponding to the final peptide **111**, as verified by ESI-MS. Following purification *via* semi-preparative RP-HPLC purification, **111** was isolated in a 22% yield and with >95% purity as confirmed by analytical RP-HPLC (Experimental Chapter, page 124).

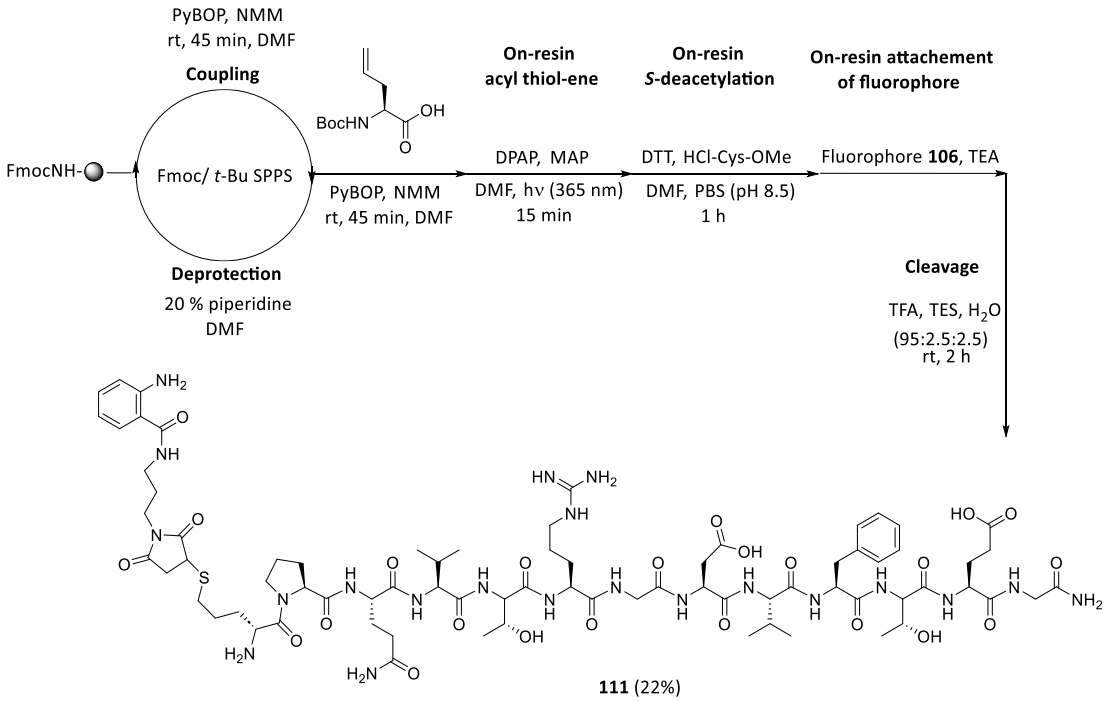

Scheme 3.14. Synthetic route undertaken to access the linear RGD **111** bearing the Abz fluorophore at the *N*-terminus.

3.3 Conclusions and Future Work

In conclusion, this study reports the application of the on-resin peptide hydrothiolation methodology developed in **Chapter 2** within the context of NCL. The synthesis of thiolated analogues of natural amino acids, commonly used in NCL and subsequent desulfurisation, is typically a laborious process requiring multiple intermediate purification steps. To address this limitation, we utilised commercially available unsaturated analogues of natural amino acids, with the aim of regioselectively introducing a thiol group in just two straightforward steps, followed by NCL and desulfurisation to regenerate the native amino acid at the ligation site. The three commercially available unsaturated amino acids, Boc-Dhv, Boc-VgI, and Boc-dehydroproline, were employed to assess the compatibility of the thiolation

methodology with NCL. Importantly, the two on-resin reactions enabled the successful thiolation of Boc-Dhv, ultimately yielding peptide fragment **69**, containing γ-thiol valine at the *N*-terminus. This peptide was subsequently ligated with the peptide thioester **80** to generate the antimicrobial peptide Ixosin [H3A, E8K, E13L, S16V], with γ-thiol valine at the ligation junction. Ongoing work focuses on desulfurising this peptide to produce the native valine at the ligation site. In contrast, attempts to thiolate Boc-VgI and Boc-dehydroproline at the *N*-terminus of two peptide targets *via* the same on-resin reactions were unsuccessful, despite multiple optimisation efforts. This failure may be attributed to the common structural feature that both amino acids share. There is only one -CH_2- group separating the alkene groups from the Boc-protected amines, thus the intermediate carbon-centred radicals formed during the TEC reaction are highly destabilised, promoting the undesired elimination process and resulting in the formation of the starting alkenes. To overcome this limitation, future work will focus on exploring unsaturated analogues of natural amino acids in which the alkene group is positioned at least two carbon atoms away from the amine group, to ensure successful thiolation, followed by NCL and desulfurisation.

To further expand the scope of the developed methodology, we demonstrated the successful on-resin, covalent attachment of the Abz fluorophore **106** onto the linear RGD peptide analogue **105**. AgI was employed and incorporated at the *N*-terminus of the RGD peptide and following on-resin thiolation, the fluorophore **106** was covalently attached on the free thiol handle under basic conditions. This approach enabled the covalent linkage of the fluorophore *via* three sequential quantitative on-resin reactions without the need for intermediate purification steps, paving the way for new developments in peptide bioconjugation. Future work will focus on extending this methodology for on-resin conjugation with sugars, lipids, and cytotoxic agents using the free thiol handle of biologically relevant peptides. Use of AgI and other commercially available unsaturated amino acids will be employed for on-resin thiolation aiming to further diversify the conjugated peptide structures.

Chapter 4

Thiol-ene Mediated Late-stage Modification of Cyclic Peptides

4.1 Introduction and Aim

As discussed in **Section 1.1.2**, macrocyclic peptides offer several advantages over their linear counterparts for drug development, including enhanced affinity and specificity towards biological targets, as well as improved *in vivo* stability. However, late-stage chemical modifications of cyclic peptides—such as glycosylation, lipidation, and fluorophore conjugation—are often required to optimise their pharmacokinetic profiles and to expand their applications in drug discovery. As described in **Section 1.4.1**, Brimble and coworkers developed a sequential process for lipidation of cyclic peptides by employing NCL for peptide cyclisation and TEC ligation for the covalent attachment of a variety of lipids onto the thiol group of the Cys residue (**Scheme 1.8.B**).[123] Nevertheless, NCL-mediated peptide cyclisation presents some major synthetic challenges as it requires the use of specific types of resins or linkers at the *C*-terminus of the peptide sequence that can enable the *in situ* formation of the thioester group. In addition, If the cyclisation kinetics are slow, competing hydrolysis of the thioester group can generate the free carboxylic group at the *C*-terminus of the peptides, terminating the cyclisation process.

In 2022, Heinis and coworkers introduced a novel strategy for peptide library synthesis involving late-stage modification of macrocyclic peptides.[172] This method employed a sequential approach to generate '*m*' number of disulfide-linked cyclic peptide scaffolds, followed by acylation of a peripheral amine group by 'o' numbers of carboxylic acid fragments, ultimately yielding '*m* x *o*' numbers of cyclic peptides. The design included three types of amino acids: one amino acid containing a primary amine group in the side chain (represented as a blue sphere), one with a random side chain (green sphere), and one with a random backbone structure (purple sphere). The disulfide bond formation was achieved on-resin through side chain deprotection, followed by spontaneous oxidative cyclisation (**Scheme 4.1**). This approach enabled the synthesis of 384 distinct cyclic peptide scaffolds, which were subsequently reacted with 12 carboxylic acids using HBTU and DIPEA as activating agents, generating a library of 4608 macrocyclic peptides. These were then screened for thrombin inhibition. Earlier this year, the same research group extended this approach by employing acylation as a

late-stage modification to construct a library of thioether-linked cyclic peptides.[173] This modification allowed the development of more structurally diverse macrocycles with improved pharmacokinetic properties. However, the post-cyclisation acylation reaction requires the use of coupling reagents, which can complicate library synthesis by generating a considerable number of byproducts in presence of other reactive side chains.

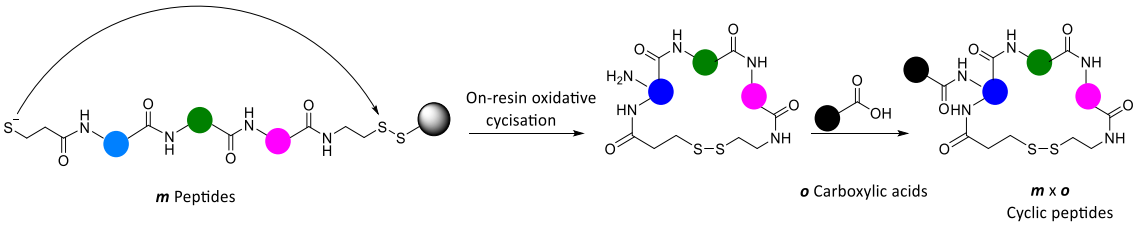

Scheme 4.1. General depiction of the library synthesis strategy developed by Heinis and coworkers.[172]

The objective of this study is to develop a novel TEC-mediated approach for the late-stage modification of cyclic peptides, enabling applications in target synthesis, peptide library synthesis, and high-throughput screening of cyclic peptide binders, such as those identified *via* mRNA display. This work describes the use of AgI within sequences and peptide cyclisation by employing the reactive chloro-acetyl group at the *N*-terminus. Under basic conditions, the chloroacetyl group undergoes intramolecular nucleophilic attack by a thiolate residue, resulting in the formation of a stable thioether linkage (**Scheme 4.2**). Following cyclisation, AgI can be serve as a versatile chemical handle for the covalent attachment of thiolated biomolecular fragments *via* TEC reaction. Notably, this post-cyclisation peptide modification strategy is entirely biorthogonal because AgI is completely stable under the basic conditions required for the cyclisation, and the TEC reaction proceeds efficiently in the presence of unprotected side chains with limited formation of by-products.

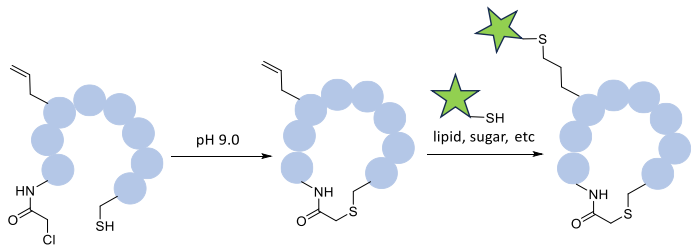

Scheme 4.2. Synthetic approach used in this project.

4.2 Results and Discussion

Vasopressin was selected as a model peptide to evaluate the applicability of this novel late-stage chemical modification strategy, owing to its biological significance. The workflow employed in this study is depicted in **Scheme 4.3**. Specifically, the Asn residue at position 4 in the native sequence was substituted with AgI to maintain a comparable chain length. During SPPS, the Cys at the *N*-terminus of the native sequence was replaced with a chloroacetyl residue which, following cleavage and deprotection, enabled the cyclisation of the linear unprotected **112** under basic conditions towards the formation of the thioether-linked **113**. Thereafter, TEC-mediated covalent attachments of various thiolated substrates to the unprotected vasopressin analogue were performed (**Scheme 4.3**).

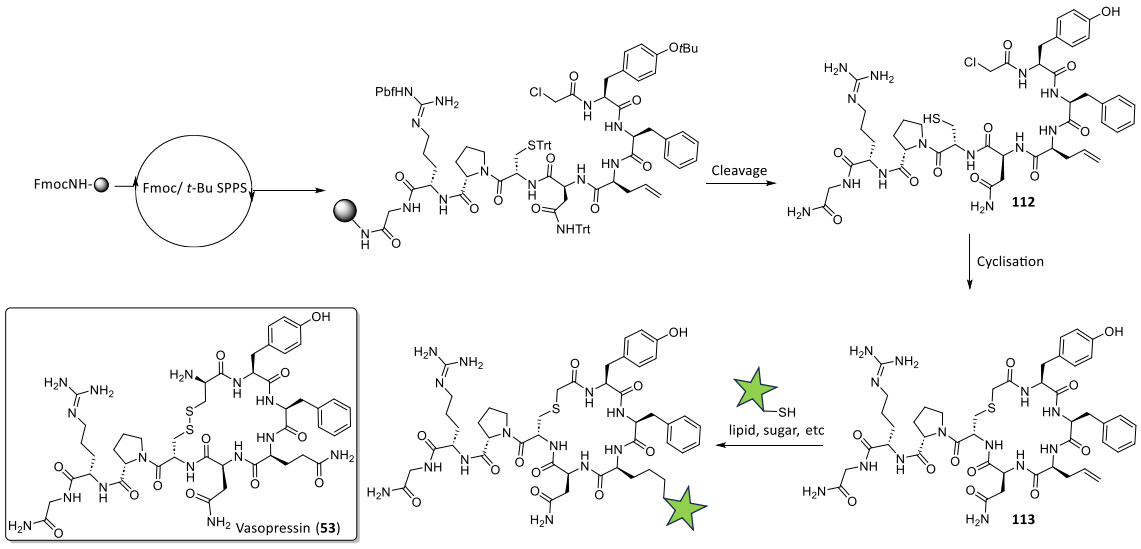

Scheme 4.3. Workflow undertaken in this project.

4.2.1 Synthesis of Thioether-linked Vasopressin Analogue **114**

The intramolecular Cys alkylation with a primary alkyl halide within the peptide sequence is a well-established reaction and is widely reported in the literature. In 2005, Dawson and Brunel demonstrated the utility of this approach by constructing a small library of constrained helical peptides featuring thioether linkages, achieved through the incorporation of a bromoacetylated ornithine (Orn) residue within peptide sequences (**Scheme 4.4.A**).[174] Boc-SPPS was employed to access the linear peptides bearing a Cys residue and an Fmoc-protected Orn residue. On-resin Fmoc deprotection followed

under basic conditions using 20% piperidine in DMF and the free amine group of Orn was subsequently coupled to bromoacetic acid preactivated with DIC in CH_2Cl_2. Following peptide cleavage and deprotection using HF, the intramolecular thioether link was formed by dissolving the linear peptides in a 1 mM solution of 6 M Gnd·HCl, 100 mM NaH_2PO_4 and pH 8.5, and the cyclic thioether peptides were finally formed in high yields and purity. More recently, Payne and coworkers developed a small library of thioether-linked cyclic peptides targeting the main protease of SARS-CoV-2.[175] In this work, the authors employed Fmoc-SPPS to access the linear peptides with *N*-terminal L- or D- Tyr residue derivatised with chloroacetic acid, enabling subsequent thioether cyclisation. Following peptide cleavage and deprotection, intramolecular Cys alkylation was achieved by dissolving the linear peptides in a 1 mM solution of H_2O/AcN (1:1) in presence of DIPEA to promote the thiolate formation. These optimised conditions were also applied by the same research group towards the development of a library of thioether-linked cyclic sulfopeptides targeting chemokine.[176]

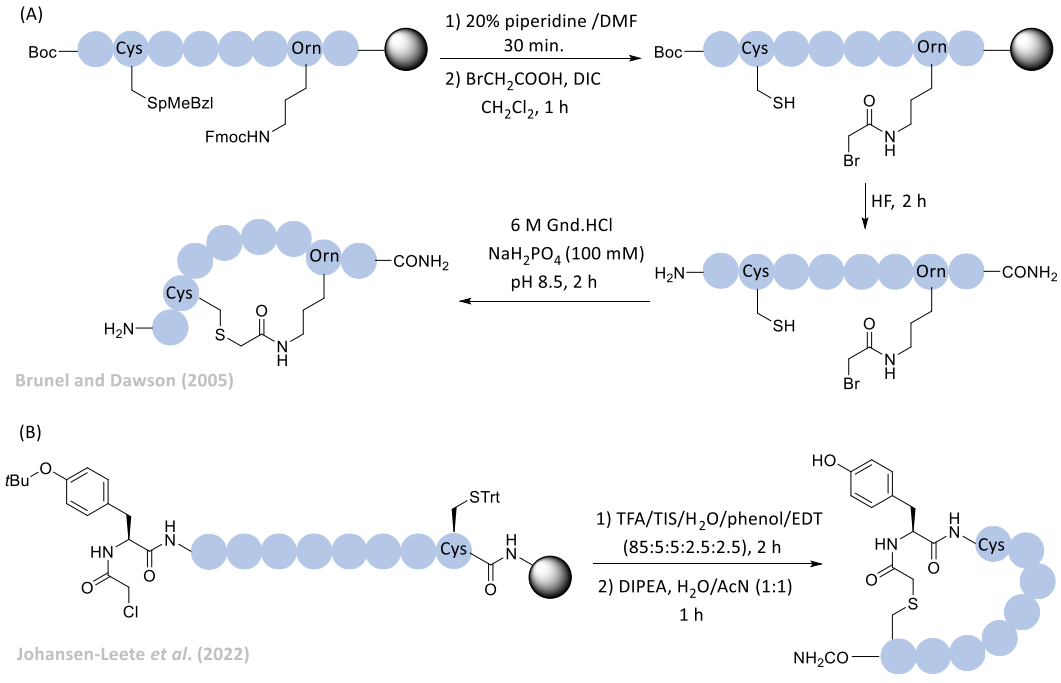

Scheme 4.4. (A) Development of helical peptides by thioether liagation.[174] (B) Development of thioether-linked cyclic peptide binders of the main protease of SARS-CoV-2.[175]

Described in this chapter, the intramolecular Cys alkylation reaction was initially applied on the linear precursor **115** bearing the native asparagine at position 4 and replacing the Cys at the *N*-terminus with a chloroacetyl group which can enable the

thioether cyclisation. **Scheme 4.5** illustrates the synthesis undertaken to access the thioether-linked vasopressin analogue **114**. The linear peptide precursor **115** was synthesised on a CEM Liberty Blue peptide synthesiser, and following the final Fmoc deprotection, the *N*-terminal Tyr was chloroacetylated on the resin. This was achieved by treating the resin-bound peptide with a solution of chloroacetic anhydride (10 equiv.) and TEA (10 equiv.) in DMF for 1 h. Successful *N*-terminal chloro-acetylation was confirmed using the bromophenol blue test. Following peptide cleavage and deprotection the linear peptide **115** was obtained in high purity as confirmed by analytical RP-HPLC and ESI-MS. Cyclisation of peptide **115** was subsequently performed in a 1 mM solution of H_2O/AcN (1:1, pH 10.0) for 2 h. Upon completion, the pH of the solution was adjusted to 5.0 and the crude material was lyophilised. RP-HPLC and ESI-MS analysis of the crude material indicated complete conversion of the linear precursor to the cyclic product **114**. Semi-preparative RP-HPLC purification afforded the final thioether-linked vasopressin analogue **114** in a 18% yield and with >90% purity as confirmed by analytical RP-HPLC (Experimental Chapter, page 126).

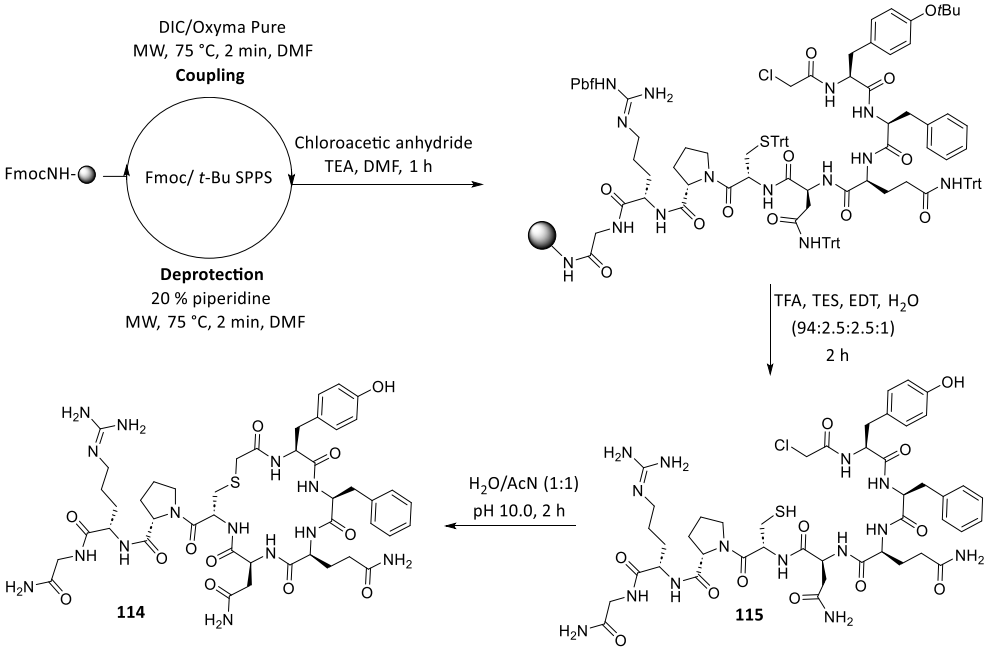

Scheme 4.5. Synthetic route undertaken to access thioether-linked vasopressin analogue **114**.

4.2.2 Synthesis of The Unsaturated Thioether-linked Vasopressin Analogue **116** and Post-Cyclisation TEC-Mediated Modifications

The synthesis of vasopressin analogue **116**, incorporating AgI at position 4, was achieved similar to vasopressin analogue **114** (**Scheme 4.6**). The linear peptide **117** was synthesised on a CEM Liberty Blue peptide synthesiser, and the on-resin chloro-acetylation was performed manually as described in **Section 4.2.1**. Upon peptide cleavage and deprotection, linear intermediate peptide **117** was obtained in good purity. The mass of the linear peptide **117** was identified under the predominant RP-HPLC peak, with a retention time of 11.743 minutes (**Figure 4.1.A**). Subsequently, the peptide **117** was subjected to cyclisation as described in **Section 4.2.1**. Gratifyingly, RP-HPLC and ESI-MS analysis of the crude product indicated a near-quantitative formation of the cyclic peptide **116** with only traces of the starting linear peptide **117** present (**Figure 4.1.B**). The mass of the cyclic peptide **116** was identified under the main RP-HPLC peak, with a retention time of 11.478 minutes (**Figure 4.1.B**). Finally, semi-preparative RP-HPLC purification yielded the final unsaturated thioether-linked vasopressin analogue **116** in a 26% yield and with >95% purity as confirmed by analytical RP-HPLC (Experimental Chapter, page 127). The terminal alkene of the pure analogue **116** served as a chemical handle for the subsequent TEC reactions incorporating various thiol-containing substrates.

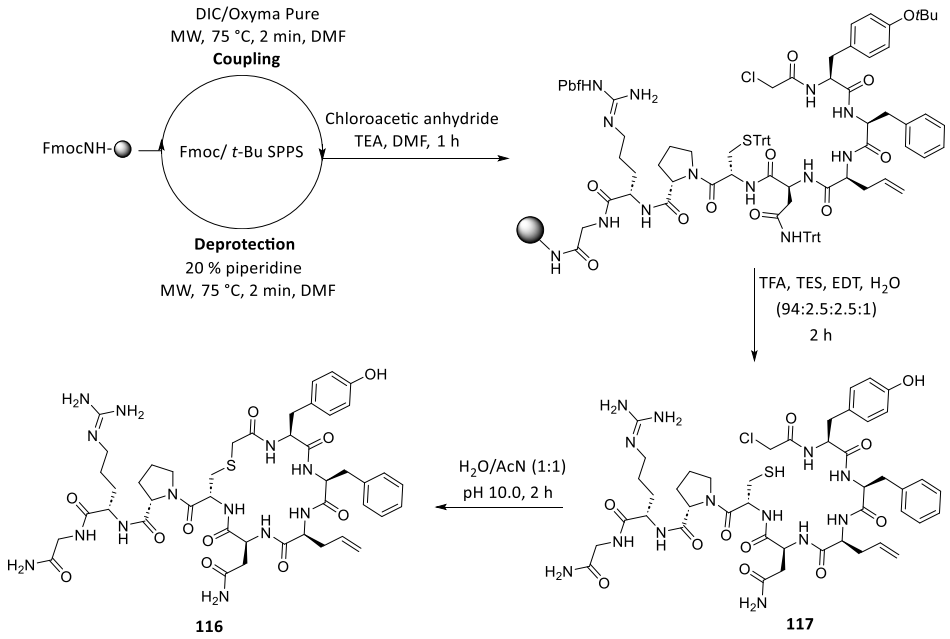

Scheme 4.6. Synthetic route undertaken to access thioether-linked vasopressin analogue **116**.

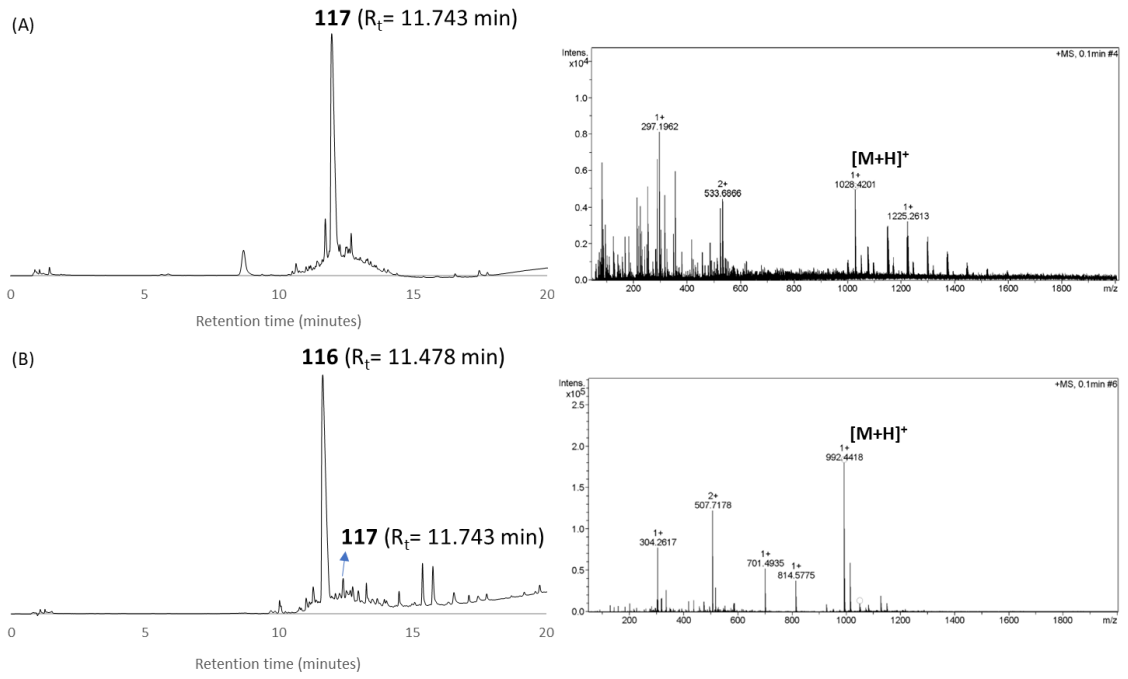

Figure 4.1. (A) Analytical RP-HPLC (254 nm) of the crude linear **117**. ESI-MS analysis of the main peak with a retention time of 11.743 minutes confirmed the mass of the linear peptide **117** (1028.4201, $[M+H]^{+1}$ requires 1028.4101). (B) Analytical RP-HPLC (254 nm) of the crude cyclic **116**. ESI-MS analysis of the predominant peak with a retention time of 11.478 minutes confirmed the mass of the cyclic peptide **116** (992.4418, $[M+H]^{+1}$ requires 992.4334).

GSH (**118**) was the first thiol-containing molecule employed in the radical TEC reaction with **116**. GSH, a tripeptide substance made from glycine, cysteine, and glutamic acid, is the most abundant non-protein thiol-containing thiol substance in human cells.[177] It plays a critical role in protecting cellular components from oxidative damage caused by reactive oxygen species (ROS), free radicals, and peroxides. Due to its low cost and commercial availability, GSH is commonly used as a thiol donor in chemical reactions. The TEC reaction between vasopressin analogue **116** (1 equiv.) and GSH (2 equiv.) was carried out in a 5 mM solution of H_2O/AcN (1:1) using DPAP (0.5 equiv.) as a photoinitiator, and the reaction mixture was irradiated at 365 nm for 2 h (**Figure 4.2.A**). Notably, these conditions led to near-quantitative formation of the desired ligated product **119** with only traces of the starting material **116** present in the crude mixture as confirmed by analytical RP-HPLC and ESI-MS. The mass of the ligated peptide **119** was identified under the RP-HPLC peak with a retention time of 10.665 minutes (**Figure 4.2.C**). The main RP-HPLC peak with a retention time of 10.822 minutes

corresponds to the DPAP fragmentation byproduct. Semi-preparative RP-HPLC purification yielded the final ligated product **119** in a 11% yield with >95% purity as confirmed by analytical RP-HPLC (Experimental Chapter, page 128).

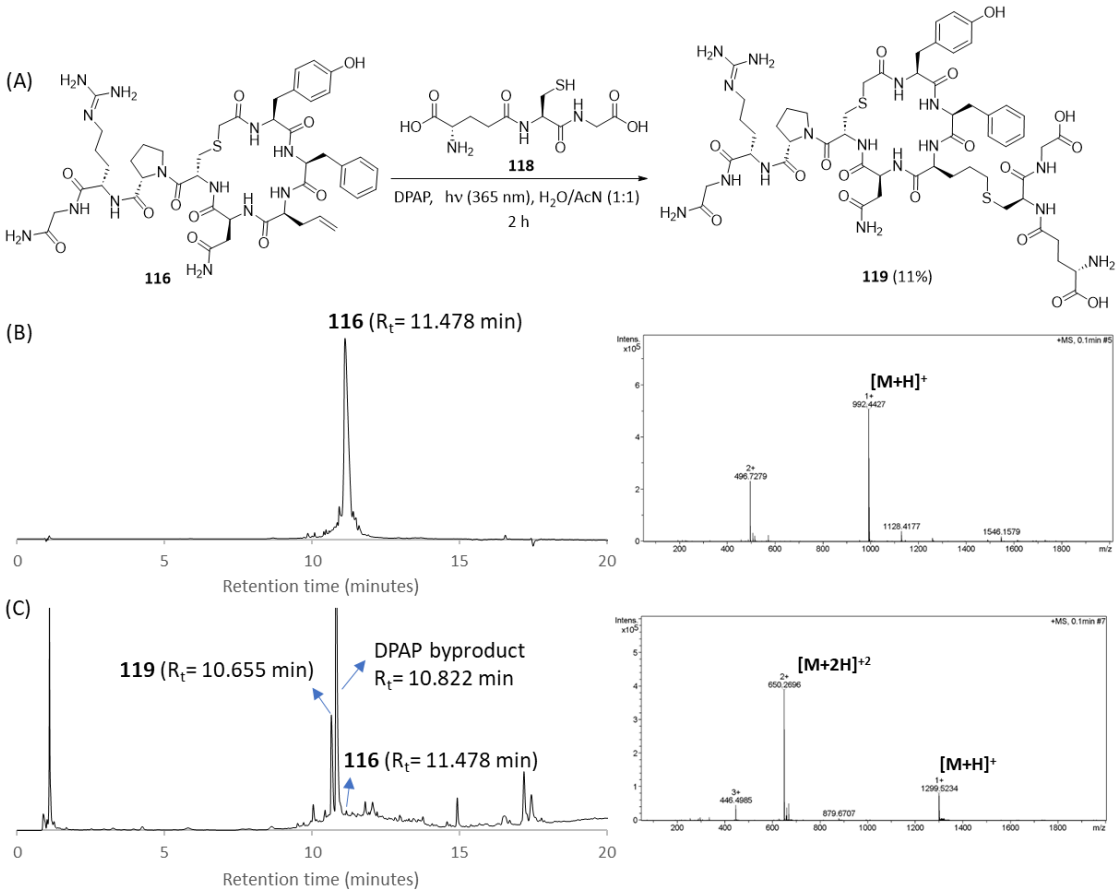

Figure 4.2. (A) Radical TEC reaction between **116** and GSH towards the formation of the ligated product **119**. (B) Analytical RP-HPLC (254 nm) and ESI-MS analysis of the pure peptide **116** (992.4427, $[M+H]^{+1}$ requires 992.4334, 496.7279, $[M+2H]^{+2}$ requires 496.7167). (C) Analytical RP-HPLC (254 nm) of the crude ligated product **119**. ESI-MS analysis of the peak with a retention time of 10.655 minutes confirmed the mass of the ligated product **119** (1299.5234, $[M+H]^{+1}$ requires 1299.5172, 650.2696, $[M+2H]^{+2}$ requires 650.2586).

Identical reaction conditions were subsequently applied for lipidation of **116** by using decanethiol **120** as a thiol donor (**Figure 4.3.A**). Incorporation of lipids onto peptide therapeutics is a well-known strategy for improvement of their enzymatic stability, potency, and bioavailability.[178] This reaction was conducted in a mixed solvent of H_2O/AcN/DMF (1:1:1) to enhance the solubility of decanethiol. The reaction mixture was irradiated at 365 nm for 2 h, and following removal of the solvents under reduced

pressure, the crude mixture was analysed by analytical RP-HPLC and ESI-MS. Notably, the RP-HPLC trace indicated complete consumption of starting material **116**, however, no new peak corresponding to the mass of the desired lapidated product **121** was observed, possibly due to very low solubility of the lipidated product **121** in H_2O (**Figure 4.3.C**). Nevertheless, ESI-MS analysis of the crude material indicated a clear formation of the desired lipidated product **121** with only traces of the starting material **116** present (**Figure 4.3.C**). Unfortunately, multiple efforts to isolate the lipidated product **121** by semi-preparative RP-HPLC were unsuccessful due to the low solubility of the product in the H_2O/AcN solvent system.

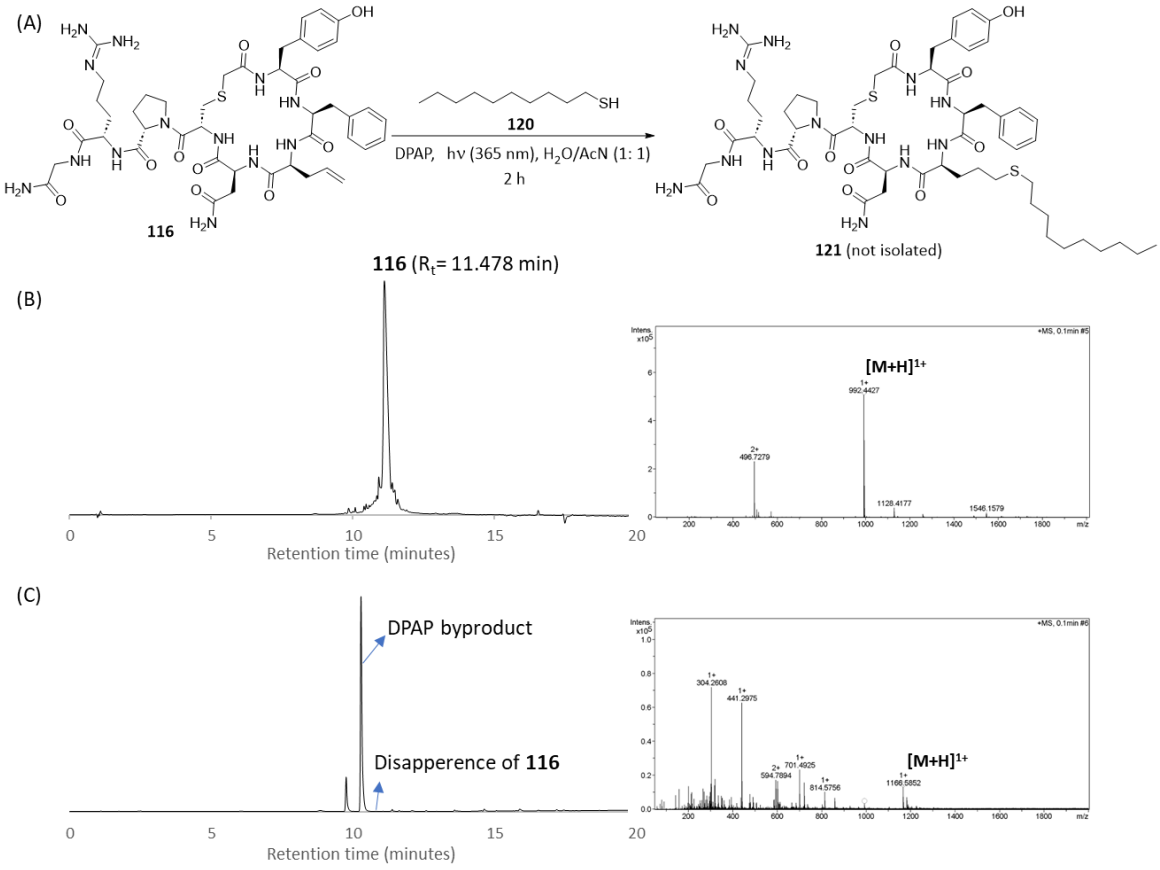

Figure 4.3. (A) Radical TEC reaction between **116** and decanethiol **120** towards the formation of the lipidated product **121**. (B) Analytical RP-HPLC (254 nm) and ESI-MS analysis of the pure peptide **116**. (C) Analytical RP-HPLC (254 nm) of the crude product **121**. ESI-MS analysis of the crude product confirmed the mass of the lipidated product **121** (1166.5852, $[M+H]^{+1}$ requires 1166.5776).

Subsequently, the post-cyclisation TEC reaction was investigated for direct glycosylation of **116** by employing 1-thio-2-acetamido-2-deoxy-β-D-glucopyranose

(**122**), (synthesised by undergraduate student Dillon Johnston as part of his final year project). Peptide glycosylation is a well-established strategy for improvement of the metabolic stability, bioavailability, and biodistribution in tissues of peptide therapeutics.[179] The reaction was performed under the same conditions used for the synthesis of **119** and RP-HPLC and ESI-MS analysis of the crude product indicated complete consumption of the starting material **116** and successful formation of the glycosylated peptide **123**. Following semi-preparative RP-HPLC purification, the glycosylated product **123** was obtained with an 8% yield and >95% purity as confirmed by analytical RP-HPLC (Experimental Chapter, page 130).

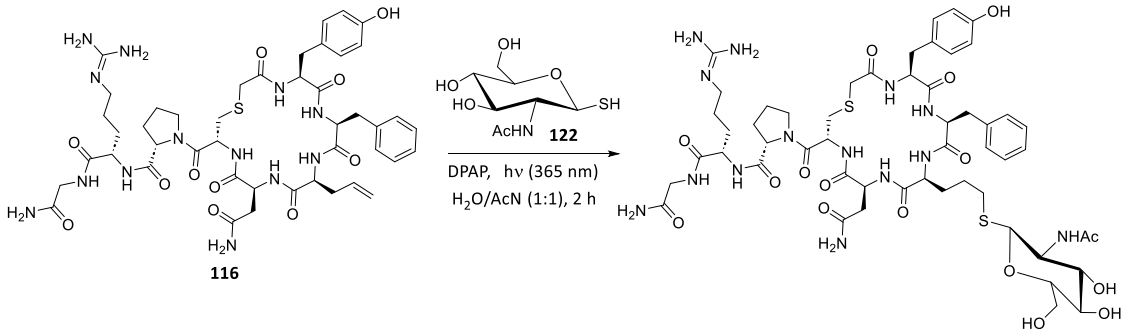

Scheme 4.7. Synthesis of glycosylated product **123**.

Finally, this new post-cyclisation TEC-mediated modification was employed to access bivalent cyclic peptide ligands by employing external dithiol-containing spacers. In this context, 1,4-butenedithiol **124,** a commercially available and cheap dithiol donor, was utilised to bridge two vasopressin analogues *via* a dual TEC reaction yielding the dimer **125** (**Figure 4.8.A**). The reaction was initially performed using 1 equiv. of vasopressin analogue **116**, 0.8 equiv. of 1,4-butenedithiol **124**, and 0.5 equiv. of DPAP in a 5 mM solution of H_2O/AcN (1:1). A reduced amount of the dithiol **124** was employed to prevent the mono-addition of the linker to the majority of the alkene sites leading to product **126** bearing a free thiol residue. The reaction mixture was irradiated at 365 nm for 2 h and the solvents were removed under reduced pressure. Analysis of the crude product by ESI-MS indicated only traces of the staring material **116**, yet the mass of the desired dimer product **125** was not identified. Interestingly, the mass of the product **126** was identified indicating that under these conditions, the mono-addition is the predominant reaction, with no dimerisation product observed. The mono-addition product **126** was also considered as a useful product, since the free thiol residue can serve as a handle for further chemical modification. Thus, following semi-preparative

RP-HPLC purification, the product **126** was obtained in an 11% yield and with >90% purity as confirmed by analytical RP-HPLC (Experimental Chapter, page 131).

Next, efforts were undertaken for the formation and isolation of the desired dimer product **125** (**Figure 4.8.A**). It was considered important to use significantly more concentrated conditions to ensure that the alkene sites are in proximity to each other which, in combination with the lower equiv. of the dithiol compared to the starting material **116**, can promote the desired dimerisation process furnishing **125**. Therefore, the reaction was carried out using 1 equiv. of vasopressin analogue **116**, 0.8 equiv. of 1,4-butenedithiol **124**, and 0.5 equiv. of DPAP in a 20 mM solution of DMF to facilitate solubilisation of all reactants. The reaction mixture was irradiated at 365 nm or 2 h and the solvents were removed under reduced pressure. Gratifyingly, ESI-MS analysis of the crude product identified the mass of the desired dimerised product **125** with no mass of either the staring material **116** or the mono-addition product **126** identified. This suggests that the concentration of the reaction plays a crucial role in selectively favouring the formation of the mono-addition product **126** or the dimer **125**. Semi-preparative RP-HPLC purification yielded the desired dimer **125** in an 10% yield and with >95% purity as confirmed by analytical RP-HPLC (Experimental Chapter, page 132). Thus, this new methodology can be applied for the development of stable thioether-based bivalent peptide ligands aimed for biological screening. Dithiols bearing different lengths can also be used for further diversification of the final bivalent peptide ligands.

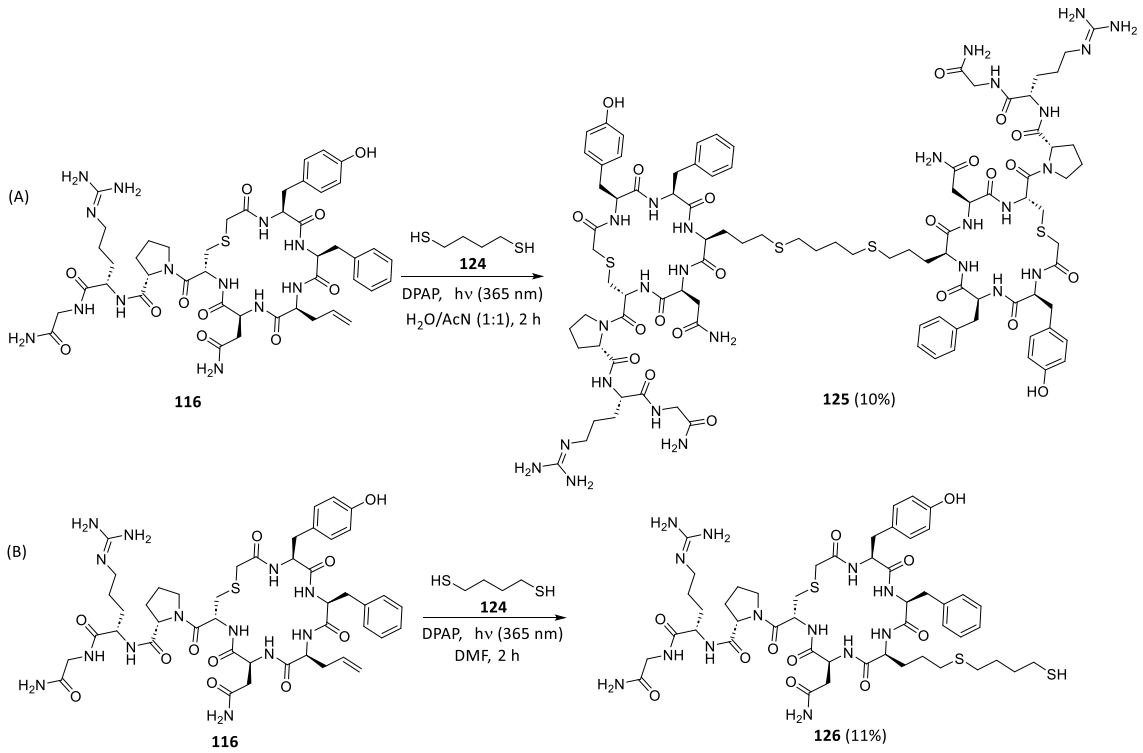

Scheme 4.8. (A) Synthesis of the dimer product **125**. (B) Synthesis of **126**.

4.3 Conclusion and Future Work

In conclusion, this study reports the development of a novel strategy for late-stage covalent modification of cyclic peptides. This was achieved by combining peptide cyclisation *via* chloroacetyl chemistry with post-cyclisation TEC reaction employing AgI within the peptide sequence. Vasopressin analogue **116** bearing AgI at position 4 was used as a model peptide for test reaction with different thiolated substrates. As detailed in **Section 4.2.2**, initial conditions using GSH as a thiol-containing donor and DPAP as a photoinitiator led to near-quantitative formation of the ligated product **119**. The same conditions, using decanethiol **120** and thiolated sugar **122** as alternative thiol sources, led to a clear formation of the respective ligated products as confirmed by analytical RP-HPLC or ESI-MS analysis. Finally, 1,4-butenedithiol **124** was employed as a cheap, commercially available dithiol to demonstrate dual TEC ligation leading to the di-thioether product **125**. This reaction was performed under concentrated conditions with reduced amounts of dithiol **124**, yielding finally the target dimer **125**.

Future directions will explore the application of this new late-stage modification in cyclic peptide library synthesis. In particular, the use of ‘m’ number of linear peptides

bearing a Cys residue, AgI and a chloroacetyl group at the *N*-terminus can cyclise under basic conditions leading to 'm' number of cyclic peptides. The stable AgI residues can then serve as chemical handles for subsequent radical TEC reactions by using 'o' number of thiolated substrates leading finally to '*m* x *o*' number of cyclic peptides that can be used for biological screening (**Scheme 4.9**).

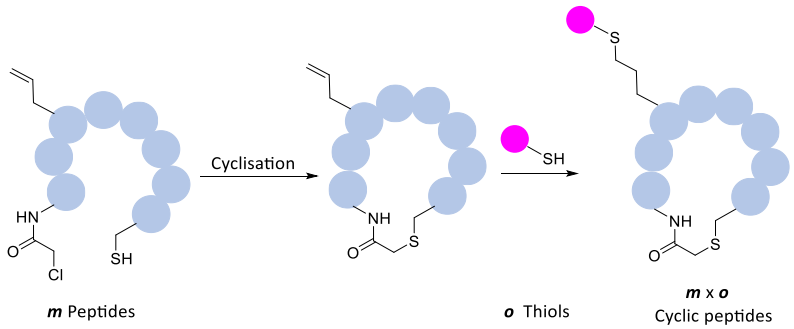

Scheme 4.9. Application of the new late-stage modification methodology in peptide library synthesis.

An additional promising application of this new methodology will be in high-throughput screening of cyclic peptides *via* mRNA display. mRNA display is a powerful *in vitro* selection used to identify high-affinity peptide ligands against biological targets of interest.[180] It establishes a covalent linkage between an mRNA molecule and its encoded peptide or protein, thereby coupling genotype with phenotype. This direct physical association enables the simultaneous screening of vast molecular libraries, often reaching sizes of up to 10^{13} variants. The process begins with the *in vitro* transcription of DNA libraries to generate mRNA, which is then translated into peptides in a cell-free system (**Scheme 4.10**). A critical step involves the covalent attachment of the mRNA to its nascent peptide, typically *via* a puromycin linker.[181] The resulting mRNA-peptide fusion molecules are then subjected to a binding assay to identify those with the desired functional properties, such as binding affinity to a target molecule. Following the selection step, the bound molecules are reverse transcribed into cDNA, amplified *via* PCR, and subjected to iterative rounds of selection and amplification to enrich for optimal sequences (**Scheme 4.10**). The final pool is sequenced to identify candidates for further validation.[181] A key advantage of this method is that it can explore a wide chemical space including non-natural AAs.

Suga and coworkers combined an engineered ribozyme (flexizyme) with the *in vitro* mRNA display technique within the Random Nonstandard Peptides Integrated Discovery (RaPID) platform.[182,183] The RaPID system enables genetic code reprogramming to incorporate noncanonical amino acids, such as those with α-*N*-chloroacetyl groups for spontaneous cyclisation *via* thioether formation for cyclic peptide libraries. Importantly, the RaPID system allows incorporation of AgI into the peptide sequences. Thus, one future direction will be to utilise the AgI of the thioether-linked cyclic peptides generated in mRNA display as a handle for radical TEC reaction with Cys-rich proteins. This can offer the advantage of identifying the exact binding sites of the high peptide binders towards the protein of interest. Covalent modification of cyclic peptides libraries with lipid moieties will also be investigated as a platform for antibiotic drug discovery.

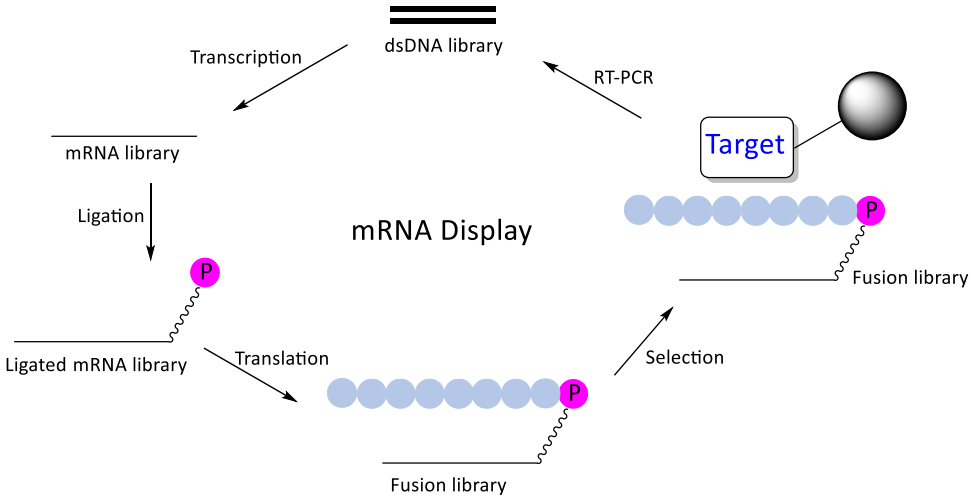

Scheme 4.10. Schematic representation of mRNA display.

Chapter 5

Development of a Photochemical Method to Specifically Label and Detect Lysine-crotonylated (KCr) Proteins.

5.1 Introduction and Aims

Proteins are essential macromolecules that perform a wide range of critical functions within biological systems. In eukaryotic cells, the majority of proteins undergo covalent modifications following ribosomal synthesis.[184] These post-translational modifications (PTMs) chemically modify specific reactive functional groups on amino acid side chains or at the *C*- and *N*-termini of proteins.[184] PTMs play a significant role in protein activity, stability, folding, localisation, and interactions with other cellular components.[185,186,187] To date, over 400 distinct types of PTMs have been identified, with the most studied being phosphorylation, acetylation, methylation, glycosylation, ubiquitination, SUMOylation, palmitoylation, myristoylation, and phenylation.[188] Dysregulation of PTMs has been implicated in various diseases, including cancer, Alzheimer's disease, Parkinson's disease, tissue injury, and cardiovascular disorders.[185,189] Consequently, targeting enzymes that regulate PTMs – referred to as "writers" for those that catalyse modifications and "erasers" for those that remove them – has become a common strategy in drug discovery. [190]

In 2011, Zhao and coworkers first identified lysine crotonylation (KCr) on histone proteins as a novel PTM.[191] Similar to the well-characterised lysine acetylation (KAc), crotonylation involves the acylation of the ε-amino group of the lysine side chain with a crotonyl moiety that contains an internal alkene group (**Figure 5.1**).[192,193] Histone crotonylation is mediated by histone crotonyl transferases (HCTs), also referred to as crotonylation "writers", which transfer the crotonyl group from the donor molecule crotonyl-CoA to specific lysine residues.[192] Conversely, histone decrotonylases (HDCs), also known as crotonylation "erasers", are responsible for the removal of the crotonyl modification (**Figure 5.1**).[192] Both histone KAc and KCr neutralise the positive charge of lysine side chains, thereby reducing the interactions between DNA and histones. This modification enhances DNA accessibility to transcription factors, subsequently promoting gene transcription. Structurally, KCr possesses an additional C-C π bond compared to KAc, resulting in a more rigid and planar structure for the crotonyl group.

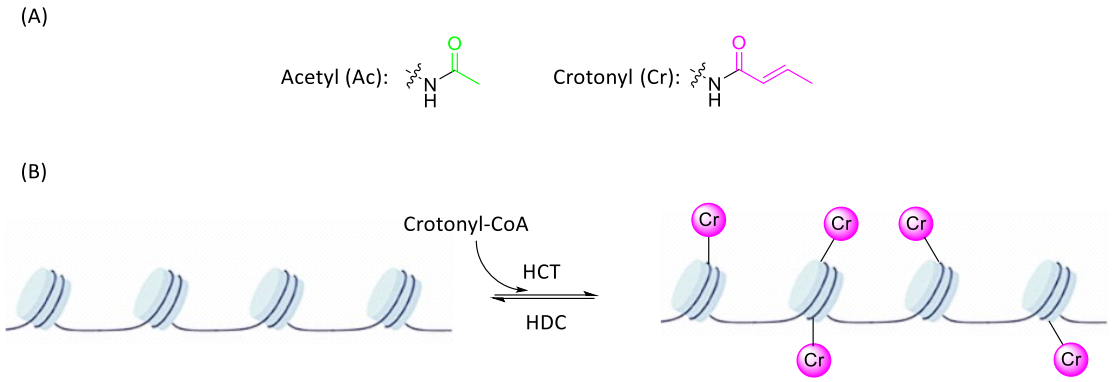

Figure 5.1. (A) Structures of an acetyl and a crotonyl group. (B) Histone crotonylation.

In 2017, Liao and coworkers reported the first observation of lysine crotonylation on non-histone proteins.[194,195] In this work, a wide array of non-histone crotonylated proteins were identified in HeLa cells through antibody-based enrichment, followed by high-resolution mass spectrometry (HRMS). Building on this, Zhang and coworkers reported the same year 2696 lysine crotonylation sites on 1024 non-histone proteins in H1299 cells.[195] These studies highlight the widespread occurrence of crotonylation within cells and suggest that this PTM plays significant roles in regulating protein activity, degradation, localization, and DNA repair. Due to the substantial impact on both protein and gene expression, crotonylation, – in both histone and non-histone contexts, – has been implicated in various diseases, including depression, HIV latency, acute kidney injury (AKI), cardiovascular diseases, and liver fibrosis.[196,197,198,199]

Despite the strong correlations between crotonylation and disease pathogenesis, robust and efficient biochemical tools that could enable in-depth investigation of this PTM in molecular processes are lacking. Currently, antibody-based techniques are the gold standard for the identification and analysis of crotonylated proteins (**Figure 5.2**). Zhao and coworkers developed the first pan-specific antibody against lysine KCr, capable of recognising peptide libraries bearing KCr moieties, and this tool has since been employed in western blotting and other assays to study protein crotonylation.[191] Following this breakthrough, the pan-KCr antibody has been widely used in combination with liquid chromatography-tandem mass spectrometry (LC-MS/MS) to identify non-histone proteins.[194,195]

However, several challenges limit the utility of this approach. Immunoaffinity proteomics is a costly and technically demanding method, and cross-reactivity of the anti-KCr antibody with acetylated histones has been observed, complicating the proteomic workflow, and raising questions about the reliability and accuracy of reported crotonylome datasets.[200,201] The primary challenge in antibody-based identification of PTMs lies in the generation of highly selective antibodies. Due to the small and structurally similar nature of many acylation PTMs, developing antibodies that are both pan-PTM-specific and independent of chemical context is difficult.[202,203] Consequently, the anti-Kcr antibody not only recognizes crotonylated proteins but also acetylated and butyrylated ones, further complicating analysis.[194,191]

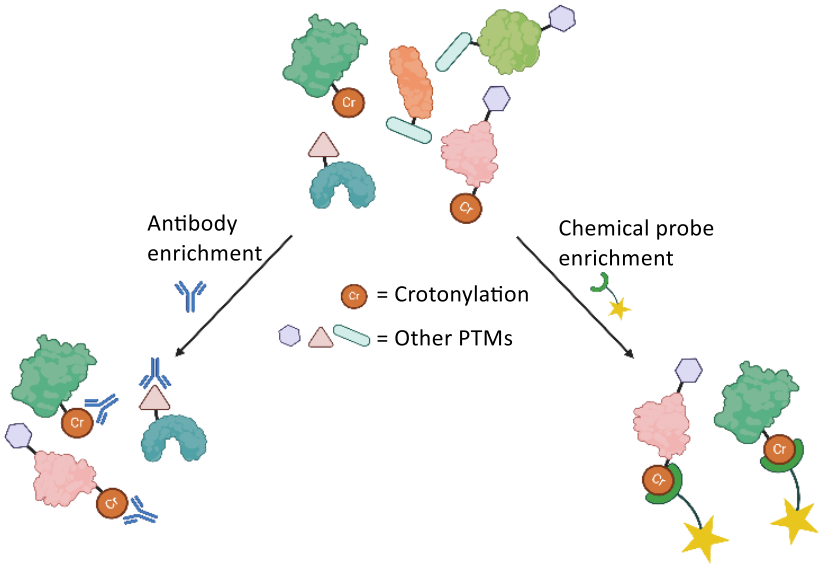

Figure 5.2. Representation of the selective chemical probe enrichment compared to the non-specific enrichment using the anti-KCr antibody.

Another enrichment approach that avoids the requirement for selective antibodies involves the use of chemical probes.[204] These probes require a tag, such as biotin, for enrichment, along with a reactive group that can selectively bind to the target PTM through bioorthogonal chemistry. This approach relies on the presence of a functional group in the PTM that can undergo selective reaction. If a bioorthogonal reaction is applicable, the use of chemical probes significantly streamlines the process, since only the probe needs to be incubated with the prepared samples. This allows for specific labelling of the target PTM, followed by pulldown enrichment for MS analysis. Employing a covalent chemoproteomics probe to selectively target PTMs can therefore

provide a more adaptable, cost-effective, and sensitive method for PTM identification (**Figure 5.2**).[204]

Bos and Muir introduced the first selective and sensitive chemical probe which reacts with crotonyl modifications.[205] The developed probe is based on a water-soluble phosphine warhead containing a pendent carboxylic acid group, which reacts with the crotonyl group to generate a β-phosphonium species (**Figure 5.3**). TCEP was found highly reactive towards crotonylated model peptides, so the authors developed a TCEP-based chemical probe wherein a biotin moiety was coupled to one of TCEP carboxylic groups to enable affinity enrichment and streptavidin-based blotting analysis of crotonylated proteins. Histone H3 with a KCr group at position 18 (H3K18Cr) was used as an initial test to investigate the reactivity of the TCEP probe and upon incubation, high biotin incorporation was found at the crotonyl units of H3 protein. The probe was also able to detect several KCr marks on the tail of H4 (H4pCr). No biotin was incorporated into nucleosomes with multiple preinstalled KAc marks (H4pAc) or into unmodified nucleosomes (WT). Furthermore, the probe was used to selectively target crotonylated histone proteins in a complex proteasome. HEK293 mammalian cell lines were grown in presence of sodium crotonate (NaCr), which is known to up-regulate crotonyl-CoA levels, and after treatment with the TCEP probe, endogenous crotonylated histone proteins were enriched.

From a mechanistic perspective, the authors proposed that the negatively charged carboxylate groups stabilise the resulting phosphonium cation through electrostatic interactions. However, they also suggested that hydrogen bonding interactions or the formation of a transient cyclic phosphorane species might contribute. Despite these speculations, the exact mechanism remains unclear, as no additional studies were conducted. Interestingly, the probe has never been applied in proteomics analysis, leading to questions about its suitability in such workflows, given that phosphine warheads typically lack selectivity, are challenging to synthesise, and have limited chemical tractability.

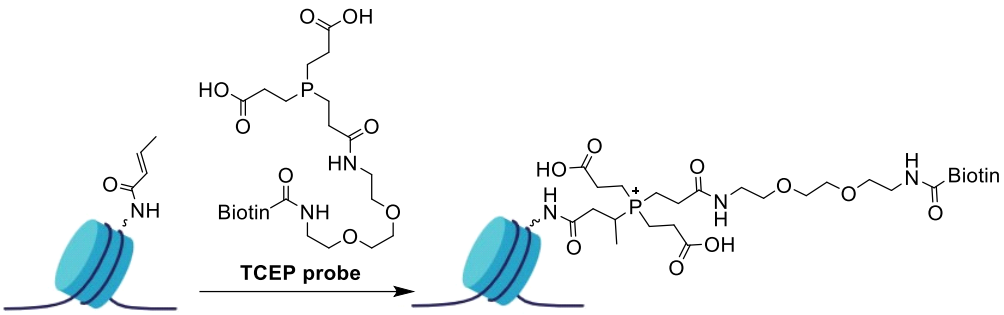

Figure 5.3. Covalent capture of crotonylated histones by the biotinylated TCEP probe, the first chemical probe for Kcr.

Thus, this work describes the development of a novel, robust and highly selective chemoproteomic approach for identification and discovery of histone and non-histone crotonylated proteins. The electron rich α,β-unsaturated internal alkene of the KCr moiety represents an excellent selective handle for the radical TEC reaction. Therefore, this project aims to develop thiol-based chemical probes that will selectively react with the unsaturated C-C bond of the KCr bond under radical-mediated conditions. The biorthogonality of the radical TEC reaction will allow the specific targeting of crotonylation among other PTMs leading to the first accurate description of crotonylome (**Figure 5.4**).

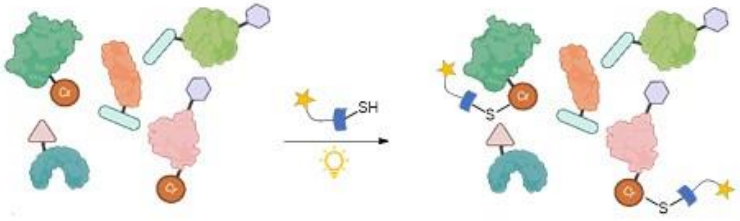

Figure 5.4. Selective covalent capture of crotonylated proteins in a mixture of proteins *via* radical TEC reaction.

5.2 Results and Discussion

5.2.1 Previous work

The initial screening to identify an optimal photoinitiator for the radical TEC reactions in aqueous media was conducted by the PhD candidate Marinda Westerveld. This study utilised a crotonylated model pentapeptide, Ac-Tyr-Gly-Lys$^{(Cr)}$-Gly-Gly (**127**),

which contains a crotonylated lysine residue at its central position, and GSH as a model thiol donor. In each experiment, GSH was added in a 10-fold molar excess relative to the model peptide, and the reaction mixtures were irradiated at 365 nm for 1 hour. The photoinitiators DPAP (**Figure 2.1.A**), Irgacure 2959 (**Figure 5.5.A**), and LAP (**Figure 5.5.B**) were each tested at different molar equivalents, and the conversion of the reaction towards the formation of the ligated product **128** was calculated based on ^{1}H NMR by measuring the consumption of the crotonyl peaks compared to an internal standard (**Table 5.1**)

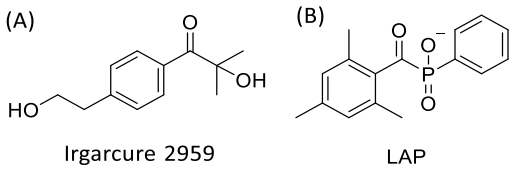

Figure 5.5. Chemical structures of (A) Irgacure 2959, and (B) LAP.

Table 5.1. Photoinitiator screening for the radical TEC reaction between pentapeptide **127** and GSH conducted by Marinda Westerveld.

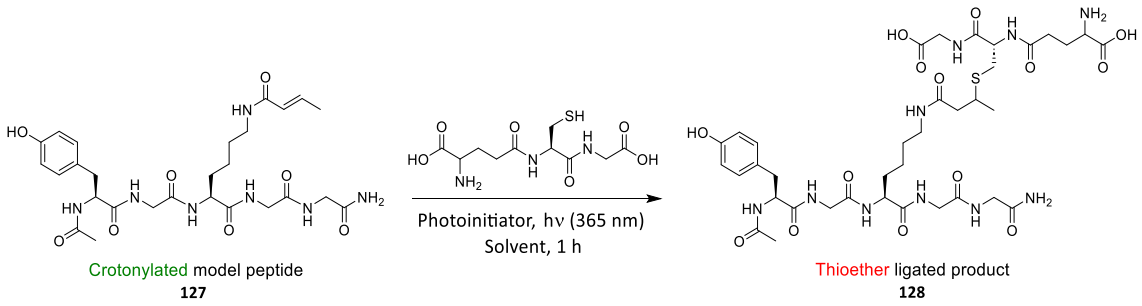

Entry	Photoinitiator	Equivalent	Solvent	Conversions
1	DPAP	5	D_2O	35%
2	DPAP	10	D_2O:AcN (1:1)	30%
3	LAP	5	D_2O	100%
4	LAP	1	D_2O	70%
5	LAP	0.5	D_2O	52%
6	Irgacure 2959	5	D_2O	93%
7	Irgacure 2959	5	D_2O:AcN (1:1)	95%

Although DPAP is a highly efficient photoinitiator, the use of 5-fold excess led to a disappointing 35% conversion based on ^{1}H NMR (**Table 5.1, Entry 1**). Further increases in DPAP concentration paradoxically led to lower conversions, likely due to DPAP's limited solubility in the D_2O solvent system used. (**Table 5.1, Entry 2**). Next, LAP was employed as a more water-soluble photoinitiator. Gratifyingly, the reaction proceeded in very high conversions with the use of 1 and 5 equivalents of LAP, respectively (**Table 5.1, Entries 3,4**). However, careful analysis of the ^{1}H NMR spectrum revealed covalent attachment of LAP to the model peptide, suggesting that the double bond of the crotonyl group underwent undesired radical addition from the LAP radicals formed upon irradiation. Thus, a significant ratio of the alkene consumption observed is attributed to the addition of the LAP radicals rather than through formation of the desired ligated product **128**. To address this limitation, Irgacure 2959 was evaluated as an alternative photoinitiator. Irgacure 2959, noted for its high aqueous solubility and lower reactivity, was intended to mitigate the undesired radical addition to the crotonyl group. Indeed, reactions conducted with 5 equivalents of Irgacure 2959 achieved >90% conversion without evidence of fragmentation byproduct addition to the alkene, as confirmed by ^{1}H NMR (**Table 5.1, Entries 6,7**). Thus, Irgacure 2959 was selected as the optimal photoinitiator for further optimisation of the TEC reaction.

5.2.2 Optimisation of The Radical TEC Reaction

The radical TEC reaction was further optimised by using the same crotonylated model penta-peptide **127**, GSH as a thiol source, and Irgarcure 2959 as a photoinitiator. The building block required for the incorporation of the KCr moiety into the peptide in SPPS, Fmoc-Lys$^{(Cr)}$OH (**129**), was synthesised following procedures described by Bruccella and coworkers.[206] Firstly, Boc-deprotection of Fmoc-Lys(Boc)-OH (**130**) was achieved in a TFA:CH_2Cl_2 mixture for 2 h yielding the TFA salt of Fmoc-Lys-OH (**131**) in quantitative yield following a simple work up procedure (**Scheme 5.1.A**). Subsequently, *N*-hydroxysuccinimide-Crotonyl (NHS-Cr) ester was prepared by treating *trans*-crotonyl chloride with *N*-hydroxysuccinimide (NHS) in the presence of DIPEA for 3 h in CH_2Cl_2. Following solvent evaporation, the NHS-Cr activated ester was isolated and used for the next acylation step without further purification. Finally, a solution of TFA salt of Fmoc-Lys-OH **131**, NHS-Cr ester and Et_3N was stirred for 18 h in CH_2Cl_2 and chromatographic

purification yielded the required building block **129** in 43% yield over two steps (**Scheme 5.1.A**).

Subsequently, the model peptide **127** was synthesised using the Liberty Blue peptide synthesiser. Notably, Fmoc-Lys$^{(Cr)}$OH was completely stable under the microwave assisted conditions and elevated temperatures used. Following the last Fmoc-deprotection, the free *N*-terminus of the sequence was manually capped by treating the resin bound peptide with a solution of acetic anhydride/DIPEA/DMF (1:1:3) for 1 h and successful acylation was confirmed by bromophenol blue test. Following peptide cleavage and deprotection, the crude product was purified by semi-preparative RP-HPLC yielding the final penta-peptide **127** in a 65% yield and with >95% purity as confirmed by analytical RP-HPLC (Experimental Chapter, page 135).

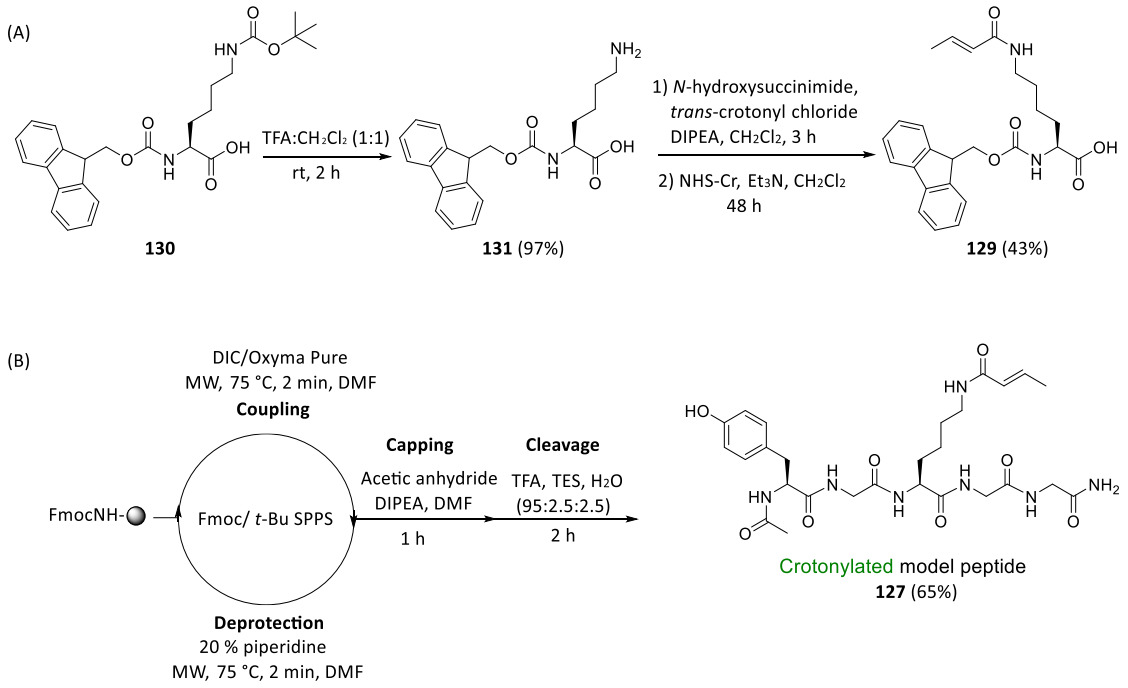

Scheme 5.1. (A) Synthesis of Fmoc-Lys$^{(Cr)}$OH (**129**). (B) SPPS of the crotonylated model peptide **127** bearing the crotonylated lysine residue in the middle of sequence.

The primary objective of this project is to develop a thiol-containing chemical probe and apply the TEC reaction in cellular environments to achieve selective targeting of crotonylated proteins. Due to the instability of cells under UV irradiation beyond 10 minutes, test reactions between the model peptide **127** and GSH were conducted in aqueous media for a maximum of 10 minutes. Various molar equivalents of Irgacure

2959 and GSH were screened, and reaction conversions toward the formation of the ligated product **128**, were quantified *via* LC-MS by integrating the product peak area relative to the starting material.

In the initial experiment, deuterated water (D_2O) was employed as the solvent alongside 2 equiv. of Irgacure 2959 and 10 equiv. of GSH. This reaction yielded the ligated product **128** with only ~20% conversion, as determined by LC-MS (**Table 5.2, Entry 1**). Interestingly, when the reaction was repeated under identical conditions but with deionized water (dH_2O) replacing D_2O, the conversion increased to >80% (**Table 5.2, Entry 2**). This observation suggests that dH_2O may promote the proton transfer during the radical reaction to a higher extent than D_2O. Therefore, dH_2O was subsequently used as the standard solvent for further optimisation. To explore catalytic loading of Irgacure, the reaction was repeated with the same equivalents of peptide and GSH but with progressively lower Irgacure concentrations of 1, 0.5, and 0.1 equiv. (**Table 5.2, Entries 3–5**). However, reductions in photoinitiator quantity led to a significant drop in conversion, with yields falling below 20% when less than 0.5 equiv. were used (**Table 5.2, Entry 4**). With 2 equiv. of Irgacure and 15 equiv. of GSH, the ligated product **128** was obtained in >85% conversion (**Table 5.2, Entry 6**). Further improvement was observed by increasing GSH to 20 equiv., which afforded the product in >95% conversion, as confirmed by LC-MS (**Table 5.2, Entry 7, Figure 5.6**). Additional attempts to achieve catalytic amounts of photoinitiator by using 20, 30, and 50 equiv. of GSH led once again to significant decrease of conversion (**Table 5.2, entries 8,9,10,11,12,13,14**). Thus, 2 equiv. of photoinitiator and 20 equiv. of thiol were determined to be the optimal conditions for 10 minutes of UV irradiation.

Table 5.2. Optimisation table for the radical TEC reaction between peptide **127** and GSH using Irgacure 2959 as a photoinitiator.

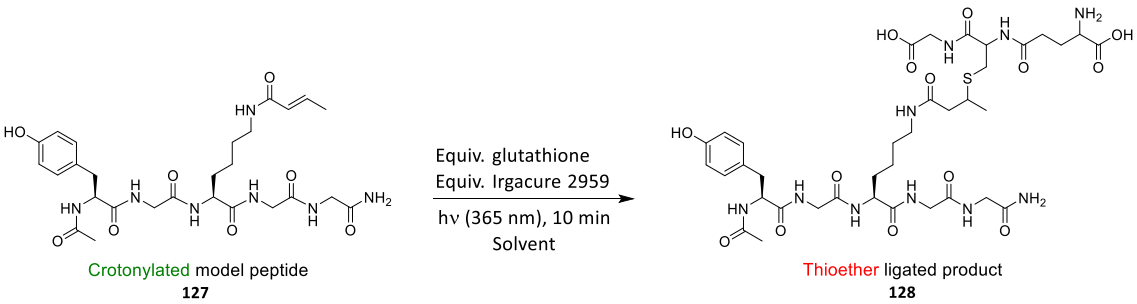

Entry	Peptide (equiv.)	Irgacure (equiv.)	Glutathione (equiv.)	Solvent (0.5 mL)	Conversion (based on RP-HPLC)
1	1	2	10	d_2O	<20%
2	1	2	10	dH_2O	>80%
3	1	1	10	dH_2O	<50%
4	1	0.5	10	dH_2O	<20%
5	1	0.1	10	dH_2O	5%
6	1	2	15	dH_2O	>85%
7	1	2	20	dH_2O	>95%
8	1	1	20	dH_2O	85%
9	1	0.5	20	dH_2O	60%
10	1	0.1	20	dH_2O	<5%
11	1	0.5	30	dH_2O	50%
12	1	0.1	30	dH_2O	<5%
13	1	0.5	50	dH_2O	60%
14	1	0.1	50	dH_2O	<5%

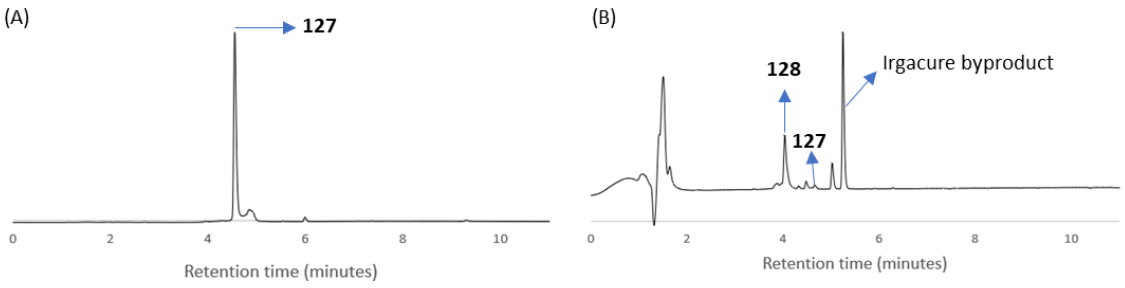

Figure 5.6. (A) RP-HPLC (214 nm) trace of the pure starting peptide **127**. (B) PR-HPLC (214 nm) trace of the crude mixture after irradiation at 365 nm for 10 minutes using the optimised conditions (**Table 5.2, Entry 7**).

Subsequently, the optimised conditions (**Table 5.2, entry 7**) were evaluated in longer peptide sequences bearing more than one crotonylated sites. The peptide **132**, with the amino acid sequence ARTK$_4$QTARK$_9$STG, originates from the tail of the H3 human histone, where both lysine residues at positions 4 and 9 are crotonylated *in vivo* (**Figure 5.7**). The PhD candidate Marinda Westerveld synthesised and purified two model peptides: Ac-ARTK$^{(Cr)}$QTARK$^{(Cr)}$STG (**133**), with both lysine residues crotonylated, and Ac-ARTKQTARK$^{(Cr)}$STG (**134**), with only the lysine residue at position 9 crotonylated. Prior to the optimisation outlined in **Table 5.2**, an initial investigation into the radical TEC reaction between the doubly crotonylated peptide (**133**) and GSH was performed by Marinda Westerveld. In this preliminary reaction, 10 equiv. of DPAP and 20 equiv. of GSH were used in an H_2O/AcN mixture, and the reaction mixture was irradiated at 365 nm for 1 hour. Analysis of the crude mixture by matrix-assisted laser desorption/ionization (MALDI) indicated the presence of unreacted starting material (**133**), a minor amount of mono-GSH addition to one of the crotonylated lysine sites, and only trace amounts of the desired product with double GSH addition to peptide **135**. As discussed in **Section 5.2.1**, this limited reactivity is primarily attributed to the low solubility of DPAP in aqueous environments.

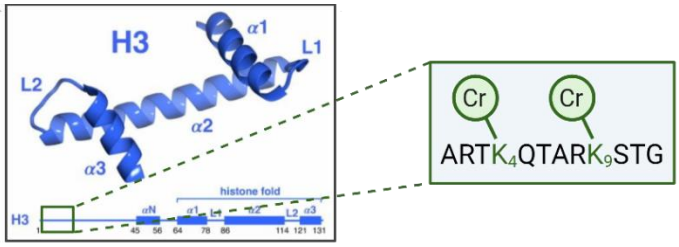

Figure 5.7. The structure of H3 human histone bearing ARTK$^{(Cr)}$QTARK$^{(Cr)}$STG at its *N*-terminus tail.

Following the optimisation process, the TEC reaction between peptide **133** and GSH was repeated under the optimised conditions (**Table 5.2, Entry 7**). Upon irradiating the reaction mixture for 10 minutes, full consumption of the starting material and quantitative formation of the desired double addition product **135** was confirmed by LC-MS analysis (**Figure 5.8.A**). Importantly, no intermediate product from mono-GSH addition to a single crotonylated lysine site was observed, indicating that the optimised conditions effectively promote covalent capture of multiple crotonylated sites within a polypeptide chain. Finally, the same reaction was performed with **134**, containing a

single crotonylated lysine at position 9. Under optimised conditions, complete consumption of the starting material **134** was achieved, with clear formation of the ligated product **136** as indicated by LC-MS (**Figure 5.8.B**).

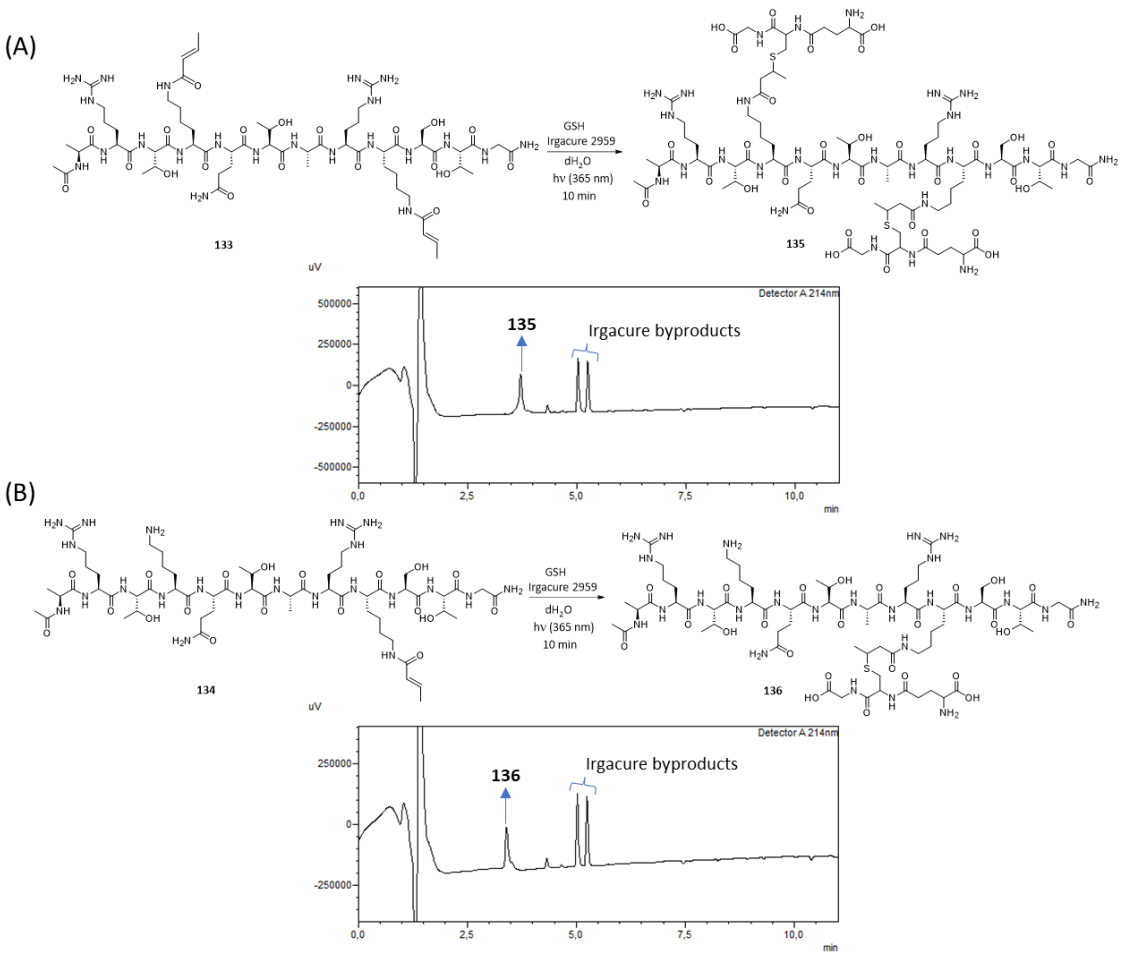

Figure 5.8. (A) TEC reaction between the doubly crotonylated **133** and GSH under the optimised conditions and the RP-HPLC trace (214 nm) of the reaction mixture after 10 minutes of irradiation at 365 nm. (B) TEC reaction between the mono crotonylated **134** and GSH and the RP-HPLC trace (214 nm) of the reaction mixture after 10 minutes of irradiation at 365 nm.

5.3 Conclusions and Future Work

In conclusion, there remains a critical need for a robust chemoproteomic approach to selectively 'tag' the crotonylation PTM. The development of a novel chemical probe capable of selectively targeting crotonylated sites within complex protein mixtures could provide significant insights into the role of this PTM in various molecular processes and disease states. This project investigates the development of

novel thiol-containing chemical probes that can enable covalent binding to the reactive double bonds of crotonylated protein sites *via* a radical TEC reaction. This work describes the initial optimisation of the TEC reaction by using a model pentapeptide bearing a crotonylated lysine residue and GSH as a thiol donor. Irgacure 2959 was selected as the most superior photoinitiator for the TEC reaction. The reaction was optimised using a maximum of 10 minutes irradiation at 356 nm, and the use of 2 equiv. of Irgacure 2959 and 20 equiv. of GSH led to the formation of the ligated product with a >95% conversion. Applying these optimised conditions to a longer peptide with two crotonylated sites resulted in the quantitative formation of the desired product with dual GSH addition, suggesting that these conditions are suitable for covalent targeting of multiple crotonylated sites within polypeptide chains.

Future directions of this project will apply the TEC reaction on the recombinant human nucleosomes containing a single crotonyl mark at position 17 (H3K27Cr). The effect of UV irradiation and Irgacure 2959 on the protein will be investigated. Further reaction optimisation will focus on parameters such as pH, salt concentration of the protein buffer, reaction time, and use of visible light irradiation. The progress of the ligation reaction will be monitored by HRMS confirming the formation of the desired thioether, and western blotting analysis using anti-H3K27Cr recombinant antibody. Finally, reactive thiol-containing chemical probes will be designed, synthesised, and tested on cell lysate to investigate their ability to selectively target crotonylated proteins in complex protein mixtures. For this purpose, the probe containing the reactive thiol moiety will be covalently linked to a biotin tag via a spacer, facilitating pull-down of crotonylated targets using streptavidin Sepharose affinity chromatography.

Chapter 6

Conclusions

6.1 Overall Conclusions

This thesis presents a comprehensive exploration of novel synthetic methodologies for peptide cyclisation and bioconjugation, and the development of tools for investigating biologically relevant interactions. Central to the work was the application of radical TEC reactions to develop versatile peptide analogues and chemical probes, contributing new insights into peptide cyclisation and functionalisation for biomedical research and drug discovery.

Chapter 2 describes the development of vasopressin and somatostatin analogues (**54**, **55**, **65**, and **66**) with extended ring sizes and preserved disulfide bonds to study how ring size affects neuropeptide activity. The radical TEC reaction was employed for the first time for direct peptide hydrothiolation on-resin, generating thiolated amino acids which were then used for peptide cyclisation *via* disulfide bond formation. The use of commercially available alkenyl amino acids, in combination with sequential ATE reaction using thioacetic acid followed by *S*-deacetylation on-resin, enabled the regioselective installation of a thiol residue onto the peptide. On-resin ATE reaction, utilising thioacetic acid (20 equiv.), DPAP (10 equiv.) and MAP (10 equiv) under irradiation at 365 nm for 15 minutes followed by on-resin *S*-deacetylation using DTT (100 equiv.) and HCl·Cys-OMe (100 equiv.) in DMF/phosphate buffer (pH 8.5), enabled the regioselective thiol installation on peptides with over 95% conversion after in depth optimization. These conditions were then applied to synthesise disulfide-based analogues of vasopressin and somatostatin by substituting Cys residues with AgI and performing regioselective hydrothiolation. Following peptide cleavage and deprotection, cyclisation occurred *via* disulfide bond formation under oxidative conditions, yielding high-purity analogues suitable for biological testing. Currently, biological evaluation of somatostatin analogues, including binding affinity studies, is ongoing with Professor Markus Muttenthaler's group. These studies aim to better understand the effect of ring size on the biological activity of somatostatin. Future research will also explore the application of disulfide bond formation on-resin to other cyclic peptides for drug discovery.

Chapter 3 presents the application of the on-resin peptide hydrothiolation methodology developed in Chapter 2 within the context of NCL. Traditionally, the synthesis of thiolated analogues of natural amino acids for NCL and subsequent desulfurisation is complex and requires multiple purification steps. This study addresses this issue by using commercially available unsaturated amino acids to introduce a thiol group in just two simple steps, followed by NCL and desulfurisation to regenerate the native amino acid at the ligation site. Three unsaturated amino acids, Boc-Dhv-OH (**67**), Boc-VgI-OH (**85**), and Boc-dehydroproline-OH (**94**), were used to test the compatibility of the thiolation methodology with NCL. The methodology was successful for Boc-Dhv-OH, which enabled the synthesis of peptide fragment **69** containing γ-thiol valine at the *N*-terminus. This peptide was ligated with peptide thioester **80** to form an analogue of antimicrobial peptide Ixosin [H_3A, E_8K, E_{13}L, S_{16}V]. However, attempts to thiolate Boc-VgI and Boc-dehydroproline at the *N*-terminus of peptide sequences were unsuccessful, likely due to structural instability of the carbon-centred radicals formed during the TEC reaction, which led to undesired elimination reactions. The study also demonstrated the successful on-resin, covalent attachment of the Abz fluorophore **106** to a linear RGD peptide analogue using the free thiol handle. This method eliminated the need for intermediate purification steps, enabling the covalent linkage of the fluorophore *via* three on-resin reactions. Future work will focus on exploring unsaturated amino acids where the alkene group is positioned further from the amine group to ensure stable on-resin thiolation and successful subsequent NCL. Additionally, this methodology will be expanded to enable conjugation with sugars, lipids, and cytotoxic agents, utilising the thiol handle of biologically relevant peptides to broaden the diversity of peptide conjugates.

Chapter 4 describes the development of a novel strategy for the late-stage covalent modification of cyclic peptides by combining peptide cyclisation *via* chloroacetyl chemistry with a post-cyclisation TEC reaction using AgI within the peptide sequence. Vasopressin analogue **116**, with AgI at position 4, served as a model peptide for testing with various thiolated substrates. Initial experiments using GSH (**118**) as a thiol donor and DPAP as a photoinitiator resulted in near-quantitative ligation. Additional thiol sources, such as decanethiol (**120**) and thiolated sugar (**122**), were also

successfully used, as confirmed by RP-HPLC and ESI-MS analysis. The reaction was further demonstrated using 1,4-butenedithiol (**124**) as a dithiol, leading to the formation of a di-thioether product **125**. Future work will focus on applying this methodology to cyclic peptide library synthesis as well as high-throughput screening of cyclic peptide binders *via* mRNA display.

Chapter 5 focuses on the development of novel thiol-containing molecules that enable selective covalent attachment to crotonylation post-translational modifications (PTM) *via* a radical TEC reaction. The initial optimisation of the TEC reaction was performed using a model pentapeptide **127** with a crotonylated lysine residue and GSH as the thiol donor. Irgacure 2959 was selected as the optimal photoinitiator, achieving >95% conversion of the ligated product **128** under optimized conditions (10 minutes of irradiation at 356 nm, 2 equiv. of Irgacure 2959 and 20 equiv. of GSH). This process was then successfully applied to a longer peptide (**133**) with two crotonylated sites, confirming the potential for covalent targeting of multiple crotonylated sites within polypeptides. Future work will focus on applying the TEC reaction to recombinant human nucleosomes containing a single crotonylation mark (H3K27Cr). Further optimization will address parameters such as pH, salt concentration, and reaction time, as well as the use of visible light irradiation. Additionally, reactive thiol-containing chemical probes will be synthesised and tested on cell lysates to evaluate their ability to selectively target crotonylated proteins in complex mixtures.

Overall, this thesis presents novel methodologies for peptide synthesis, modification, and conjugation, focusing on their application in drug discovery and chemoproteomics. The development of new synthetic strategies, including the use of the TEC reaction for peptide hydrothiolation, late-stage modifications of cyclic peptides, and the design of chemical probes for selectively targeting post-translational modifications (PTMs) is described in depth in chapters 2-5. These advancements pave the way for deeper insights into peptide-based therapies and selective protein targeting. Future work will aim to refine these strategies for broader biomedical applications.

Chapter 7

Experimental

7.1 General Experimental Details

All commercial chemicals used were supplied by Sigma Aldrich (Merck), Fluorochem, VWR Carbosynth and Tokyo Chemical Industry and used without further purification unless otherwise stated. Solvents for synthesis and purification were supplied by Sigma-Aldrich at HPLC grade. Anhydrous solvents were obtained from a PureSolv MD-4EN solvent purification system. All UV reactions were carried out in a Luzchem photoreactor, LZC-EDU (110 V/ 60 Hz) containing 10 UVA lamps centred at 365 nm. Analytical thin layer chromatography (TLC) was carried out with silica gel 60 (fluorescence indicator F254; Merck) and visualised by UV illumination (254 nm), ninhydrin staining (1.5 g ninhydrin, 3 mL acetic acid in 100 mL n-butanol) or molybdenum staining (5.0 g ammonium molybdate, 5.3 mL concentrated H_2SO_4 in 100 mL H_2O). Silica gel 60 (Merck, 230-400 mesh) was used for silica gel flash chromatography and all compounds were subject to purification using silica gel, unless otherwise stated. Manual SPPS was performed in polypropylene syringe reaction vessels (10 mL; Torviq, MI, USA) fitted with a polystyrene frit. All reactions were performed at room temperature under continuous agitation on an LBX Orb-B2 shaker set to 180 rpm. Automated SPPS was performed with a CEM Liberty Blue microwave peptide synthesiser.

Nuclear Magnetic Resonance (NMR) Spectroscopy

NMR spectra were recorded using Bruker DPX 400 (400.13 MHz for ^{1}H NMR and 100.61 MHz for ^{13}C NMR), Bruker AV 600 (600.13 MHz for ^{1}H NMR and 150.90 MHz for ^{13}C NMR), Agilent MR400 (400.13 MHz for ^{1}H NMR and 100.61 MHz for ^{13}C NMR) or Bruker AV 400 (400.13 MHz for ^{1}H NMR and 100.61 MHz for ^{13}C NMR) instruments. Deuterated solvents for NMR were purchased from Sigma Aldrich (Merck) or VWR Carbosynth. Chemical shifts, δ, are in ppm and referenced to the internal solvent signals. NMR data was processed using MestReNova (version v6.02-5475).

High Resolution Mass Spectrometry (HRMS)

ESI mass spectra were acquired using a Bruker micrOTOF-Q III spectrometer interfaced to a Dionex UltiMate 3000 LC in positive and negative modes as required. Agilent ESI-L Low Concentration Tuning Mix was used to calibrate the system, and this was also used as an internal lock mass. Masses were recorded over the range 100 – 2000 m/z. Operating conditions were asfollows: end-plate offset 500 V, capillary 4500 V, nebulizer 2.0 bar, dry gas 8.0 L min−1, and drytemperature 180 °C. APCI measurements were conducted on a Bruker micrOTOF-Q III spectrometer interfaced with a Dionex UltiMate 3000 LC or a direct insertion probe, operating in either positive or negative modes.

Reverse Phase High-performance Liquid Chromatography (RP-HPLC)

RP-HPLC analysis was performed using a Shimadzu Nexera Lite Low Pressure Gradient system. For analytical HPLC an Ascentis® Express 90 Å C18 column (100 mm × 4.6 mm, 5 µm) with a flow rate of 1.0 mL/min was utilised. For semi-preparative RP-HPLC purification, an Ascentis® C18 column (250 mm × 10 mm, 5 µm) with a flow rate of 4 mL/min was used. Gradient elution was carried out using Solvent A (0.1% TFA in water) and Solvent B (0.1% TFA in acetonitrile) for both analytical and semi-preparative HPLC runs. UV absorption signals of eluting compounds were detected using a SPD-M40 PDA detector at suitable wavelengths (220 nm, 254 nm, or 214 nm) as dictated by the resultant absorption spectrum.

7.2 Experimental Details for Chapter 2

7.2.1 General Procedures

Procedure 2A: Automated SPPS of Linear Peptides

All linear peptide sequences were assembled by automated SPPS on a CEM Liberty Blue™ Automated Microwave Peptide Synthesiser (CEM Corporation, Buckingham, UK) using repetitive steps of AA couplings and Fmoc deprotections with intermediate washes with DMF (3 × 30 s). AA couplings were carried out by treating the resin-bound peptide with Fmoc-protected AA (0.2 M in DMF), DIC (0.5 M in DMF) and Oxyma Pure (1 M in DMF) at 75 °C with a microwave potency of 170 W for 2 min. Fmoc

deprotections were carried out by treating the resin-bound peptide with 20% piperidine in DMF at 75 °C with a microwave potency of 135 W for 1 min.

Procedure 2B: On-resin ATE Reaction

100 mg of the resin bound unsaturated peptide (1.0 equiv. of peptide), DPAP (10.0 equiv.), MAP (10.0 equiv.), and thioacetic acid (20.0 equiv.) were suspended in anhydrous DMF (1 mL) and the reaction mixture was irradiated at 365 nm under continuous agitation for 15 min. The solvent and excess of reagents were removed *via* filtration and the resin was washed thoroughly with DMF (3 × 5 mL), CH_2Cl_2 (3 × 5 mL), and DMF (3 × 5 mL). The resin was finally washed with CH_2Cl_2 and dried. The progress of the reaction was monitored by small-scale peptide cleavage and deprotection by treating a small amount of the resin bound peptide with 2 mL of TFA:TES:EDT:H_2O (94:2.5:2.5:1 v/v/v/v) for 2 h. The solvent was removed under reduced pressure and the crude material was analysed by analytical RP-HPLC and ESI-MS.

Procedure 2C: On-resin S-deacetylation reaction

The resin bound peptide (1.0 equiv. of peptide), DTT (100.0 equiv.) and HCl-Cys-OMe (100.0 equiv.) were suspended in 3 mL of DMF/Phosphate buffer (pH 8.5) and the system was agitated for 1 h. The solvent and excess of reagents were removed *via* filtration and the resin was washed thoroughly with DMF (3 × 5 mL), CH_2Cl_2 (3 × 5 mL), and DMF (3 × 5 mL). The resin was finally washed with CH_2Cl_2 and dried. The progress of the reaction was monitored by small-scale peptide cleavage and as described in **Procedure 2B**. The solvent was removed under reduced pressure and the crude material was analysed by analytical RP-HPLC and ESI-MS.

Procedure 2D: Resin cleavage and global deprotection

To resin-bound peptide was added CH_2Cl_2 (5 mL), the syringe was agitated for 20 min, and then drained. The fresh cleavage cocktail (TFA:TES:EDT:H_2O; 94:2.5:2.5:1 v/v/v/v; 10 mL) was added to the syringe and it was agitated for 2 h. The syringe was drained, and the filtrate was collected. The resin was washed with cleavage cocktail (2 x 3 mL) and the washings were combined with the initial filtrate. The combined solution was concentrated under steam of N_2, followed by precipitation of the peptide with cold

Et_2O (10 mL) at 0 °C. The crude peptide suspension was centrifuged, and the supernatant was decanted. The peptide pellet was washed again with cold Et_2O (3 x 10 mL), centrifuged, and collected. The crude peptide was lyophilised.

Procedure 2E: Peptide Cyclisation via Disulfide Formation

The crude linear peptide was dissolved in a 1mM solution of H_2O/AcN (1:1) and 10% DMSO as an oxidative agent. The reaction mixture was stirred for 24 h and the crude material was subjected to purification by semi-preparative RP-HPLC.

7.2.2 Characterisation Data

(S)-N-((S)-1-((2-amino-2-oxoethyl)amino)-5-((diaminomethylene)amino)-1-oxopentan-2-yl)-1-((4R,7S,10S,13S,16S,19S)-19-amino-7-(2-amino-2-oxoethyl)-10-(3-amino-3-oxopropyl)-13-benzyl-16-(4-hydroxybenzyl)-6,9,12,15,18-pentaoxo-1,2-dithia-5,8,11,14,17-pentaazacyclodocosane-4-carbonyl)pyrrolidine-2-carboxamide (54)

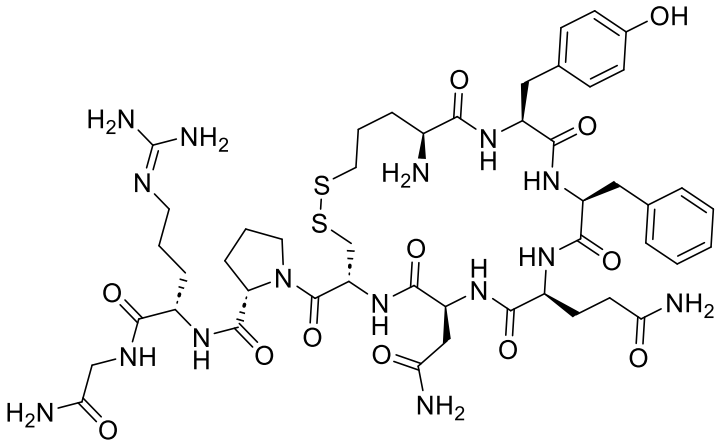

The peptide was synthesised at 0.10 mmol scale by automated SPPS as described in Procedure 2.A using Fmoc-Gly-OH, Fmoc-Arg(Pbf)-OH, Fmoc-Pro-OH, Fmoc-Cys(Trt)-OH, Fmoc-Asn(Trt)-OH, Fmoc-Gln(Trt)-OH, Fmoc-Phe-OH, Fmoc-Tyr(*t*Bu)-OH. The final Boc-AgI-OH was coupled manually with the addition of PyBOP (4 equiv.), NMM (8 equiv.), in a solution of Boc-AgI-OH (4 equiv.; 0.2 M) in DMF, activated for 2 minutes, and then added to the resin-bound peptide for 1 h. ATE and *S*-deacetylation reactions were carried out on-resin as described in Procedures 2.B and 2.C, respectively. Resin cleavage and global deprotection of the peptide were carried out as described in

Procedure 2.D. The linear peptide precursor was cyclised *via* disulfide bond formation as described in Procedure 2.E. The reaction mixture was subjected directly to purification by semi-preparative RP-HPLC (5 – 50% AcN in H_2O with 0.1% (v/v) TFA over 40 min) over multiple injections. Fractions containing pure product were combined and the solvent was lyophilised yielding the desired product as a white solid (26 mg, isolated yield: 24%, >95% purity).

Analytical RP-HPLC R_t (5 – 95% AcN in H_2O with 0.1% (v/v) TFA over 30 min, 220 nm): 9.637 min.

HRMS (*m/z* ESI^+): Found: 1112.4731 ($[M+H]^+$, $C_{48}H_{70}N_{15}O_{12}S_2$ requires 1112.4692), 556.7455 ($[M+2H]^{2+}$, $C_{49}H_{71}N_{15}O_{12}S_2$ requires 556.7346).

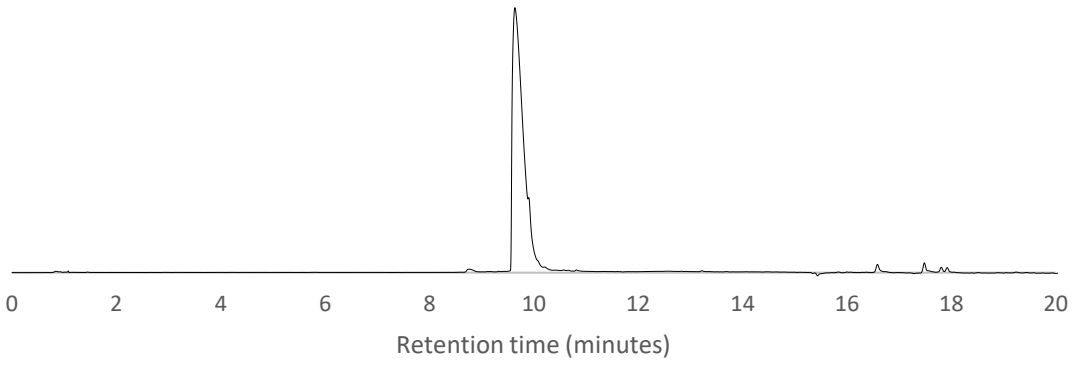

Figure 6.1. Analytical RP-HPLC trace (254 nm) of purified **54**.

(S)-N-((S)-1-((2-amino-2-oxoethyl)amino)-5-((diaminomethylene)amino)-1-oxopentan-2-yl)-1-((6S,9S,12S,15S,18S,21S)-21-amino-9-(2-amino-2-oxoethyl)-12-(3-amino-3-oxopropyl)-15-benzyl-18-(4-hydroxybenzyl)-8,11,14,17,20-pentaoxo-1,2-dithia-7,10,13,16,19-pentaazacyclotetracosane-6-carbonyl)pyrrolidine-2-carboxamide (55)

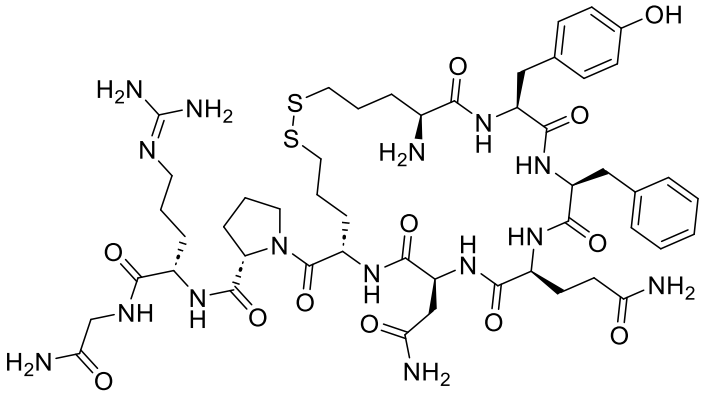

The peptide was synthesised at 0.1 mmol scale by automated SPPS as described in Procedure 2.A using Fmoc-Gly-OH, Fmoc-Arg(Pbf)-OH, Fmoc-Pro-OH, Fmoc-AgI-OH, Fmoc-Asn(Trt)-OH, Fmoc-Gln(Trt)-OH, Fmoc-Phe-OH, Fmoc-Tyr(*t*Bu)-OH, and Boc-AgI-OH. ATE and *S*-deacetylation reactions were carried out on-resin as described in Procedures 2.B and 2.C, respectively. Resin cleavage and global deprotection of the peptide were carried out as described in Procedure 2.D. The linear peptide precursor was cyclised *via* disulfide bond formation as described in Procedure 2.E. The reaction mixture was subjected directly to purification by semi-preparative RP-HPLC (5 – 50% AcN in H_2O with 0.1% (v/v) TFA over 40 min) over multiple injections. Fractions containing pure product were combined and the solvent was lyophilised yielding the desired product as a white solid (25 mg, isolated yield: 22%, >95% purity).

Analytical RP-HPLC R_t (5 – 95% AcN in H_2O with 0.1% (v/v) TFA over 20 min, 254 nm): 10.223 min.

HRMS (*m/z* ESI^+): Found: 1140.5058 ($[M+H]^+$, $C_{50}H_{74}N_{15}O_{12}S_2$ requires 1140.5005), 570.7584 ($[M+2H]^{2+}$, $C_{50}H_{75}N_{15}O_{12}S_2$ requires 570.7502).

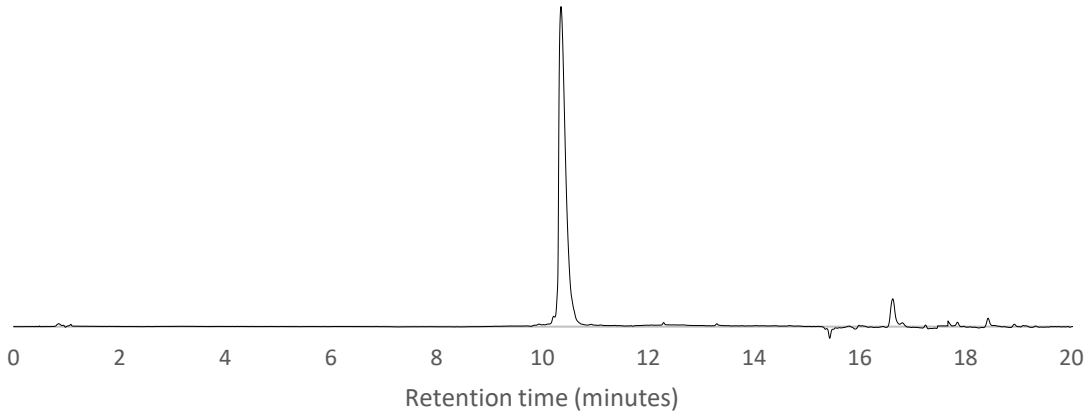

Figure 6.2. Analytical RP-HPLC trace (254 nm) of purified **55**.

(4R,7S,13S,19S,22S,25S,28S,31S,34S,37S)-22-((1H-indol-3-yl)methyl)-31-(2-amino-2-oxoethyl)-19,34-bis(4-aminobutyl)-37-(2-((S)-2-aminopropanamido)acetamido)-13,25,28-tribenzyl-10,16-bis((R)-1-hydroxyethyl)-7-(hydroxymethyl)-6,9,12,15,18,21,24,27,30,33,36-undecaoxo-1,2-dithia-5,8,11,14,17,20,23,26,29,32,35-undecaazacyclotetracontane-4-carboxamide (65)

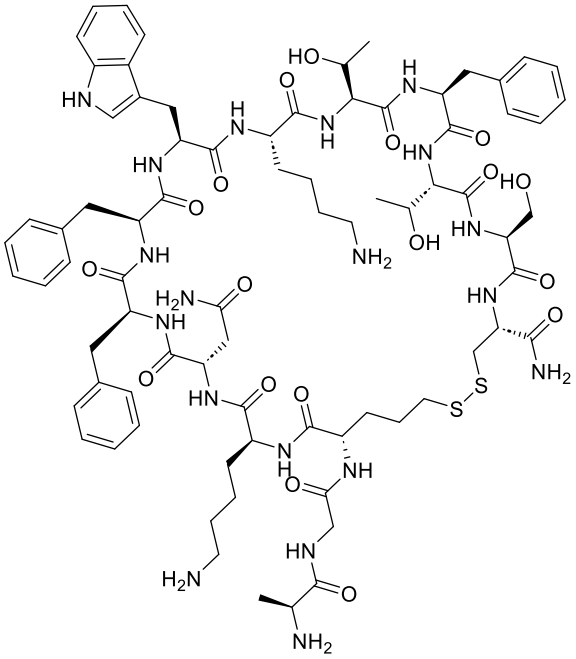

The peptide was synthesised at 0.1 mmol scale by automated SPPS as described in Procedure 2.A using Fmoc-Cys(Trt)-OH, Fmoc-Ser(*t*Bu)-OH, Fmoc-Thr(*t*Bu)-OH, Fmoc-Phe-OH, Fmoc-Thr(*t*Bu)-OH, Fmoc-Lys(Boc)-OH, Fmoc-Trp(Boc)-OH, Fmoc-Phe-OH, Fmoc-Phe-OH, Fmoc-Asn(Trt)-OH, Fmoc-Lys(Boc)-OH, Fmoc-AgI-OH, Fmoc-Gly-OH, Boc-

Ala-OH. ATE and *S*-deacetylation reactions were carried out on-resin as described in Procedures 2.B and 2.C, respectively. Resin cleavage and global deprotection of the peptide were carried out as described in Procedure 2.D. The linear peptide precursor was cyclised *via* disulfide formation as described in Procedure 2.E. The reaction mixture was subjected directly to purification by semi-preparative RP-HPLC (5 – 50% AcN in H_2O with 0.1% (v/v) TFA over 40 min) over multiple injections. Fractions containing pure product were combined and the solvent was lyophilised yielding the desired product as a white solid (23 mg, isolated yield: 14%, >95% purity).

Analytical RP-HPLC R_t (5 – 95% AcN in H_2O with 0.1% (v/v) TFA over 20 min, 254 nm): 11.548 min.

HRMS (*m/z* ESI^+): Found: 832.8817 ($[M+2H]^{2+}$, $C_{78}H_{111}N_{19}O_{18}S_2$ requires 832.8819), 555.6337 ($[M+3H]^{3+}$, $C_{78}H_{112}N_{19}O_{18}S_2$ requires 555.588).

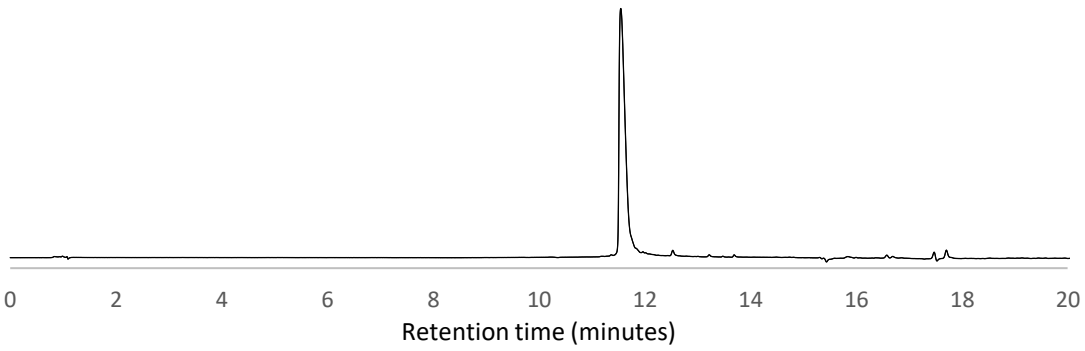

Figure 6.3. Analytical RP-HPLC trace (254 nm) of purified **65**.

(6S,9S,15S,21S,24S,27S,30S,33S,36S,39S)-24-((1H-indol-3-yl)methyl)-33-(2-amino-2-oxoethyl)-21,36-bis(4-aminobutyl)-39-(2-((S)-2-aminopropanamido)acetamido)-15,27,30-tribenzyl-12,18-bis((R)-1-hydroxyethyl)-9-(hydroxymethyl)-8,11,14,17,20,23,26,29,32,35,38-undecaoxo-1,2-dithia-7,10,13,16,19,22,25,28,31,34,37-undecaazacyclodotetracontane-6-carboxamide (66)

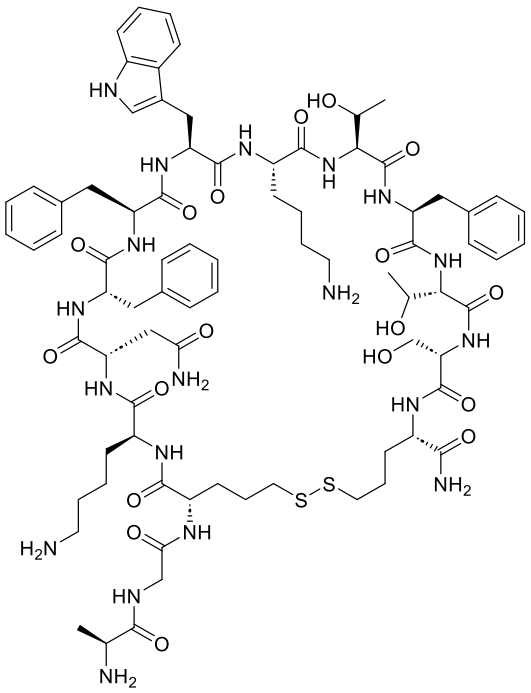

The peptide was synthesised at 0.10 mmol scale by automated SPPS as described in Procedure 2.A using Fmoc-AgI-OH, Fmoc-Ser(*t*Bu)-OH, Fmoc-Thr(*t*Bu)-OH, Fmoc-Phe-OH, Fmoc-Thr(*t*Bu)-OH, Fmoc-Lys(Boc)-OH, Fmoc-Trp(Boc)-OH, Fmoc-Phe-OH, Fmoc-Phe-OH, Fmoc-Asn(Trt)-OH, Fmoc-Lys(Boc)-OH, Fmoc-AgI-OH, Fmoc-Gly-OH and Boc-Ala-OH. ATE and *S*-deacetylation reactions were carried out on-resin as described in Procedures 2.B and 2.C, respectively. Resin cleavage and global deprotection of the peptide were carried out as described in Procedure 2.D. The linear peptide precursor was cyclised *via* disulfide formation as described in Procedure 2.E. The reaction mixture was subjected directly to purification by semi-preparative RP-HPLC (5 – 50% AcN in H_2O with 0.1% (v/v) TFA over 40 min) over multiple injections. Fractions containing pure product were combined and the solvent was lyophilised yielding the desired product as a white solid (20 mg, isolated yield: 12%, >95% purity).

Analytical RP-HPLC R_t (5 – 95% AcN in H_2O with 0.1% (v/v) TFA over 20 min, 254 nm): 11.769 min.

HRMS (*m/z* ESI^+): Found: 846.9042 ($[M+2H]^{2+}$, $C_{80}H_{115}N_{19}O_{18}S_2$ requires 846.8976), 564.9422 ($[M+3H]^{3+}$, $C_{80}H_{116}N_{19}O_{18}S_2$ requires 564.9317).

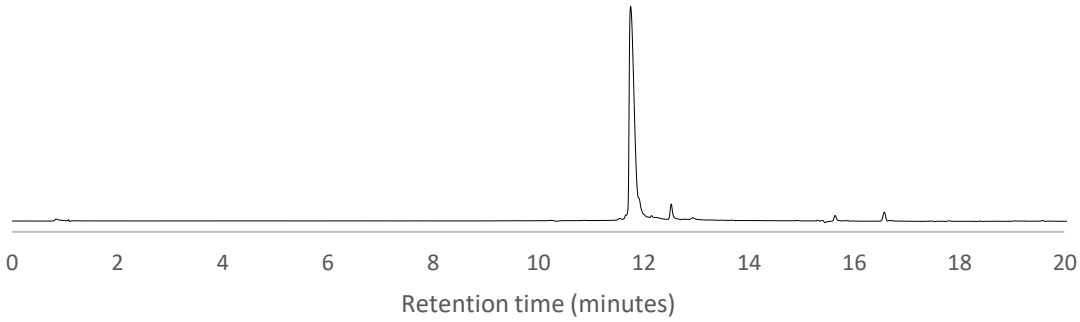

Figure 6.4. Analytical RP-HPLC trace (254 nm) of purified **66**.

7.3 Experimental Details for Chapter 3

7.3.1 General Procedures

Procedure 3A: Manual SPPS of Linear Peptides

Fmoc SPPS of peptides was performed manually in polypropylene syringe reaction vessels (10 mL; Torviq, MI, USA) fitted with a polypropylene frit. All reactions were performed at rt under continuous agitation.

First amino acid coupling to Rink amide resin

Rink amide resin (0.65 mmol, 100 - 200 mesh) was added to the SPPS syringe, swollen in DMF (5 mL) for 20 min, and then drained. The resin was washed with DMF (3 × 5 mL), CH_2Cl_2 (3 × 5 mL), and DMF (3 × 5 mL). 20% Piperidine (v/v) in DMF (5 mL) was added to the resin for 2 × 10 min to effect Fmoc deprotection and the resin was washed with the same order of solvents. PyBOP (4 equiv.) and NMM (8 equiv.) were added to a solution of the first Fmoc protected amino acid (4 equiv.; 0.2 M) in DMF, activated by mixing for 2 minutes and then added to the resin. Following agitation for 1 h, the solution was drained, and the resin as washed with DMF (3 × 5 mL), CH_2Cl_2 (3 × 5 mL), and DMF (3 × 5 mL).

Second and subsequent AA couplings and Fmoc deprotections

The subsequent amino acid coupling cycle is consisted of 1) Fmoc deprotection by the addition of 20% (v/v) piperidine in DMF (5 mL) to the resin-bound peptide for 2 x 10 min, 2) resin washes with DMF (3 × 5 mL), CH_2Cl_2 (3 × 5 mL), and DMF (3 × 5 mL), 3) amino acid coupling with addition of PyBOP (4 equiv.), NMM (8 equiv.), and Fmoc protected AA (4 equiv.; 0.2 M) in DMF to the resin-bound peptide for 1 h, 4) resin washes with DMF (3 × 5 mL), CH_2Cl_2 (3 × 5 mL), and DMF (3 × 5 mL). For the coupling of Fmoc-MeDbz-OH, HBTU (5 equiv.) and DIPEA (5.5 equiv.) were added to a solution of Fmoc-MeDbz-OH (4 equiv.; 0.2 M) in DMF, activated by mixing for 2 min and then added to the resin-bound peptide for 1 h, followed by washes with DMF (3 × 5 mL), CH_2Cl_2 (3 × 5 mL), and DMF (3 × 5 mL). For the couplings of Boc-Dhv-OH (**67**) and Boc-dehydroproline (**94**), DIC (4 equiv.) and Oxyma Pure (5 equiv.) were added to a solution of **67** or **94** (4 equiv.; 0.2 M) in DMF, activated by mixing for 2 min and then added to the resin-bound peptide for 1 h, followed by washes with DMF (3 × 5 mL), CH_2Cl_2 (3 × 5 mL), and DMF (3 × 5 mL). For the coupling of Boc-VgI-OH (**85**), IIDQ (2 equiv.) was added to a solution **85** (4 equiv.; 0.2 M) in DMF, and the solution was then added to the resin-bound peptide 120 h, followed by washes with DMF (3 × 5 mL), CH_2Cl_2 (3 × 5 mL), and DMF (3 × 5 mL).

Cyclisation of MeDbz to MeNbz (Applied only for Dbz-peptides)

The resin was first washed with CH_2Cl_2 (3 × 5 mL) and a solution of *p*-nitrophenyl chloroformate (5 eq.; 0.1 M) in dry CH_2Cl_2 was added to the resin for 2 x 40 min. The resin was then washed with DMF (3 × 5 mL), CH_2Cl_2 (3 × 5 mL), and DMF (3 × 5 mL). A solution of DIPEA (0.5 M) in 6 mL of DMF was added to the resin and agitated for 15 mins. The resin was then drained and washed with the same order of solvents. The resin was then washed with CH_2Cl_2 (3 × 6 mL) and dried under vacuum.

Procedure 3.B: Native Chemical Ligation

Ligations were performed at rt in the following ligation buffer, unless otherwise stated: Gnd·HCl (6 M), Na_2HPO_4 (200 mM), MPAA (200 mM), TCEP·HCl (20 mM). The pH was adjusted to 7.0 with $NaOH_{(aq)}$ or $HCl_{(aq)}$. Equimolar amounts of purified peptide fragments (2 mM) were dissolved in the ligation buffer and the reaction was stirred under Ar. The ligation progress was analysed by analytical RP-HPLC and ESI MS. When the ligation was complete, the ligation buffer was diluted by 10-fold ligation volume of

H_2O. TCEP·HCl (15 equiv.) was added to the solution mixture and the crude product was purified by semi-preparative RP-HPLC.

7.3.2 Characterisation Data

Methyl (*tert*-butoxycarbonyl)-D-serinate (73)

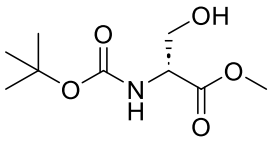

To a stirred solution of Boc_2O (16.83 g, 77.11 mmol) in CH_2Cl_2 (130 mL) was added TEA (18 mL, 129 mmol) and D-serine methyl ester hydrochloride **72** (10.00 g, 64.28 mmol), and the reaction mixture was stirred for 18 h at rt. The mixture was then washed with aq. HCl solution (1 M, 3 × 50 mL), brine (3 × 50 mL) and dried over $MgSO_4$. The solvent was removed under reduced pressure and the product was purified by silica gel flash chromatography (Hex:EtOAc– 70:30) to give a colorless oil (11.26 g, 83%). The isolated compound was in good agreement with the literature.[156]

^{1}H-NMR (400 MHz, $CDCl_3$) δ_H 5.54 (bs, NH), 4.33 (bs, 1H, Ser αCH), 3.90 (dd, *J* = 11.3, 3.7 Hz, 1H, Ser βCH_2), 3.82 (dd, *J* = 11.3, 3.7 Hz, 1H, Ser βCH_2), 3.72 (s, 3H, OCH_3), 1.40 (s, 9H, $C(CH_3)_3$).

HRMS (*m/z* APCI$^+$): Found: 242.1006 ([M + Na]$^+$, $C_9H_{17}NO_5Na$ requires: 242.1004).

3-(*tert*-Butyl) 4-methyl (*S*)-2,2-dimethyloxazolidine-3,4-dicarboxylate (75)

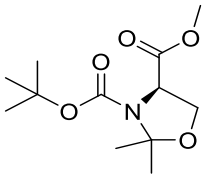

To a stirred solution of protected serine **73** (11.26 g, 51.34 mmol) in CH_2Cl_2 (60 mL) were added DMP (**74**, 31.61 mL, 256.72 mmol) and PTSA·H_2O (0.442 g, 2.57 mmol) at 0 °C. The reaction mixture was stirred at rt for 16 h and was quenched with sat. aq. $NaHCO_3$ solution (30 mL) and extracted with Et_2O (3 × 40 mL). The combined organic extracts were washed with sat. aq. $NaHCO_3$ solution (3 × 40 mL), brine (3 × 40 mL) and dried over $MgSO_4$. The solvent was removed under reduced pressure and the product

was purified via vacuum distillation to give a colorless oil (10.21 g, 76 %). The isolated compound was in good agreement with the literature.[156]

^{1}H-NMR (400 MHz, $CDCl_3$) δ_H (Isolated as a mixture of rotamers at rt): 4.39 (dd, *J* = 7.0, 2.8 Hz, 0.4H, Ser αCH), 4.29 (dd, *J* = 7.0, 2.8 Hz, 0.6H, Ser αCH), 4.05 (td, *J* = 9.5, 6.8 Hz, 1H, Ser βCH_2), 3.93 (td, *J* = 9.5, 2.8 Hz, 1H, Ser βCH_2), 3.67 (s, 3H, OCH_3), 1.57 (s, 2H, CH_3), 1.54 (s, 1H, CH_3), 1.44 (s, 2H, CH_3), 1.41 (s, 4.5H, $C(CH_3)_3$), 1.36 (s, 1H, CH_3), 1.32 (s, 4.5H, $C(CH_3)_3$).

HRMS (*m/z* APCI$^+$): Found: 282.1319 ([M + Na]$^+$, $C_{12}H_{21}NO_5Na$ requires 282.1317).

***Tert*-Butyl (*S*)-4-(2-hydroxypropan-2-yl)-2,2-dimethyloxazolidine-3-carboxylate (76)**

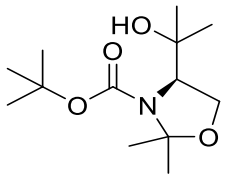

To a stirred solution of methyl magnesium bromide in Et_2O (3 M, 65 mL, 236.25 mmol) was added dropwise a solution of Boc-protected **75** (10.21 g, 39.37 mmol) solubilised in Et_2O (16 mL) while stirring at 0 °C under Ar. The reaction mixture was left under stirring at 0 °C for 1 h and then, it was quenched with dropwise addition of sat. aq. NH_4Cl solution (80 mL). The reaction mixture was extracted with EtOAc (3 × 70 mL) and the combined extracts were washed with brine (3 × 40 mL) and dried over $MgSO_4$. The solvent was removed under reduced pressure and the product was purified by silica gel flash chromatography (Hex:EtOAc– 75:25) to give a colorless oil (9.89 g, 80%). The isolated compound was in good agreement with the literature.[156]

^{1}H-NMR (400 MHz, $CDCl_3$) δ_H 4.01 – 3.92 (m, 2H, Ser βCH_2), 3.78 (bs, 1H, Ser αCH), 1.56 (s, 3H, CH_3), 1.51 (s, 3H, CH_3), 1.50 (s, 9H, $C(CH_3)_3$), 1.18 (s, 3H, CHCqC$\underline{H}_3$), 1.16 (s, 3H, CHCqC$\underline{H}_3$).

HRMS (*m/z* APCI$^+$): Found: 260.1864 ([M + H]$^+$, $C_{13}H_{26}NO_4$ requires: 260.1784).

***Tert*-Butyl (*R*)-2,2-dimethyl-4-(prop-1-en-2-yl) oxazolidine-3-carboxylate (77)**

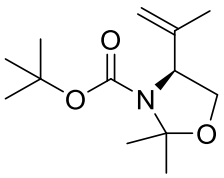

To a stirred solution of alcohol **76** (2.0 g, 7.7 mmol) and TEA (10.74 mL, 77.12 mmol) in anhydrous CH_2Cl_2 (24 mL) was added dropwise MsCl (3 mL, 38.56 mmol) at -10 ^oC under Ar and the reaction was stirred for 1 h under Ar. The reaction was then diluted with Et_2O (120 mL) and H_2O (71 mL) and washed with aq. 10% (w/v) citric acid solution (3 x 57 mL), sat. aq. $NaHCO_3$ solution (3 × 57 mL), brine (3 × 57 mL) and dried over $MgSO_4$. Solvent was removed under reduced pressure and the product was purified by silica gel flash chromatography (Hex:EtOAc– 85:15) to give a yellow oil (0.48 g, 26%). The isolated compound was in good agreement with the literature.[156]

^{1}H-NMR (400 MHz, $CDCl_3$) δ_H 4.87 (bs, 1H, C=CH_2), 4.82 (bs, 1H, C=CH_2), 4.25 – 4.17 (m, 1H, Ser αCH), 4.04 (dd, *J* = 8.9, 7.1 Hz, 1H, Ser βCH_2), 3.71 (dd, *J* = 8.9, 2.8 Hz, 1H, Ser βCH_2), 1.70 (s, 3H, CH_3), 1.66 – 1.57 (m, 3H, CH_3), 1.47 (s, 9H, C(CH_3)$_3$), 1.38 (s, 3H, CHCqC$\underline{H}_3$).

HRMS (*m/z* APCI$^+$): Found: 264.1569 ([M + Na]$^+$, $C_{13}H_{23}NO_3Na$ requires 264.1576).

Tert-Butyl (*R*)-(1-hydroxy-3-methylbut-3-en-2-yl-) carbamate (78)

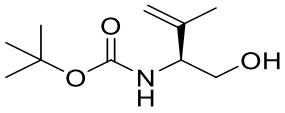

To a stirred solution of **77** (1.60 g, 6.63 mmol) in THF (10 mL) and H_2O (5 mL) at 0 °C was added ice-cold TFA (20 mL). The reaction mixture was stirred for 10 min and quenched by pouring into ice-cold sat. aq. $NaHCO_3$ solution. The resulting mixture was stirred for a further 20 min at 0 °C and extracted with EtOAc (3 × 10 mL). The combined organic extracts were washed with sat. aq. $NaHCO_3$ solution (3 × 12 mL), brine (2 × 12 mL) and dried over $MgSO_4$. The solvent was removed under reduced pressure and the product was purified by silica gel flash chromatography (Hex:EtOAc– 1:1) to give a

yellow oil (1.19 g, 91%). The isolated compound was in good agreement with the literature.[156]

^{1}H-NMR (400 MHz, $CDCl_3$) δ_H 4.92 (s, 1H, C=CH_2), 4.90 (s, 1H, C=CH_2), 4.11 – 4.00 (m, 1H, αCH), 3.62 (d, 2H, *J* = 4.2 Hz, βCH_2), 1.74 (s, 3H, CH_3), 1.41 (s, 9H, $C(CH_3)_3$).

HRMS (*m/z* APCI$^-$): Found: 202.1439 ([M + H]$^+$, $C_{10}H_{20}NO_3$ requires 202.1365).

(*S*)-2-((*tert*-Butoxycarbonyl)amino)-3-methylbut-3-enoic acid (67)

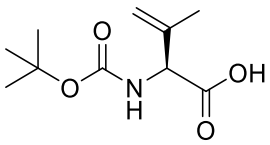

To a stirred solution of alcohol **78** (720 mg, 3.58 mmol) in acetone (120 mL) was added freshly prepared Jones reagent (2.5 M, 4.33 mL) while stirring at 0 °C. The mixture was allowed to stir at 0 °C for 3 h and quenched with IPA (10 mL). H_2O (20 mL) was added to the reaction mixture to dissolve precipitated solids and the organic solvent was removed under reduced pressure. The aq. solution was extracted with EtOAc (3 × 25 mL) and the combined organic extracts washed with brine (5 × 10 mL) and dried over $MgSO_4$. Removal of solvent under reduced pressure gave the product as a colorless oil (0.769 g, 91%). The isolated compound was in good agreement with the literature.[156]

^{1}H-NMR (400 MHz, $CDCl_3$) δ_H (mixture of rotamers at rt) 7.34 (s, 0.5H, NH), 5.33 (s, 0.5H, NH), 5.12 (s, 1H, C=CH_2), 5.04 (bs, 1H, C=CH_2), 4.78 (bs, 0.5H, αCH), 4.58 (bs, 0.5H, αCH), 1.82 (s, 3H, CH_3), 1.42 (s, 9H, $C(CH_3)_3$).

HRMS (*m/z* APCI$^+$): Found: 238.1048 ([M + Na]$^+$, $C_{10}H_{17}NO_4Na$ requires 238.1049).

4-(methylamino)-3-nitrobenzoic acid (82)

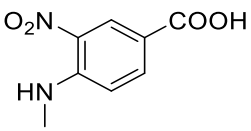

To a solution of 4-fluoro-3-niteobenzoic acid **81** (3.00 g, 16.21 mmol) in MeOH (45 mL) was added a 40% (v/v) solution of methylamine in MeOH (15 mL, 135 mmol) and the reaction mixture was stirred at rt for 18 h. The reaction mixture was poured into H_2O (45 mL) and acidified to pH 3 with dropwise addition of 37% aq. HCl to give a bright

yellow precipitate. The precipitate was filtered under vacuum, washed with H_2O (50 mL) and dried to give the product as a yellow powder (2.86 g, 90%). The isolated product was in good agreement with literature.[207]

^{1}H-NMR (400 MHz, DMSO-d_6) δ_H 12.85 (s, 1H, COOH), 8.59 (d, *J* = 2.1 Hz, 1H, Ar-CH), 8.55 – 8.47 (m, 1H, NH), 7.96 (dd, *J* = 9.0, 2.1 Hz, 1H, Ar-CH), 7.03 (d, *J* = 9.0 Hz, 1H, Ar-CH), 3.0 (d, *J*= 5.0 Hz, 3H, CH_3).

HRMS (*m/z* APCI$^+$): Found: 195.0411 ([M - H]$^-$, $C_8H_7N_2O_4$ requires 195.0484).

4-(methylamino)-3-nitrobenzoic acid (83)

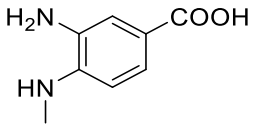

A solution of 4-(methylamino)-3-nitrobenzoic acid **82** (2.75 g, 14.58 mmol) in MeOH (150 mL) was purged with Ar for 15 min. Then 10% Pd/C (0.113 g, 1.06 mmol) was added, and the solution was purged again with Ar. The reaction was stirred at rt under an atmosphere of H_2 for 16 h. Filtration of the reaction mixture through Celite® followed and the filtrate was concentrated under reduced pressure to give a dark green powder (2.12 g, 88%). The isolated compound was in good agreement with literature.[207]

^{1}H-NMR (400 MHz, DMSO-d_6) δ_H 7.22 (dd, *J* = 8.2, 2.0 Hz, 1H, Ar-CH), 7.15 (d, *J* = 2.0 Hz, 1H, Ar-CH), 6.38 (d, *J* = 8.2 Hz, 1H, Ar-CH), 5.32 (bs, 1H, NH), 2.77 (d, *J* = 4.2 Hz, 3H, CH_3).

HRMS (*m/z* APCI$^-$): Found: 165.0670 ([M - H]$^-$, $C_8H_9N_2O_2$ requires 165.0742).

4-(methylamino)-3-nitrobenzoic acid (79)

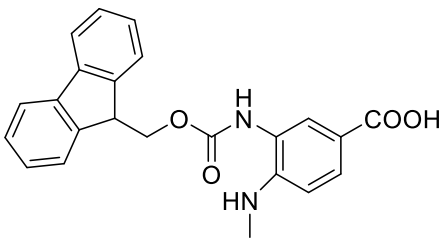

To a stirred solution of acid **83** (2.00 g, 12.04 mmol) in 1:1 H_2O/MeCN (pH 8, 40 mL) was added Fmoc-OSu (4.46 g, 13.24 mmol) in small portions over 20 min and the solution was stirred at rt for 18 h. The solution was acidified to pH 3 using 1 M aq. HCl

solution to precipitate the product which was then filtered under vacuum and washed with cold Et_2O (25 mL), hexane (25 mL) and MeOH (30 mL). The solid was dried under vacuum for 3 h to give a beige powder (3.75 g, 80%). The isolated compound was in good agreement with the literature.[158]

^{1}H-NMR (400 MHz, DMSO-d_6) δ_H 12.11 (s, 1H, COOH), 8.69 (bs, 1H, Ar-CH), 7.88 (d, *J* = 7.4 Hz, 2H, Fmoc Ar-CH) 7.80 – 7.60 (m, 3H, Fmoc Ar-CH, Ar-CH), 7.41 (t, *J* = 7.4 Hz, 2H, Fmoc Ar-CH) 7.35 – 7.25 (m, 2H, Fmoc Ar-CH), 6.58 (d, *J* = 8.6 Hz, 1H, Ar-CH), 5.85 (s, 1H, $CH_3N\underline{H}$), 4.44 – 4.18 (m, 3H, Fmoc CH, Fmoc CH_2), 2.76 (d, *J* = 4.8 Hz, 3H, CH_3).

HRMS (*m/z* APCI$^+$): Found: 411.1322 ([M + Na]$^+$, $C_{23}H_{20}N_2O_4Na$ requires 411.1321).

(*S*)-2-((2*S*,5*S*,8*S*,14*S*,17*S*,18*R*)-17-amino-2-(3-guanidinopropyl)-8-(4-hydroxybenzyl)-5,14-diisobutyl-19-mercapto-18-methyl-4,7,10,13,16-pentaoxo-3,6,9,12,15-pentaazanonadecanamido)-N1-((*S*)-1-(((*S*)-1-(((*S*)-1,6-diamino-1-oxohexan-2-yl)amino)-3-(4-hydroxyphenyl)-1-oxopropan-2-yl)amino)-3-methyl-1-oxobutan-2-yl)succinimide (69)

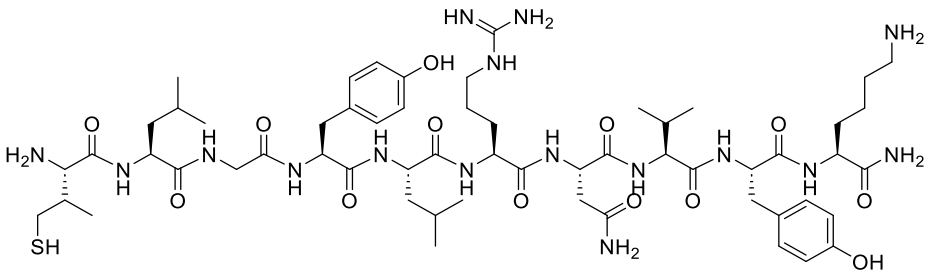

The peptide was synthesised at 0.10 mmol scale by manual SPPS as described in Procedure 3.A using Fmoc-Lys(Boc)-OH, Fmoc-Tyr(*t*Bu)-OH, Fmoc-Val-OH, Fmoc-Asn(Trt)-OH, Fmoc-Arg(Pbf)-OH, Fmoc-Leu-OH, Fmoc-Tyr(*t*Bu)-OH, Fmoc-Gly-OH, Fmoc-Leu-OH, and Boc-Dhv-OH. ATE and *S*-deacetylation reactions were carried out on-resin as described in Procedures 2.B and 2.C, respectively. Resin cleavage and global deprotection of the peptide were carried out as described in Procedure 2.D. The crude product was dissolved in H_2O:AcN (1:1, with 0.1% TFA) and subjected to purification by semi-preparative RP-HPLC (5 – 95% AcN in H_2O with 0.1% (v/v) TFA over 60 min) over multiple injections. Fractions containing pure product were combined and the solvent was lyophilised yielding the desired product as a white solid (41 mg, isolated yield: 35%, >95% purity).

Analytical RP-HPLC R_t (5 – 95% AcN in H_2O with 0.1% (v/v) TFA over 25 min, 220 nm): 9.040 min.

HRMS (*m/z* ESI^+): Found: 1255.6968 ($[M+H]^+$, $C_{58}H_{95}N_{16}O_{13}S$ requires 1255.6907), 628.3521 ($[M+2H]^{2+}$, $C_{58}H_{96}N_{16}O_{13}S$ requires 628.3453), 419.2378 ($[M+3H]^{3+}$, $C_{58}H_{97}N_{16}O_{13}S$ requires 419.2323).

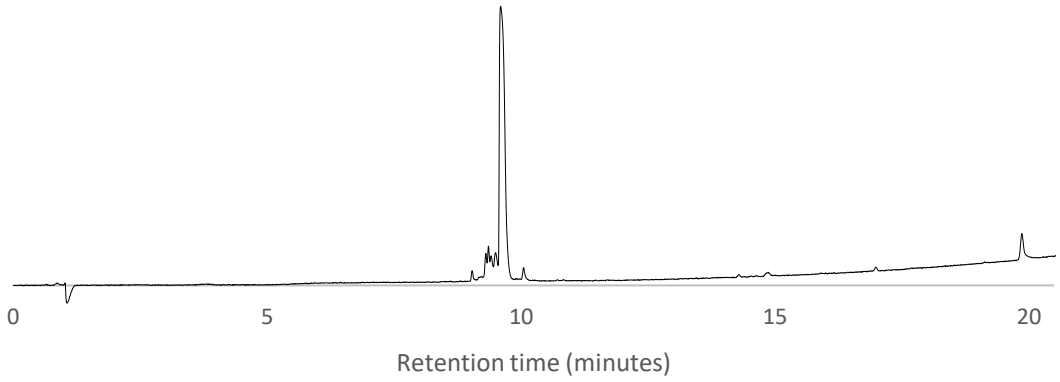

Figure 6.5. Analytical RP-HPLC trace (220 nm) of purified **69**.

_N_-(2-amino-2-oxoethyl)-3-(glycyl-L-leucyl-L-alanyl-L-lysyl-L-valyl-L-methionyl-L-arginyl-L-lysyl)-1-methyl-2-oxo-2,3-dihydro-1_H_-benzo[d]imidazole-5-carboxamide (65)

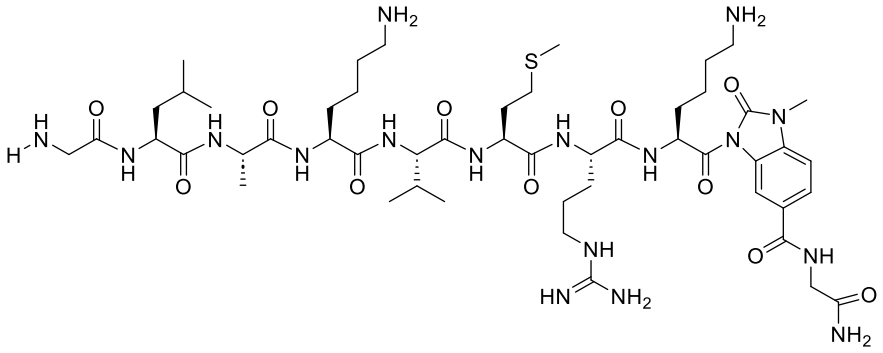

The peptide was synthesised at 0.10 mmol scale by manual SPPS as described in Procedure 3.A using Fmoc-Gly-OH, Fmoc-MeDbz-OH, Fmoc-Lys(Boc)-OH, Fmoc-Arg(Pbf)-OH, Fmoc-Met-OH, Fmoc-Val-OH, Fmoc-Lys(Boc)-OH, Fmoc-Ala-OH, Fmoc-Leu-OH, and Boc-Gly-OH. MeDbz was cyclized to MeNbz as described in in Procedure 3.A. Resin cleavage and global deprotection of the peptide were carried out as described in Procedure 2.D. The crude product was dissolved in H_2O:AcN (1:1, with 0.1% TFA) and

subjected to purification by semi-preparative RP-HPLC (5 – 95% AcN in H_2O with 0.1% (v/v) TFA over 60 min) over multiple injections. Fractions containing pure product were combined and the solvent was lyophilised yielding the desired product as a pale yellow solid (72 mg, isolated yield: 65%, >90% purity).

Analytical RP-HPLC R_t (5 – 95% AcN in H_2O with 0.1% (v/v) TFA over 30 min, 220 nm): 9.568 min.

HRMS (*m/z* ESI^+): Found: 1132.6371 ($[M+H]^+$, $C_{50}H_{86}N_{17}O_{11}S$ requires 1132.6335), 566.8239 ($[M+2H]^{2+}$, $C_{50}H_{87}N_{17}O_{11}S$ requires 566.8239), 378.2190 ($[M+3H]^{3+}$, $C_{50}H_{88}N_{17}O_{11}S$ requires 378.2111).

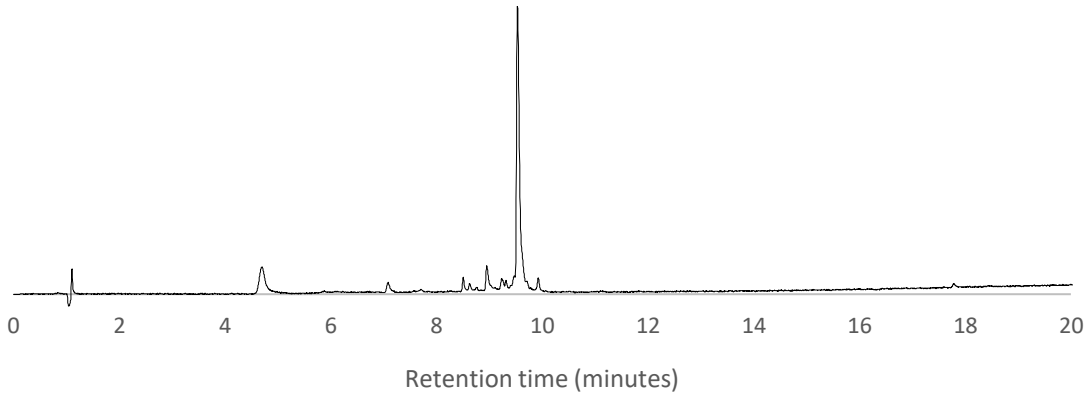

Figure 6.6. Analytical RP-HPLC trace (220 nm) of purified **65**.

Methyl (2*S*)-2-(((Benzyloxy)carbonyl)amino)-4-(methylsulfinyl)butanoate (91)

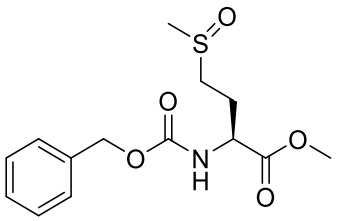

To stirred solution of Cbz-Met-OMe (5.00 g, 16.9 mmol) in MeOH (25 mL) at 0 °C, $NaIO_4$ (3.96 g, 18.6 mmol) dissolved in H_2O (25 mL) was added dropwise. The reaction mixture was stirred at rt under Ar for 14 h. The resulting mixture was filtered through Celite® and MeOH was removed under reduced pressure. The solution was extracted with CH_2Cl_2 (3 × 25 mL), and the combined extracts were washed with brine (2 × 30 mL)

and dried over $MgSO_4$ to yield the product as a colourless oil (5.15 g, 97%). The isolated compound was in good agreement with the literature.[156,161]

^{1}H-NMR (400 MHz, $CDCl_3$) δ_H 7.39 – 7.29 (m, 5H, Ar-CH), 5.66 (dd, *J* = 28.8, 5.7 Hz, 1H, NH), 5.11 (s, 2H, Ar-CH_2CO), 4.56 – 4.43 (m, 1H, αCH), 3.77 (s, 3H, OCH_3), 2.85 – 2.64 (m, 2H, γCH_2), 2.53 (s, 3H, $SOCH_3$), 2.46 – 2.32 (m, 1H, βCH_2), 2.24 – 2.06 (m, 1H, βCH_2).

HRMS (*m/z* APCI$^+$): Found: 314.1066 ([M + H]$^+$, $C_{14}H_{20}NO_5S$ requires: 314.0984).

Methyl *(S)*-2-(((benzyloxy)carbonyl)amino)but-3-enoate (92)

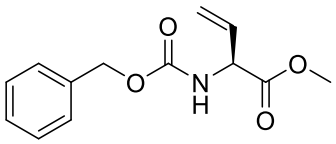

A stirred solution of **91** (4.70 g, 15.81 mmol) in xylene (50 mL) was heated under reflux for 72 h. Solvent was removed under reduced pressure and the crude mixture was purified by silica gel flash chromatography (Hex:EtOAc – 90:10 to 80:20) to yield the product as a colourless oil (0.86 g, 22%). The isolated compound was in good agreement with the literature.[156,161]

^{1}H-NMR (400 MHz, $CDCl_3$) δ_H 7.44 – 7.30 (m, 5H, Ar-CH), 5.97 – 5.81 (m, 1H, C<u>H</u>=CH_2), 5.64 (bs, 1H, αCH), 5.35 (d, *J* = 17.1, 1H, CH=C<u>H</u>$_2$), 5.27 (d, *J* = 10.3, 1H, CH=C<u>H</u>$_2$), 5.12 (s, 2H, Ar-CH_2), 4.94 (bs, 1H, NH), 3.71 (s, 1H, OCH_3).

HRMS (*m/z* APCI$^+$): Found: 272.0900 ([M + Na]$^+$, $C_{13}H_{15}NO_4Na$ requires: 272.0899), 250.1073 ([M + H]$^+$, $C_{13}H_{16}NO_4$ requires: 250.1001).

***(S)*-2-Aminobut-3-enoic acid hydrochloride (93)**

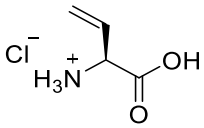

A solution of **92** (0.70 g, 2.81 mmol) in 6 M aq. HCl solution (20 mL) was heated under reflux for 2 h. The resulting mixture was cooled and washed with CH_2Cl_2 (2 × 20 mL) and solvent removed under reduced pressure. The resulting crude product was refluxed in acetone for 20 min and filtered to afford the product as a white solid (0.35 g, 75%). The isolated compound was in good agreement with the literature.[156,161]

^{1}H-NMR (400 MHz, D_2O) δ_H 5.92 (ddd, *J* = 17.6, 10.5, 7.4 Hz, 1H, C<u>H</u>=CH_2), 5.52 (dd, *J* = 2.6, 1.1 Hz, 1H, CH=C<u>H</u>$_2$), 5.48 (dd, *J* = 4.2, 1.1 Hz, 1H, CH=C<u>H</u>$_2$), 4.51 (d, *J* = 7.4 Hz, 1H, αCH).

HRMS (*m/z* APCI$^+$): Found: 102.0545 ([M + H]$^+$, $C_4H_8NO_2$ requires: 102.0550).

***(S)*-2-((*tert*-Butoxycarbonyl)amino)but-3-enoic acid (85)**

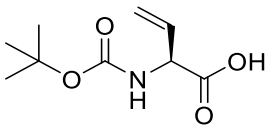

To a solution of **93** (0.6 g, 4.36 mmol) and $NaHCO_3$ (0.83 g, 10 mmol) in H_2O (24 mL) was added Boc_2O (1.14 g, 5.23 mmol) dissolved in dioxane (24 mL) and the reaction was refluxed for 3 h. Dioxane was removed under reduced pressure and the mixture acidified to pH 2 using 1 M aq. HCl solution before extraction with CH_2Cl_2 (3 × 30 mL). The combined organic extracts were washed with brine (2 × 30 mL), dried over $MgSO_4$, and concentrated under reduced pressure to afford the product as a colourless oil (0.745 g, 85%). The isolated compound was in good agreement with the literature.[156,161]

^{1}H-NMR (400 MHz, $CDCl_3$) δ_H 7.23 (s, 0.5H, NH), 5.91 (m, 1H, C<u>H</u>=CH_2), 5.39 (d, *J* = 16.9 Hz, 1H, CH=C<u>H</u>$_2$), 5.33 – 5.24 (m, 1H, CH=C<u>H</u>$_2$), 5.19 (bs, 0.5H, NH), 4.91 (bs, 0.5H, αCH), 4.68 (s, 0.5H, αCH), 1.48 (s, 9H, $C(CH_3)_3$) (mixture of rotamers at rt).

HRMS (*m/z* APCI$^-$): Found: 200.0927 ([M - H]$^-$, $C_9H_{14}NO_4$ requires: 200.0928).

(2*S*,4*R*)-4-hydroxy-2-(methoxycarbonyl)pyrrolidin-1-ium (100)

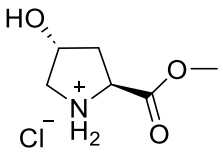

To a stirred solution of *trans*-hydroxyproline-OH (4.0 g, 30.5 mmol) in anhydrous MeOH (56 mL) was added thionyl chloride (2.45 mL, 33.55 mmol) dropwise at 0 °C. The reaction was stirred at rt for 1 h before it was refluxed for 22 h. The resulting solution was concentrated under reduced pressure, and the residue was azeotroped with MeOH yielding the product as a white solid (4.38 g, 98 %). The isolated compound was in good agreement with the literature.[208]

^{1}H-NMR (400 MHz, DMSO-d_6) δ_H 9.71 (bs, 2H, NH_2^+), 5.57 (d, *J* = 2.9 Hz, 1H, OH), 4.48 (dd, *J* = 10.8, 7.5 Hz, 1H, Pro αCH), 4.5 – 4.4 (m, 1H, Pro γCH), 3.76 (s, 3H, OCH_3), 3.38 – 3.35 (m, 1H, Pro δCH_2), 3.10 – 3.05 (m, 1H, Pro δCH_2), 2.24 – 2.16 (m, 1H, Pro βCH_2), 2.15 – 2.05 (m, 1H, Pro βCH_2).

HRMS (*m/z* APCI$^+$): Found: 146.0805 ([M + H]$^+$, $C_6H_{12}NO_3$ requires 146.0739).

1-(*tert*-butyl) 2-methyl (2*S*,4*R*)-4-hydroxypyrrolidine-1,2-dicarboxylate (101)

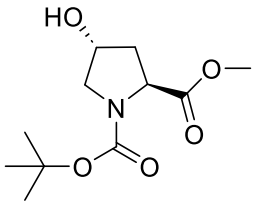

To a stirred solution of methyl ester **100** (4.38 g, 30.2 mmol) and TEA (10.6 mL, 75.5 mmol) in CH_2Cl_2 (100 mL) was added a solution of Boc_2O (7.9 g, 36.1 mmol) in CH_2Cl_2 (20 mL) at 0 °C. The solution was stirred under Ar for 18 h. Upon completion, the reaction was washed with aq. HCl (1 M) (3 × 50 mL), brine (3 × 50 mL) and dried over $MgSO_4$. The solvent was removed under reduced pressure and the crude product was purified by silica gel flash chromatography (CH_2Cl_2:MeOH– 99:1) to give a pale yellow oil (5.9 g, 79 %). The isolated compound was in good agreement with the literature.[164]

^{1}H-NMR (400 MHz, $CDCl_3$) δ_H (mixture of rotamers at rt) 4.48 – 4.30 (m, 2H, Pro αCH, Pro γCH), 3.70 (s, 3H, OCH_3), 3.66 – 3.59 (m, 1H, Pro δCH_2), 3.58 – 3.40 (m, 1H, Pro δCH_2) 3.24 (bs, 1H, OH), 2.31 – 2.17 (m, 1H, Pro βCH_2), 2.07 – 1.95 (m, 1H, Pro βCH_2), 1.41 (s, 3H, $C(CH_3)_3$), 1.36 (s, 6H, $C(CH_3)_3$).

HRMS (*m/z* APCI$^+$): Found: 268.1151 ([M + Na]$^+$, $C_{11}H_{19}NO_5Na$ requires: 268.1161).

1-(*tert*-butyl) 2-methyl (2*S*,4*S*)-4-iodopyrrolidine-1,2-dicarboxylate (102)

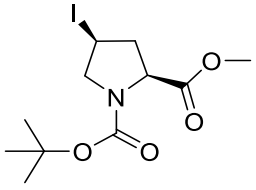

To a solution of alcohol **101** (5.9 g, 24.0 mmol) and PPh_3 (9.15 g, 34.9 mmol) in THF (100 mL) at -78 °C under N_2 was added DIAD (5.4 mL, 27.4 mmol), followed by

iodomethane (1.3 mL, 27.9 mmol). The reaction mixture was removed from the cold bath and stirred at rt for 16 h. The reaction mixture was filtered through Celite®, the filtrate was concentrated under reduced pressure, and the crude product was purified by silica gel flash chromatography (Hex:EtOAc– 19:1 to 4:1) to give a pale yellow oil (3.32 g, 39%). The isolated compound was in good agreement with the literature.[164]

^{1}H-NMR (400 MHz, $CDCl_3$) δ_H (mixture of rotamers at rt) 4.27 (td, *J* = 32.6, 7.8 Hz, 1H, Pro γCH), 4.16 – 3.99 (m, 2H, Pro δCH_2), 3.76 (s, 3H, OCH_3), 3.71 – 3.61 (m, 1H, Pro αCH), 2.93 – 2.79 (m, 1H, Pro βCH_2), 2.41 – 2.27 (m, 1H, Pro βCH_2), 1.46 (s, 3H, $C(CH_3)_3$), 1.41 (s, 6H, $C(CH_3)_3$).

HRMS (*m/z* APCI$^+$): Found: 378.0179 ([M + Na]$^+$, $C_{11}H_{18}INO_4Na$ requires: 378.0178).

1-(tert-butyl) 2-methyl (S)-2,5-dihydro-1H-pyrrole-1,2-dicarboxylate (103)

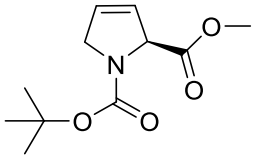

To a solution of **102** (2.0 g, 5.63 mmol) in toluene (56 mL) was added dropwise DBU (1.0 mL, 6.76 mmol) and the reaction mixture was stirred for 2 h at 80 °C. The precipitated solids were filtered and washed with toluene (10 mL) and the filtrate was concentrated under reduced pressure. The crude product was purified by silica gel flash chromatography (Hex:EtOAc– 8:1) to give a colourless oil (1.02 g, 90%). The isolated product was in good agreement with literature.[165,208]

^{1}H-NMR (400 MHz, $CDCl_3$) δ_H (mixture of rotamers at rt) 5.95 (ddt, *J* = 17.9, 6.3, 2.1 Hz, 1H, Pro γCH), 5.71 (dddd, *J* = 17.9, 6.3, 4.3, 2.1 Hz, 1H, Pro βCH), 5.06 – 4.91 (m, 1H, Pro αCH), 4.33 – 4.08 (m, 2H, Pro δCH_2), 3.72 (s, 3H, OCH_3), 1.46 (s, 3H, $C(CH_3)_3$), 1.41 (s, 6H, $C(CH_3)_3$).

HRMS (*m/z* APCI$^+$): Found: 250.1048 ([M + Na]$^+$, $C_{11}H_{17}NO_4Na$ requires: 250.1055).

(S)-1-(tert-butoxycarbonyl)-2,5-dihydro-1H-pyrrole-2-carboxylic acid (94)

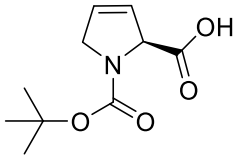

A solution of **103** (1.1 g, 4.84 mmol) and NaOH (0.21 g, 5.4 mmol) in MeOH/H_2O (1:1) was heated under reflux for 5 h. MeOH was removed under reduced pressure and the aqueous layer was washed with Et_2O (3 × 10 ml) and acidified to pH 2.0 using 1 M aq. HCl solution. The aqueous layer was extracted with Et_2O (3 × 10 ml), the combined organic layers were dried over $MgSO_4$ and the solvent was removed under reduced pressure affording the product as a white solid (0.76 g, 74%). The isolated product was in good agreement with literature.[208]

^{1}H-NMR (400 MHz, $CDCl_3$) δ_H (mixture of rotamers at rt) 6.01 (dd, *J* = 24.8, 4.6 Hz, 1H, Pro γCH), 5.83 (dd, *J* = 45.9, 4.6 Hz, 1H, Pro βCH), 5.17 – 4.93 (m, 1H, Pro αCH), 4.32 – 4.17 (m, 2H, Pro δCH_2), 1.56 (s, 4.5H, $C(CH_3)_3$), 1.46 (s, 4.5H, $C(CH_3)_3$).

HRMS (*m/z* APCI$^+$): Found: 214.1074 ([M + H]$^+$, $C_{10}H_{16}NO_4$ requires: 214.1001).

tert-butyl (3-aminopropyl)carbamate (108)

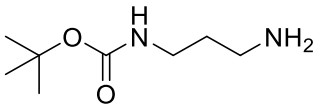

To a solution of Boc_2O (5 g, 22.9 mmol) in $CHCl_3$ (100 mL) was added slowly over 3 h a solution of 1,3-diaminopropane (**107**, 9.6 mL, 114.55 mmol) in $CHCl_3$ (50 mL) at 0^{o}C. The reaction mixture was stirred at rt for 16 h and the solvent was removed under reduced pressure. The white crude solid was dispersed in H_2O (130 mL), extracted with CH_2Cl_2 (3 × 100 mL) and the organic layers were combined, washed with brine (2 × 50 mL) and removed under reduced pressure. The crude product was purified by silica gel flash chromatography ($CHCl_3$:MeOH– 2:1) to give a pale-yellow oil (3.5 g, 88%). The isolated compound was in good agreement with the literature.[170]

^{1}H-NMR (400 MHz, $CDCl_3$) δ_H 5.09 (bs, CONH), 3.21 – 3.08 (m, 2H, CONHC$\underline{H}_2$), 2.72 (t, *J* = 6.7 Hz, 2H, C$\underline{H}_2NH_2$), 1.80 (bs, 2H, NH_2), 1.57 (app.p, 2H, $NHCH_2C\underline{H}_2$), 1.39 (s, 9H, $C(CH_3)_3$).

HRMS (*m/z* APCI$^+$): Found: 175.1442 ([M + H]$^+$, $C_8H_{19}N_2O_2$ requires 175.1368).

tert-butyl (3-(2,5-dioxo-2,5-dihydro-1H-pyrrol-1-yl)propyl)carbamate (109)

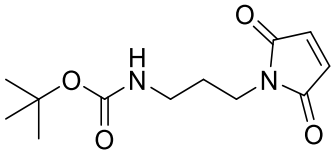

To a stirred solution of **108** (3.16 g, 18.14 mmol) in anhydrous toluene (60 mL) was added maleic anhydride (2.13 g, 21.76 mmol) in anhydrous toluene (10 mL) and the reaction mixture was stirred at rt under Ar for 16 h. The solvent was removed under reduced pressure to give a white crude solid which was used for the next cyclisation step without further purification. The crude acid was dissolved in Ac_2O (18 mL), sodium acetate (1.49 g, 18.14 mmol) was added slowly to the solution and the reaction was stirred at 60 °C under Ar for 18 h. The solvent was removed under reduced pressure to give a dark brown crude product which was purified by silica gel flash chromatography (EtOAc:Hex– 13:7) yielding a colorless oil (1.61 g, 35% over two steps). The isolated compound was in good agreement with the literature.[171]

^{1}H-NMR (400 MHz, $CDCl_3$) δ_H 6.70 (bs, 2H, C<u>H</u>=C<u>H</u>) 4.95 (bs, 1H, NH), 3.58 (t, *J* = 6.6 Hz, 2H, NHCH_2CH_2C<u>H</u>$_2$), 3.08 (dd, *J* = 12.2, 6.6 Hz, 2H, NHC<u>H</u>$_2$), 1.75 (app.p, 2H, NHCH_2C<u>H</u>$_2$), 1.43 (s, 9H, C(CH_3)$_3$).

HRMS (*m/z* APCI$^-$): Found: 254.1273 ([M - H]$^-$, $C_{12}H_{17}N_2O_4$ requires 254.1267).

3-(2,5-dioxo-2,5-dihydro-1H-pyrrol-1-yl)propan-1-aminium 2,2,2-trifluoroacetate (110)

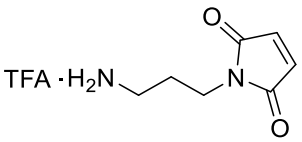

To a mixture of **109** (1.73 g, 6.00 mmol) in CH_2Cl_2 (20 mL) was added TFA (10 mL) and the reaction was stirred at rt for 3 h. The reaction mixture was diluted with CH_2Cl_2 (20 mL) and H_2O (20 mL) and extracted with H_2O (3 × 25 mL). The combined aqueous layers were washed with CH_2Cl_2 (3 × 25 mL) and concentrated under reduced pressure

yielding a pure off-white solid (1.73 g, 99%). The isolated compound was in good agreement with the literature.[209]

^{1}H-NMR (400 MHz, $CDCl_3$) δ_H 7.85 (bs, 3H, NH_3^+) 7.03 (s, 2H, C<u>H</u>=C<u>H</u>), 3.46 (t, *J* = 6.9 Hz, 2H, $NH_3CH_2CH_2C\underline{H_2}$), 2.87 – 2.67 (m, 2H, $NH_3C\underline{H_2}$), 1.85 – 1.70 (m, 2H, $NH_3CH_2C\underline{H_2}$).

HRMS (*m/z* APCI$^+$): Found: 155.0807 ([M + H]$^+$, $C_7H_{11}N_2O_2$ requires 155.0742).

tert-butyl(2-((3-(2,5-dioxo-2,5-dihydro-1H-pyrrol-1-yl)propyl)carbamoyl)phenyl)carbamate (106)

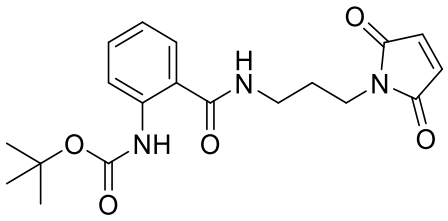

To a stirred solution of **110** (0.8 g, 3.73 mmol), EDC·HCl (1.44 g, 7.46 mmol), HOBt (0.75 g, 5.59 mmol) and TEA (2.0 mL, 14.91 mmol) in CH_2Cl_2 (40 mL) was added slowly Boc-Abz-OH (1.0 g, 3.73 mmol) at 0 °C and the reaction was stirred at rt for 18 h. The solution was washed with brine (3 × 25 mL), H_2O (3 × 25 mL), dried over $MgSO_4$ and the solvent was removed under reduced pressure. The crude product was purified by silica gel flash chromatography (EtOAc:Hex– 8:2) to give a pale yellow solid (0.96 g, 69%).

^{1}H-NMR (600 MHz, DMSO-*d*$_6$) δ_H 10.35 (s, 1H, Boc N<u>H</u>), 8.38 (d, *J* = 7.9 Hz, 1H, Abz Ar-CH), 7.58 (dd, *J* = 7.9, 1.4 Hz, 1H, Abz Ar-CH), 7.47 – 7.42 (m, 1H, Abz Ar-CH), 7.05 – 7.01 (m, 1H, Abz Ar-CH), 6.98 (s, 1H, N<u>H</u>CH_2CH_2), 6.75 (s, 2H, C<u>H</u>=C<u>H</u>), 3.70 – 3.63 (m, 2H, $NHCH_2CH_2C\underline{H_2}$), 3.38 (dd, *J* = 12.4, 6.2 Hz, 2H, $NHC\underline{H_2}CH_2CH_2$), 1.93 – 1.84 (m, 2H, $NHCH_2C\underline{H_2}CH_2$), 1.51 (s, 9H, $C(CH_3)_3$).

^{13}C NMR (151 MHz, DMSO-*d*$_6$) δ_C 171.2 (Mal C=O), 168.9 (Abz C=O), 153.1 (Boc C=O), 140.6 (Abz qC), 134.3 (<u>C</u>H=<u>C</u>H), 132.5 (Abz Ar-CH), 126.5 (Abz Ar-CH), 121.4 (Abz Ar-CH), 119.8 (Abz Ar-CH), 119.2 (Abz qC), 80.2 ($\underline{C}(CH_3)_3$), 36.1 ($NH\underline{C}H_2$), 34.7 ($NHCH_2CH_2\underline{C}H_2$), 28.7 ($C(\underline{C}H_3)_3$), 28.0 ($NHCH_2\underline{C}H_2$).

HRMS (*m/z* APCI$^+$): Found: 372.1571 ([M - H]$^-$, $C_{19}H_{22}N_3O_5$ requires 372.1638).

ν_{max} (film)/cm^{-1}: 3343 (N-H), 3086 (C-H), 2980 (CH_2), 1704 (C=O), 1690 (C=C), 1431 (Ar C-C).

(3S,6S,9S,15S)-15-((2-amino-2-oxoethyl)carbamoyl)-3-((3S,6S,12S)-3-(3-amino-3-oxopropyl)-1-((2S)-1-((2R)-2-amino-5-((1-(3-(2-aminobenzamido)propyl)-2,5-dioxopyrrolidin-3-yl)thio)pentanoyl)pyrrolidin-2-yl)-12-(3-guanidinopropyl)-9-((R)-1-hydroxyethyl)-6-isopropyl-1,4,7,10,13-pentaoxo-2,5,8,11,14-pentaazahexadecan-16-amido)-9-benzyl-12-((R)-1-hydroxyethyl)-6-isopropyl-4,7,10,13-tetraoxo-5,8,11,14-tetraazaoctadecanedioic acid (111)

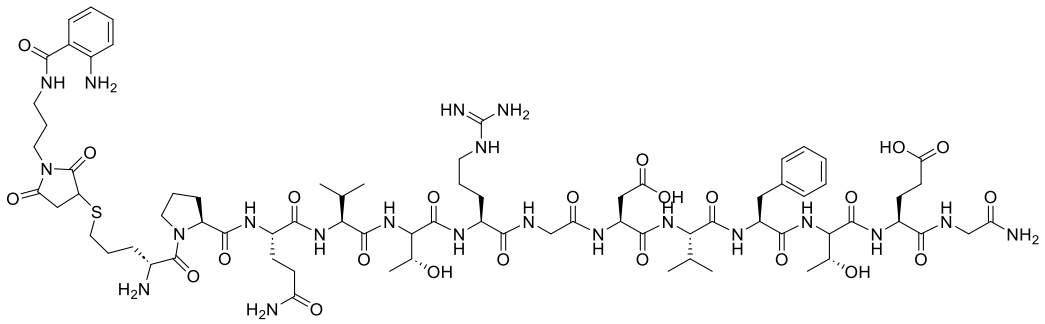

The peptide was synthesised at 0.10 mmol scale by manual SPPS as described in Procedure 3.A using Fmoc-Gly-OH, Fmoc-Glu(O*t*Bu)-OH, Fmoc-Thr(*t*Bu)-OH, Fmoc-Phe-OH, Fmoc-Val-OH, Fmoc-Asp(O*t*Bu)-OH, Fmoc-Gly-OH, Fmoc-Arg(Pbf)-OH, Fmoc-Thr(*t*Bu)-OH, Fmoc-Val-OH, Fmoc-Gln(Trt)-OH, Fmoc-Pro-OH, Boc-Agl-OH. ATE and *S*-deacetylation reactions were carried out on-resin as described in Procedures 2.B and 2.C, respectively. The on-resin covalent attachment of the fluorophore **106** at the *N*-terminus of the linear RGD peptide was achieved by treating the resin-bound peptide with a solution of **106** (10 equiv.) and TEA (10 equiv.) in DMF (3 mL) for 1 h. Resin cleavage and global deprotection of the peptide were carried out as described in Procedure 2.D. The crude product was dissolved in H_2O:AcN (1:1, with 0.1% TFA) and subjected to purification by semi-preparative RP-HPLC (5 – 95% AcN in H_2O with 0.1% (v/v) TFA over 60 min) over multiple injections. Fractions containing pure product were combined and the solvent was lyophilised yielding the desired product as a white solid (37 mg, isolated yield: 22%, >95% purity)

Analytical RP-HPLC R_t (5 – 95% AcN in H_2O with 0.1% (v/v) TFA over 30 min, 254 nm): 11.593 min.

HRMS (*m/z* ESI$^+$): Found: 854.9065 ([M+2H]$^{+2}$, $C_{75}H_{115}N_{21}O_{23}S_2$ requires 854.9019), 570.2753 ([M+3H]$^{3+}$, $C_{75}H_{116}N_{21}O_{23}S_2$ requires 570.2680).

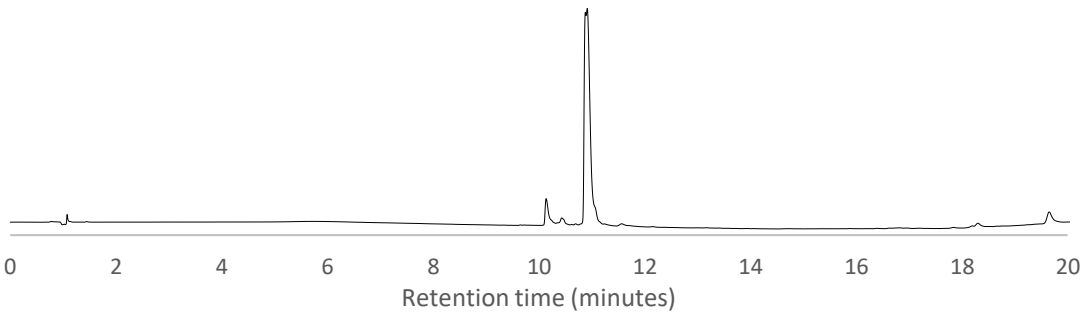

Figure 6.7. Analytical RP-HPLC trace (220 nm) of purified **111**.

7.4 Experimental Details for Chapter 4

7.4.1 General Procedures

Procedure 4A: On-resin chloroacetylation of the free N-terminus group

Following the final Fmoc-deprotection, the resin-bound peptide was treated with a solution of chloroacetic anhydride (5.0 equiv.) and TEA (5.0 equiv.) in DMF (0.2 M) under continuous agitation for 1 h. The resin was then washed with DMF (3 × 5 mL) and CH_2Cl_2 (3 × 5 mL), and the progress of the reaction was monitored qualitatively using the bromophenol blue test.

Procedure 4B: Peptide Cyclisation

The crude linear peptide precursor was dissolved in a 5 mM solution of H_2O:AcN (1:1) and the pH of the solution was adjusted to 9.0 with aq. NaOH (0.1 M). The reaction mixture was stirred at rt for 1 – 2 h and the progress of the reaction was monitored by analytical RP-HPLC and ESI-MS. Upon completion, the pH of the solution was then adjusted to 6.0 with aq. HCl (0.1 M) and the crude product was lyophilised prior to purification by semi-preparative RP-HPLC.

Procedure 4C: Post-cyclisation Radical TEC Reaction

To a 5 mM solution of the cyclic peptide (20 mg, 0.02 mmol, 1.0 equiv.) in H_2O:AcN (1:1) was added DPAP (2 mg, 0.01 mmol, 0.5 equiv.) and the thiol-containing molecule (2 equiv.). The reaction mixture was irradiated at 365 nm under stirring for 2 h. AcN was removed under reduced pressure and the crude product was lyophilised prior to purification by semi-preparative RP-HPLC.

7.4.2 Characterisation Data

(S)-1-((3R,6S,9S,12S,15S)-6-(2-amino-2-oxoethyl)-9-(3-amino-3-oxopropyl)-12-benzyl-15-(4-hydroxybenzyl)-5,8,11,14,17-pentaoxo-1-thia-4,7,10,13,16-pentaazacyclooctadecane-3-carbonyl)-N-((S)-1-((2-amino-2-oxoethyl)amino)-5-((diaminomethylene)amino)-1-oxopentan-2-yl)pyrrolidine-2-carboxamide (114)

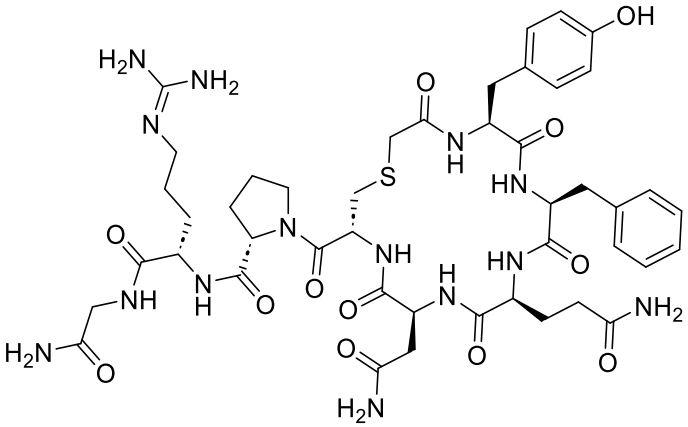

The peptide was synthesised at 0.10 mmol scale by automated SPPS as described in Procedure 2.A using Fmoc-Gly-OH, Fmoc-Arg(Pbf)-OH, Fmoc-Pro-OH, Fmoc-Cys(Trt)-OH, Fmoc-Asn(Trt)-OH, Fmoc-Gln(Trt)-OH, Fmoc-Phe-OH, Fmoc-Tyr(*t*Bu)-OH. The on-resin *N*-terminus chloroacetylation was carried out as described in Procedure 4.A. Resin cleavage and global deprotection of the peptide were carried out as described in Procedure 2.D. The linear peptide precursor was cyclised as described in Procedure 4.B. The crude product was dissolved in H_2O:AcN (1:1, with 0.1% TFA) and subjected to purification by semi-preparative RP-HPLC (5 – 50% AcN in H_2O with 0.1% (v/v) TFA over 40 min) over multiple injections. Fractions containing pure product were combined and the solvent was lyophilised yielding the desired product as a white solid (18 mg, isolated yield: 18% >90% purity).

Analytical RP-HPLC R_t (5 – 95% AcN in H_2O with 0.1% (v/v) TFA over 20 min, 254 nm): 11.558 min.

HRMS (*m/z* ESI^+): Found: 1045.4286 ($[M+Na]^+$, $C_{45}H_{62}N_{14}O_{12}SNa$ requires 1045.4290), 1023.4465 ($[M+H]^+$, $C_{45}H_{63}N_{14}O_{12}S$ requires 1023.4392), 512.2291 ($[M+2H]^{2+}$, $C_{45}H_{64}N_{14}O_{12}S$ requires 512.2196).

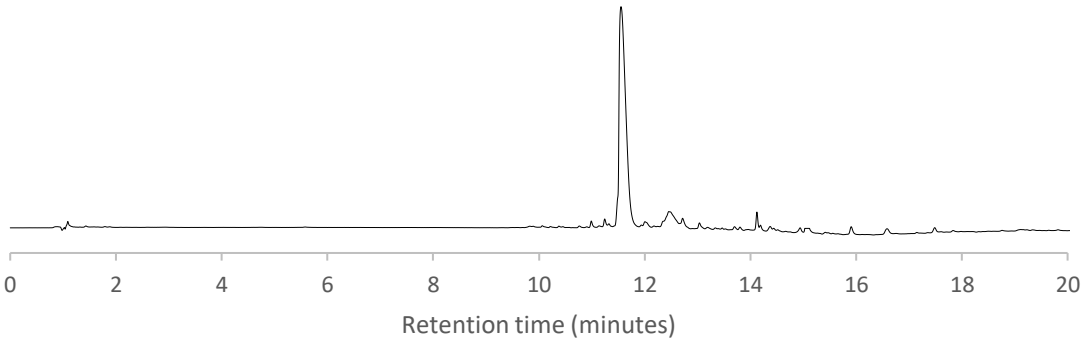

Figure 6.8. Analytical RP-HPLC trace (254 nm) of purified **114**.

(S)-1-((3R,6S,9S,12S,15S)-9-allyl-6-(2-amino-2-oxoethyl)-12-benzyl-15-(4-hydroxybenzyl)-5,8,11,14,17-pentaoxo-1-thia-4,7,10,13,16-pentaazacyclooctadecane-3-carbonyl)-N-((S)-1-((2-amino-2-oxoethyl)amino)-5-((diaminomethylene)amino)-1-oxopentan-2-yl)pyrrolidine-2-carboxamide (116)

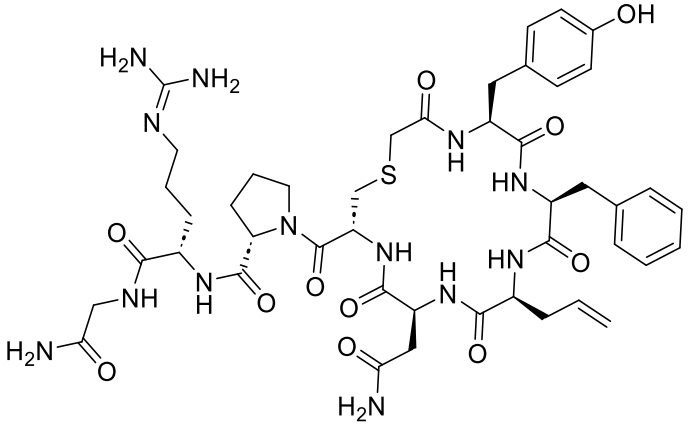

The peptide was synthesised at 0.25 mmol scale by automated SPPS as described in Procedure 2.A using Fmoc-Gly-OH, Fmoc-Arg(Pbf)-OH, Fmoc-Pro-OH, Fmoc-Cys(Trt)-OH, Fmoc-Asn(Trt)-OH, Fmoc-AgI-OH, Fmoc-Phe-OH, Fmoc-Tyr(*t*Bu)-OH. The on-resin

N-terminus chloroacetylation was carried out as described in Procedure 4.A. Resin cleavage and global deprotection of the peptide were carried out as described in Procedure 2.D. The linear peptide precursor was cyclised as described in Procedure 4.B. The crude product was dissolved in H_2O:AcN (1:1, with 0.1% TFA) and subjected to purification by semi-preparative RP-HPLC (5 – 50% AcN in H_2O with 0.1% (v/v) TFA over 40 min) over multiple injections. Fractions containing pure product were combined and the solvent was lyophilised yielding the desired product as a white solid (65 mg, isolated yield: 26%, >95% purity).

Analytical RP-HPLC R_t (5 – 95% AcN in H_2O with 0.1% (v/v) TFA over 20 min, 254 nm): 11.119 min.

HRMS (*m/z* ESI^+): Found: 992.4398 ($[M+H]^+$, $C_{45}H_{62}N_{13}O_{11}S$ requires 992.4334), 496.7179 ($[M+2H]^{2+}$, $C_{45}H_{63}N_{13}O_{11}S$ requires 496.7167).

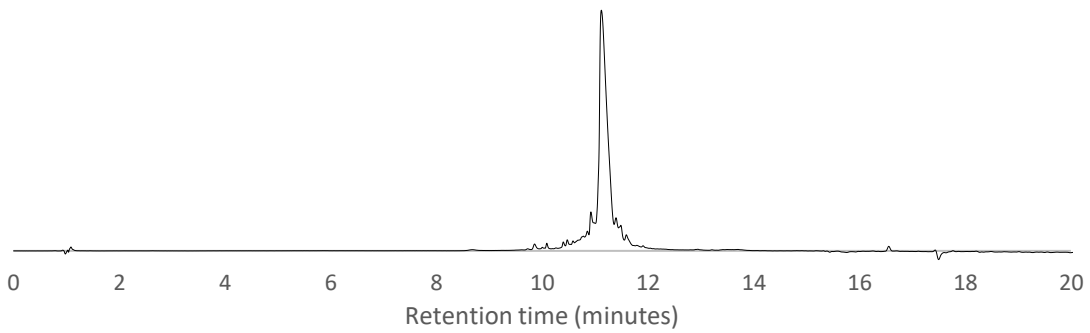

Figure 6.9. Analytical RP-HPLC trace (254 nm) of purified **116**.

N5-((R)-3-((3-((3R,6S,9S,12S,15S)-6-(2-amino-2-oxoethyl)-3-((S)-2-(((S)-1-((2-amino-2-oxoethyl)amino)-5-((diaminomethylene)amino)-1-oxopentan-2-yl)carbamoyl)pyrrolidine-1-carbonyl)-12-benzyl-15-(4-hydroxybenzyl)-5,8,11,14,17-pentaoxo-1-thia-4,7,10,13,16-pentaazacyclooctadecan-9-yl)propyl)thio)-1-((carboxymethyl)amino)-1-oxopropan-2-yl)glutamine (119)

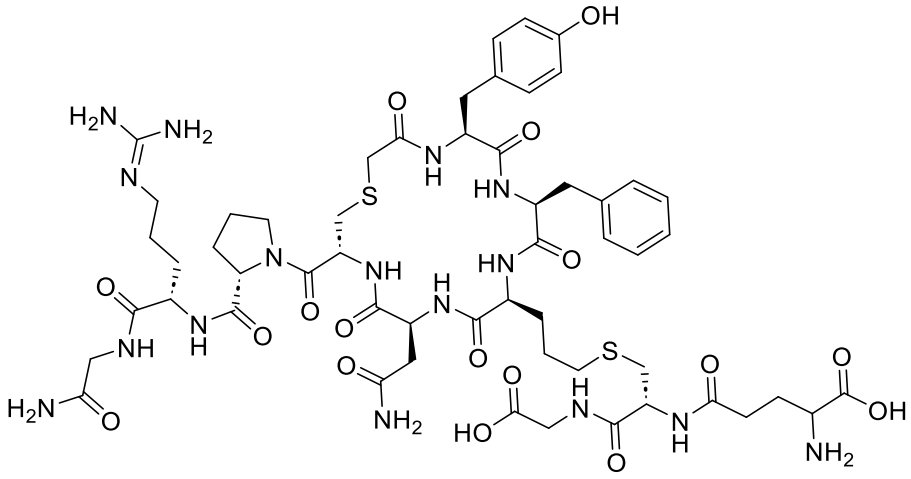

The radical TEC reaction between the cyclic peptide **116** and GSH was carried out as described in Procedure 4.C. The crude product was dissolved in H_2O:AcN (1:1, with 0.1% TFA) and subjected to purification by semi-preparative RP-HPLC (5 – 50% AcN in H_2O with 0.1% (v/v) TFA over 40 min) over multiple injections. Fractions containing pure product were combined and the solvent was lyophilised yielding the desired product as a white solid (2.8 mg, isolated yield: 11%, >95% purity).

Analytical RP-HPLC R_t (5 – 95% AcN in H_2O with 0.1% (v/v) TFA over 20 min, 220 nm): 10.671 min.

HRMS (*m/z* ESI^+): Found: 1321.5054 ($[M+H]^+$, $C_{55}H_{78}N_{16}O_{17}S_2Na$ requires 1321.5070).

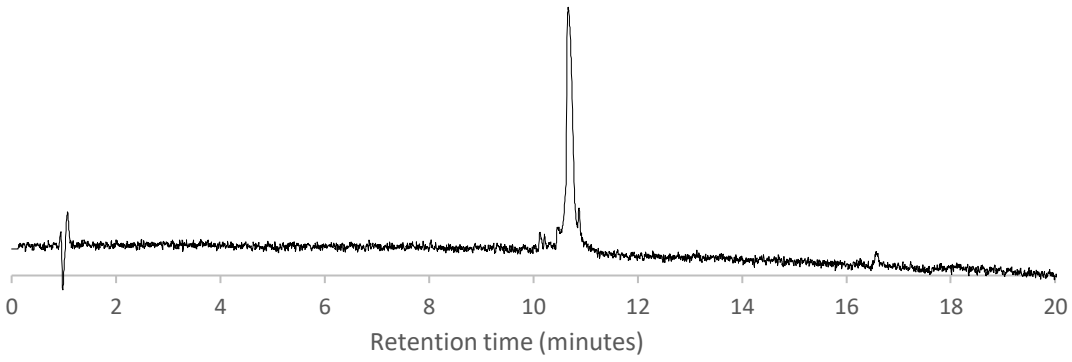

Figure 6.10. Analytical RP-HPLC trace (220 nm) of purified **119**.

(2S)-1-((3R,6S,9S,12S,15S)-9-(3-(((3R,4R,5R,6R)-3-acetamido-4,5-dihydroxy-6-(hydroxymethyl)tetrahydro-2H-pyran-2-yl)thio)propyl)-6-(2-amino-2-oxoethyl)-12-benzyl-15-(4-hydroxybenzyl)-5,8,11,14,17-pentaoxo-1-thia-4,7,10,13,16-pentaazacyclooctadecane-3-carbonyl)-N-((S)-1-((2-amino-2-oxoethyl)amino)-5-((diaminomethylene)amino)-1-oxopentan-2-yl)pyrrolidine-2-carboxamide (123)

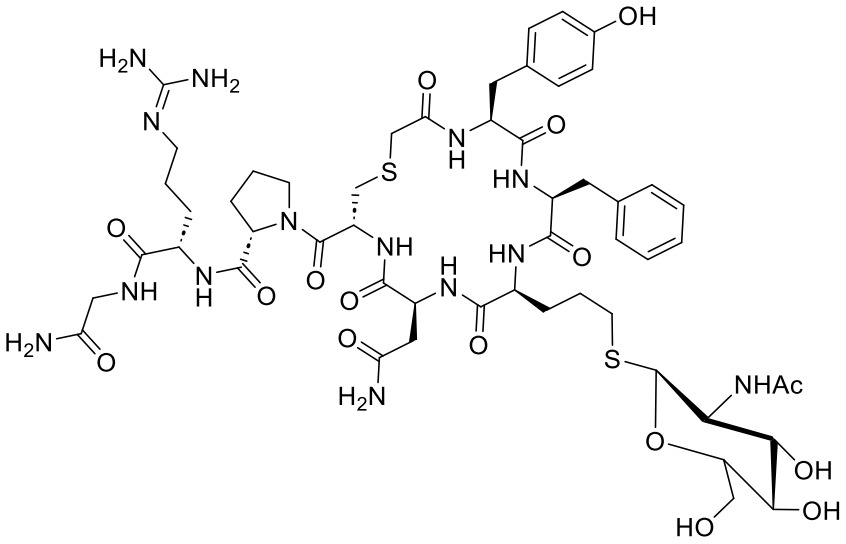

The radical TEC reaction between the cyclic peptide **116** and thiol-sugar **122** was carried out as described in Procedure 4.C. The crude product was dissolved in H_2O:AcN (1:1, with 0.1% TFA) and subjected to purification by semi-preparative RP-HPLC (5 – 50% AcN in H_2O with 0.1% (v/v) TFA over 40 min) over multiple injections. Fractions containing pure product were combined and the solvent was lyophilised yielding the desired product as a white solid (2.0 mg, isolated yield: 8%, >95% purity).

Analytical RP-HPLC R_t (5 – 95% AcN in H_2O with 0.1% (v/v) TFA over 20 min, 254 nm): 11.034 min.

HRMS (*m/z* ESI^+): Found: 1229.5078 ($[M+H]^+$, $C_{53}H_{77}N_{14}O_{16}S_2$ requires 1229.5005), 615.2576 ($[M+2H]^{2+}$, $C_{53}H_{78}N_{14}O_{16}S_2$ requires 615.2502).

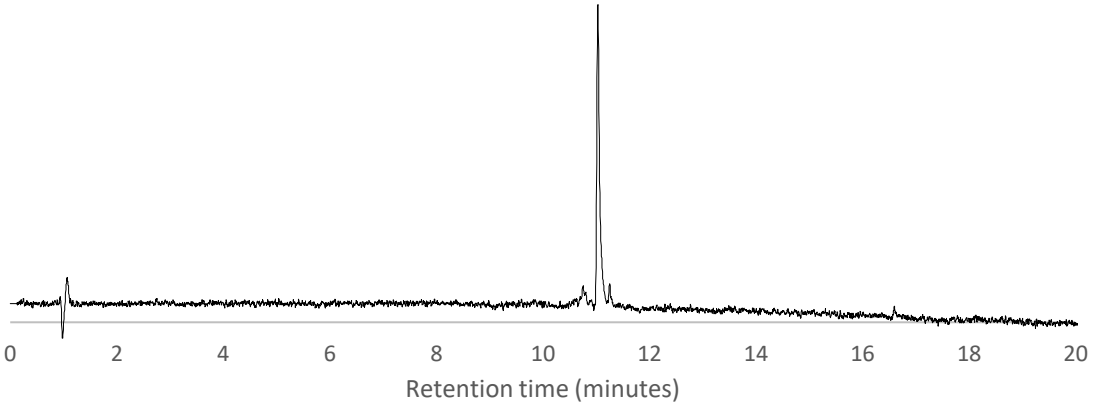

Figure 6.10. Analytical RP-HPLC trace (220 nm) of purified **123**.

(S)-1-((3R,6S,9S,12S,15S)-6-(2-amino-2-oxoethyl)-12-benzyl-15-(4-hydroxybenzyl)-9-(3-((4-mercaptobutyl)thio)propyl)-5,8,11,14,17-pentaoxo-1-thia-4,7,10,13,16-pentaazacyclooctadecane-3-carbonyl)-N-((S)-1-((2-amino-2-oxoethyl)amino)-5-((diaminomethylene)amino)-1-oxopentan-2-yl)pyrrolidine-2-carboxamide (126)

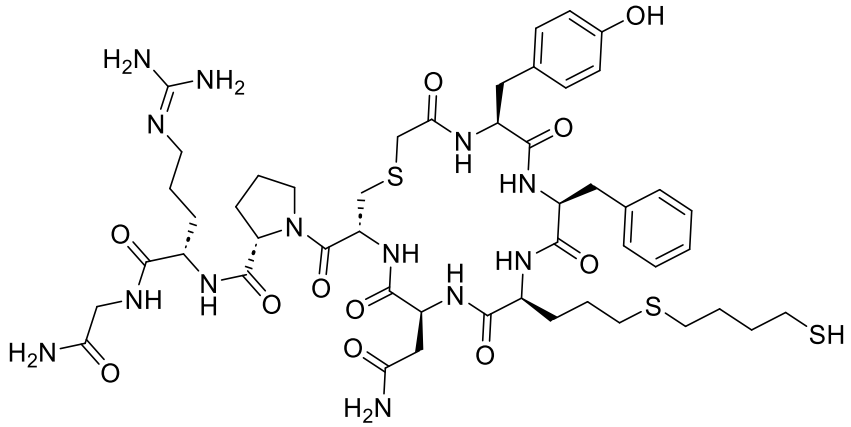

The radical TEC reaction between the cyclic peptide **116** and 1,4-butanedithiol (1.8µL, 0.016 mmol, 0.8 equiv.) was carried out as described in Procedure 4.C. The crude product was dissolved in H_2O:AcN (1:1, with 0.1% TFA) and subjected to purification by semi-preparative RP-HPLC (5 – 50% AcN in H_2O with 0.1% (v/v) TFA over 40 min) over multiple injections. Fractions containing pure product were combined and the solvent was lyophilised yielding the desired product as a white solid (2.0 mg, isolated yield: 10%, >90% purity).

Analytical RP-HPLC R_t (5 – 95% AcN in H_2O with 0.1% (v/v) TFA over 20 min, 254 nm): 13.187 min.

HRMS (*m/z* ESI$^+$): Found: 1229.5078 ([M+H]$^+$, $C_{53}H_{77}N_{14}O_{16}S_2$ requires 1229.5005), 615.2576 ([M+2H]$^{2+}$, $C_{53}H_{78}N_{14}O_{16}S_2$ requires 615.2502).

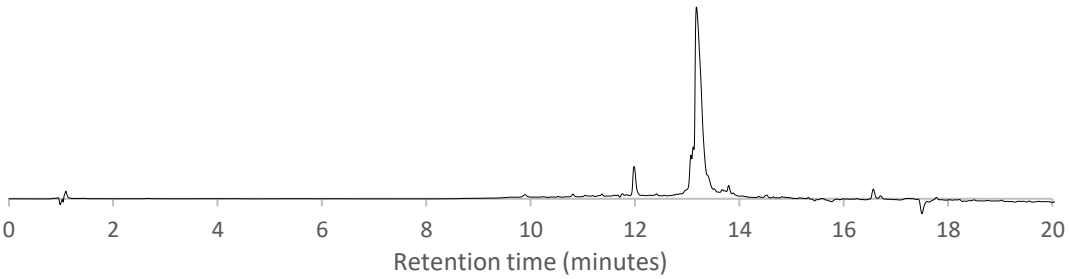

Figure 6.11. Analytical RP-HPLC trace (254 nm) of purified **126**.

(2S,2'S)-1,1'-((3R,3'R,6S,6'S,9S,9'S,12S,12'S,15S,15'S)-9,9'-((butane-1,4-diylbis(sulfanediyl))bis(propane-3,1-diyl))bis(6-(2-amino-2-oxoethyl)-12-benzyl-15-(4-hydroxybenzyl)-5,8,11,14,17-pentaoxo-1-thia-4,7,10,13,16-pentaazacyclooctadecane-9,3-diyl-3-carbonyl))bis(N-((S)-1-((2-amino-2-oxoethyl)amino)-5-((diaminomethylene)amino)-1-oxopentan-2-yl)pyrrolidine-2-carboxamide) (125)

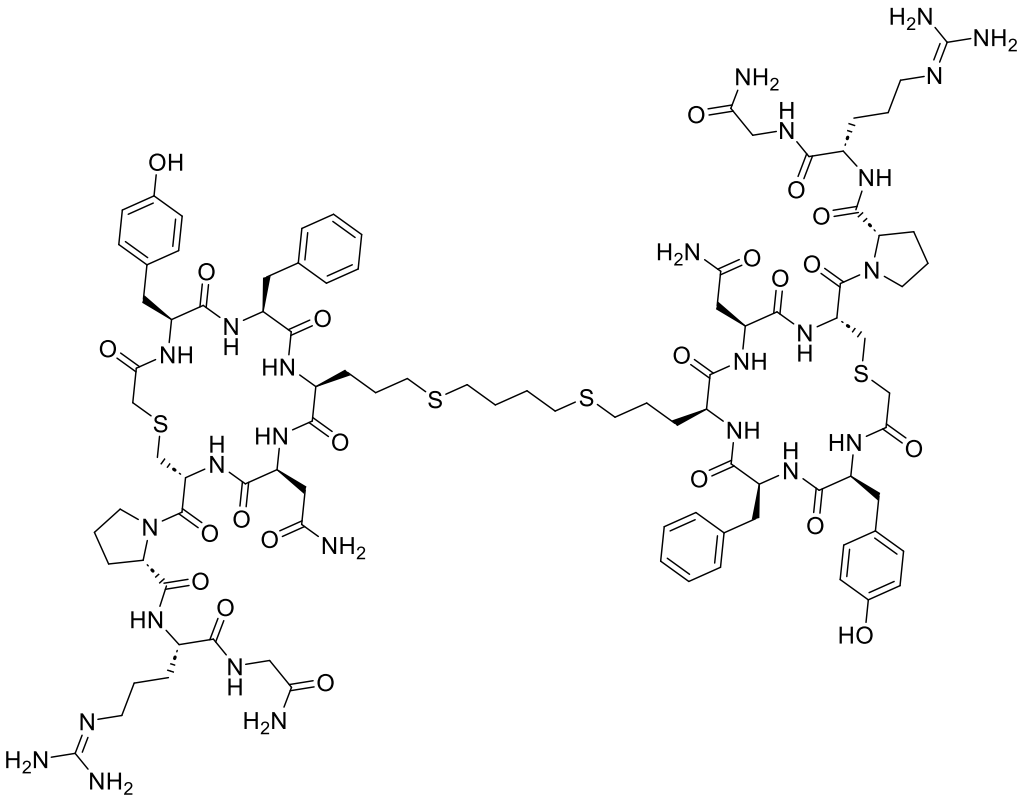

1,4-butanedithiol (1.8µL, 0.016 mmol, 0.8 equiv.) and DPAP (2 mg, 0.01 mmol, 0.5 equiv.) were added to a 20 mM solution of **116** (20 mg, 0.02 mmol, 1.0 equiv.) in DMF (1mL) and the reaction mixture was irradiated at 365 nm under stirring for 2 h. DMF was removed under reduced pressure, the crude product was dissolved in H_2O:AcN (1:1, with 0.1% TFA) and subjected to purification by semi-preparative RP-HPLC (5 – 50% AcN in H_2O with 0.1% (v/v) TFA over 40 min) over multiple injections. Fractions containing pure product were combined and the solvent was lyophilised yielding the desired product as a white solid (5.0 mg, isolated yield: 12%, >90% purity).

Analytical RP-HPLC R_t (5 – 95% AcN in H_2O with 0.1% (v/v) TFA over 20 min, 254 nm): 12.616 min.

HRMS (*m/z* ESI^+): Found: 1053.4540 ($[M+2H]^{2+}$, $C_{94}H_{133}N_{26}O_{22}S_4$ requires 1053.4446).

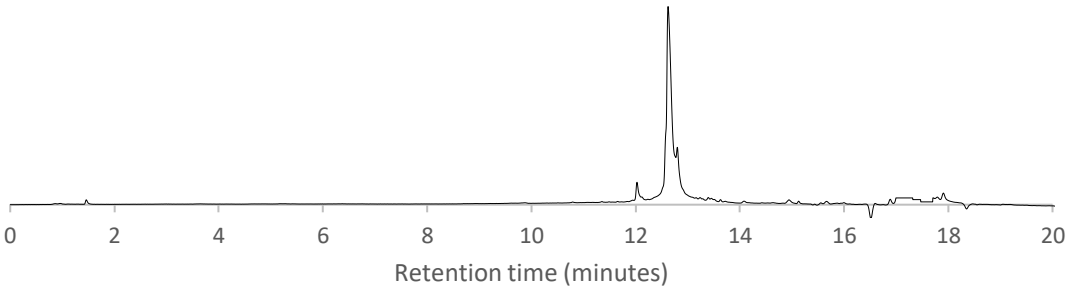

Figure 6.12. Analytical RP-HPLC trace (254 nm) of purified **125**.

7.5 Experimental Details for Chapter

7.5.1 Characterisation Data

(((9H-fluoren-9-yl)methoxy)carbonyl)-*L*-lysine (131)

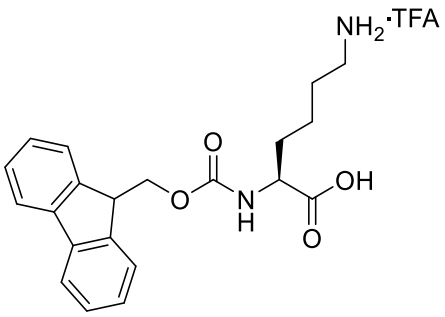

Fmoc-Lys(Boc)-OH (3.00 g, 6.40 mmol) was dissolved in 48 mL of CH_2Cl_2:TFA (1:1) and the mixture was stirred for 2 h. The solvent mixture was removed under reduced pressure, and the remaining TFA was co-evaporated three times with CH_2Cl_2. the product was dissolved in H_2O and extracted with Et_2O (3 × 25 mL). The aqueous layers were combined and removed under reduced pressure yielding the product as a white solid (3.05 g, 99%). The isolated compound was in good agreement with the literature.[206]

^{1}H-NMR (400 MHz, DMSO-*d_6*) δ_H 7.90 (d, *J* = 7.5 Hz, 2H, Fmoc Ar-CH), 7.76 – 7.66 (m, 5H, Fmoc Ar-CH, NH_3), 7.63 (d, *J* = 8.1 Hz, 1H, NH), 7.43 (t, *J* = 7.5 Hz, 2H, Fmoc Ar-CH), 7.34 (t, *J* = 7.5, 2H, Fmoc Ar-CH), 4.37 – 4.20 (m, 3H, Fmoc CH, Fmoc CH_2), 3.97 – 3.90 (m, 1H, αCH), 2.83 – 2.72 (m, 2H, εCH_2), 1.78 – 1.45 (m, 4H, βCH_2, δCH_2), 1.45 – 1.30 (m, 2H, γCH_2).

HRMS (*m/z* APCI$^+$): Found: 369.1808 ([M + H]$^+$, $C_{21}H_{25}N_2O_4$ requires 369.1736).

(E)-N2-(((9H-fluoren-9-yl)methoxy)carbonyl)-N6-(but-2-enoyl)-*L*-lysine (129)

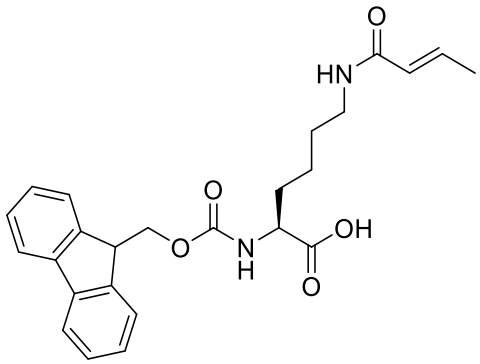

To a stirring solution of *N*-hydroxysuccinimide (0.345 g, 3.0 mmol) and DIPEA (0.52 mL, 3.0 mmol) in CH_2Cl_2 (7.5 mL) at 0 °C was added dropwise *trans*-crotonyl chloride (0.29 mL, 3.0 mmol). The reaction was warmed at rt and stirred for 3 h. The

mixture was then diluted with EtOAc (50 mL) and washed with sat. NH_4Cl (30 mL) and brine (3 × 30 mL). The organic layer was dried over $MgSO_4$, filtered, and removed under reduced pressure. The residue was then dissolved in a solution of **131** (0.78 g, 2.1 mmol) and Et_3N (0.83 mL, 6.0 mmol) in CH_2Cl_2 (30 mL) and the reaction mixture was stirred at rt for 48 h. The solvent was then removed under reduced pressure, the crude residue was dissolved in H_2O (30 mL) and acidified to pH 2 using with aq. HCl (1 M). The aqueous layer was extracted with EtOAc (3 × 30 mL) and the combined organic layers were dried over $MgSO_4$ and removed under reduced pressure. The crude compound was purified by silica gel flash chromatography (CH_2Cl_2:MeOH– 90:10) to give a white solid (0.40 g, 43% over two steps). The isolated compound was in good agreement with the literature.[206]

^{1}H-NMR (600 MHz, DMSO-d_6) δ_H 7.90 (d, *J* = 7.5 Hz, 2H, Fmoc Ar-CH), 7.70 (d, *J* = 7.5 Hz, 2H, Fmoc Ar-CH), 7.42 (t, *J* = 7.4, 2H, Fmoc Ar-CH), 7.35 – 7.30 (m, 2H, Fmoc Ar-CH), 7.74 (bs, 1H, Fmoc NH), 6.58 (dq, *J* = 13.8, 6.8 Hz, 1H, COCH=C<u>H</u>CH_3), 5.88 (d, *J* = 13.8, 1H, CO<u>C</u>H=CHCH_3), 4.37 – 4.17 (m, 3H, Fmoc CH, CH_2), 3.80 – 3.70 (m, 1H, αCH), 3.10 – 3.00 (m, 2H, εCH_2), 1.76 (d, *J* = 6.8 Hz 3H, CH_3), 1.74 – 1.40 (m, 4H, βCH_2, δCH_2), 1.33 – 1.21 (m, 2H, γCH_2).

HRMS (*m/z* APCI$^+$): Found: 437.2074 ([M + H]$^+$, $C_{25}H_{29}N_2O_5$ requires 437.1998), 459.1876 ([M + Na]$^+$, $C_{25}H_{28}N_2O_5Na$ requires 459.1896), 475.1589 ([M + K]$^+$, $C_{25}H_{28}N_2O_5K$ requires 475.1635).

(S)-2-(2-((S)-2-acetamido-3-(4-hydroxyphenyl)propanamido)acetamido)-N-(2-((2-amino-2-oxoethyl)amino)-2-oxoethyl)-6-((E)-but-2-enamido)hexanamide (127)

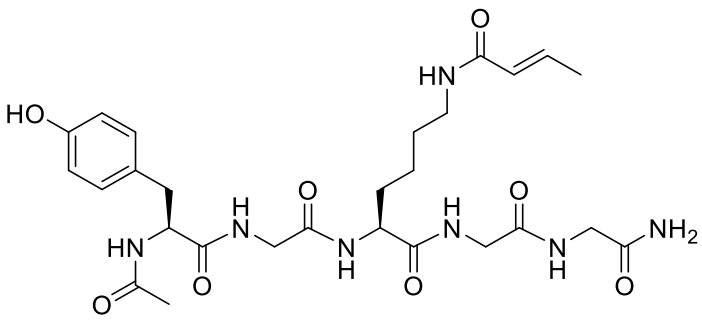

The peptide was synthesised at 0.25 mmol scale by SPPS as described in Procedure 2.A using Fmoc-Gly-OH, Fmoc-Lys(Cr)-OH, and Fmoc-Tyr(*t*Bu)-OH. Following

the final Fmoc deprotection, the *N*-terminus of the peptide was capped twice using a solution of 20% acetic anhydride in DMF. Resin cleavage and global deprotection of the peptide were carried out as described in Procedure 2.D. The crude product was dissolved in H_2O:AcN (1:1, with 0.1% TFA) and subjected to purification by semi-preparative RP-HPLC (5 – 60% AcN in H_2O with 0.1% (v/v) TFA over 60 min). Fractions containing pure product were combined and the solvent was lyophilised yielding the desired product as a white solid (70 mg, isolated yield: 65% >95% purity).

Analytical RP-HPLC R_t (5 – 95% AcN in H_2O with 0.1% (v/v) TFA over 10 min, 214 nm): 4.234 min.

HRMS (*m/z* ESI^+): Found: 590.2920 ($[M+H]^+$, $C_{75}H_{115}N_{21}O_{23}S_2$ requires 590.2860),

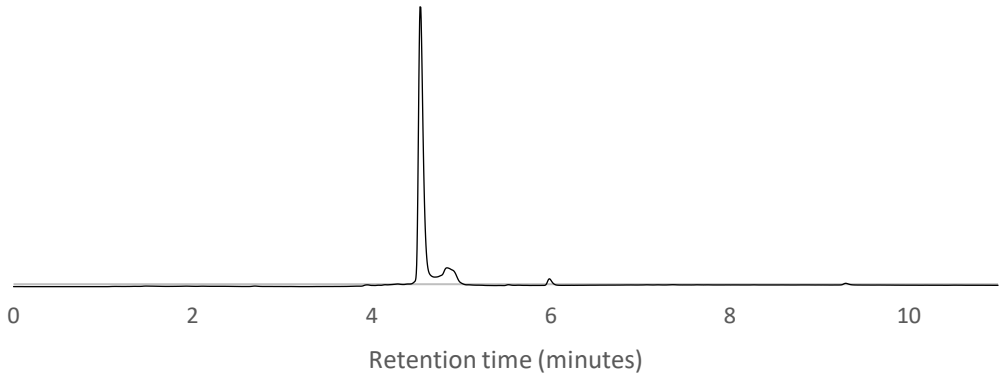

Figure 6.12. Analytical RP-HPLC trace (214 nm) of purified **127**.

Chapter 8

References

1 L. Wang, N. Wang, W. Zhang, X. Cheng, Z. Yan, G. Shao, X. Wang, R. Wang and C. Fu, *Signal Transduct. Target. Ther.* 2022, **7**, 1–27.

2 E. Fisher, K. Pavlenko, A. Vlasov and G. Ramenskaya, *Pharmaceut. Med.*, 2019, **33**, 9–20.

3 S. Iyengar, M. H. Ossipov and K. W. Johnson, *Pain*, 2017, **158**, 543–559.

4 S. C. Peterson and A. R. Barry, *Curr. Diabetes Rev.*, 2018, **14**, 273–279.

5 M. D. T. Torres, S. Sothiselvam, T. K. Lu and C. de la Fuente-Nunez, *J. Mol. Biol.*, 2019, **431**, 3547–3567.

6 I. Vecchio, C. Tornali, N. L. Bragazzi and M. Martini, *Front. Endocrinol. (Lausanne)*, 2018, **9**, 613.

7 V. du Vigneaud, C. Ressler, J. M. Swan, C. W. Roberts and P. G. Katsoyannis, *J. Am. Chem. Soc.,* 1954, **76**, 3115-3121.

8 H. J. Lee, A. H. Macbeth, J. H. Pagani and W. Scott Young, *Prog. Neurobiol*., 2009, **88**, 127–151.

9 V. du Vigneaud, C. Resslbr, J. M. Swan, C. W. Roberts and P. G. Katsoyannis, *J. Am. Chem. Soc.*, 1954, **76**, 3115–3121.

10 M. Muttenthaler, G. F. King, D. J. Adams and P. F. Alewood, *Nat. Rev. Drug Discov.*, 2021, **20**, 309–325.

11 H. F. Stähelin, *Experientia*., 1996, **52**, 5–13.

12 J. F. Borel, C. Feurer, H. U. Gubler and H. Stähelin, *Agents Actions*, 1976, **6**, 468–475.

13 G. F. King, *Expert. Opin. Biol. Ther*., 2011, **11**, 1469–1489.

14 L. J. Miller, P. M. Sexton, M. Dong and K. G. Harikumar, *Int. J. Obes. Suppl.*, 2014, **4**, S9–S13.

15 A. M. Ali, J. Atmaj, N. Van Oosterwijk, M. R. Groves and A. Dömling, *Comput. Struct. Biotechnol. J.*, 2019, **17**, 263–281.

16 M.S. Mitra, S. DeMarco, B. Holub, L. Thiruneelakantapillai and E.A. Thackaberry, *Regul. Toxicol. Pharmacol*., 2020, **117**, 104766.

17 N. Tsomaia, *Eur. J. Med. Chem.*, 2015, **94**, 459–470.

18 I. W. Taylor, R. Linding, D. Warde-Farley, Y. Liu, C. Pesquita, D. Faria, S. Bull, T. Pawson, Q. Morris and J. L. Wrana, *Nat. Biotechnol*., 2009, **27**, 199–204.

19 T. Tuller, S. Atar, E. Ruppin, M. Gurevich and A. Achiron, *Genes Immun.*, 2013, **14**, 67–82.

20 C. Lamers, *Future Drug Discov.*, 2022, **4**, FDD75.

21 P. Vlieghe, V. Lisowski, J. Martinez and M. Khrestchatisky, *Drug Discov. Today*, 2010, **15**, 40–56.

22 J. F. Woodley, *Crit. Rev. Ther. Drug Carrier Syst*., 1994, **11**, 61–95.

23 N. J. Yang and M. J. Hinner, *Methods Mol. Biol*., 2015, **1266**, 29–53,

24 A. Patel, K. Cholkar and A. K. Mitra, *Ther. Deliv*., 2014, **5**, 337–365.

25 L. Gentilucci, R. De Marco and L. Cerisoli, *Curr. Pharm. Des.*, 2010, **16**, 185–203.

26 A. Zorzi, K. Deyle and C. Heinis, *Curr. Opin. Chem. Biol.*, 2017, **38**, 24–29.

27 J. He, P. Ghosh and C. Nitsche, *RSC.*, 2024, **15**, 2300–2322.

28 M. A. Abdalla and L. J. Mcgaw, *Molecules*, 2018, **23**, 2080.

29 D. Lipovsek and A. Plückthun, *J. Immunol. Methods*, 2004, **290**, 51–67.

30 G. Bhardwaj, J. O'Connor, S. Rettie, Y. H. Huang, T. A. Ramelot, V. K. Mulligan, G. G. Alpkilic, J. Palmer, A. K. Bera, M. J. Bick, M. Di Piazza, X. Li, P. Hosseinzadeh, T. W. Craven, R. Tejero, A. Lauko, R. Choi, C. Glynn, L. Dong, R. Griffin, W. C. van Voorhis, J. Rodriguez, L. Stewart, G. T. Montelione, D. Craik and D. Baker, *Cell*, 2022, **185**, 3520–3532.

31 B. F. Erlanger and L. Goode, *Nature*, 1954, **174**, 840-841.

32 C. González, G. M. Langdon, M. Bruix, A. Gálvez, E. Valdivia, M. Maqueda and M. Rico, *Proc. Natl. Acad. Sci. U S A*., 2000, **97**, 11221–11226.

33 J. A. Orwa, C. Govaerts, R. Busson, E. Roets, A. Van Schepdael and J. Hoogmartens, *J. Chromatogr. A*, 2001, **912**, 369–373.

34 A. P. Zavascki, L. Z. Goldani, J. Li and R. L. Nation, *J. Antimicrob. Chemother*., 2007, **60**, 1206–1215.

35 S. Ullrich and C. Nitsche, *Pept. Sci*., 2024, **116**, e24326.

36 R. W. Sparidans, E. Stokvis, J. M. Jimeno, L. López-Lázaro, J. H. M. Schellens and J. H. Beijnen, *Anticancer. Drugs*, 2001, **12**, 575–582.

37 K. Jin, I. H. Sam, K. H. L. Po, D. Lin, E. H. Ghazvini Zadeh, S. Chen, Y. Yuan and X. Li, *Nat. Commun.*, 2016, **7**, 12394.

38 L. D. Lavis, *ACS Chem. Biol.*, 2008, **3**, 203–206.

39 C. A. G. N. Montalbetti and V. Falque, *Tetrahedron*, 2005, **61**, 10827–10852.

40 S. J. De Veer, M. W. Kan and D. J. Craik, *Chem. Rev*., 2019, **119**, 12375–12421.

41 O. Saether, D. J. Craik, I. D. Campbell, K. Sletten, J. Juul and D. G. Norman, *Biochemistry*, 1995, **34**, 4147–4158.

42 T. M. Postma and F. Albericio, *Eur. J. Org. Chem.*, 2014, 3519–3530.

43 P. W. R. Harris, S. H. Yang, A. Molina, G. Lõpez, M. Middleditch and M. A. Brimble, *Chemistry*, 2014, **20**, 5102–5110.

44 D. M. Ziegler, *Annu. Rev. Biochem.*, 1985, **54**, 305–329.

45 B. S. Jursic and Z. Zdravkovski, *Synth. Commun.*, 1993, **23**, 2761–2770.

46 S. Zuffanti, *J. Chem. Ed*. 1948, **25**, 481.

47 D. C. Washington, R. Adams and L. H. Ulich, *J. Am. Chem. Soc*., 1920, **42**, 509–611.

J. 48 S. Bräse, C. Gil, K. Knepper and V. Zimmermann, *Angew. Chem. Int. Ed. Engl.* 2005, **44**, 5188–5240.

49 A. Mata, U. Weigl, O. Flögel, P. Baur, C. A. Hone and C. O. Kappe, *React. Chem. Eng*., 2020, **5**, 645–650.

50 N. Thieriet, F. Guibé and F. Albericio, *Org. Lett*. 2000, **29**, 1815–1817.

51 J. C. Sheehan and G. P. Hess, *J. Am. Chem. Soc.*, 1955, **77**, 1067–1068.

52 L. A. Carpino and A. El-Faham, *Tetrahedron*, 1999, **55**, 6813–6830.

53 P. Acosta-Guzmán, A. Ojeda-Porras and D. Gamba-Sánchez, *Adv. Synth. Catal.*, 2023, **365**, 4359–4391.

54 C.A.G.N. Montalbetti and V. Falque, *Tetrahedron*, 2005, **61**, 10827–10852.

55 R.B. Merrifield, *J. Am. Chem. Soc*., 1963, **85**, 2149–2154.

56 J. M. Palomo, *RSC Adv*., 2014, **4**, 32658–32672.

57 R. B. Merrifield, *Angew. Chem. Int. Ed. Engl.*, 1985, **24**, 799–810.

58 K. B. Højlys-Larsen and K. J. Jensen, *Methods Mol. Biol.*, 2013, **1047**, 191–199.

59 M. C. Galan, P. Dumy and O. Renaudet, *Chem. Soc. Rev.*, 2013, **42**, 4599.

60 S. Vilà, E. Badosa, E. Montesinos, L. Feliu and M. Planas, *Org. Biomol. Chem*, 2013, **11**, 3365.

61 I. Avan, C. Dennis and A. R. Katritzky, *Chem. Soc. Rev.*, 2014, **43**, 3575.

62 J. P. Tam, J. Xu and D. Eom, *Biopolymers*, 2001, **60**, 194–205.

63 R. B. Merrifield, *Recent Prog. Horm. Res.*, 1967, **23**, 451–482.

64 S. Sakakibara, Y. Shimonishi, Y. Kishida, M. Okada and H. *Sugihara, Bull. Chem. Soc. Jpn*., 1967, **40**, 2164–2167.

65 A. Kluczyk, I. Z. Siemiona and Z. Wieczorek, Peptides, 2000, **21**, 1411–1420.

66 B. Gutte and R. B. Merrifield, *J. Am. Chem. Soc.*, 1969, **91**, 501–502.

67 M. Schnolzer, P. Alewood, A. Jones, D. Alewood and S. B. Kent, *Int. J. Peptide Protein Res.*, 1992, **40**, 180–193.

68 M. Muttenthaler, F. Albericio and P. E. Dawson, *Nat. Protoc*., 2015, **10**, 1067–1083.

69 R. Behrendt, P. White and J. Offer, *J. Pept. Sci.*, 2016, **22**, 4–27.

70 L. A. Carpino and G. Y. Han, *J. Org. Chem.*, 1972, **37**, 3404–3409.

71 C. -D Chang and J. Meienhofer, *Int. J. Pept. Protein Res.*, 1978, **11**, 246–249.

72 R. H. Angeletti, L. F. Bonewald and G. B. Fields, *Methods Enzymol.*, 1997, **289**, 697–717.

73 R. Behrendt, P. White and J. Offer, *J. Pept. Sci*, 2016, **22**, 4–27.

74 T. W. Overton, *Drug Discov. Today*, 2014, **19**, 590–601.

75 J. M. Chalker, *Chem. Biol. Drug Des.*, 2013, **81**, 122–135.

76 L. R. Malins and R. J. Payne, *Curr. Opin. Chem. Biol.*, 2014, **22**, 70–78.

77 P. E. Dawson, T. W. Muir, I. Clark-Lewis and S. B. H. Kent, *Science*, 1994, **266**, 776–779.

78 H. M. Burke, L. McSweeney and E. M. Scanlan, *Nat. Commun*., 2017, **8**, 1–16.

79 A. C. Conibear, E. E. Watson, R. J. Payne and C. F. W. Becker, *Chem. Soc. Rev.*, 2018, **47**, 9046–9068.

80 W. Jiang, B. Zhang, C. Fan, M. Wang, J. Wang, Q. Deng, X. Liu, J. Chen, J. Zheng, L. Liu and T. F. Zhu, *Cell Discov*., 2017, **3**, 1–7.

81 G. G. Kochendoerfer, S. Y. Chen, F. Mao, S. Cressman, S. Traviglia, H. Shao, C. L. Hunter, D. W. Low, E. N. Cagle, M. Carnevali, V. Gueriguian, P. J. Keogh, H. Porter, S. M. Stratton, M. Con Wiedeke, J. Wilken, J. Tang, J. J. Levy, L. P. Miranda, M. M. Crnogorac, S. Kalbag, P. Botti, J. Schindler-Horvat, L. Savatski, J. W. Adamson, A. Kung, S. B. H. Kent and J. A. Bradburne, *Science*, 2003, **299**, 884–887.

82 V. Y. Torbeev and S. B. H. Kent, *Angew. Chem. Int. Ed.*, 2007, **46**, 1667–1670.

83 W. Xu, W. Jiang, J. Wang, L. Yu, J. Chen, X. Liu, L. Liu and T. F. Zhu, *Cell Discov*., 2017, **3**, 1–10.

84 P. A. Cistrone, M. J. Bird, D. T. Flood, A. P. Silvestri, J. C. J. Hintzen, D. A. Thompson and P. E. Dawson, *Curr, Protoc, Chem, Biol*., 2019, **11**, e61.

85 D. Bang, B. L. Pentelute and S. B. H. Kent, *Angew. Chem. Int. Ed.*, 2006, **45**, 3985–3988.

86 V. Agouridas, O. El Mahdi, V. Diemer, M. Cargoët, J. C. M. Monbaliu and O. Melnyk, *Chem. Rev.*, 2019, **119**, 7328–7443.

87 J. B. Blanco-Canosa and P. E. Dawson, *Angew. Chem. Int. Ed.*, 2008, **47**, 6851–6855.

88 S. Bondalapati, M. Jbara and A. Brik, *Nat. Chem.*, 2016, **8**, 407–418.

89 G. M. Fang, Y. M. Li, F. Shen, Y. C. Huang, J. Bin Li, Y. Lin, H. K. Cui and L. Liu, *Angew. Chem. Int. Ed.*, 2011, **50**, 7645–7649.

90 N. Ollivier, J. Dheur, R. Mhidia, A. Blanpain and O. Melnyk, *Org. Lett.*, 2010, **12**, 5238–5241.

91 D. W. Low, M. G. Hill, M. R. Carrasco, S. B. H. Kent and P. Botti, *Proc. Natl. Acad. Sci. U S A*, 2001, **98**, 6554.

92 L. Z. Yan and P. E. Dawson, *J. Am. Chem. Soc.*, 2001, **123**, 526–533.

93 S. S. Kulkarni, J. Sayers, B. Premdjee and R. J. Payne, *Nat. Rev. Chem*., 2018, **2**, 1–17.

94 Q. Wan and S. J. Danishefsky, *Angew. Chem. Int. Ed.*, 2007, **46**, 9248–9252.

95 K. Jin and X. Li, *Chem. Eur. J*., 2018, 10.1002/chem.201802067.

96 D. Crich and A. Banerjee, *J Am Chem Soc*, 2007, **129**, 10064–10065.

97 J. Li, S. Dong, S. D. Townsend, T. Dean, T. J. Gardella and S. J. Danishefsky, *Angew. Chem. Int. Ed.*, 2012, **51**, 12263–12267.

98 G. S. Creech, C. Paresi, Y. M. Li and S. J. Danishefsky, *Proc, Natl, Acad, Sci, U S A*, 2014, **111**, 2891–2896.

99 M. Murakami, R. Okamoto, M. Izumi and Y. Kajihara, *Angew. Chem. Int. Ed.*, 2012, **51**, 3567–3572.

100 B. Fauvet, S. M. Butterfield, J. Fuks, A. Brik and H. A. Lashuel, *Chem. Comm.*, 2013, **49**, 9254–9256.

101 T. Posner, *Berichte der Dtsch. Chem. Gesellschaft*, 1905, **38**, 646–657.

102 C. E. Hoyle and C. N. Bowman, *Angew. Chem. Int. Ed.*, 2010, **49**, 1540–1573.

103 M. D. Nolan and E. M. Scanlan, *Front. Chem.*, 2020, **8**, 583272.

104 B. H. Northrop and R. N. Coffey, *J. Am. Chem. Soc.*, 2012, **134**, 13804–13817.

105 E. Denisov, C. Chatgilialoglu, A. Shestakov and T. Denisova, *Int. J. Chem. Kinet.*, 2009, **41**, 284–293.

106 K. Owusu-Adom, J. Schall and C. A. Guymon, *Macromolecules*, 2009, **42**, 32753284.

107 C. E. Hoyle, C. N. Bowman and C. N. Bowman, *Angew. Chem. Int. Ed.*, 2010, **22**, 1540–1573.

108 L. McSweeney, F. Dénès and E. M. Scanlan, *Eur. J. Org. Chem.*, 2016, 2080–2095.

109 M. Ahangarpour, I. Kavianinia, P.W.R. Harris and M. A. Brimble, *Chem. Soc. Rev*, 2021, **50**, 898–944.

110 J. T. Mclean, A. Benny, M. D. Nolan, G. Swinand and E. M. Scanlan, *Chem. Soc. Rev*, 2021, **50**, 10857.

111 R. Apweiler, H. Hermjakob and N. Sharon, *Biochim, Biophys. Acta, Gen. Subj*. 1999, **1473**, 4–8.

112 O. Seitz, *Chembiochem*., 2000, **1**, 214–246.

113 A. Dondoni, A. Massi, P. Nanni and A. Roda, *Chem. Eur. J.*, 2009, **15**, 11444–11449.

114 N. Floyd, B. Vijayakrishnan, J. R. Koeppe, B. G. Davis, N. Floyd, B. Vijayakrishnan, J. R. Koeppe and B. G. Davis, *Angew. Chem. Int. Ed.*, 2009, **48**, 7798–7802.

115 S. A. Cochrane and J. C. Vederas, *Med. Res. Rev.*, 2016, **36**, 4–31.

116 P. Simerska, P. M. Moyle and I. Toth, *Med. Res. Rev.*, 2011, **31**, 520–547.

117 L. Zhang and G. Bulaj, *Curr. Med. Chem.*, 2012, **19**, 1602–1618.

118 M. H. Gelb, D. Kadereit, J. Kuhlmann, H. Waldmann, A. Chembiochem ; Wittinghofer, P. Konstantinopoulos, M. V Karamouzis, A. G. Papavassiliou, A. I. Magee, L. Gutierrez, I. A. Mckay, C. J. Marshall, A. Hall, J. A. Embo J. ; Duncan and A. G. Gilman, *Nat. Rev. Drug Discov.*, 2006, **2**, 3646–3649.

119 T. H. Wright, A. E. S. Brooks, A. J. Didsbury, G. M. Williams, P. W. R. Harris, P. R. Dunbar and M. A. Brimble, *Angew. Chem. Int. Ed.*, 2013, **52**, 10616–10619.

120 V. Yim, I. Kavianinia, M. K. Knottenbelt, S. A. Ferguson, G. M. Cook, S. Swift, A. Chakraborty, J. R. Allison, A. J. Cameron, P. W. R. Harris and M. A. Brimble, *Chem. Sci.*, 2020, **11**, 5759–5765.

121 S. H. Yang, C. A. Clemett, M. A. Brimble, S. J. O'Carroll and P. W. R. Harris, *RSC Med. Chem.*, 2020, **11**, 1041–1047.

122 V. V. Yim, A. J. Cameron, I. Kavianinia, P. W. R. Harris and M. A. Brimble, *Front. Chem.*, 2020, **8**, 538272.

123 V. V. Yim, I. Kavianinia, A. J. Cameron, P. W. R. Harris and M. A. Brimble, *Org. Biomol. Chem.*, 2020, **18**, 2838–2844.

124 Y. H. Lau, P. De Andrade, Y. Wu and D. R. Spring, *Chem. Soc. Rev.*, 2014, **44**, 91–102.

125 C. Hoppmann, P. Schmieder, N. Heinrich and M. Beyermann, *ChemBioChem.*, 2011, **12**, 2555–2559.

126 P. J. Levalley, E. M. Ovadia, C. A. Bresette, L. A. Sawicki, E. Maverakis, S. Bai and A. M. Kloxin, *Chem. Comm.*, 2018, **54**, 6923–6926.

127 M. D. Nolan, C. Shine, E. M. Scanlan and R. Petracca, *Org. Biomol. Chem.*, 2022, **20**, 8192–8196.

128 A. A. Aimetti, R. K. Shoemaker, C. C. Lin and K. S. Anseth, *Chem. Comm.*, 2010, **46**, 4061–4063.

129 B. Zhao, Q. Zhang and Z. Li, *J. Pept. Sci.*, 2016, **22**, 540–544.

130 Y. Wang and D. H. C. Chou, *Angew. Chem. Int. Ed.*, 2015, **54**, 10931–10934.

131 Y. Wang, B. J. Bruno, S. Cornillie, J. M. Nogieira, D. Chen, T. E. Cheatham, C. S. Lim and D. H. C. Chou, *Chem, Eur. J.*, 2017, **23**, 7087–7092.

132 D. L. Paterson, J. U. Flanagan, P. R. Shepherd, P. W. R. Harris and M. A. Brimble, *Chem. Eur. J.*, 2020, **26**, 10826–10833.

133 N. Narendra, V. M. Thimmalapura, B. Hosamani, G. Prabhu, L. R. Kumar and V. V. Sureshbabu, *Org. Biomol. Chem.*, 2018, **16**, 3524–3552.

134 S. A. Svarovsky, Z. Szekely and J. J. Barchi, *Tetrahedron: Asymmetry*, 2005, **16**, 587–598.

135 M. Yüce and H. Kurt, *RSC Adv.*, 2017, **7**, 49386–49403.

136 Y.-J. Chen, S.-H. Chen, Y.-Y. Chien, Y.-W. Chang, H.-K. Liao, C.-Y. Chang, M.-D. Jan, K.-T. Wang, C.-C. Lin, Y. Chen, Y. Chang, H. Liao, C. Chang, M. Jan, C. Lin, S. Chen, Y. Chien and K. Wang, *ChemBioChem.*, 2005, **6**, 1169–1173.

137 E. Katz, I. Willner, I. Willner and E. Katz, *Angew. Chem. Int. Ed*, 2004, **43**, 6042–6108.

138 R. O. McCourt and E. M. Scanlan, *Org. Lett.*, 2019, **21**, 3460–3464.

139 R. O. McCourt, F. Dénès, G. Sanchez-Sanz and E. M. Scanlan, *Org. Lett.*, 2018, **20**, 2948–2951.

140 A. Benny and E. M. Scanlan, *7950 | Chem. Comm.*, 2024, **60**, 7950.

141 P. Shu, J. Zeng, J. Tao, Y. Zhao, G. Yao and Q. Wan, *Green Chem.*, 2015, **17**, 2545–2551.

142 H. R. Kim, Y. K. Park and S. H. Lee, *Bioorg. Med. Chem.*, 2016, **24**, 4023–4031.

143 J. L. Vincent and F. Su, *Best Res Clin Anaesthesiol*., 2008, **22**, 243–252.

144 T. A. Treschan and J. Peters, *Anesthesiology*, 2006, **105**, 599–612.

145 T. R. Insel, *Neuron.*, 2010, **65**, 768–779.

146 M. Christ-Crain and O. Gaisl, *Presse Med.*, 2021, **50**, 104093.

147 S. R. Manne, A. Sharma, A. Sazonovas, A. El-Faham, B. G. de la Torre and F. Albericio, *ACS Omega*, 2022, **7**, 6007–6023.

148 V. Krchňák, J. Vágner and M. Lebl, *Int. J. Pept. Protein Res.*, 1988, **32**, 415–416.

149 C. E. Paulsen and K. S. Carroll, *Chem. Rev*., 2013, **113**, 4633–4679.

150 U. Wirth, K. Raabe, P. Kalaba, E. Keimpema, M. Muttenthaler and B. König, *J. Med. Chem.*, 2023, **66**, 14853–14865.

151 M. Gomes-Porras, J. Cárdenas-Salas and C. Álvarez-Escolá, *Int. J. Mol. Sci*., 2020, **21**, 1682.

152 P. Barnett, *Endocrine*, 2003, **20**, 255–264.

153 J. Chen, Q. Wan, Y. Yuan, J. Zhu and S. J. Danishefsky, *Angew. Chem. Int. Ed. Engl.*, 2008, **47**, 8521.

154 D. Yu, Z. Sheng, X. Xu, J. Li, H. Yang, Z. Liu, H. H. Rees and R. Lai, *Peptides (N.Y.)*, 2006, **27**, 31–35.

155 M. Daben, J. Libardo, V. Y. Gorbatyuk and A. M. Angeles-Boza, *ACS Infect. Dis.*, 2016, **2**, 71–81.

156 J. T. McLean, P. Milbeo, D. M. Lynch, L. McSweeney and E. M. Scanlan, *Eur. J. Org. Chem.*, 2021, 4148–4160.

157 T. Yamakawa, E. Ideue, J. Shimokawa, T. Fukuyama, T. Yamakawa, E. Ideue, J. Shimokawa and T. Fukuyama, *Angew. Chem. Int. Ed.*, 2010, **49**, 9262–9265.

158 J. B. Blanco-Canosa, B. Nardone, F. Albericio and P. E. Dawson, *J. Am. Chem. Soc.*, 2015, **137**, 7197–7209.

159 P. A. Cistrone, M. J. Bird, D. T. Flood, A. P. Silvestri, J. C. J. Hintzen, D. A. Thompson and P. E. Dawson, *Curr. Protoc. Chem. Biol.*, 2019, **11**, e61.

160 J. M. Conlon, E. Ahmed and E. Condamine, *Chem. Biol. Drug Des.*, 2009, **74**, 488–493.

161 A. Afzali-Ardakani and H. Rapoport, *J. Org. Chem.*, 1980, **45**, 4817–4820.

162 B. Colak, J. C. S. Da Silva, T. A. Soares and J. E. Gautrot, *Bioconjug. Chem.*, 2016, **27**, 2111–2123.

163 B. F. Tack, M. V. Sawai, W. R. Kearney, A. D. Robertson, M. A. Sherman, W. Wang, T. Hong, L. M. Boo, H. Wu, A. J. Waring and R. I. Lehrer, *Eur. J. Biochem.*, 2002, **269**, 1181–1189.

164 J. Sayers, P. M. T. Karpati, N. J. Mitchell, A. M. Goldys, S. M. Kwong, N. Firth, B. Chan and R. J. Payne, *J. Am. Chem. Soc.*, 2018, **140**, 13327–13334.

165 K. Okamoto, T. Shoji, M. Tsutsui, N. Shida and K. Chiba, *Chemistry*, 2018, **24**, 17902–17905.

166 F. Wang, Y. Li, Y. Shen, A. Wang, S. Wang and T. Xie, *Int. J. Mol. Sci.,* 2013, **14**, 13447–13462.

167 H. Javid, M. A. Oryani, N. Rezagholinejad, A. Esparham, M. Tajaldini and M. Karimi-Shahri, *Cancer Med.*, 2024, **13**, e6800.

168 J. L. Sutcliffe-Goulden, M. J. O'Doherty, P. K. Marsden, I. R. Hart, J. F. Marshall and S. S. Bansal, *Eur. J. Nucl. Med.*, 2002, **29**, 754–759.

169 R. F. Turchiello, M. T. Lamy-Freund, I. Y. Hirata, L. Juliano and A. S. Ito, *Biophys. Chem.*, 1998, **73**, 217–225.

170 D. Muller, I. Zeltser, G. Bitan and C. Gilon, *J. Org. Chem.*, 1997, **62**, 411–416.

171 D. alia, P. V Malekar, and Manikandan Parthasarathy, D. Kalia, P. V Malekar and M. Parthasarathy, *Angew. Chem. Int. Ed*, 2016, **55**, 432–1435.

172 S. Habeshian, M. L. Merz, G. Sangouard, G. K. Mothukuri, M. Schüttel, Z. Bognár, C. Díaz-Perlas, J. Vesin, J. Bortoli Chapalay, G. Turcatti, L. Cendron, A. Angelini and C. Heinis, *Nat. Comm*., 2022, **13**, 1–14.

173 M. L. Merz, S. Habeshian, B. Li, J. A. G. L. David, A. L. Nielsen, X. Ji, K. Il Khwildy, M. M. Duany Benitez, P. Phothirath and C. Heinis, *Nat. Chem. Biol.,* 2023, **20**, 624–633.

174 F. M. Brunel and P. E. Dawson, *Chem. Comm.*, 2005, 2552–2554.

175 J. Johansen-Leete, S. Ullrich, S. E. Fry, R. Frkic, M. J. Bedding, A. Aggarwal, A. S. Ashhurst, K. B. Ekanayake, M. C. Mahawaththa, V. M. Sasi, S. Luedtke, D. J. Ford, A. J. O'Donoghue, T. Passioura, M. Larance, G. Otting, S. Turville, C. J. Jackson, C. Nitsche and R. J. Payne, *Chem. Sci.*, 2022, **13**, 3826–3836.

176 J. Johansen-Leete, T. Passioura, T. Passioura, T. Passioura, T. Passioura, S. R. Foster, R. P. Bhusal, D. J. Ford, M. Liu, S. A. K. Jongkees, H. Suga, M. J. Stone and R. J. Payne, *J. Am. Chem. Soc.*, 2020, **142**, 9141–9146.

177 A. Pompella, A. Visvikis, A. Paolicchi, V. De Tata and A. F. Casini, *Biochem. Pharmacol.*, 2003, **66**, 1499–1503.

178 R. Kowalczyk, P. W. R. Harris, G. M. Williams, S. H. Yang and M. A. Brimble, *Peptides and Peptide-based Biomaterials and their Biomedical Applications*, 2017, **1030**, 185.

179 S. V. Moradi, W. M. Hussein, P. Varamini, P. Simerska and I. Toth, *Chem. Sci.*, 2016, **7**, 2492.

180 D. Lipovsek and A. Plückthun, *J. Immunol. Methods*, 2004, **290**, 51–67.

181 T. T. Takahashi, R. J. Austin and R. W. Roberts, *Trends Biochem. Sci.*, 2003, **28**, 159–165.

182 Y. Goto, A. Ohta, Y. Sako, Y. Yamagishi, H. Murakami and H. Suga, *ACS Chem. Biol.*, 2008, **3**, 120–129.

183 Y. Goto and H. Suga, *Acc. Chem. Res.*, 2021, **54**, 3604–3617.

184 K.-C. Chou, *Int. J. Pept. Res. Ther.*, 2020, **26**, 873–888.

185 Y. L. Deribe, T. Pawson and I. Dikic, *Nat. Struct. Mol. Biol*., 2010, **17**, 666–672.

186 M. Mann and O. N. Jensen, *Nat. Biotechnol*. 2003, **25**, 255–261.

187 G. Duan and D. Walther, *PLoS Comput. Biol.*, 2015, **11**, 1004049.

188 J. Bobalova, D. Strouhalova and P. Bobal, *J. Agric. Food Chem.*, 2023, **71**, 14825.

189 B. R. Sabari, D. Zhang, C. David Allis and Y. Zhao, *Nat. Rev. Mol. Cell Biol*. 2017, **18**, 90–101.

190 F. Meng, Z. Liang, K. Zhao and Cheng Luo, *Med Res Rev.* 2021, **41**, 1701–1750.

191 M. Tan, H. Luo, S. Lee, F. Jin, J. S. Yang, E. Montellier, T. Buchou, Z. Cheng, S. Rousseaux, N. Rajagopal, Z. Lu, Z. Ye, Q. Zhu, J. Wysocka, Y. Ye, S. Khochbin, B. Ren and Y. Zhao, *Cell*, 2011, **146**, 1016–1028.

192 A. Ntorla and J. R. Burgoyne, *Front Cell Dev. Biol.*, 2021, **9**, 624914.

193 G. Jiang, C. Li, M. Lu, K. Lu and H. Li, *Cell Death & Disease*, 2021, **12**, 1–11.

194 W. Wei, A. Mao, B. Tang, Q. Zeng, S. Gao, X. Liu, L. Lu, W. Li, J. X. Du, J. Li, J. Wong and L. Liao, *J. Proteome Res.*, 2017, **16**, 1743–1752.

195 W. Xu, J. Wan, J. Zhan, X. Li, H. He, Z. Shi and H. Zhang, *Cell Res.*, 2017, **27**, 946–949.

196 S. Wang, G. Mu, B. Qiu, M. Wang, Z. Yu, W. Wang, J. Wang and Y. Yang, *Int. J. Biol. Sci.*, 2021, **17**, 3441–3455.

197 O. Ruiz-Andres, M. D. Sanchez-Niño, P. Cannata-Ortiz, M. Ruiz-Ortega, J. Egido, A. Ortiz and A. B. Sanz, *DMM*, 2016, **9**, 633–645.

198 Y. Liu, M. Li, M. Fan, Y. Song, H. Yu, X. Zhi, K. Xiao, S. Lai, J. Zhang, X. Jin, Y. Shang, J. Liang and Z. Huang, *Biol. Psychiatry*, 2019, **85**, 635–649.

199 B. R. Sabari, D. Zhang, C. D. Allis and Y. Zhao, *Nat. Rev. Mol. Cell Biol.*, 2017, **18**, 90–101.

200 Q. Wu, W. Li, C. Wang, P. Fan, L. Cao, Z. Wu and F. Wang, *J. Proteome Res*., 2017, **16**, 3664–3671.

201 G. Drewes and S. Knapp, *Trends Biotechnol.,* 2018, **36**, 1275–1286.

202 Y. Zhao and O. N. Jensen, *Proteomics*, 2009, **9**, 4632–4641.

203 W. H. Dunham, M. Mullin and A. C. Gingras, *Proteomics*, 2012, **12**, 1576–1590.

204 G. Drewes and S. Knapp, *Trends Biotechnol.*, 2018, **36**, 1275–1286.

205 J. Bos and T. W. Muir, *J. Am. Chem. Soc.*, 2018, **140**, 4757–4760.

206 D. R. Rooker, Y. Klyubka, R. Gautam, E. Tomat and D. Buccella, *ChemBioChem.*, 2018, **19**, 496–504.

207 C.N. Kuzniewski, J. Gertsch, M. Wartmann and K-H. Altmann, *Org. Lett.*, 2008, **10**, 1183–1186.

208 C. Priem and A. Gayer, *Org. Lett*., 2017, **20**, 162–165.

209 L.D. Turner, A.L. Nielsen, L. Lin, S. Pellett, T. Sugane, M.E. Olson, E.A. Johnson and K.D. Janda, *RSC Med. Chem*., 2021, **12**, 960–969.